



UNIVERSITAT DE
BARCELONA

Characterization of the pulmonary and systemic immune response in relation with lung stem cells in patients with COPD

Tamara Cruz Santa Cruz

ADVERTIMENT. La consulta d'aquesta tesi queda condicionada a l'acceptació de les següents condicions d'ús: La difusió d'aquesta tesi per mitjà del servei TDX (www.tdx.cat) i a través del Dipòsit Digital de la UB (diposit.ub.edu) ha estat autoritzada pels titulars dels drets de propietat intel·lectual únicament per a usos privats emmarcats en activitats d'investigació i docència. No s'autoritza la seva reproducció amb finalitats de lucre ni la seva difusió i posada a disposició des d'un lloc aliè al servei TDX ni al Dipòsit Digital de la UB. No s'autoritza la presentació del seu contingut en una finestra o marc aliè a TDX o al Dipòsit Digital de la UB (framing). Aquesta reserva de drets afecta tant al resum de presentació de la tesi com als seus continguts. En la utilització o cita de parts de la tesi és obligat indicar el nom de la persona autora.

ADVERTENCIA. La consulta de esta tesis queda condicionada a la aceptación de las siguientes condiciones de uso: La difusión de esta tesis por medio del servicio TDR (www.tdx.cat) y a través del Repositorio Digital de la UB (diposit.ub.edu) ha sido autorizada por los titulares de los derechos de propiedad intelectual únicamente para usos privados enmarcados en actividades de investigación y docencia. No se autoriza su reproducción con finalidades de lucro ni su difusión y puesta a disposición desde un sitio ajeno al servicio TDR o al Repositorio Digital de la UB. No se autoriza la presentación de su contenido en una ventana o marco ajeno a TDR o al Repositorio Digital de la UB (framing). Esta reserva de derechos afecta tanto al resumen de presentación de la tesis como a sus contenidos. En la utilización o cita de partes de la tesis es obligado indicar el nombre de la persona autora.

WARNING. On having consulted this thesis you're accepting the following use conditions: Spreading this thesis by the TDX (www.tdx.cat) service and by the UB Digital Repository (diposit.ub.edu) has been authorized by the titular of the intellectual property rights only for private uses placed in investigation and teaching activities. Reproduction with lucrative aims is not authorized nor its spreading and availability from a site foreign to the TDX service or to the UB Digital Repository. Introducing its content in a window or frame foreign to the TDX service or to the UB Digital Repository is not authorized (framing). Those rights affect to the presentation summary of the thesis as well as to its contents. In the using or citation of parts of the thesis it's obliged to indicate the name of the author.

Universidad de Barcelona
Facultad de Medicina
Centro de investigación CELLEX

Characterization of the pulmonary and systemic
immune response in relation with lung stem cells in
patients with COPD.

Memoria de Tesis presentada para la obtención del título europeo de
Doctor en Biomedicina por la Universidad de Barcelona

Tamara Cruz Santa Cruz

Barcelona, 21 de Julio del 2017

CLÍNIC
BARCELONA
Hospital Universitari


UNIVERSITAT DE BARCELONA

ciberes
Centro de Investigación Biomédica en Red
Enfermedades Respiratorias

IDIBAPS
Institut
d'Investigacions
Biomèdiques
August Pi i Sunyer

Centro de Investigación CELLEX
Facultad de Medicina, Hospital Clinic
Casanova, 143, 08036 Barcelona

Álvar Agusti Profesor Asociado de Medicina de la Universidad de Barcelona y Director del institut clínic de respiratori y Rosa Faner investigadora Miguel Servet del CIBER de enfermedades Respiratorias.

Certifican:

Que la tesis titulada “*Characterization of the pulmonary and systemic immune response in relation with lung stem cells in patients with COPD*” ha sido realizada por Tamara Cruz Santa Cruz bajo su dirección y consideran que es apta para ser presentada y optar al grado de Doctor en Biomedicina por la Universidad de Barcelona.

Para que quede en constancia, se firma la presente certificación a Barcelona 15 de Junio del 2017.

Dr. Álvar Agustí

Dra. Rosa Faner

ABSTRACT

Rationale: Chronic obstructive pulmonary disease (COPD) is characterized by chronic airflow limitation caused by a combination of airways disease (bronchiolitis) and parenchymal destruction (emphysema), whose relative proportion varies from patient to patient. An abnormal immune response to tobacco smoke is one of the main factors, both in the lungs and circulating blood. Both the relation between the pulmonary and systemic inflammation and the regenerative capacity of the lung are also unclear.

Objectives: Divided into 3 specific objectives:

1. To explore and contrast the molecular pathogenesis of emphysema and bronchiolitis in COPD.
2. To characterize and contrast the cellular pulmonary and systemic immune response in COPD patients and healthy controls smokers and non-smokers.
3. To identify, characterize and compare the immunomodulatory capacity of a putative resident stem cell population in the lung.

Methods: For the first objective differential expression and gene co-expression in bronchiolitis and emphysema were analyzed by lung transcriptomics. For the second, flow cytometry from lung tissue and blood was performed to evaluate the cellular immune response. For the third objective, a new cell culture methodology was developed.

Results: Specific results for each objective

1. Emphysema signature is different from bronchiolitis with an up-regulated expression of ontologies related with B-cell homing and activation.
2. The lung of mild COPD patients has increase macrophages and decrease T lymphocytes associated to both COPD and smoking status, that is not co-related with systemic immune response.
3. A putative lung resident stem cell population was identify with transcriptional signature of mesenchymal origin and immunomodulatory properties.

Conclusions: The lung immune response is heterogeneous and associated with both the lung regenerative capacity and the clinical heterogeneity/complexity of COPD.

ÍNDICE

ABSTRACT	5
ÍNDICE.....	7
ABBREVIATIONS	11
1 - INTRODUCCION.....	16
1.1 - CHRONIC OBSTRUCTIVE PULMONARY DISEASE (COPD).....	17
1.1.1 - Burden of COPD	17
1.1.2 - Diagnosis	18
1.1.3 - Natural history.....	18
1.1.3 - Pathology:	20
1.1.3.1 – Functional changes: chronic bronchitis	20
1.1.3.2 - Structural changes: airway and parenchymal abnormalities	21
1.1.3.2.1 - Small airways disease.....	21
1.1.3.2.2 - Emphysema.....	22
1.1.4 - Mechanism leading to COPD.....	22
1.1.4.1 - Proteinases-antiproteinases balance	22
1.1.4.2 - Inflammation – immune response	23
1.1.4.2.1 - Autoimmune process.....	28
1.1.4.3 - Oxidative stress	30
1.2 – LUNG REGENERATION-REPAIR	31
1.2.1 - Human airway epithelium.....	31
1.2.1.1 - Airway epithelium in COPD	34
1.2.1.1.1 - Similarities of COPD lung epithelium and aging	36
1.2.1.1.2 - DNA methylation.....	36
1.2.2 - Adult stem cells.....	37
1.2.2.1 - Mesenchymal stem cells	40
1.2.2.2 - MSC in the lung	40
1.2.2.3 - Sphere formation as a source of stem cells.....	41
1.2.2.4 - Animal models that use MSC cell therapy.....	42
1.2.2.5 - Cell based therapies in human patients	43
1.3 - NETWORK MEDICINE.....	44
1.3.1 - Network analysis	48
1.3.2 - Network medicine in COPD	51
2-HYPOTHESIS.....	57
2.1 - GENERAL HYPOTHESES	58
2.2 - SPECIFIC HYPOTHESES	58
3 - OBJECTIVES	59

3.1 - GENERAL OBJECTIVE	60
3.2 – SPECIFIC OBJECTIVES	60
4 - METHODS	61
4.1 – DESIGN, POPULATION AND ETHICS.....	62
4.1.1 - Clinical and functional characterization	62
4.2 – METHODS IN RELATION TO OBJECTIVE-1: MOLECULAR PULMONARY IMMUNE RESPONSE NETWORK	64
4.2.1 – RNA extraction	64
4.2.1.1 - Microarray processing and raw data generation	64
4.2.1.1.1 - Differential gene expression	65
4.2.1.1.2 - Gene Set Enrichment Analysis (GSEA).....	65
4.2.1.1.3 - Gene Enrichment Profiler (GEP).....	66
4.2.1.1.4 - Gene co-expression networks and their comparison.....	66
4.2.1.2 - Validation of microarray results	67
4.2.1.2.1 - Quantitative Real Time PCR	67
4.2.1.2.2 - Immunofluorescent determination of lymphoid follicles and CD20+lung tissue area calculation.....	67
4.2.1.2.3 - CXCL13 and BAFF ELISA	68
4.3 - METHODS IN RELATION TO OBJECTIVE-2: CELLULAR CHARACTERIZATION OF THE IMMUNE RESPONSE	69
4.3.1 - Processing of lung tissue	69
4.3.2 - Processing of peripheral blood	70
4.3.3 - RNA extraction and microarray analysis	70
4.3.4 - Flow cytometry staining.....	70
4.3.4.1 - Gating strategies	73
Tube 1: Neutrophils	73
Tube 2: T Lymphocytes	74
Tube 3: B, NK lymphocytes	75
Tube 4: NKT lymphocytes.....	76
Tube 5: Monocytes (Blood only)	78
Tube 6: (lung only) Macrophages.....	78
Tube 7: Dendritic cells.....	79
Tube 8: Mast Cells.....	80
Tube 9: Mesenchymal stem cells (MSC).....	81
4.3.5 - Statistical analysis.....	83
4.3.5.1 - Population statistics	83
4.3.5.2 Network Analysis:.....	83
4.3.5.2.1 Spearman correlation networks:.....	83
4.3.5.2.2 Weighed gene co-expression Networks Analysis (WGCNA):.....	83
4.4 – METHODS IN RELATION TO OBJECTIVE-3: LRMSC	85

4.4.1 - Isolation of Lung Resident Mesenchymal-like Stem Cells, LRMSC:	85
4.4.2 - Cell surface marker characterization	86
4.4.3 - Expression of pluripotency associated genes:	88
4.4.3.1 - Microarray data analysis:	89
4.4.3.2 - RT-PCR validation of the microarray results.....	89
4.4.4 - Adipogenic, osteogenic and chondrogenic differentiation:	90
4.4.5 - Immunofluorescence:	91
4.4.6 - Proliferation assay:	92
4.4.7 - Senescence and telomere length:	93
4.4.8 - Immunomodulation assay:	94
4.4.8.1 - <i>In vitro</i> co-culture assays:	94
5 - RESULTS	97
5.1 – RESULTS IN RELATION TO OBJECTIVE-1: MOLECULAR PULMONARY IMMUNE RESPONSE NETWORK	98
5.1.1 - Characterization of patients and analysis strategy	98
5.1.1.1 - Comparison 1: Severe emphysema vs. bronchiolitis	100
5.1.1.1.1 - Gene Set Enrichment Analysis (GSEA).....	101
5.1.1.1.2 - Network structure of the immune response in severe emphysema vs. bronchiolitis.....	101
5.1.1.2 - Comparison 2: Intermediate group vs. bronchiolitis	105
5.1.1.3 - Comparison 3: Moderate vs. mild emphysema.....	106
5.1.1.4 - Comparison 4: Assessment of airflow limitation severity influence	107
5.1.2 - Functional translation of transcriptomic results	108
5.2 – RESULTS IN RELATION TO OBJECTIVE 2: CELLULAR CHARACTERIZATION OF THE IMMUNE RESPONSE	112
5.2.1 –Study population	112
5.2.2 - Characterization of the immune cell infiltrate in lung tissue	112
5.2.3 - Characterization of blood immune response	117
5.2.4 - Effects of cigarette smoke vs. disease status	117
5.2.5 –Pulmonary and systemic immune cell correlation network	118
5.2.6 –Weighted gene co-expression network analysis	119
5.3 – RESULTS IN RELATION TO OBJECTIVE 3: LRMSC	125
5.3.1 - Study population	125
5.3.2 – LRMSC isolation procedure	125
5.3.3 - Characterization of LRMSC	127
5.3.3.1 - Cell surface characterization by flow cytometry	128
5.3.3.2 –Transcriptomics profile comparison	128
5.3.3.2.1 - Rohart test	130
5.3.3.2.2 – Expression of stemness related genes	131
5.3.3.3 - Differentiation capacity.....	133
5.3.3.4 – Senescence status	133
5.3.3.5 - Localization in the lung.....	134

5.3.3.6 - Immunomodulatory capacity	138
5.3.4 - LRMSC differences between study groups	140
5.3.4.1 –LRMSC quantification in lung homogenates.....	140
5.3.4.2 - Proliferation capacity	140
5.3.4.3 –Telomere length	141
5.3.4.4– Differences in the MSC Rohart score.....	142
5.3.4.5 –Differences in gene expression.....	142
5.3.4.6 - Immunomodulatory capacity	143
6 - DISCUSSION	146
6.1 – OBJECTIVE 1. MOLECULAR IMMUNE RESPONSE	147
6.1.1 - Comparison with previous studies.....	147
6.1.2 - Interpretation of findings.....	148
6.1.3 - Potential clinical implications.....	150
6.1.4 – Potential Limitations	151
6.2 – OBJECTIVE 2. CELLULAR IMMUNE RESPONSE.....	152
6.2.1 - Comparison with previous studies.....	152
6.2.2 - Interpretation of findings.....	153
6.2.3 - Potential limitations	155
6.2.4 - Potential clinical implications.....	156
6.3 – OBJECTIVE 3. REGENERATIVE CAPACITY	157
6.3.1 - Comparison with previous studies.....	157
6.3.2 - Interpretation of findings.....	158
6.3.3 - Potential limitations	160
6.4 INTEGRATIVE, DISUSSION	161
7 - CONCLUSIONS.....	163
7.1 - GENERAL CONCLUSION	164
7.2 - SPECIFIC CONCLUSIONS.....	164
8 - BIBLIOGRAPHY.....	165
9- ANNEX I: PUBLISHED ARTICLES	185

ABBREVIATIONS

ABBREVIATIONS

7-AAD	7-AminoActinomycin D
AEC	Alveolar Epithelial Cell
APC	Allophycocyanin
AREG	Amphiregulin
BAFF	B cell Activating Factor
BAL	Bronchoalveolar Lavage
BALT	Bronchus Associated Lymphoid Tissue
BD	Becton, Dickinson
GBLAP	Bone Gamma-Carboxyglutamate Protein (osteocalcin)
BM-MSC	Bone Marrow Mesenchymal Stem Cell
BMI	Body Mass Index
BV421	Brilliant Violet 421
CCL	CC chemokine ligand family
CCR	CC chemokine receptor family
CD	Clinical diseasome
CD	Cluster of Differentiation
CFSE	Carboxyfluorescein Succinimidyl Ester
CIBERES	Centro Investigaciones Biomédicas en Red de Respiratorio
CLGN	Calmegin
CO ₂	Carbon dioxide
COPD	Chronic Obstructive Pulmonary Disease
COPD-CS	Chronic Obstructive Pulmonary Disease – Current Smoker
COPD-FS	Chronic Obstructive Pulmonary Disease – Former Smoker
CT	Computer Tomography
CTL	Cytolytic T Lymphocyte
CXCL	CXC chemokine ligand family
CXCR	CXC chemokine receptor family
DAMPs	Danger Associated Molecular Patterns
DAPI	4',6-diamino-2-fenilindol
DCs	Dendritic cells
DEPC	DiEthyl PyroCarbonate
DLCO	Diffusing capacity of the Lung for Carbon Monoxide
DMEM	Dulbecco's Modified Eagle Medium

DNA	DesoxiriboNucleic Acid
DPPA3	Developmental Pluripotency Associated 3
ECLIPSE	evaluation of COPD Longitudinally to Identify predictive Surrogate End-Point
EDTA	Ethylenediaminetetraacetic acid
EGF	Epithermal Growth Factor
EGFR	Epithermal Growth Factor Receptor
EGLN2	EGL Nine homolog 2
ELISA	Enzyme-Linked Immunosorbent Assay
EMT	Epithelial to Mesenchymal Transition
EPAS1	Endothelial PAS domain containing protein 1
ES	Enrichment Score
FACS	Fluorescence-Activated Cell Sorting
FABP-4	Fatty Acid Binding Protein 4
FBS	Fetal Bovine Serum
FDR	False Discovery Rate
FDR	Fold Discovery Rate
FEV1	Forced Expiratory Volume in the first second
FGFR	Fibroblast Growth Factor Receptor
FITC	Fluorescein isothiocyanate
FMO	Fluorescence Minus One
FOX	Forkhead Box Protein family
FS	Former Smoker
FSC	Forward Scattered Light
FVC	Forced Vital Capacity
FWER	Family-Wise Error Rate
G-CSF	Granulocyte Colony Stimulator Factor
GM-CSF	Granulocyte-Macrophage Colony Stimulator Factor
Gapdh	Gliceraldehído-3-fosfato deshidrogenasa
GEP	Gene Enrichment Profiler
GSEA	Gene Set Enrichment Analysis
GO	Gene Ontology
GOLD	Global Initiative for Chronic Obstructive Lung Disease
H/E	Hematoxylin and eosin stain
HLA	Human leukocyte Antigen

IDO	Indoleamine-pyrrole 2,3-dioxygenase
IFN γ	Interferon- γ
Ig	ImmunoGlobulin
IL	InterLeukin
IMDM	Iscove's Modified Dulbecco's Media
iNOS	inducible Nitric Oxide Synthase
IP-10	Interferon inducible Protein 10
IQR	Inter Quartile Range
I-TAC	Interferon-inducible T cell Alpha Chemoattractant
KEGG	Kyoto Encyclopaedia of Genes and Genomes
KLF4	Kruppel-like factor 4
KRT5	Keratine-5
LIF	Leukemia Inhibitor Factor
LRMSC	Lung Resident Mesenchymal-like Stem Cells
LPS	LipoPolySaccharide
LTBP4	Latent TGB Binding Protein 4
M-CSF	Macrophage Colony Stimulating Factor
MACS	Magnetic Activated Cell Sorted
MD	Molecular diseasome
MDSCs	Myeloid Derived Suppressor Cells
MHC	Major Histocompatibility Complex
MIG	Monokine induced by Interferon Gamma
MMP	Matrix Metalloprotease
MSC	Mesenchymal Stem Cell
NaHCO ₃	Sodium Bicarbonate
NES	Normalized Enrichment Score
NF-Kb	Nuclear Factor of K light chains of B cells
NFKB1B	NF- $\kappa\beta$ Inhibitor β
NH ₄ Cl	Ammonium Chloride
NK	Natural Killer
NKT	Natural Killer T cell
NRF2	Nuclear factor (erythroid-derived 2)-like 2
O.C.T	Optimal Cutting Temperature compound
Oct-4	Octamer Binding transcription Factor 4
PBS	Phosphate Buffer Saline

PCA	Principal Components Analysis
PE	Phycoerythrin
PerCP	Peridinin chlorophyll
PGE2	Prostaglandin E2
PKH	Membrane fluorescencet marker
RFX	Regulatory factor X gene family
RMA	Robust Multiarray Average
RT-PCR	Real Time - Polymerase Chain Reaction
R&D	Research and Development
SCF	Stem Cell Factor
SCM	Sphere Culture Medium
SDC	Sphere Derived Cells
SLPI	Secretory Leukocyte Protease Inhibitor
SMG	Submucosal Glands
Sox-2	Sex determining region Y Box 2
SPD	Surfactant Protein D
SPDEF	SAM pointed domain-containing Ets transcription factor
SSC	Side Scattered Light
TcR	T cell Receptor
TGFB1	Transforming Growth Factor β 1
TLR	Toll Like receptor
TNF	Tumor Necrosis Factor
TPER	Tissue Protein Extraction Reagent
VIStA	diVISive Shuffling Approach
WHO	World Health Organization
μ l	microlitro
μ m	micrometro
μ M	micromolar

1 - INTRODUCCION

1 - INTRODUCTION

1.1 - Chronic obstructive pulmonary disease (COPD)

Chronic obstructive pulmonary disease (COPD) is characterized by persistent respiratory symptoms and airflow limitation due to airway and/or alveolar abnormalities (i.e., emphysema) [1]. Airflow limitation seems, in turn, related to the structural changes induced by an abnormal inflammatory response of the lungs to harmful particles or vapors [2]. In high- and middle-income countries tobacco smoke is the main risk factor for COPD [3], while in low-income countries exposure to indoor air pollution [4], such as the use of biomass fuels for cooking and heating, causes most of the COPD burden. Of note however, not all exposed individuals develop the disease, which suggest that the genetic and or epigenetic background of each person is key for the development of the disease. Other well-established risk factors for COPD include occupational dusts and chemicals [5] (such as vapors, irritants, and fumes) and, as shown by recent research from our group and others, abnormal lung development, which in turn can be due to genetic, epigenetic and/or environmental factors such as passive smoking, frequent lower respiratory infections and/or poor diet during childhood [6].

1.1.1 - Burden of COPD

The World health Organization (WHO) estimates that 65 million people currently suffer moderate to severe COPD and that more than 3 million people died of COPD annually, which corresponds to 5% of all deaths globally. In 2002, COPD was the fifth leading cause of death worldwide. Approximately 50% of all individuals with COPD are not aware of the disease and its prevalence is thus considerably underestimated [7]. Total deaths from COPD are projected to increase by more than 30% in the next 10 years in relation to the aging of the population [8, 9], which estimates that COPD will become the third leading cause of death worldwide in 2030 [2].

Historically, COPD was more common in men, but because of increased tobacco use among women in high-income countries and the higher risk of exposure to indoor air pollution (such as biomass fuel used for cooking and heating) in low-income countries, the disease now affects men and women almost equally [10].

1.1.2 - Diagnosis

The diagnosis of COPD requires the spirometry confirmation of airflow limitation as indicated by the ratio of volume of gas exhaled in the first second (Forced Expiratory Volume, FEV1) over the total volume exhaled (Forced Vital Capacity, FVC) lower than 70%, in the appropriate clinical context [2]. The severity of airflow limitation is then graded according to the value of FEV1, expressed as % of a reference value that takes into consideration the age, sex, race, and height of the individual (www.goldcopd.org), as shown in Table 1 below.

Grade	Severity	FEV1/FVC	FEV1 (% reference)
I	Mild	<0.70	≥ 80%
II	Moderate	<0.70	50-79%
III	Severe	<0.70	30-49%
IV	Very Severe	<0.70	<30%

Table 1: GOLD classification of airflow-limitation severity

1.1.3 - Natural history

As Fletcher and Peto described in 1977, FEV1 declines continuously and smoothly over an individual's life in healthy non-smokers, who lose FEV1 slowly and almost never developed clinically significant airflow limitation [11]. By contrast, there seems to be two subgroups of smokers; one that loses FEV1 as slowly as non-smokers and never develop airway limitation either. They appeared to be resistant to the deleterious effects of the smoke (hence, they were originally named “non-susceptible”). On the other hand, there is another subgroup of smokers (“susceptible smokers”) who are susceptible to the damaging effects of smoking and, therefore, lose lung function at an accelerated rate and develop different degrees of airway limitation (hence COPD), . A susceptible smoker who stops smoking will, according to Fletcher and Peto, not recover the FEV1 already lost, but the subsequent rate of loss of FEV1, will (in theory) revert to normal (Figure 1) [11].

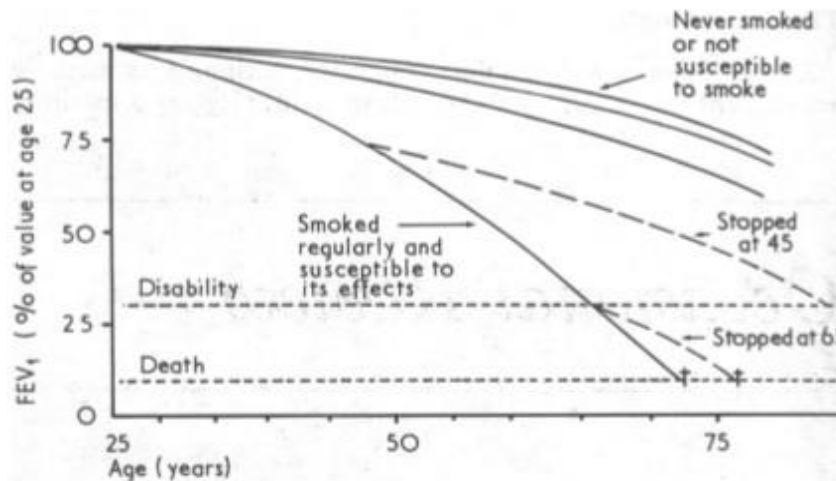


Figure 1: Natural history of COPD from the original work by Fletcher and Peto (1977) [11].

The mechanisms of susceptibility to smoking are not precisely known but researchers suspect that environmental and genetic factors play a significant role [2, 12]. The genetic hypothesis is supported by the familiar aggregation that has been described in siblings of COPD patients [13]. More recent research by our group and others, however, has challenged this traditional dogma (Figure 1) by showing that low maximally attained peak lung function in early adulthood can also result in COPD later in life, even when the rate of decline in FEV₁ is within the normal range [14] (Figure 2).

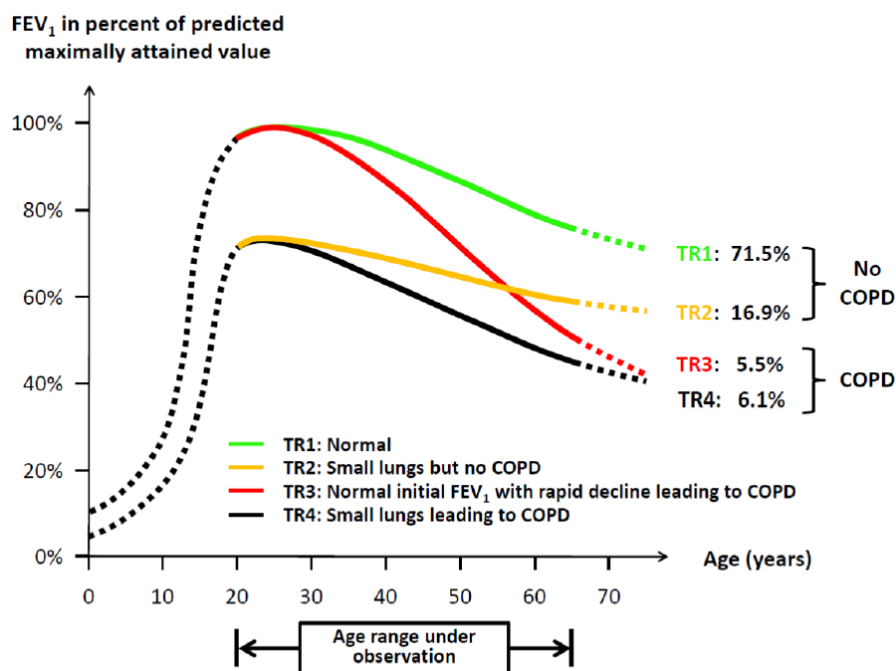


Figure 2: Schematic representation of lung function trajectories represented as decline of FEV₁ over time [14].

1.1.3 - Pathology:

Airflow limitation in COPD is due to two different pathological processes: airway remodeling (chronic bronchitis and bronchiolitis) and/or parenchymal (i.e. alveolar) destruction (emphysema). The relative proportion of airway remodeling and emphysema varies greatly between patients. These pathological abnormalities appear to be related by an abnormal and/or enhanced inflammatory response, which seems to be responsible for specific effects on mucociliary function as well as structural changes in the airways and lung parenchyma. Further, it is likely related too to some of the effects outside the lung (the systemic effects of COPD). In this context, COPD can be considered a multicomponent disease, comprising structural and functional changes, inside and outside the lungs (Figure 3) [15]. Among the extra-pulmonary manifestations of COPD, cardiovascular diseases, skeletal muscle dysfunction, osteoporosis, metabolic syndrome and (lung) cancer appear to be particularly prevalent and relevant clinically [2].

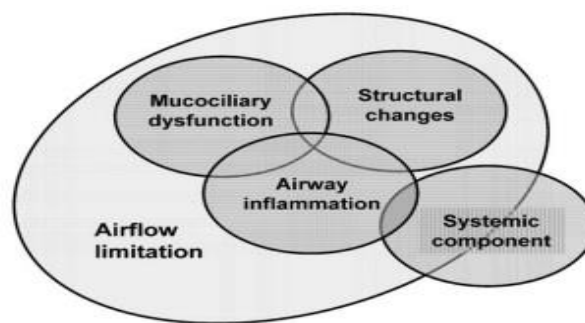


Figure 3: Principal alterations in COPD pathophysiology [2].

Current treatment of COPD is effective in improving the symptoms of these patients (mostly dyspnea with or without chronic cough and expectoration). Yet, no available treatment so far is curative, and there is debate on whether current therapies do alter or not the natural course of the disease [2].

1.1.3.1 – Functional changes: chronic bronchitis

Chronic bronchitis is a clinical syndrome defined by the presence of cough and sputum production for more than three months during two consecutive years, in the absence of other diseases that can explain it (e.g., bronchiectasis) [16]. It can also occur in smokers

with normal lung function but, in patients with COPD, it increases the risk of bacterial infections and exacerbations, thus influencing the natural course of the disease [17].

Exposure to environmental factors (mostly, but not exclusively, cigarette smoke) causes an enlargement of the mucous glands (hypertrophy) of the airways and increases the number of the mucus-secreting goblet cells [18, 19]. In addition, the damage to the ciliated epithelium decreases the mucociliary transport (Figure 4). The combination of these two processes leads to an accumulation of mucus in the airways which, in turn, increases the likelihood of infections [17].

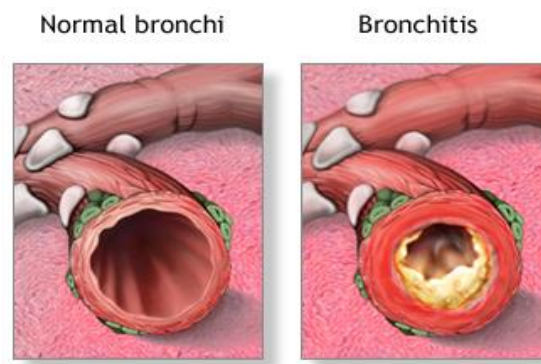


Figure 4: Chronic bronchitis in COPD (extracted from <https://medlineplus.gov/chronicbronchitis.html>).

1.1.3.2 - Structural changes: airway and parenchymal abnormalities

The structural changes that characterize COPD include small airways disease (obstructive bronchiolitis) and parenchymal destruction (emphysema).

1.1.3.2.1 - Small airways disease

The inflammatory response to the repetitive tissue damage that long term smoking causes can lead to a repair process that aims at restoring the epithelium and microvasculature by adding connective-tissue matrix in an attempt to return the tissue architecture and function to its previous state. This remodeling mechanism results in bronchial wall thickening that obstructs airways smaller than 2 mm internal diameter. There is a relationship between the severity of airflow limitation in COPD and the extent of occlusion of the airway lumen [18, 20].

1.1.3.2.2 - Emphysema

Emphysema is characterized by destruction of the alveolar walls that leads to permanent enlargement of the airspaces distal to the terminal bronchioles, see Figure 5. Emphysema reduces the alveolar surface available for pulmonary gas exchange and decrease the elastic recoil of the lung parenchyma, thus limiting the force that drives air out of the lungs. The latter can also cause shortness of breath due to lung hyperinflation and gas trapping [21, 22].

The destruction of the alveolar walls results both from protease-mediated degradation of connective tissue elements, particularly elastin, as well as from apoptosis of type I pneumocytes and endothelial cells [23, 24]. About 40% of heavy smokers develop severe emphysema, although it can also be found in smokers with normal lung function [18].

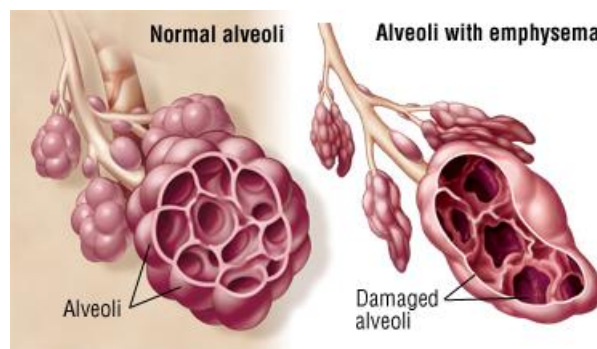


Figure 5: Emphysema in COPD (extracted from <https://www.drugs.com/health-guide/emphysema.html>)

1.1.4 - Mechanism leading to COPD

There are several pathobiological mechanisms that, alone or in combination, can lead to COPD. These are briefly reviewed below.

1.1.4.1 - Proteinases-antiproteinases balance

Neutrophil and macrophage proteases are able to enzymatically degrade a variety of lung matrix proteins. Also CD8+ T cells produce granzyme B that contribute to the degradation and remodeling. Granzyme B accumulates in the milieu during the chronic inflammation that characterizes of COPD, and their levels correlate with disease severity [25].

In order to protect the tissue, the structural cells of the lung produce antiproteases which inactivate these proteases. Protease-antiprotease imbalance is likely to have an important pathogenic role in the development of emphysema [26]. A mutation in the gene of the α -1 antitrypsine has been described as a risk factor for the development of severe emphysema [27].

1.1.4.2 - Inflammation – immune response

The mechanism by which harmful particles or gases, such as cigarette smoke, trigger an innate immune response is still unknown but the danger hypothesis of Matzinger could be a possible explanation [28]. This hypothesis proposes that the cellular stress or tissue damage produce biological signals that are responsible of starting an innate immune response. Each puff of a cigarette contains more than 4.000 xenobiotic compounds and 10^{14} free radicals that can injure lung epithelial cells to a degree that is directly proportional to their concentration [29].

A breakdown of connective tissue has also been described in smokers and mice models exposed to cigarette smoke [30, 31]. TLR2 and TLR4 can recognize products derived from epithelial injury and produce mediators of inflammation that activate macrophages and neutrophils [32], which in turn secrete proteolytic enzymes that, in combination with reactive oxygen species, can damage the lung tissue further [33].

Macrophages play a key role in the defense of the respiratory track. Their number is increased in the lung of smokers and correlate with the degree of airflow limitation [34, 35]. Activated macrophages release several chemotactic factors and pro-inflammatory cytokines that perpetuate the inflammatory response. Macrophages produce matrix metalloproteases (MMP) that contribute to the degradation of the extracellular matrix. In particular MMP12 is increased in COPD lungs, and mice MMP12 knock out model is protected against cigarette induced emphysema, revealing an important role for this protease [36].

Neutrophils produce elastases, serine proteases and proteinase-3 that contribute to the degradation of the matrix [37]. Neutrophil elastase levels are associated with the severity of airflow limitation in COPD [38]. Neutrophils also generate oxidants and release cytokine/chemokine that can further potentiate inflammation and trigger an

immune response [39, 40]. Figure 6 shows a representation of all these mechanisms as initial immune responses against smoke.

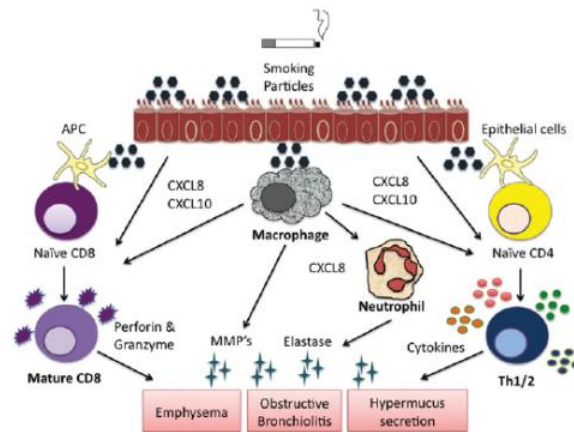


Figure 6: Initial mechanism of immune response against cigarette smoke [41]

Macrophage proteases and neutrophil elastases produce the release of more apoptotic DNA, extracellular matrix proteins, auto-antigens, modify proteins and damaged mitochondria than enhance the immune response [42, 43]. This process originates a close-circle mechanism that perpetuates tissue damage and triggers the innate immune system. In addition some of these products could be recognized as a foreign antigens and trigger an adaptive immune response [23, 24]. This possible interaction between the innate and the adaptive immune responses is represented in the Figure 7.

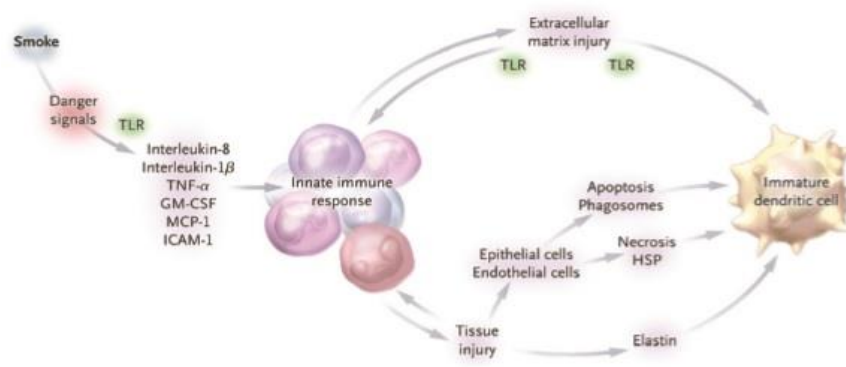


Figure 7: Process by which the innate immune response could trigger an adaptive immune response [44].

The resolution of the inflammation (also known as *catabasis*) is not a passive process, instead is a highly regulated one [45]. Catabasis requires the coordinated action of specific lipid mediators, pro-resolution and repair proteins, anti-inflammatory nuclear receptors and the elimination of apoptotic cells by macrophages, a process known as *efferocytosis* [46]. In alveolar macrophages, the surface expression of CD44, a key molecule involved in efferocytosis, was significantly reduced in comparison with

smokers with normal lung function [47], supporting the hypothesis that catabasis may be impaired in COPD. It has been proposed that the smokers with normal lung function can in fact control the innate immune response at this initial step hence avoiding the activation of the adaptive immune system [44].

Immature dendritic cells are present in the lung tissue and could recognize some of the products generated from tissue damage that can act as foreign antigens. When TLRs binds a ligand, the dendritic cell matures, expresses high levels of class II major-histocompatibility-complex (MHC-II) and the co-stimulatory molecules CD80 and CD86, that direct these cells to the local lymph nodes, where they present the antigens to the T lymphocytes [48, 49].

Naive, quiescent T cells cannot enter the lung parenchyma until they are activated by antigen-bearing dendritic cells and express their tissue-specific chemokine receptors [50], process shown in Figure 8. Several studies have found in the lungs of COPD patients: (a) CD4+ T cells expressing the tissue-specific chemokine receptors CXCR3, CCR5 and CXCR6; and, (b) structural cells in the airways and pulmonary arteries expressing interferon-inducible protein 10 (IP-10), monokine induced by interferon gamma (MIG), and interferon-inducible T cell alpha chemoattractant (I-TAC), three known ligands for CXCR3 and CXCR6 ligand (CXCL6) [51, 52]. These chemokines are homing of a CD4+ Th1 T cell response which is different from the Th2 response of asthma patients characterized by CCR2 and CCR4.

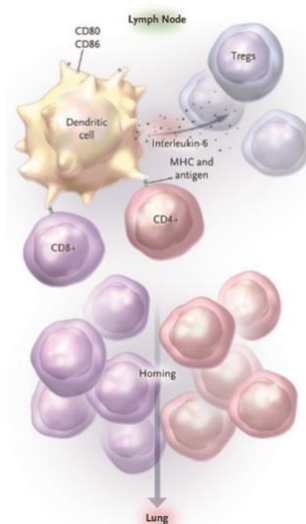


Figure 8: Activation of naive T cells in the lymph node leads to the expression of tissue specific chemokine receptors that direct the T cells to the lung tissue [44].

In the BAL of COPD patients there is also an increased number of mature dendritic cells producing IL-12, that can polarized CD4⁺ T lymphocytes towards a Th1 response that produces IFN γ and an up regulation of the macrophage matrix metalloproteases (MMP) [53]. Of note, levels of the chemokines receptors and ligands as well as that of IFN γ correlate with the degree of airflow limitation [51, 54].

Cell survival signals depend on the integrin family that senses the extracellular milieu [55]. The disruption of this milieu by the action of matrix metalloproteases contributes to perpetuate the apoptosis of epithelial and endothelial cells, which is not balanced by cell proliferation, hence contributing to lung destruction in COPD [24]. In addition, the deficient phagocytosis of alveolar macrophages (i.e., efferocytosis; see above) [56, 57], also contribute to the accumulation of antigenic material that can, in turn, induce and facilitate an autoimmune response [49, 58].

All these pathobiological mechanisms underlie the association between a COPD Th1 driven adaptive immunity and lung tissue destruction, so the severity of the disease at this point is greatly determined by the immunomodulatory capacity of the dendritic cells [44]. It has been proposed that dendritic cells in smokers with normal lung function are partially activated by autoantigens but given that they would lack the co-stimulatory signal (DAMPs), they develop tolerance against these autoantibodies. By contrast in smokers with COPD, dendritic cells are fully activated and thus activate T cells [44, 47].

In severe COPD, it has been shown that CD8⁺ cytotoxic T cell are the predominant lymphocyte type in the lung tissue and the numbers of this cells correlates with the degree of airflow limitation and the severity of emphysema [59-61]. CD8⁺ T cells can attack any cell presenting abnormal antigens via MHC-I molecules by releasing their cytotoxic enzymes and inducing a necrotic or apoptotic process. In the lungs of COPD patients, apoptotic endothelial and epithelial cells increase in relation to smoking exposure and correlate with the number of CD8⁺ T cells [22, 62, 63].

Furthermore, traditionally in COPD it has been considered that CD4⁺ T cells that are mainly polarized toward a Th1 response, producing cytokines which promote transendothelial migration of inflammatory cells. The recruitment and activation of inflammatory cells, macrophages, neutrophils, eosinophils, CD4⁺ and CD8⁺ T cells, and B cells increase as COPD worsens [18, 64].

The presence of B cells, organized in lymphoid follicles, has also been described in the lung parenchyma of patients with COPD [18, 65]. Immunoglobuline analysis reveals an antigen driven selection process that, suggest a process against lung autoantigens, although it is not clear yet which are the antigens associated to these B cell expansion [65]. This adaptive immune response is represented in the Figure 9.

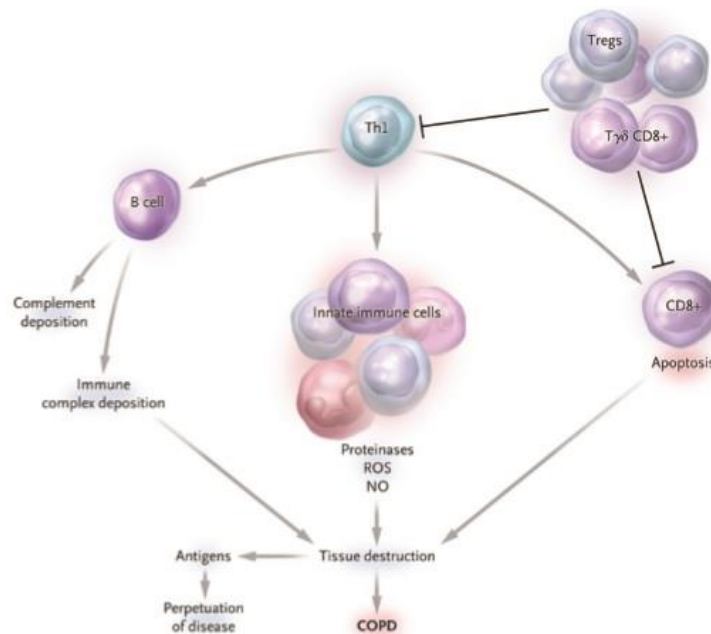


Figure 9: Adaptive immune response in COPD [44].

It has been proposed that genetic predisposition, enhance dendritic cell antigen presentation and that failure to control this adaptive immune response results in severe disease. Supporting this hypothesis is the fact that patients with severe COPD present large numbers of activated oligoclonal Th1 T cells [52, 66], B cells [32, 34] and CD8+ T cells [59-61, 67], which persist after quitting smoking [38] suggesting a self-perpetuating process that might be due to a response to self-antigen, typical feature of autoimmune diseases. Likewise, the presence of sub-epithelial lymphoid aggregates rich in T and B cells, known as “bronchus associated lymphoid tissue, BALT”, correlates with the severity of airflow limitation [18, 68]. The intensity of this immune infiltrate seems to increase with the severity of the disease, see Figure 10 [47].

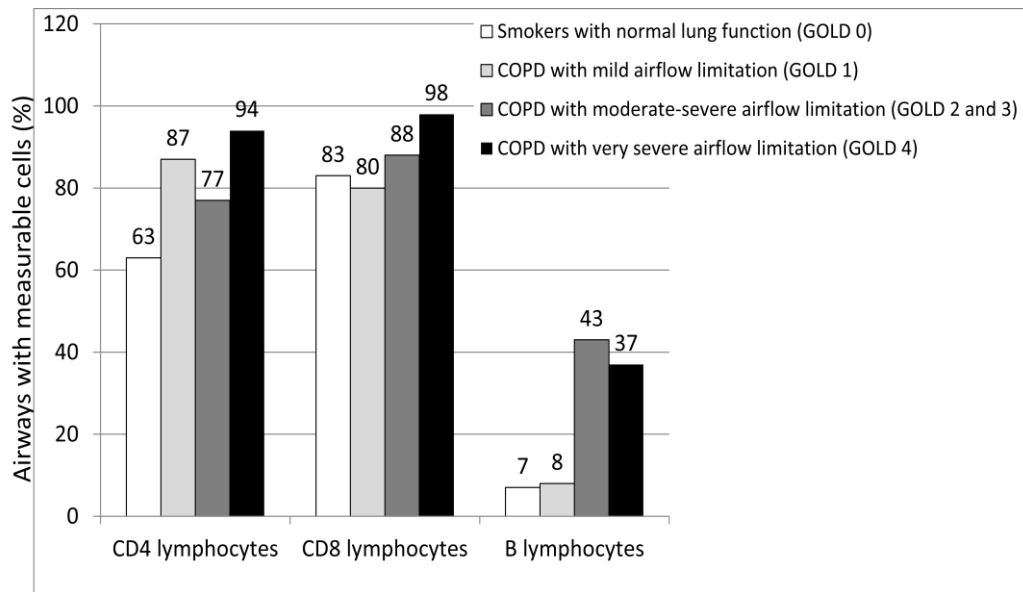


Figure 10: The immune infiltrate increase with COPD severity (GOLD grades) [47].

It is important to note that there are no longitudinal studies investigating the temporal sequence of inflammation in COPD, and that all available studies merge data obtained cross-sectionally. Therefore, the above-mentioned data has to be taken with caution since an equally possible interpretation is that patients with more severe disease were already more inflamed in the initial steps of the disease and that, it was precisely because of this more intense inflammation, the disease progress to more severe forms [47].

1.1.4.2.1 - Autoimmune process

The fact that patients with COPD that quit smoking for more than a decade still present evidence of abnormal inflammation suggest the presence of some form of self-perpetuating mechanism, either due to abnormalities in the resolution of inflammation (catabasis) and/or to mechanisms capable of maintaining the inflammatory response despite that the trigger that originated it, has disappeared, a situation that occurs in autoimmune processes.

In this context, it is worth noting that several mechanism of autoimmunity have been described in COPD and that most of the clinical evidences supporting an autoimmune component in the pathogenesis of COPD refers to patients with severe airflow limitation and emphysema [47]. Following Witebsky autoimmunity postulates [69] a number of

direct, indirect and circumstantial pieces of evidence support the possibility of an autoimmune component in the pathogenesis of COPD.

Direct evidence is provided by mice models injected with antibodies against endothelial cells (or T cells reactive against endothelial cells) which present enhanced apoptosis of alveolar cells and accumulation of CD4⁺ T cells in the lung, as well as emphysema [70].

Indirect evidence is provided by the presence of circulating antibodies against elastin, pulmonary epithelium and endothelium and CD4⁺ T cells that respond to elastin and collagen by secreting IFN γ and IL-10 [71, 72]. Likewise, CD4⁺ T cells appeared to be activated with an oligoclonal TcR that also persist after smoking cessation. Although the specific antigen of this CD4⁺ T cells is still unknown, their oligoclonality suggest specific T cell differentiation.

Finally **circumstantial evidence** is provided by the accumulation of effector memory CD4⁺ CD28^{null} T cells have been reported in patients with severe COPD [73, 74]. This cell population has also been described in several autoimmune diseases and it is interesting to note that these cells display some special pathogenic features, including a lower susceptibility to regulatory mechanisms and lack the co-stimulatory molecule [75].

Infiltrating CD8⁺ cells were found to have increase expression of CCR7 and CD45RA effector memory phenotype in COPD patients [76]. Also mice cigarette smoking models have shown an oligoclonal TcR profile in CD4⁺ T cells that persists after smoking cessation suggesting a specific differentiation process [76, 77]. TcR $\gamma\delta$ T cells are present in the mucosal surfaces of the gut and, in smaller numbers, also in the lungs. Its function is not clear yet but they are increased in BAL from smokers with normal lung function (vs. non smokers) but not for COPD patients [78].

Recently, it has been shown a Th17 profile in CD4⁺ and CD8⁺ T cells in patients with COPD [79, 80]. B cell infiltrate has also been described in the lung tissue of patients with severe COPD, with increased production of B cell activating factor (BAFF), a crucial mediator of the persistent immune activation in autoimmune disorders [81]. This B cells present immunoglobulins with variable regions suggesting an antigen driving in

situ selection process. Also CXCL13, TLRs and lymphotoxin receptor signaling is overexpressed in severe COPD, indicating a lymphoid follicle neogenesis [82].

Finally, a blunted regulatory T-cell response to tobacco smoking has been observed in COPD patients in the form of lower numbers of TCD4⁺CD25⁺ FOXP3 cells in these patients as compared to smokers with normal lung function [47].

1.1.4.3 - Oxidative stress

Another important pathobiological mechanism of emphysema is oxidative stress, which is intimately linked with inflammation, activation of proteases, inactivation of antiproteases, and apoptosis, all of which play a major role in the pathogenesis of COPD.

Several pieces of evidence support a role for oxidative stress in the pathogenesis of COPD, including the increased expression of markers of oxidative stress both in the lung tissue as well as in the systemic circulation [83]. An animal model of a mouse deficient in the transcription factor NRF2, which regulates multiple antioxidant enzymes, develops severe emphysema, hence showing a direct relation between oxidative stress and the destruction of the alveolar tissue [84]. Another animal model of emphysema shows co-localization of oxidative stress and apoptosis markers in the alveoli. Also the inhibition of the oxidative stress by administration of superoxide dismutase abrogated alveolar cell apoptosis and emphysema [23].

There is evidence of mitochondrial dysfunction and accumulation of macromolecular imprints of oxidative injury with aging. In this context, it is of interest that *in vitro* hyperoxia increases free radicals stress and leads to molecular changes typical of aging and, conversely, increases in antioxidants increase life span of cultured cells [85]. Mitochondrial dysfunction of aging can also be an important factor for the development of COPD.

1.2 – LUNG Regeneration-repair

1.2.1 - Human airway epithelium

The human airway epithelium is composed of 4 major cell types: ciliated cells, secretory cells, intermediate cells and basal cells, see Figure 11A [86]. Ciliated and secretory cells are terminally differentiated cells joined by tight junctions that form a relative impermeable barrier central to pulmonary host defense. This physical barrier protects the airways and provides the mucociliary escalator function that clears the respiratory tract from inhaled pathogens, particulates, and other foreign material [87]. Basal cells are keratin 5 (KRT5) positive cuboidal cells that are tightly attached to the basement membrane (Figure 11B) and play an essential role as progenitors of the ciliated and secretory cells [88, 89]. Intermediate cells (also known as “parabasal” and “undetermined” cells) are located between the basal cells and differentiated cells and are believed to represent basal cell derived precursors of ciliated and secretory cells (Figure 11C)[90].

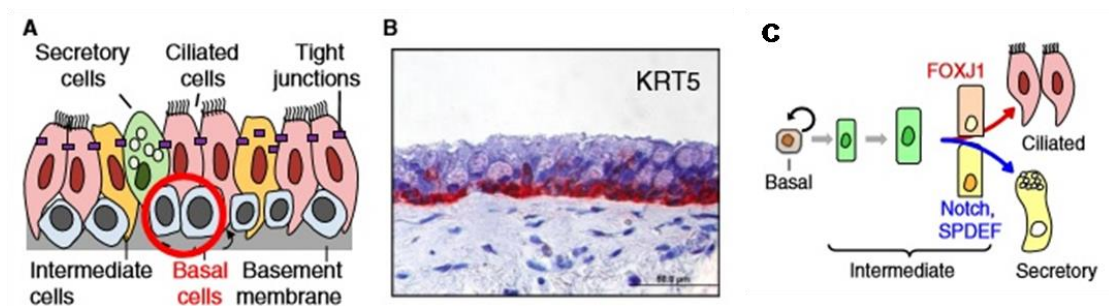


Figure 11: Structure of human airway epithelium [86].

The composition and proportion of these different cell types vary along the airway epithelium. The ratio of ciliated to secretory cells is tightly controlled around 10 to 1 through the tracheobronchial airway, but this proportion decreases in the small airway. In the larger airways the mucus producing goblet cells constitute the predominant secretory cells, while in the small airways the secretory population change to non-mucus producing cells producing secretoglobulins and other proteins with antimicrobial, anti-inflammatory and antioxidant properties, the “Clara” cells [91].

Basal cells are a population of progenitor cells that drives both homeostasis of the normal epithelium and its orderly regeneration after injury [87]. The proportion of basal cells in the airway epithelium is highest in the large airways and progressively decreases

going down the tracheobronchial tree, representing an average of 30% in the upper respiratory system down to 6% in the small airways [92]. In the trachea, basal cells are located in the submucosal glands (SMG) whereas in the bronchi they are located in the intercartilaginous area (see Figure 12). A subset of the Clara cells in the small airways function as progenitor cells, the variant Clara cells [93]. In the alveoli, the alveolar epithelial cell type 2 (AEC2) are the progenitor population giving origin to the alveolar epithelial type 1 cells (AEC1) specialized in gas exchange (see Figure 12) [93]. This later population is not completely undifferentiated since AEC2 also expressed genes associated with specialized functions, such as surfactant protein synthesis [94].

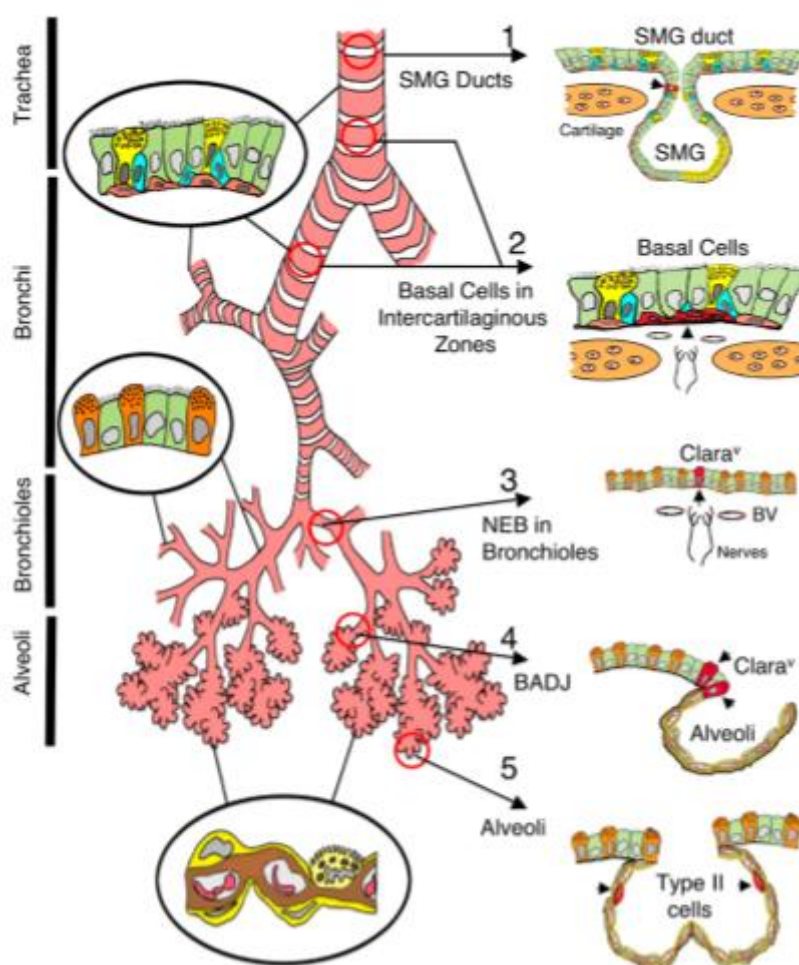


Figure 12: Progenitors cells in relation to lung structure [93].

Because stem cells are classically defined on the basis of their potential to indefinitely self-renew and differentiate, an argument could be made in support of referring to all these populations as stem cells. Yet, it is preferred to call them as progenitors rather than stem cells, as their self-renewal capacity may be transient and they differentiate

into one or more distinct lineages, but it is unclear that they could regenerate all lung cell types [95].

Under physiological conditions the normal adult human airway epithelium turns over relatively slowly, approximately every 1 to 4 months. Basal cells are relatively quiescent, and only few intermediate cells can be observed [92, 96]. In response to injury, airway basal cells proliferate forming clonal patches and expanding the pool of intermediate cells regenerating a normally differentiated epithelium.

However under the presence of several microenvironment factors, such as cigarette smoke, this process could generate an altered phenotype [91, 97-100]. Also lung regeneration capacity of self-renewal from differentiated cells by a dedifferentiation (lost of differentiation and re-differentiation) or trans-differentiation (directly differentiation into another cell type) is strongly influenced by the particular kind of injury sustained [101]. This phenotypic plasticity is not unique to the lung and dedifferentiation or trans-differentiation apparently occurs quite frequently in response to adverse events in various tissues, such liver or pancreas (Figure 13)[95]. In addition, lung regenerative capacity is higher than in other organs as brain or heart but not as good as for the blood or the intestine [95].

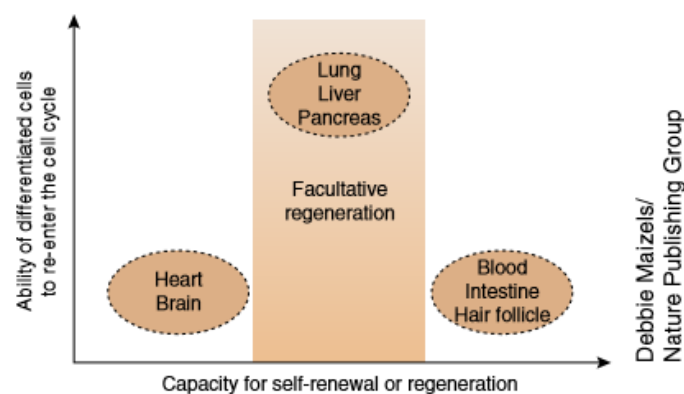


Figure 13: Representation of the regeneration capacity of several organs [95].

Although relatively little is known about the plasticity of human airway epithelial cells *in vivo*, mouse studies suggests that many, if not most, lung epithelial cell lineages have the capacity to re-enter the cell cycle and replace lost cells through their ability to proliferate [95]. Also, there are evidences of the capacity of a phenotypic swift of differentiated cells. In some studies it has been shown that this phenotypic switching involves a process of de-differentiation to a less specialized, multipotent intermediate,

followed by a re-differentiation. Other studies have not been able to identify the precise steps involved and it remains possible that this plasticity was a direct process and didn't involve an undifferentiated intermediate [87].

The mechanism that controls the specificity of basal cell differentiation process into ciliated or secretory cells is only partially understood. Studies of the transcription factors involved are based principally in mice models. Ciliated cell differentiation process is governed by FOXJ1, multicilin, cyclin O, Myb, and RFX family proteins [102]. The differentiation to the secretory lineage is mediated by the Notch pathway and for the mucus producing cells that transcription factors SPDEF and FOXA3 are needed [103].

1.2.1.1 - Airway epithelium in COPD

Basal cell hyperplasia is one of the first abnormalities seen in the airways of smokers [86]. With the development of COPD, important changes in the airway epithelium occur (see Figure 14), including squamous metaplasia and replacement of differentiated ciliated and secretory cells with squamous deficient cells, not present in the normal airways [86]. This results in a shortening of cilia and altered ciliary beating, which reduce the efficiency of the mucociliary escalator to eliminate respiratory pathogens and foreign particles. The secretory cells suffer a mucus cell hyperplasia that in small airways is paralleled by the loss of protective non-mucous secretoglobin secreting cells that could lead to airway obstruction. The reduced expression of the polymeric immunoglobulin receptor/secretory component in the small airway epithelium, which normally transports secretory immunoglobulin A to the mucosal surface to sample pathogens present in the airway lumen, correlates with the severity of airflow limitation in smokers with COPD [104]. There is also an increase airway permeability, through the broad suppression of the components that maintain junctional barrier assembly and integrity, and induces some features of epithelial–mesenchymal transition (EMT)[105].

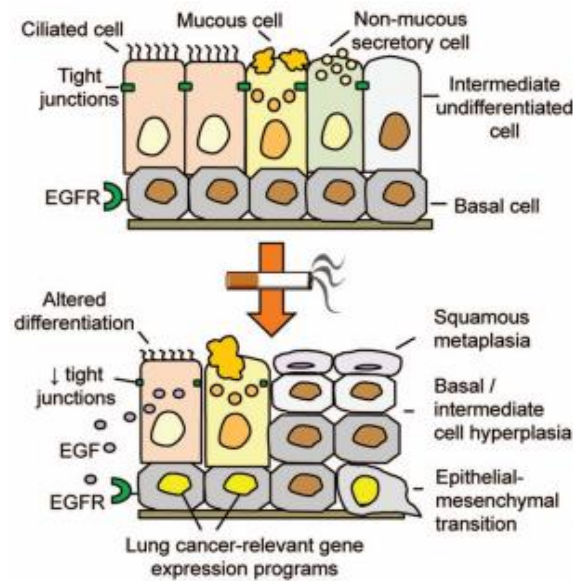


Figure 14: Basal cell hyperplasia in the early abnormalities of smoker airways [91].

There is not a well established pathobiology process that leads to these alterations in the epithelium. As reviewed below, several pieces of evidence support the concept that airway basal cells are the origin of the earliest molecular and histologic changes in the airway epithelium of smoking-induced lung diseases [86, 91].

Basal cells are directly exposed to the environment, and can influence the surrounding cells by secreting polypeptides. Various cytokines and growth factors, such as IL1 α , IL-33, and TGF- β , have been found to be up-regulated in airway basal cells of smokers and patients with COPD. This suggests the generation of a proinflammatory microenvironment that alters epithelial–mesenchymal interactions that can be relevant to the pathogenesis of COPD [91].

Another potential mechanism of smoking induced epithelial alterations points to the epidermal growth factor receptor (EGFR) pathway in the reprogramming of basal progenitor cells. EGF and AREG (both ligands of EGFR) are up regulated in ciliated cells of smokers which, in combination with the decreased junctional barrier integrity caused by smoking, can potentially interact with EGFR-expressing basal cells inducing chronic stimulation (see Figure 14). *In vitro* exposure of differentiating basal cells to EGF recapitulates the major pathologic phenotypes observed in the airway epithelium of smokers *in vivo* [91, 105], suggesting that the EGFR axis is an important pathway in the initiation of the pathologic disorders that characterize the airways in COPD.

COPD associated changes in the airway epithelium contribute to lung inflammation. The loss of Clara cells in the small airways leads to a decrease in the production of the anti-inflammatory protein secretoglobin [97, 106]. In addition, the squamous cell metaplasia increases the production of the pro-inflammatory cytokines IL-1 α and IL-1 β and decreases the production of antimicrobial factors such as SLPI that limits the damage of the lung by inhibiting the neutrophil elastases [107, 108]. Further, the disorganization of the junctional barrier results in increase permeability to microbial components and cigarette smoke components to diffuse through the epithelial barrier and activate the inflammatory cells in the airway mucosa [100].

1.2.1.1.1 - Similarities of COPD lung epithelium and aging

It has been proposed that COPD can represent an accelerated aging of the lung [109]. Like COPD, aging is also associated with decreased epithelial barrier function, abnormalities in respiratory cilia structure and function, and reduced antimicrobial/anti-inflammatory protein production by epithelial cells, including SLPI. Likewise, aging is associated with increased numbers of macrophages and neutrophils that are deficient in their capacity of host defense [110, 111]. In COPD there is chronic low grade inflammation that leads to innate immunity dysregulation and a situation of under-responsiveness to pathogens, which is similar to the immune senescence phenotype of the elderly. Smoking is also associated with induction of senescence of the structural cells of the lung, and may also cause premature aging of the innate immune cells [112]. In addition, telomere shortening in circulating leukocytes has been observed in COPD patients. Further, as well as aging-associated immunosenescence contributes to an increased susceptibility of the elderly to malignance, the suppression of the innate immune mechanisms in COPD patients may explain why COPD is associated with increased risk of lung cancer [113].

1.2.1.1.2 - DNA methylation

Changes in DNA methylation have been described in relation to cigarette smoke, and DNA methylation is known to influence the renewal and differentiation capacities of adult tissue stem cells [114-116]. In fact, basal cells from smokers and patients with COPD are limited in their capacity to generate a fully differentiated epithelium, and

their methylation profile is altered. This opens the possibility that the lung microenvironment of smokers and, particularly, patients with COPD alter the capacity of stem/progenitor cells to maintain a normally differentiated epithelium [117].

Since, as discussed above, the genetic background of smokers seems to play an important role in modulating the risk of developing COPD, and basal cells plays a central role in the early pathogenic changes that characterize the disease, it has been hypothesized that this genetic susceptibility could be related with the biology of basal cells. In fact, several dysregulated genes in basal cells from patients with COPD have been already identified. They are located to 19q13.2, a known COPD risk locus. Particularly four of these genes (EGLN2, LTBP4, TGFB1, and NFKB1B) have been linked by genome-wide association studies or candidate gene studies to COPD risk [86, 118, 119].

1.2.2 - Adult stem cells

Adult stem cells are defined as infrequent, morphologically unrecognizable cells endowed with the potential to maintain and replenish their own population and generate large numbers of functionally differentiated progeny for replace senesce and damage cells [120]. Stem cells are a hierarchical population that forms a continuum of stem and transit amplifying progenitor cells of progressively restricted proliferative and differentiation potential that in turn give rise to functionally differentiated cells (Figure 15) [121]. Generally stem cells are in G0 state and descendent lineages are derived from a small number of active clones, thus ensuring the preservation of a stem cell reserve while mitigating the risk of error-prone stem cell replication and transformation [122, 123].

According to this paradigm, stem cells divide asymmetrically to replenishing the more committed transit amplifying progenitor cell compartments in order to meet the increased demand for differentiated cells following tissue injury, while simultaneously retaining the ability to divide symmetrically to expand stem cell numbers and homeostatically regulate stem cell pool size [121, 124].

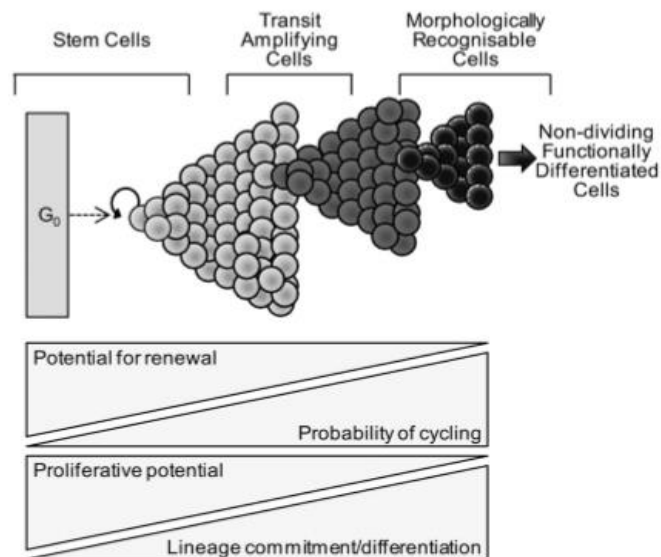


Figure 15: Proliferative - differentiation potential of the stem cells and their hierarchical asymmetrical division system [121]

Embryonic stem cells are totipotent, they can proliferate indefinitely and differentiate into all cell lines, but the adult stem cells may have less proliferation and differentiation capacities. Adult stem cells usually are multipotent giving arise to a limited number of different cell lineages with their normal environs [125]. However recent studies have shown that tissue specific stem cells have grater plasticity than it has been thought before [126-128].

The definitions and the hierarchical structure of the adult stem cells have not yet been standardized. This difficult the investigation of their proliferative-differentiation potential and the comparison of different studies. Mesenchymal stem cells (MSCs) are multipotent cells with the capacity of differentiate into the connective tissue cells. MSC can be isolated from several tissues, but bone marrow is their main reservoir and it is thought to be the main source of these cells for the population of the MSC in the organs [129, 130]. It is unknown whether MSC isolated from tissues reside and self-renew locally or whether they are recruited from bone marrow [131-133]. The lack of specific markers and standardization of growing cultures methods difficult again the comparison between studies. MSC are thought to be the adult stem cell with the higher multipotentiality, but it is still controversial whether tissue resident MSC have the same properties than bone marrow MSC [126-128].

Adult stem cells reside in specific anatomical sites termed *niches* that preserve their potential, regulate their proliferation and inhibit their differentiation preserving their

stemness throughout life [134]. The resident somatic or adult stem cells are responsible for replacing naturally apoptotic cells (homeostasis) or as a response to injury. The decision to lie dormant, self-renew, or differentiate is a consequence of the diverse cocktail of signals provided by the stem cell niche. How these niches develop and establish themselves is still an area of active research [135]. There is a great diversity in the niche design, since quiescent individual cells attach to the basal lamina (muscle-skeletal system) to small substructures establish to house clusters of stem cells such as subventricular and subglandular zones of the brain or the hair follicles [136].

Recent studies propose that the niche not only affects the homeostatical pool of the stem cells, but it also affects profoundly the functionality and behavior of the cells [134, 137, 138]. The specialized niche cells and the extracellular proteins provide the essential signals of the niche. In addition the extracellular matrix is highly dynamic, changes in the microenvironment induce rapid remodeling of the matrix [139]. In this context the microenvironment in which the MSC reside acts as a director that could polarize the MSC into a proinflammatory MSC1 population or immunosuppressive MSC2 phenotype [140].

Trans-differentiation is the process by which a circulating cell engrafts into another organ and assumes some of the phenotypic traits of that organ. But only in a few cases it has been reported that the engrafted cells becomes a stem cell of the new organ. This would require the isolation and transplantation of single cells with clonogenic potential that produce functional cells. There is still controversy on this definition as some researchers added the quality of occur “naturally”, not after severe organ damage, while another part argue that it is precisely because of severe organ damage that trans-differentiation occur when an organ’s own regenerative capacity is overwhelmed [141]. Recent studies have eliminated the theory of the fusion of the stem cells with the differentiated organ cells instead of the trans-differentiation by studies of sex mismatch transplant receptors [142, 143].

The lung is an organ continuously exposed to a variety of potentially injurious pathogens and noxious environmental agents that necessitates cellular turnover and renewal. It was thought that the MSC that participating in lung repair derive from the bone marrow, but a recent study has demonstrated the existence of MSC engrafted in the adult lung by studies in sex mismatched lung transplants [144].

1.2.2.1 - Mesenchymal stem cells

MSCs are multipotent stromal cells that can be isolated from numerous tissues, the most study sources being the bone marrow, skeletal muscle, amniotic fluid, and adipose tissue. They are plastic adherent cells that exhibit trilineage differentiation into adipocytes, chondrocytes, and osteoblasts [145]. MSCs can be purified based on their ability to adhere to plastic. They express several mesenchymal markers CD105, CD90, CD73, CD13, CD166, CD44, CD29 and do not express hematopoietic and endothelial markers CD45, CD31 and CD34 [146].

A unique feature of MSCs is their ability to produce an immunosuppressive effect both *in vitro* and *in vivo*, inhibiting T-cell proliferation and supporting the development of T regulatory cells. Several studies has reported the production of a range of immunomodulators as transforming growth factor β (TGF- β), prostaglandin E 2 (PGE2), IL-10, nitric oxide, and indoleamine 2,3-dioxygenase, as the paracrine mediators of this immunosuppressive mechanism. MSC mediated immunosuppression could also result from the recruitment and modulation of other immune cells. In particular it has been shown that MSC affects dendritic cell maturation modifying their ability to stimulate allogenic T cells [147].

1.2.2.2 - MSC in the lung

MSC in the lung were first describe in BAL samples from transplanted patients as CD105+ CD90+ and CD73+ cells, negative for hematopoietic markers, exhibiting clonal proliferation and ability to differentiate into adipocytes, osteocytes and chondrocytes [144]. Next MSC were successfully isolated and culture from human lung tissue [148, 149]. More recently a study in sex-mismatched lung transplanted patients for more than 10 years, it has been demonstrated their homing in the lung tissue, being most of the MSC from the donor and only a small population derive from the patients [150].

It is still unknown if these lung resident MSCs represent an endogenous MSC population or more lung specialized stem cell. MSC are thought to have great immunomodulatory properties in the transplanted lung, but their presence in fibrotic lesions could indicate polarization to a more myofibrotic progenitor [121]. The international criteria for MSC definition is not specific enough to differentiate between

MSC and closely related populations such as fibroblast [149], being difficult to define the type of cell involve in different studies. Transcriptional profiling and bioinformatics are emerging as potentially useful tools for the categorization of MSC population [151].

A recent study found MSC in lung tissue and in BAL from lung transplant patients but no in healthy subjects. BAL MSC from transplanted patients express an atypical immunophenotype characterized by reduced multipotency, diminished colony forming efficacy and altered transcription profile, as compared with lung tissue MSC. These BAL MSCs fail to fulfill some of the criteria for MSC definition but express the typical MSC transcriptome and share high level of similarities with lung tissue MSC. It is possible that this population derives from dysregulated lung tissue MSC that migrate to the alveolar space. These finding support the theory of a MSC heterogeneous community with distinct but phenotypically similar populations. Whether these cells are hierarchical organized or represent completely distinct populations remains to be determined [152]. Up to date no studies have investigated the functionality and presence of lung MSC in patients with COPD.

1.2.2.3 - Sphere formation as a source of stem cells

A new technique for the isolation of stem cells, based on their ability to form 3D spheres, has emerged during the last decade. Sphere forming cells are putative immature regenerative cells which spontaneously migrate from small pieces of tissue (explants). They were first describe in cardiac samples in 2004 and were called cardiospheres [153]. These cells are clonogenic, express stem and endothelial markers and appear to have properties of adult cardiac stem cells because they present long-term self renewal and can differentiate *in vitro* and *in vivo* to the majority of heart cell types. Since then, several groups had reproduced similar results and validate this new methodology for the isolation of stem cell from cardiac biopsies [154-157].

The method of growing the cells as three dimensional cardiospheres seems to recapitulate a stem cell niche like environment, favoring cell survival and enhancing their functional properties for transplantation. In comparison with cells growing in traditional monolayer cultures, cardiospheres show enhanced expression of stem related

factor and extracellular matrix proteins, which translates in improved heart function after transplantation [158].

Any of the available methods for the isolations of stem-progenitor cells have the difficulty of how to expand this population *in vitro* while maintaining their multipotent capacity. To overcome this limitation, a repeated sphere formation strategy (with an intermediate adhesion phase) was developed. Compared to the adhesion phase (primary spheres), secondary spheres recover the expression of stemness genes like Oct-4 and c-kit. In addition, secondary spheres showed higher differentiation potential and, when transplanted into infarcted myocardium, engrafted robustly, improved ventricular function and reduced infarcted areas [159, 160].

Several recent studies that used sphere 3D culture to isolate BM-MSc showed that isolated cells present high anti-inflammatory capacity, express increased levels of anti-inflammatory and anti-cancer proteins, and have increased suppression of the inflammatory response both in co-culture with LPS activated macrophages as well as in a mice model of peritonitis [161]. This 3D culture method has also been used as a tool to pre-activate anti-inflammatory MSC for use in clinical applications [162, 163]. Also the 3D culture has been shown to be pro-angiogenic and increase endothelial cell proliferation and survival [164].

So far, however, only one study has previously tried to obtain stem cells from lung tissue using the sphere 3D culture method [165]. Results showed a epithelial phenotype polarization and a characteristic secretome distinct from adherent cultures.

1.2.2.4 - Animal models that use MSC cell therapy

Animal models of fibrosis (bleomycin induce), COPD-emphysema (smoke-induce) and microbial inflammation (LPS) showed that treatment with MSC ameliorates the injury-induced pathologic changes [166-169]. Little is known, however, about the mechanisms involved, which may be different for each disease model. A couple of them have however been proposed. The first, would be the release by MSC of a wide range of paracrine factors that have potent immunosuppressive activity [166]. The second, can be the MSC mitochondrial transfer to the epithelial and alveolar cells in order to, restore their impaired activity [170, 171].

In any case, MSC obtained from BAL samples and instilled intratracheally into healthy mice showed alveolar engraftment [166, 168, 172].

1.2.2.5 - Cell based therapies in human patients

Based on their anti-inflammatory properties MSC are currently being evaluated in several clinical trials for a variety of autoimmune disorders such as Chron's disease, multiple sclerosis, diabetes mellitus and acute graft *vs.* host disease, with promising results [173, 174]. Due to their natural ability to migrate to sites of injury or inflammation, MSCs are also being develop as a tool to deliver specific molecules to a localized area [175].

In respiratory medicine, there is one trial with *ex vivo* expanded adult human MSC administrated intravenously for the treatment of patients with COPD with the aim of delaying disease progression by reducing lung inflammation [176]. However further studies are necessary to evaluate in depth the efficacy and safety of MSC cell therapy in respiratory diseases [177].

1.3 - NETWORK MEDICINE

Human biology is extremely *complex* because it is *multilevel*, *redundant*, and *dynamic*. A *complex* system is a collection of linked individual elements with so-called *emerging properties* that cannot be attributed to each element separately. Human health is an emerging property of the complex system that the human body is, and human diseases are also an emerging property of the system when one or several of its components are not working properly. *Multilevel* means here that it involves the interactions between molecules, metabolites, nucleic acids, proteins, cells, tissues and organs. *Redundancy* means that, often, there are several processes implicated in the same biological response [178]. This facilitates a better control both within and between biological levels. It is continuously sensing the environment and has the ability to vary in response to the changes. Finally, *dynamic* means that the system is constantly influenced by the changing conditions of the (micro) environment [178].

A plane is an example of a (mechanical) complex system. It is composed of many different elements (nodes of the network system), such wings, engines, wheels and so on. that are linked (i.e., related) in a specific manner (each plane has two wings, one in each side, a plane with one wing would not fly). The plane has one emergent property: it flies. Yet none of the individual elements can fly on its own, and it is necessary that the essential elements of the system are linked in the appropriate manner [178]. A complex system can have, however, redundant components (e.g. several engines) and non essential parts (e.g. seats). Engineers know very well how the different components of the system need to be connected for the plane to fly [178]. Biologists are far from there in most if not all biological systems. Traditionally, biological complexity has been investigated using a reductionist approach, i.e. studying the structure and function of isolated genes, proteins or cells. This strategy has been successful in many aspects but now it is essential to provide a more general and integrated overview of the biological system considered if we are going to develop novel, more effective and safe therapies [178]. *Systems biology*, and its human counterpart, *network medicine* are novel research strategies that sought to provide a better understanding of human biology complexity both in health and disease.

In essence, systems biology offers the potential to deliver an integrative and dynamic view of complex biological conditions, rather than focusing on a specific molecule at a given time. The principal feature of systems biology is to integrate data from different

levels (genes, proteins, molecules, cells, tissues or organs) and develop a mathematical (i.e., engineer like) model of the system that explains its emerging properties and the response to perturbations [179, 180]. According to Kitano [181], one of the founders of systems biology, this approach requires the understanding of four key properties of the system. First, the *structure* of the system, which includes the network of gene interactions and biochemical pathways and how intracellular and in multicellular systems modulate their properties. Second, the system *dynamics* that explains how the system behaves over time in response to perturbations. Third, the *control methods* that sought to minimize malfunction of the system, which can therefore be a potential target for therapeutic treatments. Fourth and final, *design* methods which can be used to modify and/or construct biological system directed for specific purposes.

To achieve these goals, systems biology usually follows an iterative process. First, it is necessary to generate a multi-level database from high-throughput omics in one or more biological samples and phenotypically well characterized animals. Next is the analysis of the data with the aim of generating a predictive mathematical model of the system. The model is then used to formulate a hypothesis on the mechanism and pathways involved in the process studied. These novel hypotheses are tested with perturbation experiments *in silico* (computer modeling), *in vitro* (cell culture) or *in vivo* (animal models). The experimental responses observed are finally compared with those predicted by the mathematical model and discrepancies are used to adjust the model. This process should be iterated until the predictive model fits well enough with the observed response [182].

Human health and disease are emergent properties of a extremely complex system (the human body) that relies on the interaction of many components, within and across cells and organs (i.e., *interactome*). The complexity of the human interactome is daunting; 25000 protein coding genes, 1000 metabolites, an undefined number of proteins and RNA molecules and more than 10000 cellular components. The interconexions of this system implies that the impact of a specific abnormality is not restricted to the activity of that individual component of the interactome, but can spread along the different links of the network and alter the activity of other components which will eventually modulate the final phenotype (e.g., the clinical presentation of a disease or the response (or absence of response) of a given disease to a specific therapeutic intervention). In

essence, network medicine define human disease as a consequence of one or more biological networks that have become disease perturbed through genetic and/or environmental pathogenic changes [183].

The actual concept of network medicine has evolved the original concept of a gene as the determinant of the phenotype. As Figure 16 [184] illustrates, a gene is not longer the single determinant of a phenotype (the traditional concept) but just a DNA sequence that codes for a protein, whose final function is modulated by many biological networks (in turn influenced by environmental conditions) that, eventually, contribute to a certain phenotype [184].

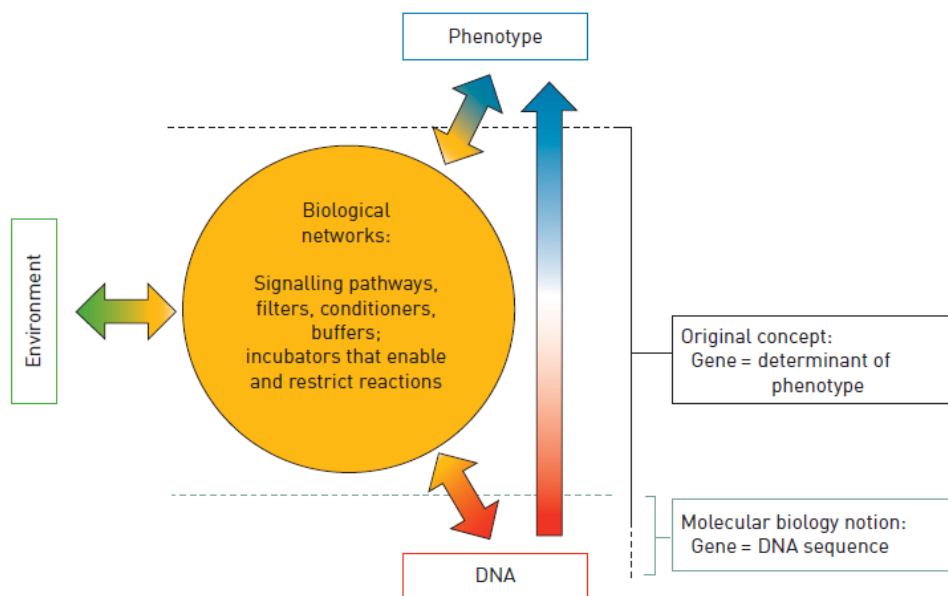


Figure 16: Network medicine evolution of the relation between gene, phenotype and environment [184, 185].

Figure 17 [185] presents a pictorial representation of the multi-level components of human biology (specifically referred here to COPD) in a four story building. Traditionally, clinical practice focuses on the clinical network (blue level) where patients often suffer several simultaneous diseases or *comorbidities*. Below this clinical level, there is a biological level (orange) and, in the basement of the building, a genetic level (yellow); these two levels had been the traditional focus of biological research. In the roof there is a environmental network (green) that represents all the factors that could influence on human health (typically investigated by epidemiologists).

This environmental network is also called *exposome* and, ideally, it takes into account a wide spectrum of exposures (diet, dietary supplements, food additives, pesticide residues, microbial organisms and infections, geophysical exposures, environmental

pollution, smoking, alcohol consumption, exercise, infections, vaccinations, occupational exposures, consumer products, therapeutic drugs, severe stress, etc.) a individual can be exposed to, the time of the exposure and the type of response to the exposure (chronic or acute). In contrast to genome, the exposome is highly variable and dynamic and evolves throughout life of an individual [186, 187].

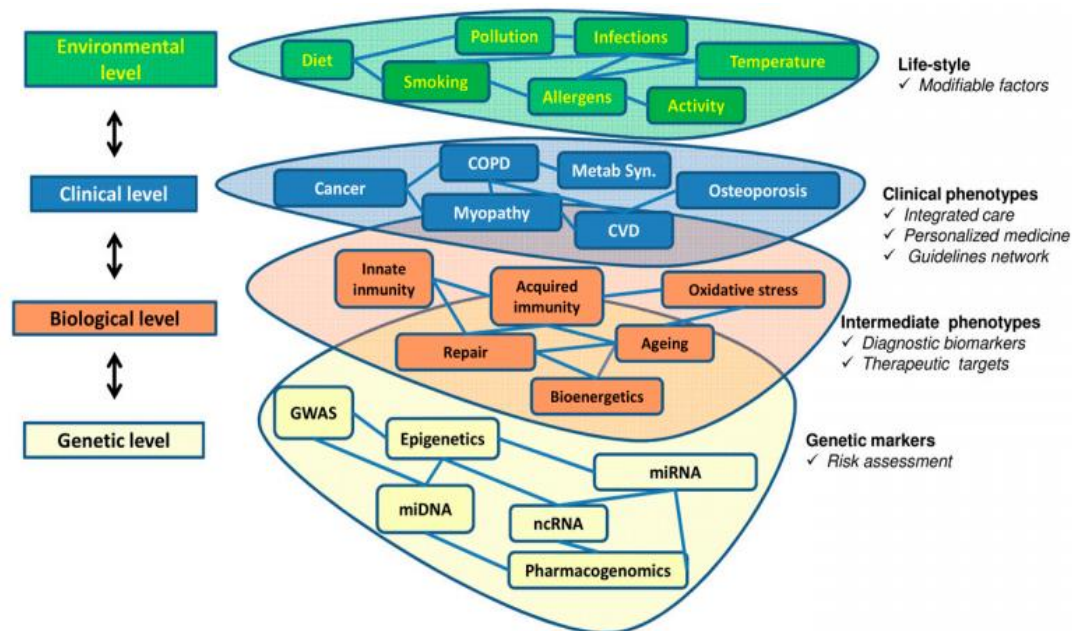


Figure 17: Multi-level components of network medicine approach to COPD [185].

Changes in the environmental level could affect to the genetic level, through so-called epigenetics. Therefore this building is complex at each level but also the interactions between levels are complex. Finally, another important concept is its dynamic component changing with time [185]. This Figure 17, therefore, illustrates another important characteristic of modern network medicine approaches: the need of multi-disciplinary cooperation.

Each of these four levels can produce clinical information of potential relevance. At the genetic level, the identification of genes associated with the disease can help to determine the future risk of a patients, the prognosis of the disease or a possible response to a given therapy [185]. The biological level can provide information of the biological process associated to a particular disease feature (i.e., end types) that could be used to asses and monitor patients [188]. At the clinical level a deeper understanding of the relationship between comorbidities can facilitate better strategies for integrative care

[189, 190]. Finally the environmental network will promote healthier life-styles and preventive measures.

This network perspective has direct implications for the understanding of COPD, since a disease phenotype is rarely the consequence of an abnormality in a single component of the system (no matter what level). Rather, it very likely reflects various pathobiological processes that interact in this complex network [178].

1.3.1 - Network analysis

A network is a useful tool to represent graphically a complex system. In a network the different structural elements are represented as nodes, and their structural and/or functional relationship as edges (or links) [191]. Depending on the research question of interest, nodes could represent genes, proteins, diseases, people, environmental factors or any other element of potential relevance for a better understanding of the system/disease. Similarly, the connection between nodes (links or edges) can represent functional or structural interactions, co-occurrences of diseases, environmental perturbations (e.g. smoking), sharing genes or proteins or any other type of relationship. Further, edges can have directionality that indicates what is the direction in which one node relate or influence other. Importantly, as the reader may have already guessed, there is not a single, universal, predefined network. On the contrary, the researcher customizes the characteristics of the networks of interest depending on the specific research question being investigated.

Laszlo Barabasi, one of the founders of the network medicine, proposed the term *diseasome* to describe the network of human diseases. In the *diseasome*, nodes are diseases, and two diseases are linked if they share genes, proteins, regulatory or metabolic components. This approach has illustrated that most human diseases that are treated separately are not really independent (see Figure 18) [192] [193].

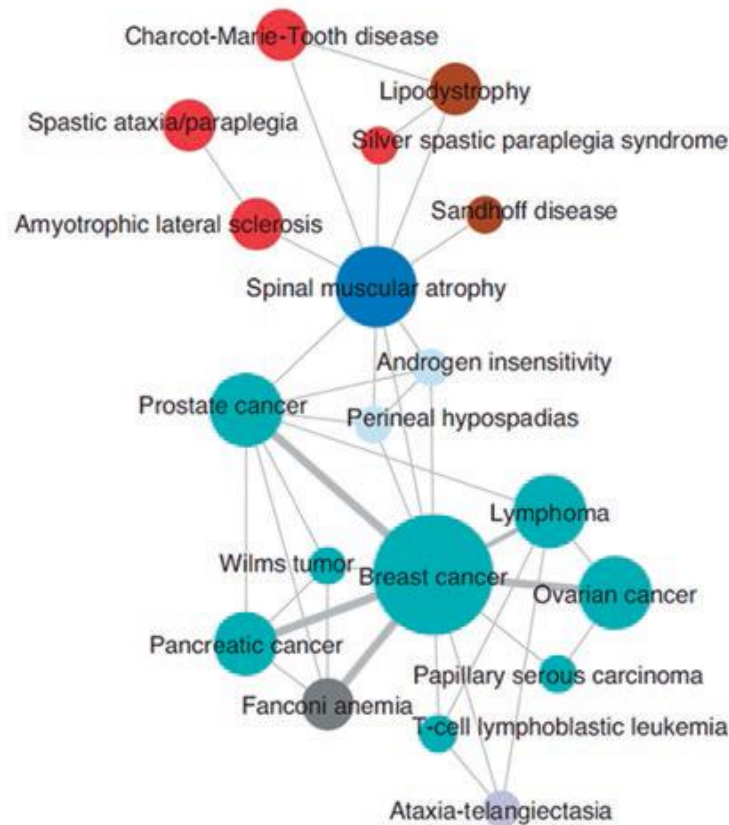


Figure 18: Enlarged part of the diseasesome network representing diseases by nodes and shared genes by edges, image modified from [193].

Barabasi *et al.* showed that most biological (and other) networks have a so-called scale free structure [193]. As shown in Figure 19 [194], scale free networks are characterized by having the majority of their nodes connected to other nodes by a relatively small number of links, whereas a few nodes are highly connected and are called *hubs* [195]. This is very different from a Poisson network where the majority of the nodes have similar amount of links. This distribution makes scale free network differentially sensitive to damage, which means that in front perturbations in a peripheral node, the network is very likely to continue working without problem, whereas damage of a hub could affect the functionality of the entire network [196].

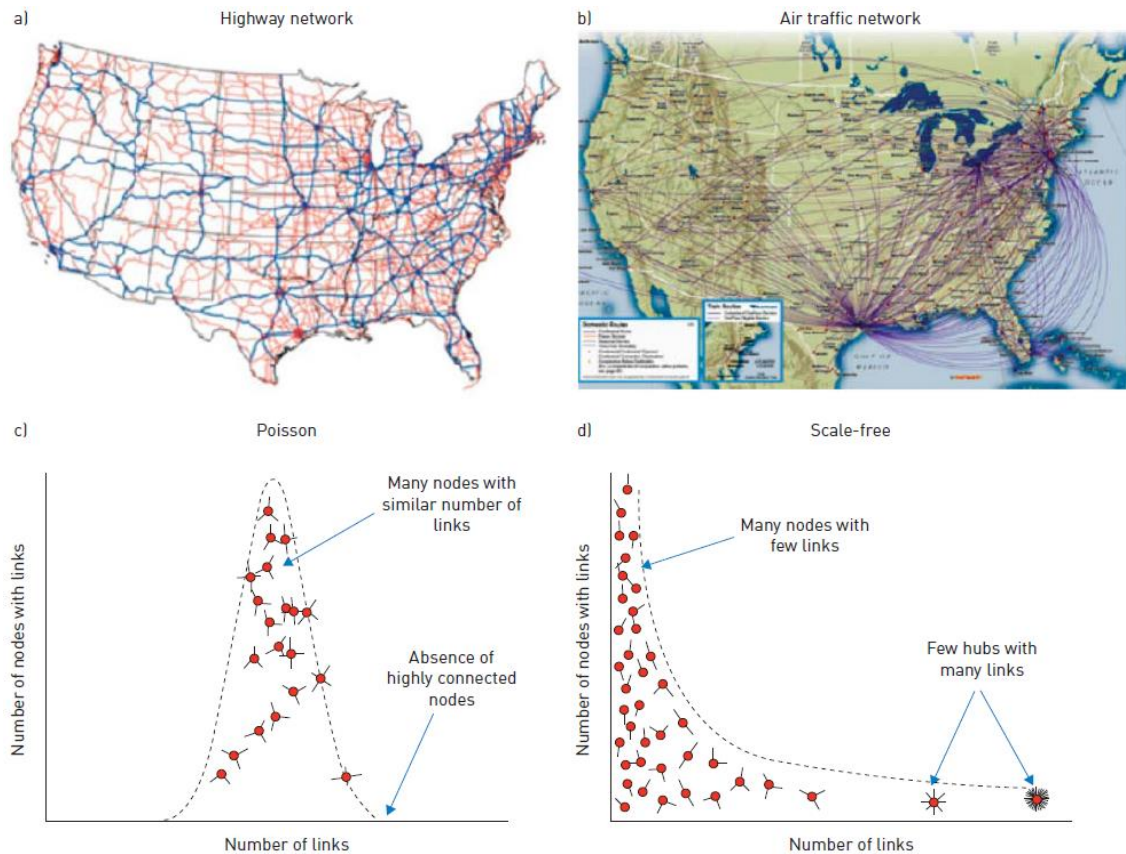


Figure 19: Poisson and scale-free network distributions [194].

Interestingly, non-essential genes are located in the functional periphery of the network and usually do not encode hubs, while essential genes encoded hub proteins and play a central role in the dynamics of the network. Of note, hub genes are expressed widely in most tissues [193, 194].

Finally, the disease module hypothesis proposes that the cellular components (genes, proteins, metabolites) of a disease segregate into the same region (or neighborhood) of the human interactome [197-199]. Disease modules can be identify by combining high-throughput “omics” results and bioinformatics analysis [183]. Network based location of each disease module determinate its relationship to other diseases and diseases with overlapping modules show significant co-occurrence [197].

The human disease network illustrates the potential of network medicine to explore both the molecular pathways of a particular disease and the molecular relationships between apparently distinct phenotypes. Furthermore, network medicine can facilitate the identification of better and more accurate biomarkers and can lead to a more accurate classification of disease phenotypes [183].

1.3.2 - Network medicine in COPD

Network analysis is in its early steps, but there are already a few studies on respiratory medicine in general and COPD in particular. Several of them have focused on establishing molecular relationships between comorbidities frequently occurring in patients with COPD. For instance, the prevalence of the comorbidities and their relationship with mortality in COPD patients was studied by Divo et al [200], twelve specific comorbidities were significantly associated with an increased risk of death. This was graphically represented in the form of a *comorbidome* (see Figure 20), where the prevalence of each comorbidity is proportional to the size of each node whereas the associated risk of death is proportional to the distance of the node to the centre of the network.

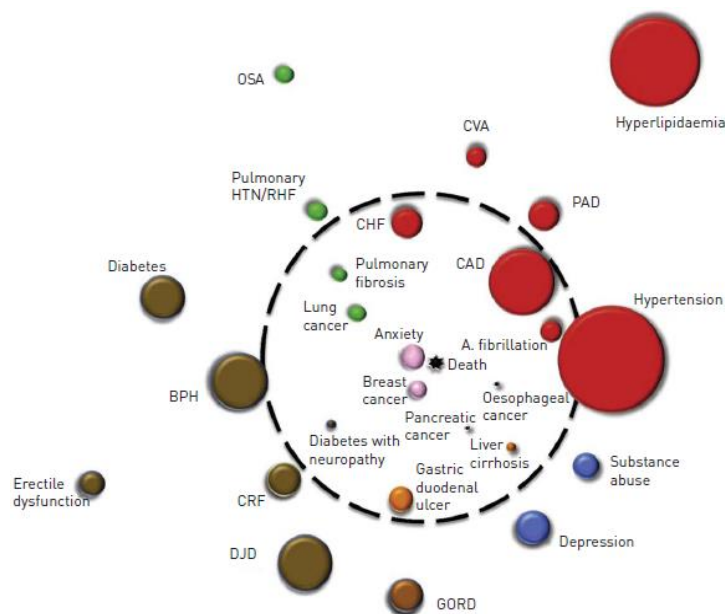


Figure 20: The COPD comorbidome [200].

Cluster analysis is another unbiased analytical approach that, when applied to this same question by other group of investigators, identified five clusters of patients based on 13 comorbidities: “psychological”, “methabolical”, “cachectic”, “cardiovascular” or “less comorbidity”. Cluster differed in health status but were comparable in terms of airflow limitation. The methabolical cluster presented increased levels of $TNF\alpha$ whereas the cardiovascular cluster showed increased IL-6 [201].

Alternatively, Van Remoortel *et al.* [202] related smoking status, age and physical inactivity with premorbid risk factors and comorbid diseases, and found that premorbid

risk factors and comorbidities were higher in what they called “preclinical COPD” and in smokers than in never smokers. The study showed that smoking and physical inactivity were independent risk factors for comorbidities, challenging the concept of COPD as an independent risk factor. In addition, age, rather than COPD severity, was related with most comorbidities [202].

Our group has also explored the molecular relationships between comorbid diseases and COPD [203]. To this end, we mined data from published literature and used a novel network analysis approach that sought to integrate the *diseasome* (i.e., relationship between comorbidities), *interactome* (i.e., molecular relationships), biological pathways and tobacco exposure (*exposome*) with 16 highly prevalent comorbidities. Main results showed that all studied comorbidities shared genes, proteins and molecular pathways related with inflammation, endothelial dysfunction and apoptosis. It also showed that tobacco smoke targets more than 70% of the proteins related with COPD comorbidities, showing a plausible molecular link between COPD and comorbid diseases that interestingly is target by the tobacco *exposome* [203].

This study was later expanded by the information provided by two large COPD audits [204-206] that included more than 5.000 patients in order to study the relationships between comorbidities in patients hospitalized because of an exacerbation of COPD [207]. We constructed and compared the *clinical diseasome* (CD), where diseases are linked if they co-occur more frequently than expected at random, with the *molecular diseasome* (MD), that links diseases that share genes or proteins. About half of the disease pairs in the CD were also related in the MD, particularly in relation to inflammation and vascular tone regulation, supporting the previous results of shared molecular mechanism between comorbidities in COPD [207, 208].

Systems biology has also been used in the study of the molecular pathobiological mechanisms of COPD. Using this approach, Xie *et al.* [209] identified the serum levels of the microRNAs miR-21 and miR-181a as potential biomarkers of COPD susceptibility among heavy smokers. Ezzie *et al.* [210] identified 70 microRNAs and 2667 mRNAs differentially expressed in lung tissue from smokers with and without COPD. Turan *et al.* investigated the relationship between muscle skeletal dysfunction, pulmonary gas exchange, systemic inflammation and response to training. Results showed that there is an alteration in remodeling and bioenergetic pathways in the skeletal muscle that may be linked with an abnormal expression of histone modifiers

and appears to correlate with tissue oxygen utilization. This point to hypoxia as a key factor driving skeletal muscle dysfunction in COPD [211].

The evaluation of COPD Longitudinally to Identify predictive Surrogate End-Point (ECLIPSE) study was a large 3-years international study (NCT00292552) aimed at defining clinically relevant subtypes of COPD, novel biomarkers and genetic factors [212]. Using data from ECLIPSE study Agusti *et al.* [213] described the systemic inflammation of smoking and COPD, a network representation of the systemic inflammation observed in smokers with normal lung function and with COPD, see Figure 21 [213].

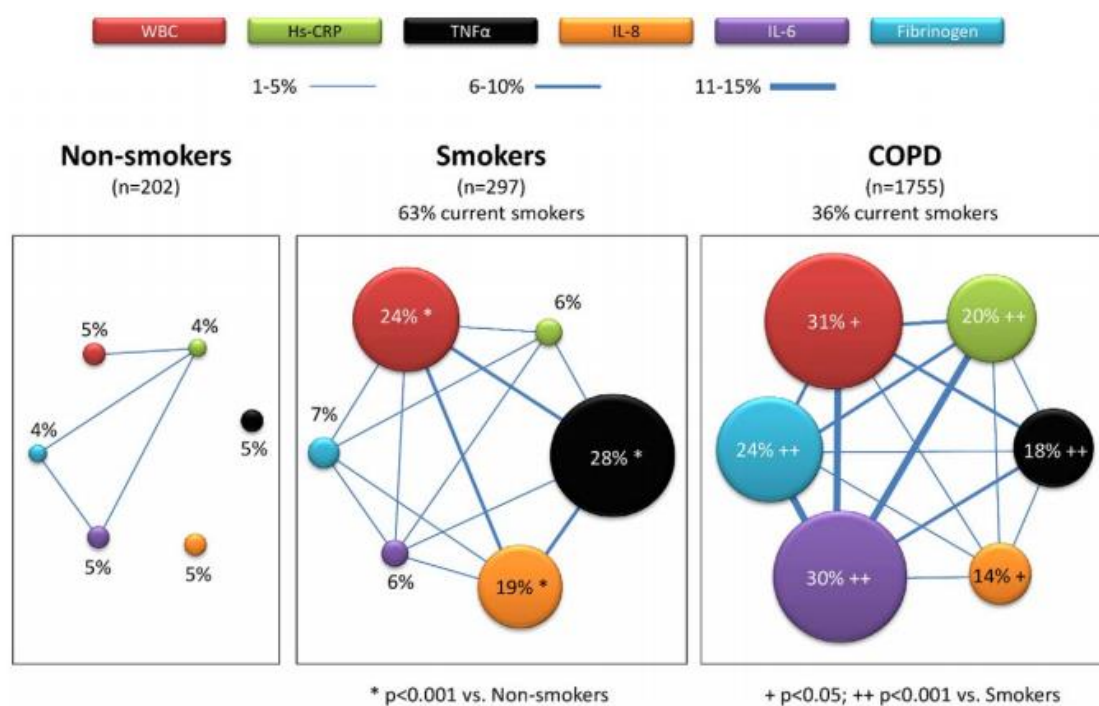


Figure 21: Inflammome representation of systemic inflammation in smokers with normal lung function and patients with COPD [213].

Results showed that the systemic inflammation differs between healthy subjects, smokers and COPD patients (see Figure 21) [213]. This analysis also showed that 20% of COPD patients are persistently inflamed whereas 30% are never inflamed, despite similar lung structural and functional abnormalities. Yet, those persistently inflamed had six times higher mortality and a twice higher incidence of COPD exacerbations than the never inflamed during the 3 years follow up [213]. The identification of novel phenotypes of the disease can potentially identify novel and better therapeutic alternatives [200, 214].

Menche *et al.* [199] develop a novel dual network strategy to identify the genetic basis of COPD. They used the sputum transcriptomic data generated also by the ECLIPSE study. They first compared the number of differentially expressed genes in the two extreme quartiles of several clinically relevant phenotypes. Secondly, they identified groups of patients with maximally differential gene expression, reverse approach. To this end, they developed an unbiased bioinformatic algorithm (diVIIsive Shuffling Approach or VISTa) that maximize gene differences (see Figure 22). This algorithm makes a first random division of the available patients into 3 groups comparing the different gene expression between groups 1 and 2 a keeping group 3 as a reservoir. Then, it randomly swaps one patients from group 1 o 2 with the reservoir (group 3) and compare the differential gene expression again. If the differential gene expression increases, swap is accepted. If not, it is rejected. This step is iterated until the number of differentially expressed genes reached a plateau, at around 1000 iterations. At this point the resulting groups 1 and 2 include patients with maximal gene expression differences.

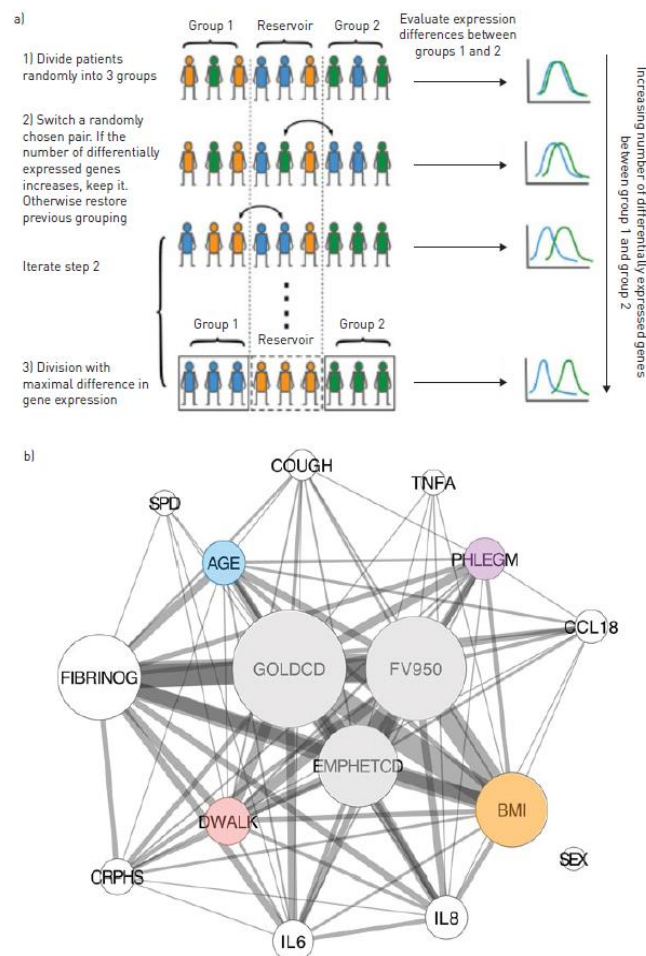


Figure 22: Alternative VISTa algorithm; a) methodology for maximize gene differences between groups and b) network representation of the clinical variables altered between groups [199].

The first approach comparing groups with different clinical phenotypes, only found differentially expressed genes related with airflow limitation, indicating that mild-moderate COPD is associated with significantly different gene signature (in sputum). The results of the reverse approach (i.e., using VISTA algorithm) showed that airflow limitation in combination with the severity of emphysema was the most important hub of the network. However age, Body Mass Index (BMI), exercise capacity, chronic bronchitis, some inflammatory biomarkers (IL-6, IL-8 and SP-D) and sputum findings (elevated neutrophils and decreased lymphocytes) could provide discriminant power.

Another study of Faner *et al.* [215] that used network analysis explored the hypothesis that the systemic inflammatory response to tobacco smoking would differ in smokers with or without COPD. To explore this hypothesis, the systemic leukocyte transcriptomic response after tobacco exposure was analyzed in smokers with and without COPD. The more striking result was a remarkable difference in the inflammatory response to smoking between males and females, regardless the presence or absence of COPD. Yet, within both genders, differentially expressed networks were identified in COPD patients (COPD-related signature) and in healthy smokers (smoking-related signature).

Very recently an integrative approach of genome-wide DNA methylation, gene expression and phenotypic data in lung tissue from COPD patients and healthy smokers identified 126 key molecular regulators. Among these genes, the EPAS1 downstream genes were significantly overlapped with COPD associated genes [216].

Finally Agusti *et al.* [217] have proposed a novel network approach to COPD based on the idea that COPD is not a single organ (i.e., lung) condition, but a complex inter-organ network (Figure 23). In this multi-organ network the smoke affect not only the lungs, but also more distant organs. Specifically, these authors proposed a vascularly connected network, where the lungs are the main external sensor and the source of the “danger signals”, the endothelium the internal sensor and bone marrow and adipose tissue the key effectors producing inflammatory and repair signals. This network model propose that COPD and comorbidities actually depend on how this vascular connected network responds to cigarette smoke, mainly dictated by the genetic and epigenetic background of the individual.

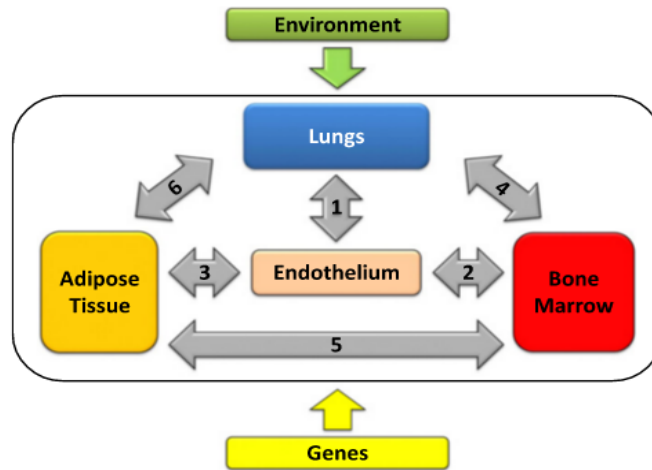


Figure 23: Model propose for a inter organ network of COPD [217].

All in all, these previous studies illustrate the power of systems biology to unravel the complexity of human diseases. However, systems biology results are most often hypothesis generators, since results need to be validated using experimental interventions.

2-HYPOTHESIS

2- HYPOTHESIS

2.1 - GENERAL HYPOTHESES

The general hypothesis of this PhD dissertation is that the clinical heterogeneity and complexity of COPD is associated with different types of immune response and lung regeneration/repair capacity.

2.2 - SPECIFIC HYPOTHESES

In patients with COPD:

1. The **molecular pulmonary immune response** network varies according to the degree of airflow limitation and/or presence and severity of emphysema.
2. The **cellular pulmonary immune response** network is altered and related to the systemic cellular immune response network.
3. The **regenerative and immunomodulatory capacity of the lungs** is compromised due to the micro-environment in which lung resident mesenchymal cells reside.

3 - OBJECTIVES

3 – OBJECTIVES

3.1 - GENERAL OBJECTIVE

The main general objective of this PhD dissertation is to better understand the relationships between the immune response and the lung regenerative capacity in patients with COPD.

3.2 – SPECIFIC OBJECTIVES

This general objective is translated here, in this PhD dissertation, into the following three specific objectives:

1. To characterize and compare the molecular pulmonary immune response network in former smokers with COPD with different degrees of airflow limitation and emphysema.
2. To characterize, relate and compare the cellular pulmonary and systemic immune response in COPD patients with mild/moderate airflow limitation, non-smokers and smokers with normal lung function.
3. To identify, characterize and compare the immunomodulatory capacity of a putative resident stem cell population in the lung of COPD patients mild/moderate airflow-limitation, non-smokers and smokers with normal lung function.

4 - METHODS

4 - METHODS

To facilitate the presentation and understanding of the methodology used, methods will be detailed on a *per objective* basis, with the exception of the study population and ethics details, which are provided below.

4.1 – DESIGN, POPULATION AND ETHICS

This PhD dissertation is based on a prospective, controlled observational study. A total of ? former/current smokers with (n=198) or without COPD (n=20), or non-smokers (n=36) were included in the analysis. Not all individuals (hence, biological samples) could be used to investigate all objectives.

Lung tissue samples were obtained from patients requiring thoracic surgery because of localized lung cancer or those undergoing bilateral lung transplant. We used two sources of lung tissue: 1) the CIBERES pulmonary biobank platform [218] was used as a source of RNA later preserved lung tissue and paraffin imbedded sections, used to address objective 1; and, 2) Fresh lung tissue and circulating blood were obtained from patients undergoing thoracic surgery at the Hospital Clinic of Barcelona and used for objectives 2-3.

The Ethics Committee of the Hospital Clinic of Barcelona and/or of the CIBERES pulmonary biobank platform approved the studies, and all subjects signed their informed consent.

4.1.1 - Clinical and functional characterization

Age, gender, body mass index (BMI), tobacco exposure history, current medication, and presence of comorbidities were recorded in each patient. The presence and degree of airflow limitation was measured using spirometry according to international guidelines [1] and reference values used correspond to Spanish population [219]. The carbon monoxide diffusing capacity (DLCO) was measured too [220] and computed tomography (CT) lung scans were obtained as part of the routine clinical management of patients. For objective 1 CT scans were assessed qualitatively for the presence/absence of emphysema by the attending radiologist and validated by a second

experienced radiologist. The specific clinical characteristics of the patients included for each objective are presented in Table 10 (objective 1), Table 12 (objective 2) and Table 16 (objective 3). Patients presenting pulmonary diseases other than COPD, metastatic cancer, history of substance abuse, acquired or congenital immunodeficiency or used systemic corticoids were excluded.

4.2 – METHODS IN RELATION TO OBJECTIVE-1: MOLECULAR PULMONARY IMMUNE RESPONSE NETWORK

In this objective only lung tissue from COPD former smokers (>6 months) was collected.

4.2.1 – RNA extraction

Total RNA was extracted from 70 lung tissue preserved with RNAlater (Life technologies, US) using the marinas mini kit (Qiagen, Valencia CA, US) with DNase Set treatment (Qiagen, Valencia CA, US). Quantity and purity of RNA was determined with Nanodrop 800 Spectrophotometer (Thermo Scientific, Germany), and its integrity with the Agilent 2100 Bioanalyzer (Agilent technologies, Waldbronn, Germany). Only samples with RNA integrity numbers (RIN) ≥ 7 were considered acceptable.

4.2.1.1 - Microarray processing and raw data generation

RNA samples (n=70) were hybridized to a Affymetrix HG-U219 array plate following Affymetrix's protocols at the IDIBAPS genomic platform. In brief, from 150 ng of total RNA a biotin labeled cRNA was generated by reverse transcription followed by *in vitro* transcription (IVT). After cRNA fragmentation, samples were hybridized on a GeneChip HT HG-U219 perfect-match only (PM) Array Plate. Scanning was processed in the Gene Titan Platform at our institution, a fully automated array system. Scanned images were analyzed with the GeneChip Operating Software (GCOS, Affymetrix). Microarray data quality assessment was conducted using the Expression Console Software (EC, Affymetrix).

Robust Multichip Analysis normalization was performed using the Affymetrix Expression Consol, US. As all samples were processed in one plate, no batch effects were considered. Filtering of the adjusted matrix was performed, keeping those probe-sets with expression values larger than 6 in at least 95% of the samples using the Partek software (Partek, US). Raw and processed microarray data has been deposited in GEO (GSE69818).

4.2.1.1.1 - Differential gene expression

Four differential gene expression comparisons were performed:

1. Patients with severe emphysema n=25 (CT scan+ and DLCO<60% ref.) vs. patients with absence of emphysema here termed as “Bronchiolitis” n=15 (no emphysema in CT scan and DLCO >80% ref.).
2. Patients with “Bronchiolitis” vs. the intermediate group (n=30, with or without CT emphysema and a DLCO value between 60- 80% ref.).
3. This latter group of patients with intermediate characteristics was divided into those with moderate emphysema (DLCO 60-70% ref. and CT emphysema; n=12) vs. those with mild emphysema (DLCO >70-80% ref. and no CT emphysema; n=11). Seven intermediate patients did not meet any of these criteria and were therefore not included in comparison 3. These two groups are likely to have varying degrees of both airway and parenchymal disease.
4. Finally we compared patients with the same GOLD grade of airflow limitation (GOLD 2) with severe emphysema (n=12) or bronchiolitis (n=9), using the same criteria as per the extreme group comparison presented above (see 1).

In all cases, differential gene expression was performed using the non-parametric RankProd method [221] by IDIBAPS bioinformatics platform. Significantly expressed genes were considered as those with a Fold Discovery Rate (FDR) below 1% and with a Log ratio of fold change $\geq|0.4|$.

Finally, to get an insight of the biological process involved in the differentially expressed genes, gene ontology functional over-representation was assessed using DAVID (Database for Annotation, Visualization, and Integrated Discovery, v6.7) [222].

4.2.1.1.2 - Gene Set Enrichment Analysis (GSEA)

GSEA [223] was used to identify similarities of the expression matrix with previously published microarray datasets [224]. Enrichment p-values were calculated by gene set permutation (n=1000), and significant enrichment was determined by an FDR-corrected p-value of <0.05. The key outcomes of GSEA are: (1) Enrichment Score (ES) which reflects the degree to which a gene set is overrepresented at the top or bottom of a

ranked list of genes; (2) Normalized Enrichment Score (NES), which accounts for differences in gene set size and in correlations between gene sets and the expression dataset. NES can be used to compare GSEA results across gene sets; (3) Nominal P Value, which estimates the statistical significance of ES for a single gene set; (4) False Discovery Rate (FDR), which is the estimated probability that a gene set with a given NES represents a false positive finding. (5) Family-wise error rate (FWER), that is a more conservatively estimated probability that the normalized enrichment score represents a false positive finding.

4.2.1.1.3 - Gene Enrichment Profiler (GEP)

From a list of genes of your interest (in our case, up-regulated genes in comparison 1), GEP [225] identifies the enrichment of each of them in different human healthy tissues, and expresses it as an “enrichment score” (ES). For each gene in each tissue; the higher ES, the more tissue specific is that particular gene.

4.2.1.1.4 - Gene co-expression networks and their comparison

Gene co-expression networks for severe emphysema individuals and bronchiolitis were calculated, selecting the probes corresponding to the 2,189 genes included in the GO term “Immune System Process” (GO:0002376), if several probes corresponded to the same genes they were collapsed to have a unique intensity value per gene. The correlation matrix was computed using Pearson correlation ($|R| > 0.8$, $p\text{-value} < 0.0001$) [226] with the R platform [227] and visualized with Cytoscape [228].

To compare the emphysema and bronchiolitis networks, we calculated and compared the connectivity of each gene (K_i) and the number of hubs, as previously described [226]. The gain (or loss) of connectivity (Diff K) was calculated as $K(i)$ emphysema – $K(i)$ bronchiolitis, and the threshold to accept a connectivity gain (or loss) was set at $\text{Diff}K > 0.4$ (or < 0.4). Hub genes were defined as genes with a node degree (K) > 70 [226]. All these analysis were done at the bioinformatics platform of the IDIBAPS.

4.2.1.2 - Validation of microarray results

In order to expand the original population and validate the results obtained in the microarray analysis, lung tissue was available from 24 additional COPD, supplementary table E13 of the included article.

4.2.1.2.1 - Quantitative Real Time PCR

One μg of RNA was retro-transcribed with random hexamers with the Transcriptor First Strand cDNA synthesis Kit. cDNA was diluted $\frac{1}{2}$ with DEPC water and amplified in triplicate with Taqman assays on demand (Hs00241027, Hs00757930, Hs1573371, Hs00922012) in a LightCycler 480 (Roche, Manenheim, Germany). We used actin (Hs99999903_m1) as a housekeeping gene.

4.2.1.2.2 - Immunofluorescent determination of lymphoid follicles and CD20+lung tissue area calculation

5 μM sections lung tissue sections were used for the CD20+ area quantification and lymphoid follicle characterization. Sections were de-parafinized, rehydrated and subjected to an antigen retrieval step with citrate buffer pH 6. Blocked with 10% normal goat/donkey serum (Millipore, US), washed and incubated overnight at 4°C with primary antibody, detected with specific secondary antibody for 1 h and mounted with prolong Gold with DAPI (Life technologies, US). Slides were analyzed in at 20x in a TCS-SP5 confocal microscope (Leica, at the confocal unit of the University of Barcelona) using the Matrix screener software application. The list of the primary antibodies with their corresponding secondary antibody is listed in the following Table 2.

Primary antibody	Secondary antibody
IgG2a mouse anti-human CD20 (Dako. US) 0.5 µl en 100 µl	Goat anti mouse IgG2a 555 (Life Technologies. US) 0.5 µl en 100 µl
IgG1k mouse anti human IgM (Novus. US) 1 µl en 100 µl	Goat anti Mouse IgG1k 647 (Life Technologies. US) 0.5 µl en 100 µl
IgG1k mouse anti human IgG (Southern Biotech. US) 1 µl en 100 µl	Goat anti Mouse IgG1k 647 (Life Technologies. US) 0.5 µl en 100 µl
Rabbit anti human Ki-67 (Novus. US) 2 µl en 100 µl	Donkey anti rabbit 488/647 (Life Technologies. US) 0.5 µl en 100 µl
Rabbit anti human NF-Kb Phosporilated p65 (Abcam. US) 1 µl en 100 µl	Donkey anti rabbit 488/647 (Life Technologies. US) 0.5 µl en 100 µl

Table 2: Antibodies used in the lymphoid follicle characterization

For the quantification of the area belonging to CD20+ cells in lung tissue a minimum of 2 matrices of 56 fields each from two different tissue sections from two blocs was scanned for each tissue. Using Image J we calculated: (i) the total area of each matrix stained with CD20; and (ii) the total area of the tissue stained with DAPI. Next we compared in patients with emphysema with different grades of airflow limitation, and in patients with bronchiolitis: (the total area of CD20 staining/total Dapi area) x100 with a Kruskal Wallis followed by a non-parametric Mann Whitney test.

4.2.1.2.3 - CXCL13 and BAFF ELISA

Total lung protein was extracted from flash frozen lung tissue using TPER tissue reagent (Pierce, Rockford, US) with complete Mini Protease Inhibitor Cocktail Tablets (Roche, Germany): 1 tablet per 10ml of TPER. Tissue homogenization was done in a GentleMACS (Miltenyi Biotech, Germany) instrument following manufacturer instructions. Lysates were centrifuged at 10,000 g for 5 min at 4°C. Supernatants were aliquoted and frozen at -80°C until use. CXCL13 and BAFF were measured by ELISA (R&D) following manufacturer instructions.

4.3 - METHODS IN RELATION TO OBJECTIVE-2: CELLULAR CHARACTERIZATION OF THE IMMUNE RESPONSE

To investigate this specific objective, we used fresh lung tissue and peripheral blood obtained from former and current smokers with or without COPD and non-smoking controls.

4.3.1 - Processing of lung tissue

Fresh lung tissue was collected in PBS on ice within an hour post-surgery, in all cases samples were assessed by a pathologist and only non-affected lung tissue far from the affected cancer nodule was processed. Tissue was processed for several applications:

- A) For RNA isolation: a 1cm x 1cm piece was minced and preserved with RNAlater at 4°C 24 hours and then stored at -20°C.
- B) For the lung disaggregation: the tissue was washed twice with PBS (5' with gentle agitation) to reduce the red cell content. Next, it was cut into small pieces and digested enzymatically with 0,5mg/ml collagenase P (Roche) and 0,1 mg/ml DNase I (Roche) and mechanically with the GentleMACS (Miltenyi Biotec), a maximum of 2 gr of tissue per tube were processed. The pieces are transfer with the enzymes in medium without antibiotics to a GentleMACS C tube (Miltenyi Biotec) and run a first GentleMACS program "m_lung 1.1". Then the tubes are place for 30 minutes at 37°C with shaker and finally the tubes run another GentleMACS program "m_lung 1.2". Obtained cells are first filter through a 100 µm cell strainer (BD) to eliminate the undigested tissue. Second, a hemolysis step with buffer (8,3g NH₄Cl, 1 g NaHCO₃ and 0,04g of disodium EDTA in 1l distillate water and sterilized by filtration) is performed to eliminate the erythrocytes. Finally an additional two filtration steps through 70 µm and 40 µm cell strainer (BD) are made to assure a single cell suspension in PBS for cell staining.

4.3.2 - Processing of peripheral blood

10ml of whole blood drawn in one EDTA tube was obtained the same day of the surgery, before starting any procedure, and processed within 30' from extraction. One ml of whole blood was used for flow cytometry stainings, 1ml stored at -80°C for later DNA extraction and the remaining 8 ml are centrifuged at 400g 6 min at 4°C to isolate the plasma and the buffy coat. The plasma is removed, aliquoted and storage at -80°C, the buffy coat is washed in PBS, erythrocytes are lysed with EL buffer 15' at 4°C (Quiagen, Germany), centrifuged at 400g 6 minutes 4°C, the pellet is then lysed in 1 ml of RTL buffer (Quiagen, Germany) and storage at -80°C for subsequent RNA isolation.

4.3.3 - RNA extraction and microarray analysis

From lung tissue preserved in RNA later, total RNA was extracted with the PureLink RNA kit (Ambion, LifeTechnologies, US). RNA quantity and purity was determined with Nanodrop 800 Spectrophotometer (Thermo Scientific, Germany), and its integrity with the Agilent 2100 Bioanalyzer (Agilent technologies, Waldbronn, Germany). Only samples with RNA integrity numbers (RIN) were ≥ 7 were considered acceptable. Next, 72 lung tissue RNA samples were hybridized to a Affymetrix HG-U219 array plate following Affymetrix's protocols at the IDIBAPS genomic platform (as described above).

4.3.4 - Flow cytometry staining

For each patient, 8 tubes, plus a negative control (no staining) and (3 FMO) are processed (see Table 3) for the lung homogenates and the peripheral blood. Tube 5 is only performed in blood and 6 and 10 only in lung tissue, this is because macrophages are not found in circulating blood.

During the set-up phase of the project, the FMI for each antibody was compared in parallel in lung tissue digested with collagenase and DNAase or without it (only in the GentleMACS tube). Only those antibodies for which we did not observe differences were selected for their inclusion in the study.

For each immune population $5 \cdot 10^5$ cells of lung homogenates in 50 μl (except for the MSC determination that $2 \cdot 10^6$ cells were stained in 100 μl) and 50 μl of whole blood were stained with the antibodies listed in Table 3 and incubated 30' at 4°C in the dark. Then cells are washed with 2ml of PBS, centrifuged at $400g \cdot 6'$. Lung cells are then resuspended in 100 μl of PBS + 10% fixative (Immunochemistry technologies, US), except MSC that are resuspended in 300 μl . In blood tubes erythrocytes are lysed with BD FACS lysing solution (BD, US), incubated 10' at RT in the dark, centrifuged at $400g \cdot 6'$ and resuspended in 100 μl of PBS + 10% fixative.

Cell suspensions are then acquired in a 2 laser BD FACS-CANTO II (BD, US). For each tubes, a minimum of $3 \cdot 10^5$ cells (10^6 cells for the MSC population) was acquire for each population.

Tube, populations and volume	Dye	Brand and reference number	μl of antibody
#1: Neutrophils (50 μl)			
CD45	PECy7	BD 560915	5
CD16	PE	BD 555407	5
CD15	APC	BD 551376	5
CD66b	FITC	BD 555724	2.5
#2: T lymphocytes (50 μl)			
CD45	FITC	BD 555482	5
CD3	Alexa Fluor 750	Beckman Coulter A66329	5
CD4	APC	BD 345771	5
CD8	PECy7	BD 557750	2.5
CD28	PerCPCy5.5	BD 560685	2.5
#3: B and NK lymphocytes (50 μl)			
CD45	FITC	BD 555482	5
CD3	Alexa Fluor 750	Beckman Coulter A66329	5
CD19	PerCPCy5.5	BD 561295	2.5
CD16	PE	BD 555407	5
CD56	PE	BD 555516	5
#4: NKT lymphocytes (50 μl)			
CD45	FITC	BD 555482	5
CD3	Alexa Fluor 750	Beckman Coulter A66329	5
CD56	PE	BD 555516	5
CD4	APC	BD	5
CD8	PECy7	BD 557750	2.5
#5: Monocytes in blood (50 μl)			
CD45	FITC	BD 555482	5

CD64	PECy7	BD 561191	2.5
CD33	Alexa Fluor 750	Beckman Coulter A70200	5
# 6: Macrophages in lung (50 µl)			
CD45	FITC	BD 555482	5
CD64	PECy7	BD 561191	2.5
CD33	Alexa Fluor 750	Beckman Coulter A70200	5
CD163	Alexa Fluor 647	BD 562669	2.5
CD80	PE	BD 557227	10
#7: Dendritic cells (50 µl)			
CD45	FITC	BD 555482	5
CD33	Alexa Fluor 750	Beckman Coulter A70200	5
CD11b	PECy7	BD 557743	2.5
CD11c	APC	BD 559877	5
HLA-DR	PE	BD 555812	10
#8: Mast cells (50 µl)			
CD45	FITC	BD 555482	5
CD34	PECy7	BD 348811	5
c-kit	PE	DAKO R 7145	10
#9: Mesenchymal stem cells (MSC) (100 µl)			
CD45	Alexa Fluor 750	Beckman Coulter A79392	10
CD34	PECy7	BD 348811	5
c-kit	PE	DAKO R 7145	10
CD90	APC	BD 559869	5
CD73	PerCPCy5.5	BD 561260	5
CD105	FITC	BD 561443	5
# 10: FMO lymphocytes (50 µl)			
CD45	FITC	BD 555482	5
CD3	Alexa Fluor 750	Beckman Coulter A66329	5
CD4	APC	BD 345771	5
CD8	PECy7	BD 557750	2.5
# 11: FMO for CD80 in lung Macrophages (50 µl)			
CD45	FITC	BD 555482	5
CD64	PECy7	BD 561191	2.5
CD33	Alexa Fluor 750	Beckman Coulter A70200	5
CD163	Alexa Fluor 647	BD 562669	2.5
# 12: FMO for CD163 in lung Macrophages (50 µl)			
CD45	FITC	BD 555482	5
CD64	PECy7	BD 561191	2.5
CD33	Alexa Fluor 750	Beckman Coulter A70200	5
CD163	Alexa Fluor 647	BD 562669	2.5

Table 3: Monoclonal antibodies for flow cytometry

4.3.4.1 - Gating strategies

Compensation was set using single staining tubes and the FACSDiva (BD, US) automatic compensation. Further compensation adjusts for specific tubs and flow cytometry analysis was performed after the acquisition using FlowJo V10 software (FlowJo LLC, US).

As the same markers were used to stain blood and lung populations, similar gating strategies were used for most of the cell populations. In this section we describe the strategy used and provide examples for both lung and blood.

In all the tubes the first step was to select the living cells from the debris (plot FSC vs. SSC) and determine the G1. Next, SCC is plot against the CD45+ in order to select the live cells of hematopoietic lineage cells (G2), and then the gating strategy is different according to the population of interest.

Tube 1: Neutrophils

Non-lymphocyte populations in lung tissue have auto fluorescence, for this reason, two empty channels (with no fluorochrome) were plotted and used to select the double negative cells, those with no autofluorescence (G3). Neutrophils are selected from G3 as the CD15+ and CD16+ cells, see Figure 24 a-G4 and b-G3).

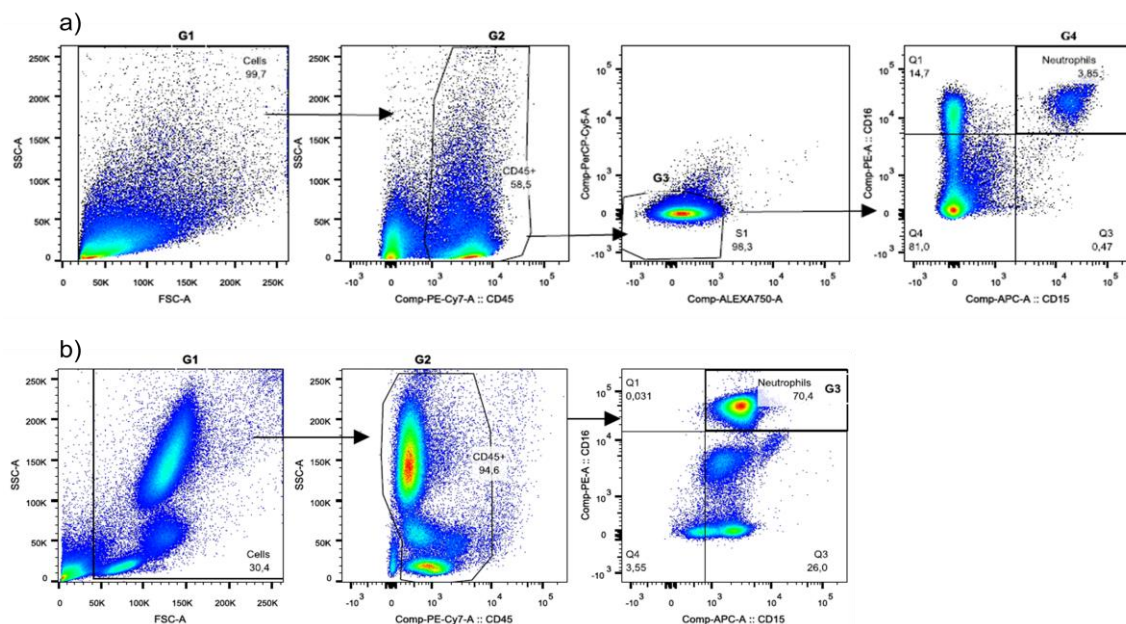
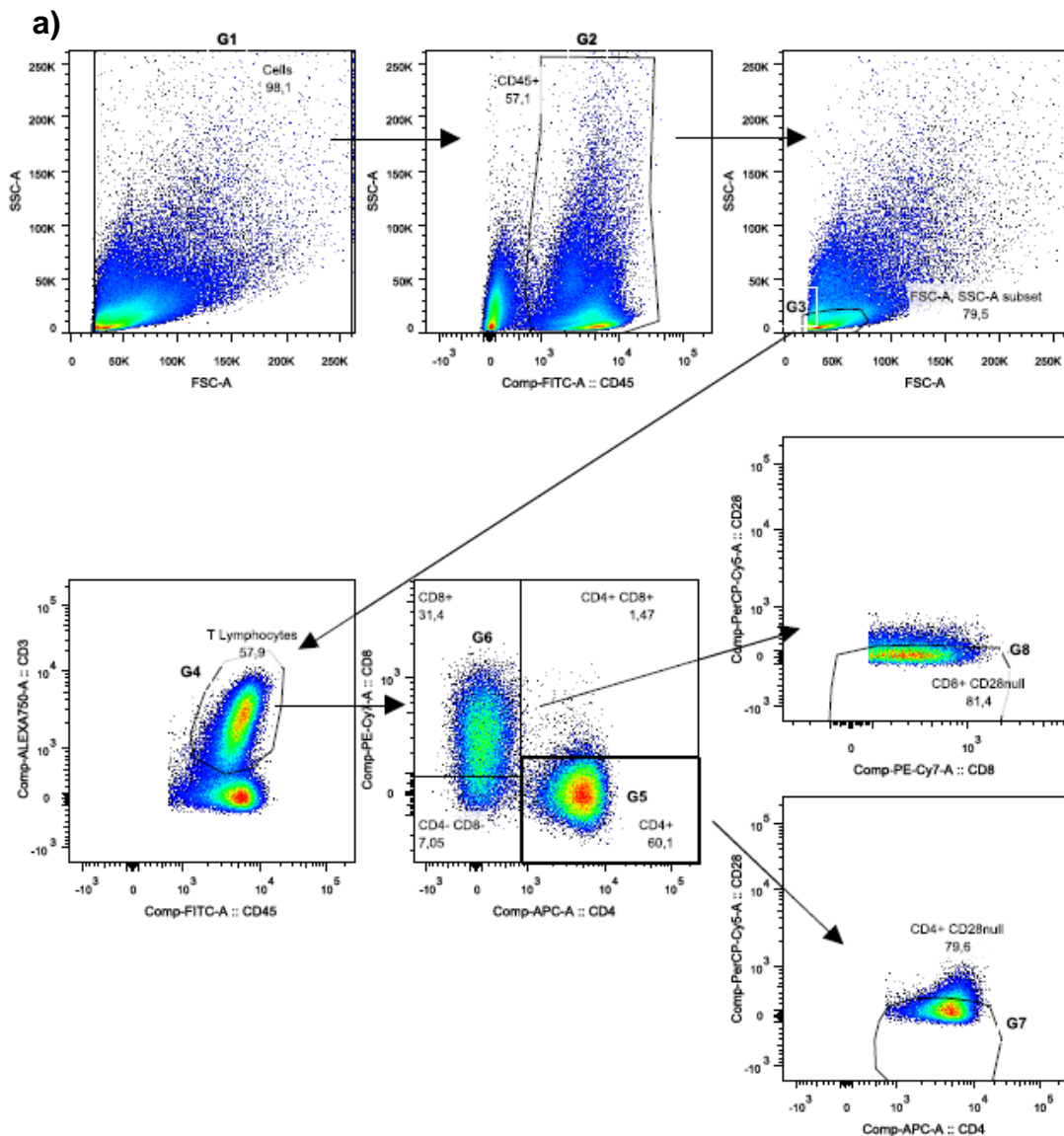


Figure 24: Neutrophils gating strategy for a) lung tissue and b) peripheral blood

Tube 2: T Lymphocytes

The gating strategy for lung and blood T lymphocytes is represented in Figure 25. First, the lymphocyte population is selected by FSS-A vs. SSC-A (G3) and next, T cells are selected by the expression of the CD3 (G4) and then the CD3⁺ population is split in CD3⁺CD4⁺ cells (G5) and the CD3⁺CD8⁺ cells (G6). Finally, in these two populations the expression of the CD28 is evaluated (G7 and G8). To fix the gate for CD28 the FMO tube of lymphocytes (tube 10) was used.



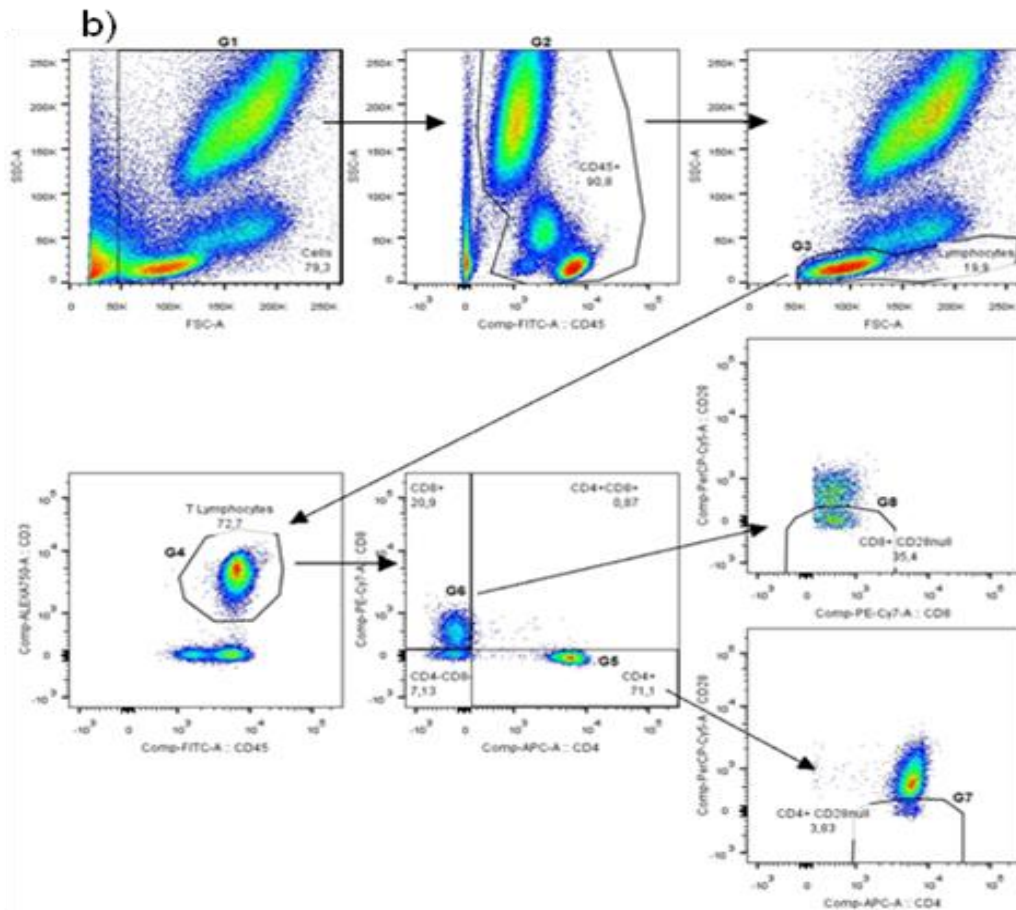


Figure 25: T Lymphocyte gating strategy for a) lung tissue and b) peripheral blood.

Tube 3: B, NK lymphocytes

The NK-lymphocyte and B-lymphocyte populations are determined at the same time (Figure 26). From the lymphocyte population (G3) the $CD3^+CD56^+CD16^+$ population represents the NK cells (G4) and the $CD45^+CD19^+$ population the B cells (G5).

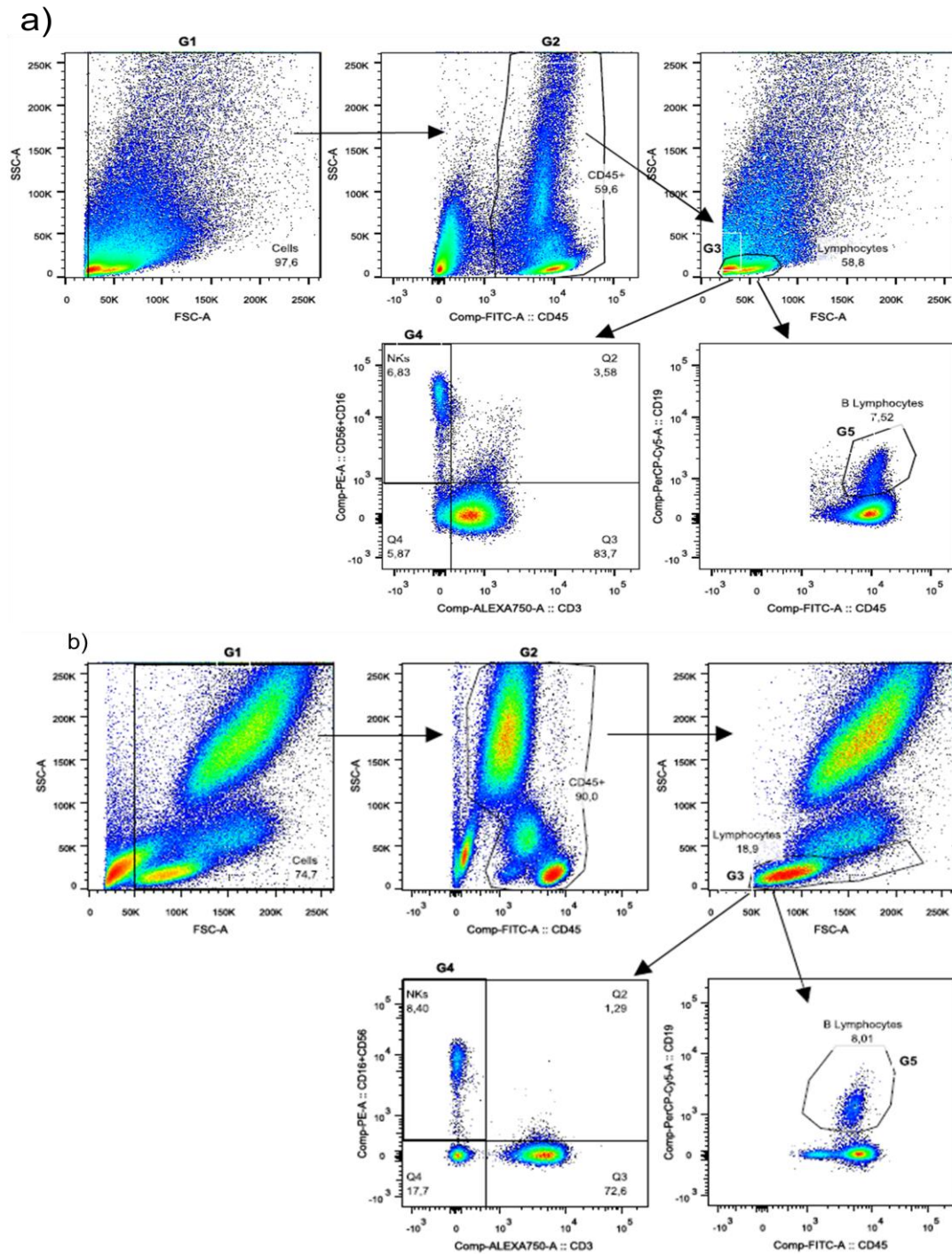


Figure 26: NK Lymphocytes and B Lymphocytes for a) lung tissue and b) peripheral blood

Tube 4: NKT lymphocytes

From the lymphocyte population (G3) NKT-like lymphocytes are selected as CD3+CD56+ (G4), see Figure 27. As the CD3+CD56+ and CD3+CD56- population do not split completely, a FMO without the CD56 (Tube 10, FMO for lymphocytes) was

used to set the gate and to differentiate them. In the CD3+CD56+ NKT-like population the expression of the CD4 and CD8 was evaluated.

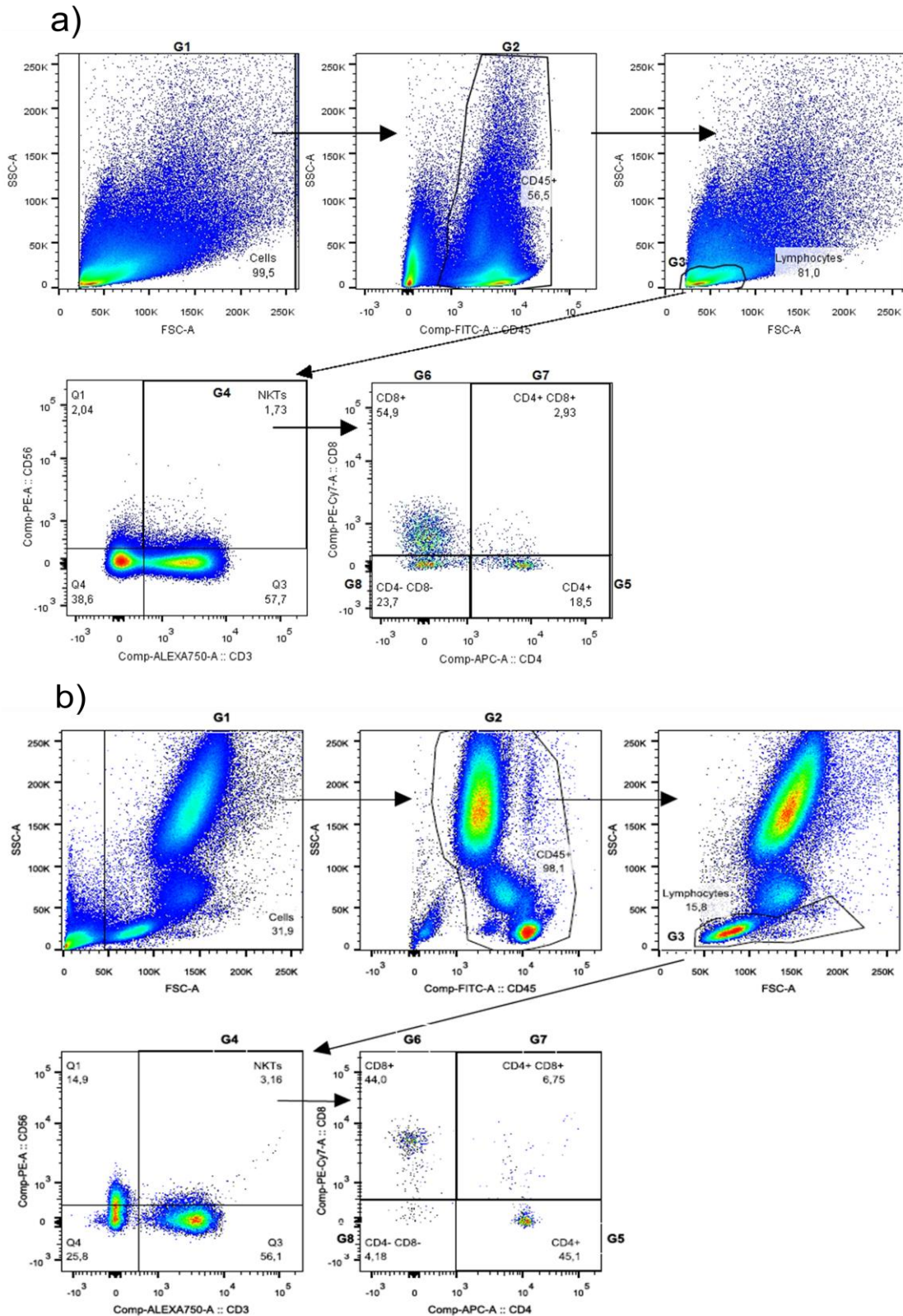


Figure 27: NKT Lymphocyte gating strategy for a) lung tissue and b) peripheral blood.

Tube 5: Monocytes (Blood only)

In peripheral blood the CD64 and CD33 markers are evaluated for the monocyte population (G3) (Figure 28).

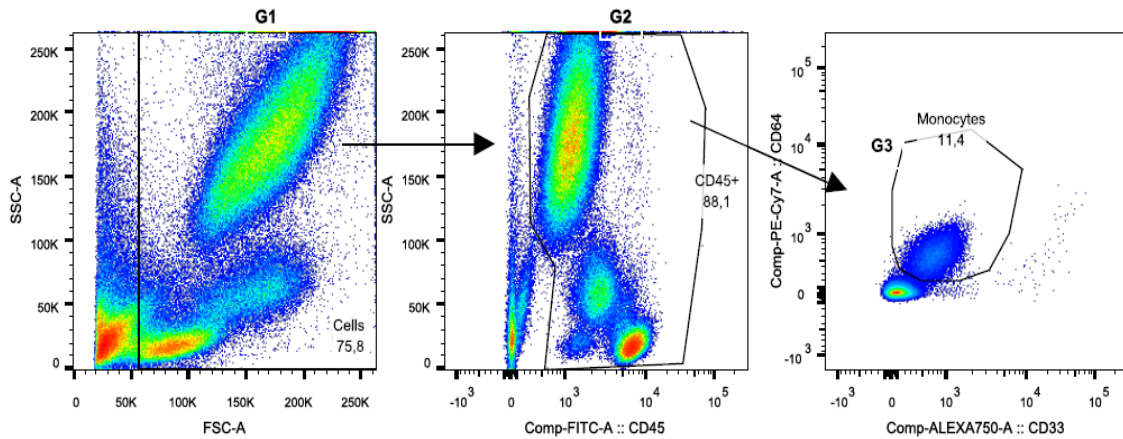


Figure 28: Monocyte gating strategy for blood

Tube 6: (lung only) Macrophages

After the selection of the CD45+ fraction, the SSC vs. CD64 plot is used to select the macrophages (G3) and monocytes (G4), see Figure 29. In these two populations the expression of the M1 and M2 markers CD80 and CD163 is evaluated. To obtain the fraction of M1 (G5), M2 (G6) and M1-2 (G7) macrophages, two FMO tubes (Tubes 11 and 12) are used to set the gates.

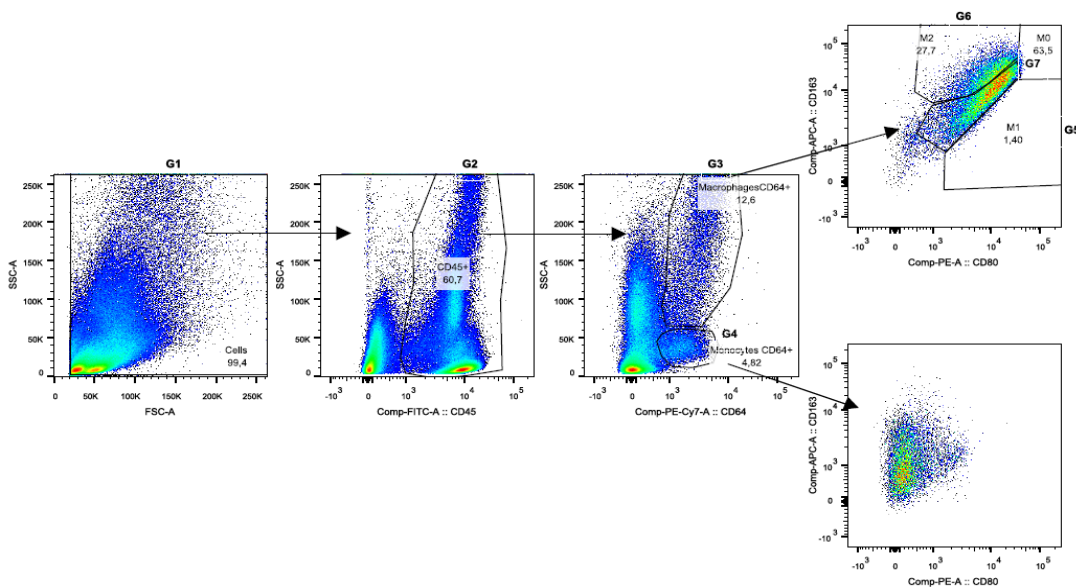


Figure 29: Macrophage gating strategy for lung tissue

Tube 7: Dendritic cells

In lung tissue, due to the high number of cells analyzed in this tube and their natural tendency of self-aggregation a first step for the exclusion of cell aggregates is performed using the FSC-A vs. FSC-H (G2), see Figure 30. Then the hematopoietic cells are selected with the CD45 (G3) and autofluorescent cells are excluded selecting the negative population in a channel with no fluorochrome (G4).

From G4 the Dendritic cells (DCs) are first split in two population according to the expression of the CD11c (G6 and G7) and then in each one the expression of CD11b and HLA-DR is evaluated giving the final 4 DCs population: CD11c^{high}HLA-DR^{high}CD11b⁺ (G9), CD11c^{high}HLA-DR⁺CD11b^{high} (G10), CD11c^{low}HLA-DR⁺CD11b^{low} (G12) and CD11c^{low}HLA-DR⁺CD11b^{high} (G11).

Finally MDSC are defined from G4 as CD33⁺CD11b⁺ (G5) and HLA-DR⁻(G8).

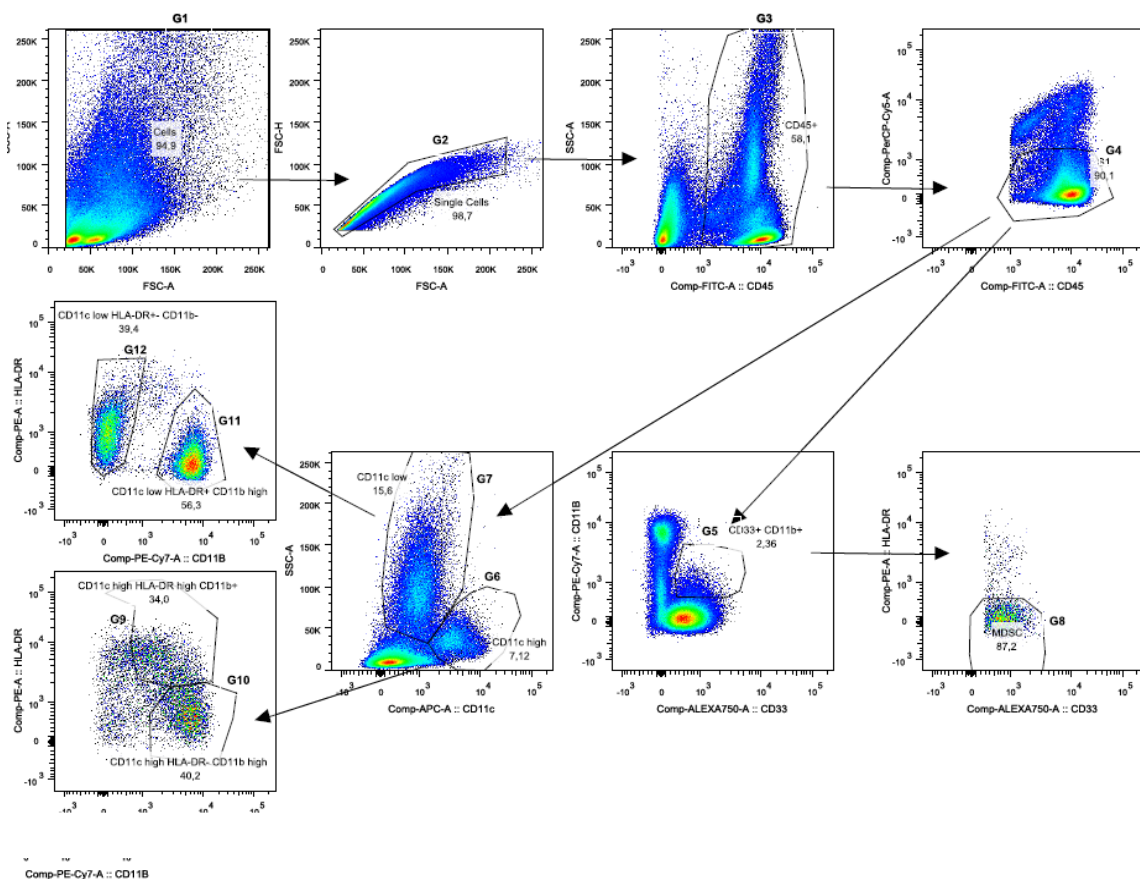


Figure 30: DCs and MDSC gating strategy for lung tissue.

In peripheral blood DCs (Figure 31) mononuclear cells are selected using the FSC vs. SSC (G3), then expression of CD11c and HLA-DR is evaluated to define the CD11c+

DCs (G4) and the CD123+ DCs (G5). From the CD45+ cells the CD33+CD11b+ population (G4) was selected and then analyze for the expression of the HLA-DR, to select the CD33+CD11b+HLA-DR- population (G7)

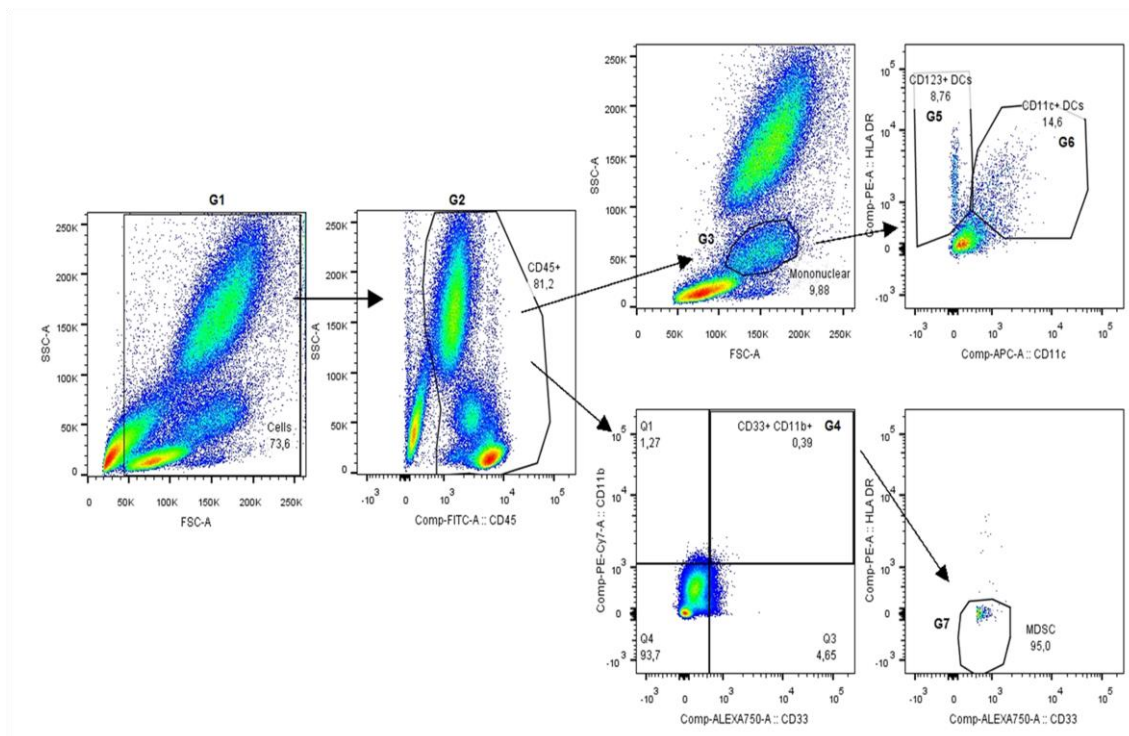


Figure 31: DCs and MDSC gating strategy for peripheral blood.

Tube 8: Mast Cells

In this work, mast cells are defined as CD45+ c-kit+ and CD34- cells. Figure 32 shows the gating strategy, starting excluding cell aggregates (G2) due to the large number of cells analyzed in this tube. Next the CD45+ population (G3) is selected and then the autofluorescent cells are excluded (G4). The c-kit is represented against the CD34 for the selection of the c-kit+CD34- population (G5). The analysis for the blood sample (Figure 32B) is similar but the aggregate exclusion step is not performed.

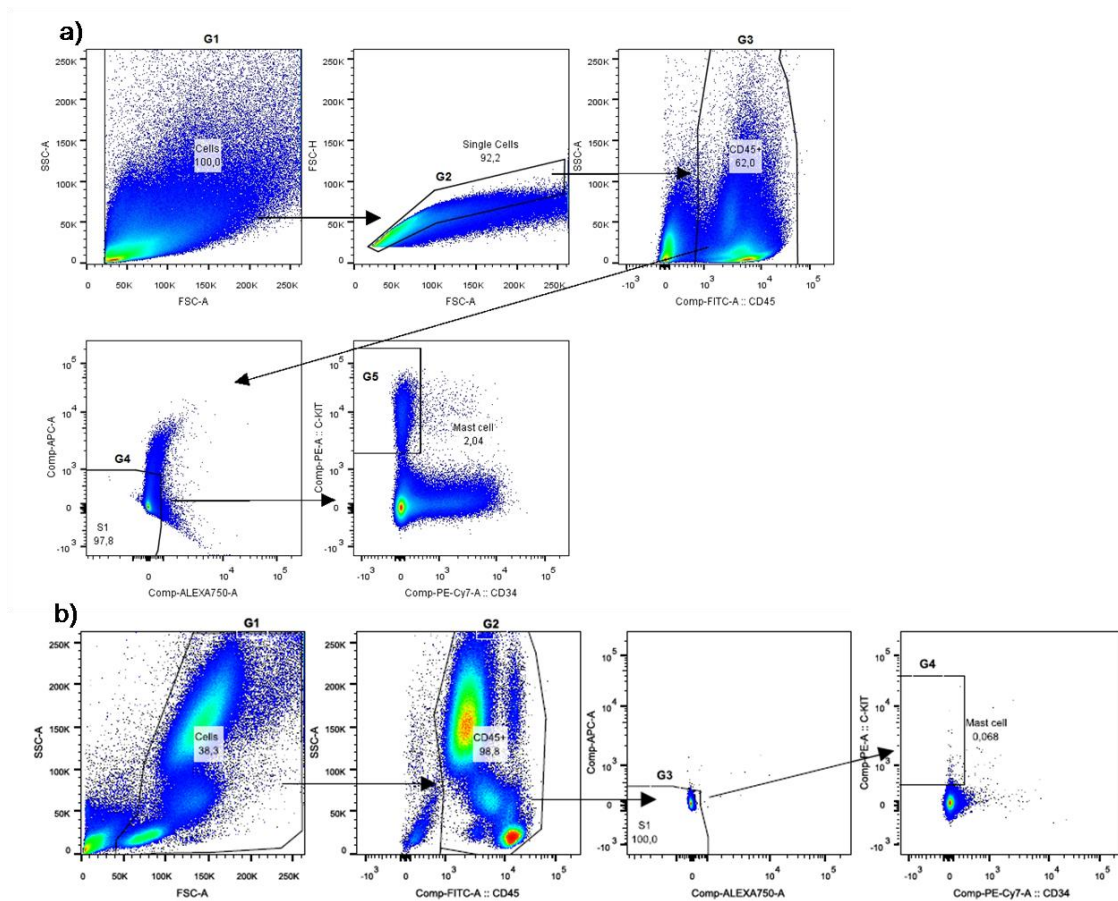


Figure 32: Mast cell gating strategy for a) lung tissue and b) peripheral blood

Tube 9: Mesenchymal stem cells (MSC)

For this population (see Figure 33A), due to the high number of cells analyzed, we first exclude the cell doublets (G1: FSC-A vs. FSC-H), then the CD45 negative population was selected (G2) and from it the CD34 negative (G3). From this double negative CD45⁻CD34⁻ population the expression of the CD90 (G4), CD105 (G5) and CD73 (G6) was evaluated, gates were established using a FMO tube. In blood the gating strategy is the same, but the doublet removal step is not required, see Figure 33B.

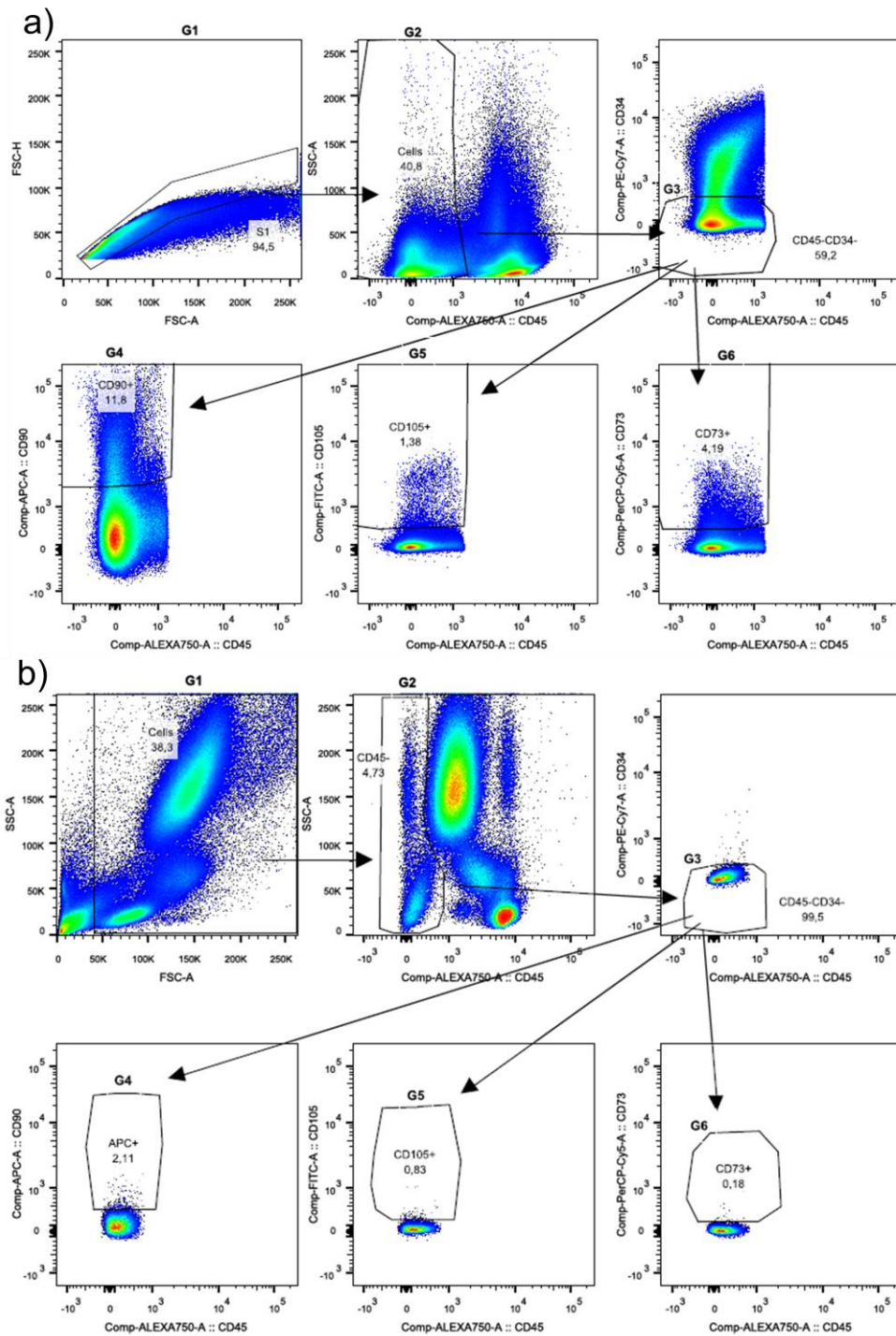


Figure 33: MSC gating strategy for a) lung tissue and b) peripheral blood

4.3.5 - Statistical analysis

4.3.5.1 - Population statistics

Clinical data is presented in Table 12 (result sections) as mean \pm standard deviation or percentage. Between groups comparisons were performed using a non-parametric one-way ANOVA.

Immune cell populations of interest are calculated as % of CD45+ cells, and differences between study groups were assessed using non-parametric one-way ANOVA with a Mann-Whitney post-hoc analysis when appropriated. To check if smoking status and disease status contributed both to the observed differences, variables were log scale transformed and the analysis was performed with a two-way ANOVA . A P value <0.05 was considered significant.

4.3.5.2 Network Analysis:

4.3.5.2.1 Spearman correlation networks:

To assess the correlation between pulmonary and systemic immune cell populations, a Spearman correlation matrix was computed with all variables of each individual, for all the studied subjects and by groups: non-smokers, COPD patients, and smokers with normal lung function.

Only correlations with a Spearman (r) coefficient $> |0.3|$ and a p-value < 0.05 were considered. All statistical analysis were performed using the R platform [227] and networks were visualized using Cytoscape [228].

4.3.5.2.2 Weighed gene co-expression Networks Analysis (WGCNA):

Microarray was performed over the same lung tissue samples in which the cell populations were determined. Raw microarray results were normalized with the RMA algorithm (oligo package [229], R platform). Probes in the lowest quartile of variability were removed. U219 array probes were collapsed to genes [230] with the WGCNA function [231], and 16000 genes were considered for analysis.

Weighted gene co-expression networks were built using the WGCNA package [231]. Briefly, the adjacency matrix was built using the biweight midcorrelation, with a softpower threshold of 12. The DeepSplit for module identification was 2 and the minimum module size 30. WGCNA produced a set of modules (labeled by color), each containing a set of unique genes. The module eigengene is defined as the first principal component of the expression matrix of the probes within the module.

Module eigengenes were correlated with clinical variables and cell population frequencies to identify modules associated with them [231]. For gene ontology enrichment genes with both high gene significance (GS) with the variable of interest and high module membership (MM) metrics were selected. Ontology enrichment was performed as described above.

4.4 – METHODS IN RELATION TO OBJECTIVE-3: LRMSC

In this objective only fresh lung tissue from former or current smokers with or without mild/moderated COPD and non-smoking controls was used.

4.4.1 - Isolation of Lung Resident Mesenchymal-like Stem Cells, LRMSC:

Fresh lung tissue was washed in PBS to reduce the blood content, minced in 0.3cm x 0.3cm pieces (explants) plated on 12 multi-well plates with DMEM (Gibco, US), 10% FBS (Gibco, US) 2% pen-strep (Gibco, US). After 5-6 days, explants are transferred to a new well, the well is washed with PBS (Gibco, US) to eliminate the erythrocytes and the hematological non adherent cells and the explants are returned to the plate with DMEM (Gibco, US), 10% FBS (Gibco, US) 2% pen-strep (Gibco, US) and 20ng/ml fibroblast growth factor (Gibco, US) . Explants are left in the diffusion phase during 15-20 days until the surface of the well is occupied by a layer of cells. This monolayer is composed by both a fibroblast population which is tightly attached to the plastic surface (including macrophages) and a population of clear phase bright cells, round and attached to the top of the fibroblast monolayer (see Figure 34A). In other organs (heart tissue) this cells have been described to be sphere forming progenitor cells [153, 160].

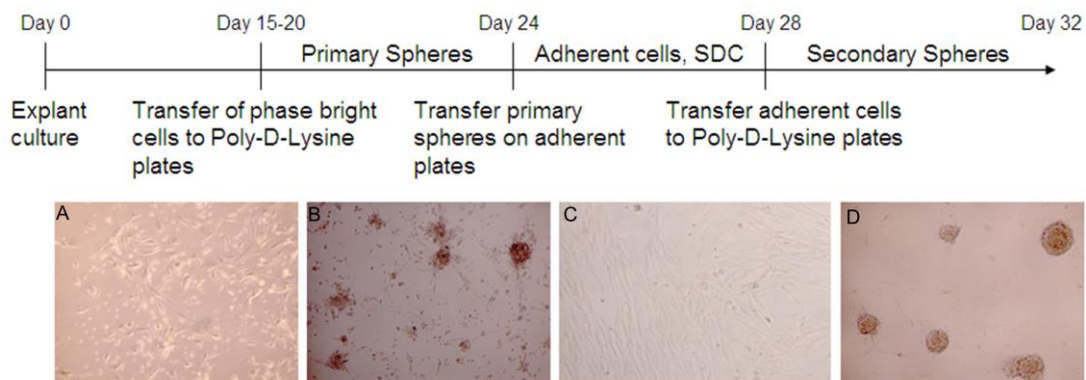


Figure 34: Scheme of lung resident stem cell culture methodology and representative images of each phase. A) Representative image of the diffused cells from the explant, B) 1st spheres, C) Sphere derived cells (SDC) and D) 2nd spheres.

To isolate these cells, 0,2 ml of 0,05% trypsin (Gibco, US) are added to each well, incubated 1' at room temperature, cells are recovered with PBS (Gibco, US) and

centrifuged 600g 4 mins. Fibroblasts and macrophages remain attached to the plastic surface of the plates.

Next, stem cell isolation is performed in the basis of the sphere formatting capacity (3D structure formation) of these cells. To do so, the recovered fraction is plated on 96 well poly-D-lysine plates (Corning, US). 10^5 cells/ml are plated with sphere culture medium (SCM): 35% IMDM/65% DMEM:F12 (Gibco, US) supplemented with 2% B27 (Gibco, US), 10ng/ml epidermal growth factor (Gibco, US), 20ng/ml fibroblast growth factor (Gibco, US) and 2% pen-strep (Gibco, US). In 24h culture in these plates, spheres appear as self-assembling, multicellular and floating cell clusters, while the rest of the cells remain attach to the plate, see Figure 34B. After 4 days, spheres are replated in polystyrene 96 multi-well plates (Corning, US) in SCM supplemented with 3,5% FBS (Gibco, US) and they expand as monolayer that is referred as sphere derived cells (SDC) Figure 34C. This part supposes an important purification step as the contaminant cells remain attach to the plastic surface.

When the culture become confluent (4-5 days in culture approx.), the cells are harvested and replated in poly-D-lysine coated culture plates with a 1.2 dilution in SCM without FBS to generate the secondary spheres, see Figure 34D. Again after 4 days in spheres the cells could be transfer for a new proliferation step. There cells were frozen at $5 \cdot 10^5$ cells/ml and stored in N_2 .

4.4.2 - Cell surface marker characterization

During all the steps of the culture the cells were analyze by flow cytometry to determine the cell surface markers. The staining procedure was performed in a volume of 50 μ l of PBS (10^5 cell approx). The antibodies used per tube and the volume are listed in the following Table 4, 3 different tubes were used in order to make the whole characterization. Cells were stained 30' on ice in the dark, washed with PBS (Gibco, US) and resuspended in 100 μ l of PBS + 10% fixative (Immunochemistry technologies, US).

Tube	Dye	Brand and reference number	µl of antibody
Tube 1			
CD45	Alexa750	Beckman Coulter A79392	5
CD90	APC	BD 559869	2.5
CD73	PerCPCy5.5	BD 561260	2.5
CD105	FITC	BD 561443	2.5
c-kit	PE	DAKO R 7145	5
CD34	PECy7	BD 348811	2.5
Tube 2			
CD45	Alexa750	Beckman Coulter A79392	5
CD13	FITC	ImmunoTools 21270133	2.5
CD44	PE	ImmunoTools 21270444	2.5
CD29	APC	BD 561794	2.5
CD140b	PerCPCy5.5	BD 562714	2.5
CD31	PECy7	BioLegend 303117	2.5
CD166	PerCPCy5.5	BD 5124700	2.5
Tube 3			
CD45	Alexa750	Beckman Coulter A79392	5
EGFR	FITC	BD 612554	2.5
FGFR	PE	Cell Signaling 12777S	2.5
CD133	APC	Miltenyi Biotec 130-098-129	2.5

Table 4: Antibodies used for flow cytometry characterization of LRMSC

Cell suspensions were acquired, compensated and analyzed as described previously for blood and lung homogenates (4.3.4 - Flow cytometry staining). A minimum of $5 \cdot 10^4$ live cells were considered per each tube. The gating strategy for each tube is found in Figure 35. Briefly, the live cells were selected using the FSC Vs SSC (G1) and then, the CD45- cells were gated (G2). From this CD45- population the expression of all the markers was evaluated and express as a percentage of the CD45 negative population.

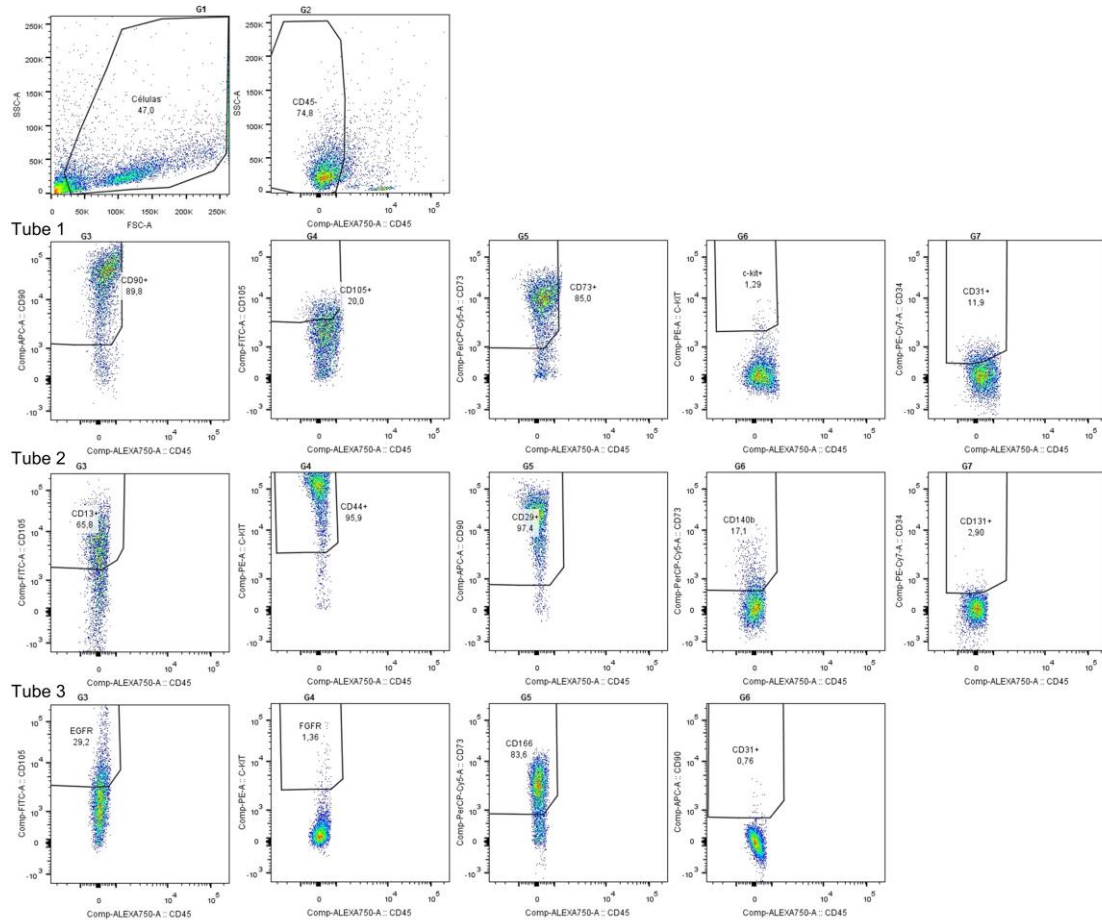


Figure 35: Gating strategy for the characterization of the LRMSC

4.4.3 - Expression of pluripotency associated genes:

Total RNA was extracted from lung tissue preserved in RNA later as described in section (4.2.1 – RNA extraction, microarray processing and raw data generation). Dry pellets from each cell culture step were performed and total RNA was isolated from them using the RNeasy Micro Kit (Ambion, Life technologies, US). DNase treatment was performed in both, RNA quantity and purity was determined with Nanodrop 800 Spectrophotometer (Thermo Scientific, Germany), and its integrity with Agilent 2100 Bioanalyzer (Agilent technologies, Waldbronn, Germany). RNA integrity numbers (RIN) ≥ 7 were considered acceptable. 150ng of RNA were used for microarray determination using the U219 Array Plate described above.

4.4.3.1 - Microarray data analysis:

Raw microarray results were RMA normalized and filtered as described in section (4.2.1 – RNA extraction, microarray processing and raw data generation). Raw microarray results (.cel files) from second spheres were used to perform the Rohart test, which is an *in silico* test that has been optimized in order to discriminate mesenchymal stem cells (MSC) from fibroblasts and other progenitor cells or differentiated stromal cells [151] with a classifier accuracy of 97%. As controls in the test we included .cel files from 3 bone marrow mesenchymal stem cells (BM-MSC, provided by Carlos Rio in IDISPA), and the blood and tissue signatures from the same individuals of which LRMSC were isolated. Finally the differentially expressed genes between the different groups of LRMSC was performed as described in section (4.2.1.1.1 - Differential gene expression).

4.4.3.2 - RT-PCR validation of the microarray results

One µg of RNA was retro-transcribed with random hexamers with the Transcriptor First Strand cDNA synthesis Kit (Roche, Mannheim, Germany). cDNA was diluted ½ with DEPC water and amplified in triplicate with the 0,5µM of each of the primers described in Table 5, LightCycler ® 480 SYBR Green I Master (Roche) in a LightCycler 480 instrument (Roche, Mannheim, Germany).

Gene	Primer Sequence	T °C	Fragment size (bp)
Gapdh	F: TCTTCTTTTGCCTCGCCAG R: AGCCCCAGCCTTCTCCA	60	372
Oct-4	F: GACAGGGGGAGGGGAGGAGCTAGG R: CTTCCCTCCAACCAGTTGCCCAAAC	60	144
KLF4	F: GACTTCCCCCAGTGCTTC R:CGTTGAACTCCTCGGTCTC	60	144
DPPA3	F: GTTACTGGGCGGAGTTCGTA R: TGAAGTGGCTTGGTGTCTTG	60	168
Nestin	F: GCGGTGGCTCCAAGACTTC R: ACTGGGAGCAAAGATCCAAGAC	60	100
c-kit	F: GCACCTGCTGAAATGTATGACATAAT R: CTGCAGTTTGCTAAGTTGGAGTAAAT	60	146
Sox2	F: CCAGCTCGCAGACCTACA R: CCTGGAGTGGGAGGAAGA	60	155
Lin28	F: TCTGGAATCCATCCGTGTC R: TTGGCATGATGATCTAGACCT	60	146
c-Myc	F: GTGCGTAAGGAAAAGTAAGG R: AAGACTCAGCCAAGGTTG	60	117

Table 5: Primer sequences for some of the validated genes

We used *gapdh* as a housekeeping gene and relative quantification was performed with the $2^{(\Delta\text{CP})}$ method²⁰. The cycling conditions are in Table 6.

Denaturalization and activation	
95°C	10 minutes
Amplification cycles: 50	
95°C	5 seconds
60°C	5 seconds
72°C	15 seconds
Generation of melting curves	
65-95°C	

Table 6: Thermal cycling conditions of the RT-PCR

4.4.4 - Adipogenic, osteogenic and chondrogenic differentiation:

To prove the stem cell properties, LRMSC were differentiated towards adipocytes, osteocytes and chondrocytes in the presence of specific differentiation media (Human Mesenchymal Stem Cell Functional Identification Kit, R&D Systems, Germany).

Adipogenic and osteogenic differentiation were performed in 24 well plates in triplicates (Corning, US). For adipogenic differentiation $5 \cdot 10^4$ cells were plated and expanded 4 days until 100% confluence. For the osteogenic differentiation $3 \cdot 10^4$ cells were plated and expanded 2 days until reaching the 50-70% of confluence. Cells were differentiated for two weeks, changing the medium every 3-4 days. At the end of the differentiation, the medium was removed, the cells were washed with PBS, one well was lysed for RNA extraction and the two others fixed with PBS + 4% paraformaldehyde 20 minutes, washed twice with PBS, and then plates were allowed to dry 2 hours. Finally the plate was stored at -80°C until staining.

To identify adipocytes, both oil-red staining (Sigma, US) and goat anti mouse FABP-4 (fatty acid binding protein-4, from the Human Mesenchymal Stem Cell Functional Identification Kit, R&D Systems, US) with a secondary donkey anti-goat-555 (LifeTechnologies, US) were employed. For osteocyte detection a mouse anti-human osteocalcin (from the Human Mesenchymal Stem Cell Functional Identification Kit, R&D Systems, US) with a secondary donkey anti-mouse-555 (LifeTechnologies, US) and alizarin red staining (Sigma, US) were used following manufacturer instructions. Negative controls of differentiated cells without staining and non-differentiated cells were included. Plates were defrost, rehydrated, blocked and permeabilized with 10%

normal goat/donkey serum (Millipore, US) and 0,01% triton (Sigma, US), washed and incubated overnight at 4°C with primary antibody, detected with specific secondary antibody for 1 h and mounted with prolong Gold with DAPI (Life technologies, US). Slides were analyzed in at 20x in a TCS-SP5 confocal microscope (Leica, at the confocal unit of the University of Barcelona).

For the chondrogenic differentiation $2,5 \cdot 10^5$ cells were transferred to a 15ml polypropylene conical tube (Corning, US), cells were centrifuged and left as a pellet in the incubator (with the tub cap loosen to allow gas exchange) the medium was replace each 3-4 days without disrupting the pellet. After 3 weeks the medium was remove, the pellet was washed with PBS and transferred to a tissue-tek cryomold (Sakura, Fisher Scientific, US) imbibed in tissue-tek O.C.T compound (Sakura, Fisher Scientific, US) and frozen with cold Isopentane. Sections of 5µm were made and stained with the Alcian blue dye (Sigma, US) for chondrocyte visualization following manufacturer instructions.

4.4.5 - Immunofluorescence:

Three triple stainings were performed: 1) CD45/CD90/CD73; 2) CD45/CD90/CD105; 3) CD45/CD90/ against MMP-3, MMP-1, CD31, CLGN or FoxF1.

Fresh lung tissue was fixed overnight with 4% paraformaldehyde, and then O.C.T imbibed (Sakura, Fisher Technologies) and frozen in Isopentane. Tissue Blocks were kept at -80 until cut at -20°C into 5µM sections by the IDIBAPS tissue platform. The sections were stored at -80°C until staining.

For staining, the sections were defrost at room temperature and allowed to dry with a fan for at least 2h. Then were rehydrated with PBS, blocked and permeabilized with 10% normal goat/donkey serum (Millipore, US) and 0,01% triton (Sigma, US), washed and then incubated overnight at 4°C with corresponding concentration of the primary antibodies (Table 7). Then sections are washed three times with PBS, and the corresponding secondary antibody (Table 7) was added for 1 hour at room temperature in the dark, washed again three times with PBS and slides were mounted with prolong Gold with DAPI (Life technologies, US). Slides were analyzed in a TCS-SP5 confocal microscope (Leica, at the confocal unit of the University of Barcelona). Tissue mosaics

of 8x8 fields with the 63x objective were made in order of having a representative area (using the Matrix Scanner software) for the first two stainings.

Primary antibody Brand and concentration	Secondary antibody Brand and concentration
Sheep anti-human CD90 (R&D. US) 10 µl en 100 µl	Donkey anti-sheep 555 (Life Technologies. US) 0.5 µl en 100 µl
Mouse anti-human CD73 (Thermo Scientific. US) 2 µl en 100 µl	Donkey anti-mouse 647 (Life Technologies. US) 0.5 µl en 100 µl
Mouse anti-human CD105 (Thermo Scientific. US) 10 µl en 100 µl	Donkey anti-mouse 555 (Life Technologies. US) 0.5 µl en 100 µl
Rat anti-human CD45 (NovusBio. US) 1 µl en 100 µl	Donkey anti-rat 488 (Life Technologies) 0.5 µl en 100 µl
Mouse IgG1 anti-human CD31 (Thermo Scientific. US) 1 µl en 100 µl	Donkey anti-mouse 647 (Life Technologies. US) 0.5 µl en 100 µl
Rabbit anti-human MMP-3 (CUSb. US) 1 µl en 100 µl	Donkey anti-rabbit 555 (Life Technologies. US) 0.5 µl en 100 µl
Rabbit anti-human CLGN (CUSb. US) 1 en 100 µl	Donkey anti-rabbit 647 (Life Technologies. US) 0.5 µl en 100 µl
Rabbit anti-human FoxF1 (Abcam. US) 2 µl en 100 µl	Donkey anti- rabbit 647 (Life Technologies. US) 0.5 µl en 100 µl
Rabbit anti-human MMP-1 (CUSb. US) 1 µl en 100 µl	Donkey anti-rabbit 647 (Life Technologies. US) 0.5 µl en 100 µl

Table 7: Antibodies used in the determination of the LRMSC

4.4.6 - Proliferation assay:

Differences in cell proliferation were determined by the growth in the amount of DNA in culture during 3 days using CyQUANT® Cell Proliferation Assay Kit (Invitrogen). Cells were plated on 96 well plate (Thermo Fisher, US) at a density of $5 \cdot 10^3$ and 10^4 cell/well to generate two proliferative curves. For each day a plate was washed and froze at -80°C . For determination, the CyQUANT (a green fluorescent dye when bound to nucleic acids) were added and the readings were performed in the spectrophotometer Synergy (Biotek, US) Ratios of the fluorescence from day 2 and 3 respect day 1 were calculated.

4.4.7 - Senescence and telomere length:

In order to determine the aging status of the LRMSC, the senesce status was tested and the telomere length quantified.

Senesce assay was performed using the senescence cells histochemical staining kit (Sigma, US) following manufacturer instructions. Briefly, SDC cells at various passages were washed in PBS, fixed with the kit fixative for 7 mins, washed 3 times with PBS and incubated overnight at 37°C (without CO₂) with the X-gal staining solution. At the end of the incubation the cells were washed with PBS and watched under light microscope.

At passage 5 of all the cultured cells a part of them was harvested, centrifuged at 400 g 6 min and flash-frozen (dry pellet). Genomic DNA from LRMSC dry pellets was extracted using Purelink genomic DNA Mini Kit (Invitrogen, US) and stored at 20°C until analysis. From the same subjects DNA from blood and lung tissue was also extracted using the QiaAmp DNA Blood mini kit (Qiagen, Valencia CA, US) and Purelink genomic DNA Mini Kit (Invitrogen, US) respectively.

Telomere length was measured in relation to the concentration to the single copy gen albumin following the methodology developed by Cawthon, et.al. [232], primers are listed in Table 8. In this multiplex reaction the primers pairs had different melting temperatures allowing the specific acquisition of the SYBR green signal at different temperatures. The telomere is more abundant than the albumin, in this manner the early value of the CP at 74°C represents only telomere amplification. The second acquisition at 88°C is specific for the albumin because the telomere amplimer at this temperature is melted and gives no signal.

Gene	Primer Sequence	Fragment size (bp)
Telomere	F: AACTAAGGTTTGGGTTTGGGTTTGGGTTTGGGTTAGTGT R: TGTTAGGTATCCCTATCCCTATCCCTATCCCTATCCCTAACA	79
Albumin	F: CGGCGGCGGGCGGGCGGGCTGGGCGGAAATGCTGCACAGAATCCTTG R: GCCCGGCCCGCCGCGCCCGTCCCGCCGAAAAGCATGGTGCCTGTT	98

Table 8: Primer sequences for the telomere determination

For the qPCR reaction, telomeres primers were used at a concentration of 1500 nM each, with 100 nM of each albumin primer, 1X of SYBR Green 480 PCR Master Mix (Roche) and 20 ng of DNA (quantified by Qubit, Life Technologies, US). Samples were

run in triplicate and the standard curves of the two genes were generated using serial dilution of DNA (50ng to 6,25ng). Relative telomere length was calculated as the ratio between the two genes. Thermal cycling conditions were specifying in the Table 9.

Denaturalization and activation	
95°C	15 minutes
Pre-amplification: 2 cycles	
94°C	15 seconds
49°C	15 seconds
Amplification cycles: 40	
94°C	15 seconds
62°C	10 seconds
74°C	15 seconds with signal acquisition
74°C	10 seconds
88°C	15 seconds with signal acquisition
Generation of melting curves	
72°C to 95°C	

Table 9: Thermal cycling conditions for the RT-PCR

4.4.8 – Immunomodulation assay:

4.4.8.1 - *In vitro* co-culture assays:

In order to determine the immunomodulatory properties of LRMSC an *in vitro* co-culture experiment to assess their ability to suppress T and B lymphocytes proliferation was set up. LRMSC from 8 non-smokers, 4 smokers with normal lung function, 7 COPD former smoker patients, 8 COPD current smokers and as controls 3 lung fibroblast cell lines and 2 BM-MSc cell lines were evaluated in triplicates at the same time.

A donor buffy coat (obtained from the Hospital Clinic) was diluted 1:10 in PBS and carefully added 3 parts of the diluted buffy on the top of one part of Ficoll (Fresenius Kabi, Norway) without mixing the two phases. The two phases tubes were centrifuge 2000 rpm 20 mins to make a gradient separation of the cells. The obtaining interphase contains the peripheral blood mononuclear cells (PBMC) that were collected and washed in PBS 2 times.

T and B lymphocytes (CD3pos T cells and CD19pos B cells) were purified from the PBMCs using appropriate negative selection kits (Miltenyi Biotec, Germany). Purity of the cell separations was evaluated by flow cytometry with an anti-CD3 and anti-CD19

(same antibodies described in section 4.3.4 – Flow cytometry staining) and at least 95% cell purity was obtained.

The lymphocytes were stained with 5 mM carboxyfluorescein succinimidyl ester, CFSE cell trace (Life Technologies, US). T cells were activated with T cell activation/expansion Kit (Miltenyi Biotec, Germany) one bead for 2 cells in sphere culture medium supplemented with 10% human FBS (Life Technologies, US) at $5 \cdot 10^5$ cells/ml. B cells were activated with 2 $\mu\text{g/ml}$ F(ab')₂ anti-human IgM+IgG (Affymetrix eBioscience), 1 $\mu\text{g/ml}$ CD40L (R&D, US), 20 IU/ml rhIL-4 (Sigma, US), in sphere culture medium supplemented with 10% FBS (Life Technologies, US) at $1,5 \cdot 10^5$ cells/ml.

LRMSC were plated 24 h before to form spheres at 10^4 cells/well for the T lymphocyte assay and $3 \cdot 10^4$ cells/well for the B lymphocyte assay. The LRMSC were then mixed with the T or B lymphocytes in 96-well adherent plates (Termo Fisher, US) with LRMSC at a ratio (1:1) for the B cells and (1:10) for the T cells. The experiment was run in triplicate during 4 days for the T lymphocyte co-culture and 7 days for the B lymphocytes. A summary of the *in vitro* assay was represented in the Figure 36.

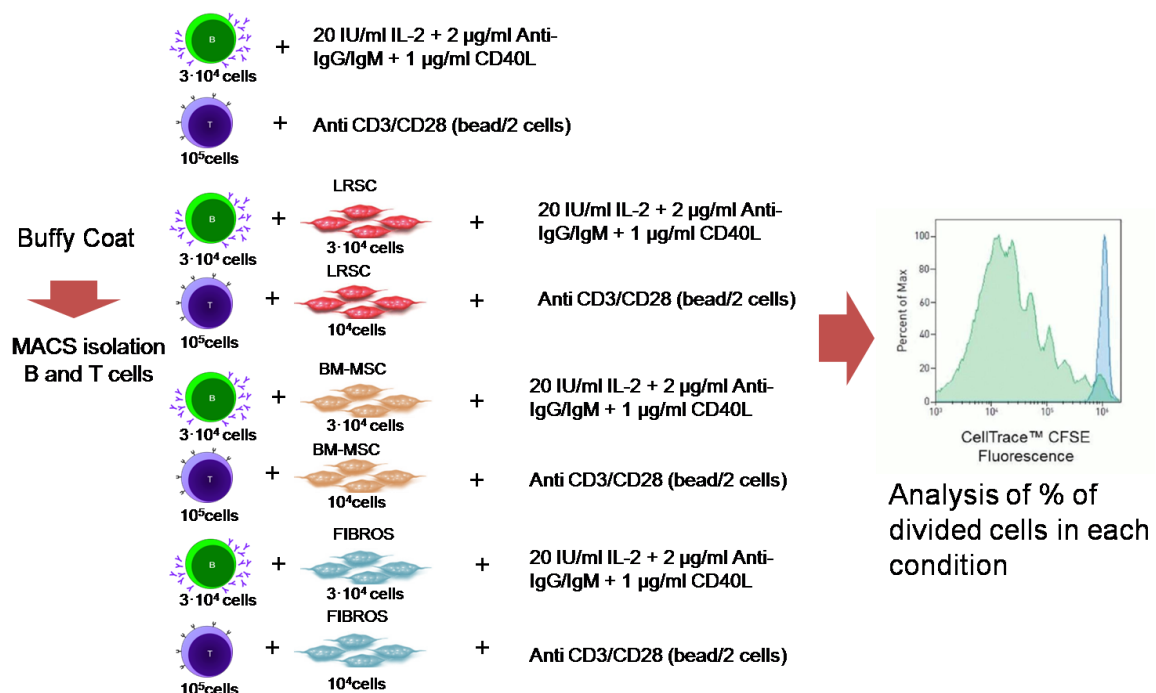


Figure 36: Schematic representation of the *in vitro* co-culture assay

At the end of the co-culture, cells were detached, resuspended and stained with: CD3-Alexa750 (Beckman), CD8-PECy7 (BD), CD4-APC (BD) and 7-AAD (BD) for T cells and CD19-BV421 (BD), and 7-AAD (BD) for B cells. The 7-AAD allows the exclusion of the dead cells and the evaluation of the proliferation was made by the CFSE (FITC) intensity dilution on the CD3⁺CD4⁺/CD8⁺ for the T cells and on the CD19⁺ for the B cells. FACS tubes were read in a BD LSRFortessa with 4 lasers in the Flow cytometry facility of the Institut Investigació Germans trias i Pujol (IGTP).

5 – RESULTS

The results in relation to objective-1 have been already published [233]. The rest are being written now, and I hope to be able to submit them for publication during the summer.

5.1 – RESULTS IN RELATION TO OBJECTIVE-1: MOLECULAR PULMONARY IMMUNE RESPONSE NETWORK

5.1.1 - Characterization of patients and analysis strategy

Figure 37 shows that, in the 70 patients studied: (*Panel A*) the proportion of patients with CT emphysema increased in relation to the severity of airflow limitation (GOLD grade¹), so CT emphysema was present in 89% of patients with GOLD grade 3-4 and only in 47% of those with GOLD grades 1-2 (Fisher $p = 0.0021$; 95% confidence interval [CI] 37.3- 74.4); (*Panel B*) the presence of CT was highly related to a reduced carbon monoxide diffusing capacity of the lung (DL_{CO}), a well validated surrogate marker of emphysema [234]. Hence, no patient with $DL_{CO} > 80\%$ reference value had CT emphysema, whereas more than 80% of patients with $DL_{CO} < 60\%$ ref. presented it; and, (*Panels C-D*) there was a clear relationship between the severity of DL_{CO} impairment and that of airflow limitation.

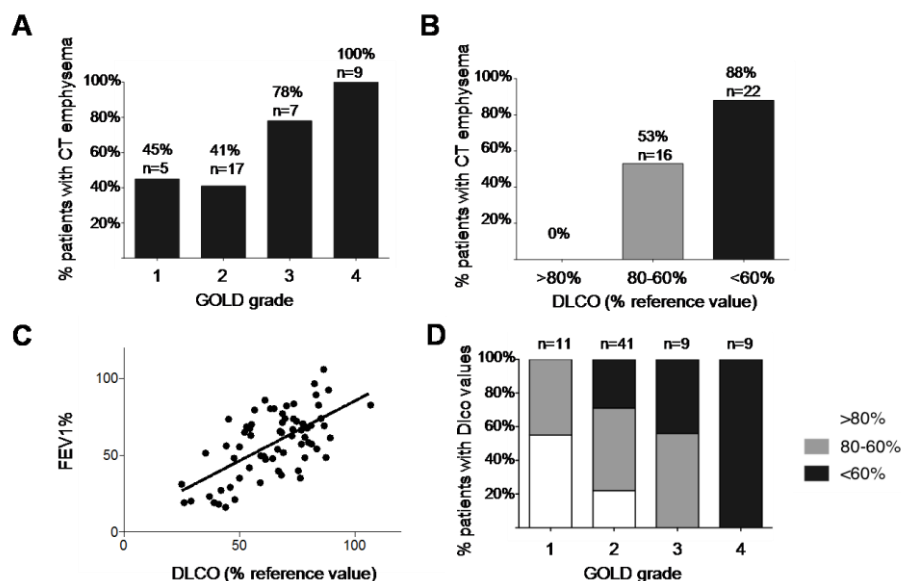


Figure 37: Proportion and number of patients with CT emphysema by GOLD airflow limitation (Panel A) and DLCO values (>80%, 60-80% and <60% reference) (Panel B). Panel C shows the correlation between FEV1 (% ref.) with DLCO (% ref.) values, and Panel D the distribution of DLCO values by GOLD airflow limitation

Based upon these observations, and in order to explore our working hypothesis, we designed an *analysis plan* that included four different lung tissue gene expression comparisons (Table 10): (1) the two most *extreme* groups, this is, 25 patients with *severe emphysema* ($DL_{CO} < 60\%$ ref. and/or CT emphysema) vs. 15 patients with *bronchiolitis* ($DL_{CO} > 80\%$ ref. and absence of CT emphysema). We acknowledge that patients with severe emphysema may also have a component of bronchiolitis, but recent pathological [235] and imaging data [236] support this operational classification because terminal bronchioles are extremely reduced in patients with emphysema; (2) the group of patients with bronchiolitis studied above with a group of patients with intermediate characteristics (n=30, with or without CT emphysema and a DLCO value between 60-80% ref.); (3) we divided this latter group of patients with intermediate characteristics into those with *moderate emphysema* (DL_{CO} 60-70% ref. and CT emphysema; n=12) vs. those with *mild emphysema* (DL_{CO} >70-80% ref. and no CT emphysema; n=11). Seven intermediate patients did not meet any of these criteria and were therefore not included in comparison 3. These two groups are likely to have varying degrees of both airway and parenchymal disease. And, finally (4): given the tight association between the severity of airflow limitation and the presence of emphysema (Figure 37), to dissect the influence of these two factors we compared patients with the same GOLD grade of airflow limitation (GOLD 2) with severe emphysema (n=12) or bronchiolitis (n=9), using the same criteria as per the extreme group comparison presented above (see (1)).

	Comparison 1			Comparison 2		
	Severe emphysema n=25	Bronchiolitis n=15	p value	Intermediate group n=30	Bronchiolitis n=15	p value
CT emphysema (Yes/No)	23/2	0/15		16/13	0/15	
DL_{CO} group	<60% ref.	>80% ref.		60-80% ref.	>80% ref.	
Gender F/M	3/22	2/13	ns	2/28	2/13	ns
Age (yrs.)	62.8±9.7	70.5±6.1	0.013	67.1±7.9	70.5±6.1	ns
Body mass index (Kg/m ²)	26.8±4	28.2±5.1	ns	27.5±4.5	28.2±5.1	ns
Smoking exposure (pack-years)	54.4±28.2	48.7±25.5	ns	61.9±23.6	48.7±25.5	ns
FEV ₁ /FVC (%)	44.2±14.5	58.4±8.8	0.002	55.8±9.0	58.4±8.8	ns
FEV ₁ (% reference)	40.9±20.7	73.9±16.9	<0.0001	62.4±14.7	73.9±16.9	ns
DLco (% reference)	44.8±10.3	95.2±24.6	<0.0001	70.9±5.3	95.2±24.6	<0.0001

	Comparison 3			Comparison 4		
	Mild Emphysema n=11	Moderate Emphysema n=12	p value	Severe Emphysema GOLD grade 2 n=12	Bronchiolitis GOLD grade 2 n=9	p value
CT emphysema (Yes/No)	0/11	12/0		10/2	0/9	
DL _{CO} group	>70-80	<70-80		<60	>80	
Gender F/M	1/10	1/11	ns	1/11	1/8	ns
Age (yrs.)	66.8±7.9	68.3±4.39.3	ns	71.6±6.7	68.3±5.8	ns
Body mass index (Kg/m ³)	27.1±5.1	28.6±4.3	ns	28.4±3.2	29.1±5.0	ns
Smoking exposure (pack-years)	57.2±25.9	61.18±32.7	ns	67.6±30.2	45.7±26.5	ns
FEV ₁ /FVC (%)	58.1±9.0	53±10.7	ns	56.8±7.1	54.8±7.5	ns
FEV ₁ (% reference)	63.3±9.4	61.6±17.4	ns	62.1±7.7	68.8±6.6	ns
DL _{CO} (% reference)	76.2±2.5	66±2.9	<0.0001	50.3±6.8	99.6±30.9	0.0002

Table 10: Characteristics of COPD patients included in the study. Statistically significant differences between the three groups were calculated using the Kruskal-Wallis test, followed by post-hoc comparisons (Mann-Whitney) if appropriate.

5.1.1.1 - Comparison 1: Severe emphysema vs. bronchiolitis

We found 249 differentially expressed (DE) genes (FDR<0.01 and LogRatio >0.5) in lung tissue samples of patients with severe emphysema vs. bronchiolitis (Table 10), 120 of which were up- and 129 down-regulated in severe emphysema.

Amongst the *up-regulated* genes in emphysema: (i) there were 4 immunoglobulin chains and MS4A1 (CD20), a B lymphocyte marker [237], among the top ten DE genes; (ii) we observed enrichment of ontologies related to the immune response, including inflammation, B cell response, response to bacteria and fungi.

Amongst *down-regulated* genes in emphysema (i.e., relatively up-regulated in bronchiolitis) we: (i) identified circadian cycle regulators (PER2 and PER 3) among the top DE genes (ii) found enrichment in ontologies related to remodeling and scarring including extracellular matrix changes (adhesion), cell development and mechanisms regulating cell shape.

5.1.1.1.1 - Gene Set Enrichment Analysis (GSEA)

GSEA of C7 immunologic signatures in severe emphysema showed a trend to enrichment of genes expressed in B cells. To complement and extend this observation we also used GSEA to mine the *Immune Response in Silico* (IRIS) transcriptional compendia [238], which includes patterns of gene expression that are distinct among immune cell lineages [239]. This analysis also identified an enrichment of B cell related genes in severe emphysema. Likewise, using the Gene Enrichment Profiler tool [225], we confirmed that up-regulated genes in emphysema were related to B cell containing tissues and activated B cells. Finally, to validate *in silico* our observations, we also used GSEA to contrast our results with those published by Campbell *et al*, who used micro CT and laser capture dissection to investigate the transcriptomic signature of emphysema [224]. We found a significant enriched core of genes up-regulated in both datasets (normalized enrichment score (NES) = 1.36, FDR= 0.04).

5.1.1.1.2 - Network structure of the immune response in severe emphysema vs. bronchiolitis

To contrast the organization of the pulmonary immune response in emphysema and bronchiolitis, we selected the list of 2,189 genes included in the GO term “Immune System Process” (GO:0002376) (<http://www.ebi.ac.uk/QuickGO>) to build gene co-expression correlation networks both in emphysema (Figure 38) and bronchiolitis (Figure 3).

In *emphysema*, 636 of the 2,189 GO genes (29%) showed strongly related co-expression ($|R| > 0.8$, $p < 10^{-5}$) and formed (Figure 38) one large (A) and 3 smaller and independent co-expression networks (B, C, D). Thirty-six of these 636 genes (5.6%) were DE *vs.* bronchiolitis and, interestingly, 34 of them (94%) were integrated into the large co-expression network (yellow shaded area in A, Figure 38), whereas only two (DEFA4 and DEFA1) were identified in one of the small, independent, ones (Figure 38, Panel C). Of note: (i) DE genes related to B cell activation, homing, lymphoid follicle formation and immunoglobulin production (CXCL13, LTB, CCL19, TNFRSF17, MS4A1, POU2AF1 and immunoglobulin chains) occupied a central position in these yellow shaded area (Figure 38, Panel A); and, (ii) CXCL13 expression correlated with

that of (Figure 38, Panel A) AIM2, TLR10 and ISG20 (innate immune receptors for viruses and bacteria [240]), CD19, MS4A1 (CD20) and CR2 (markers of B cell lineage [241]) and FOXF1, RHOH, BLK (molecules related to B cell activation [242, 243]).

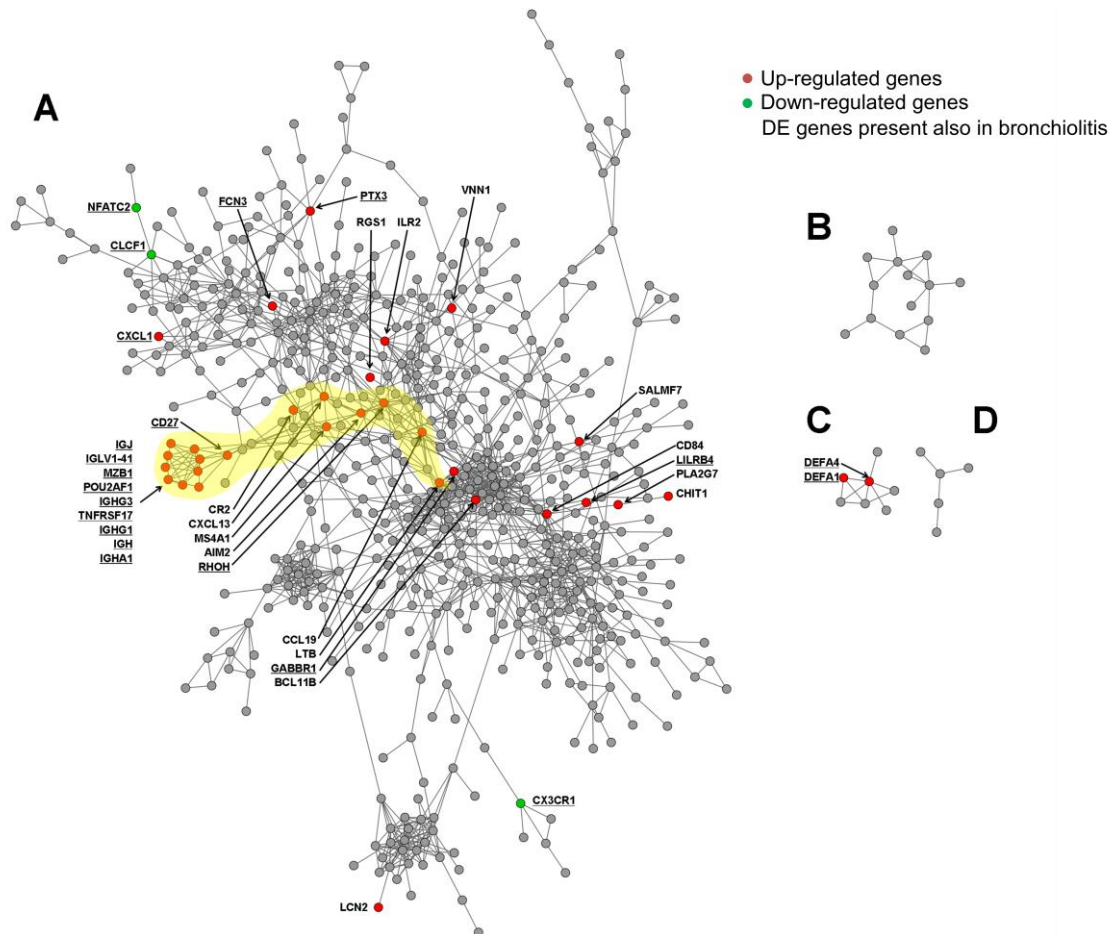


Figure 38: Correlation ($|R| > 0.8$, $p < 10^{-5}$) gene expression network of the 2,189 genes included in GO:0002376 (“Immune System Process”) in patients with emphysema. Red and green nodes indicate DE vs. bronchiolitis. Underlined genes indicate that they were DE in the bronchiolitis network also. Panels A, B, C, D highlight the different sub-networks identified. The yellow shaded area indicate a group of DE genes related to B cell activation, lymphoid follicle formation and immunoglobulin production (CXCL13, LTB, CCL19, TNFRSF17, MS4A1, POU2AF1, Immunoglobulin chains) occupying a central position in the main network.

In *bronchiolitis* (Figure 39), 851 out of the 2,189 GO genes (39%) showed significant ($|R| > 0.8$, $p < 10^{-5}$) co-expression and formed one large (A) and seven smaller and independent co-expression networks (B to H). Thirty of these 851 (3.5%) genes were DE genes vs. emphysema. Of note: (i) 11 DE genes identified in the emphysema network related to immunoglobulin production (Figure 38, Panel A, yellow shaded area) were no longer integrated into the large network in bronchiolitis (Figure 39, Panel A) but formed a small and independent network (Figure 39, Panel B, blue shaded area); and, (ii) at variance with emphysema too, CXCL13, CCL19, MS4A1 and LTB (related

to lymphoid follicle formation) were not included in the core co-expression network and were not connected to the immunoglobulin core.

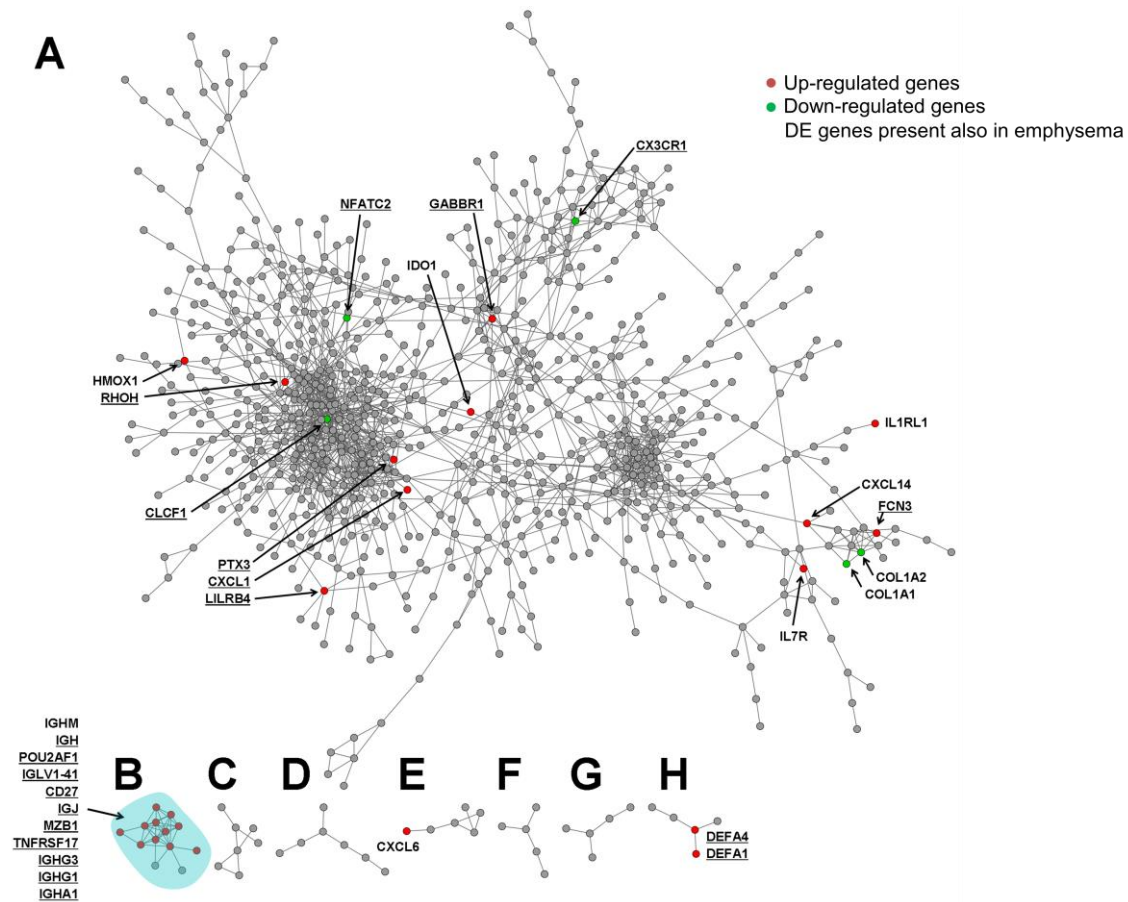


Figure 39: Correlation ($|R| > 0.8$, $p < 10^{-5}$) gene expression network of the 2,189 genes included in GO:0002376 (“Immune System Process”) in patients with bronchiolitis. Red and green nodes indicate DE vs. bronchiolitis.

Underlined in blue DE genes also present in the emphysema network. Panels A to H highlight the different sub-networks identified. The blue shaded area indicates a group of DE genes related to B cell activation, lymphoid follicle formation and immunoglobulin production (CXCL13, LTB, CCL19, TNFRSF17, MS4A1, POU2AF1, Immunoglobulin chains) which, at variance with what occurs in patients with emphysema (Fig. 3, yellow shaded area), are no longer incorporated into the main network.

The comparison of the emphysema (Figure 38) and bronchiolitis (Figure 39) co-expression networks, revealed that: (i) they shared 362 genes (57% of the emphysema and 43% of the bronchiolitis genes) and only 21 of them were DE genes including B cell related genes; (ii) among the genes identified exclusively in the emphysema network ($n=274$), functions related to the B cell response, T cell response and NF- κ B cascade were enriched, whereas biological processes related to lung development, proliferation and activation (Wnt, EGFR and MAPK pathways) were enriched among those identified exclusively in the bronchiolitis network ($n=489$). As we constructed

Results show that: (1) DE genes related to B cell activation, homing and lymphoid follicle formation (red dots), including CXCL13, LTB, CCL19, TNFRSF13B and MS4A1, are strongly correlated in emphysema but not in bronchiolitis (orange and green edges in Figure 40); (2) the immunoglobulin production sub network (blue circled area) is linked to the main network through two genes (blue arrows): TNFRSF13B (also known as TACI, a BAFF receptor important in B cell activation and survival [244]) and CD19 (a B cell receptor with a key function to enhance B cell antigen recognition and signaling [245]).

5.1.1.2 - Comparison 2: Intermediate group vs. bronchiolitis

Given that most COPD patients have varying proportions of both emphysema and bronchiolitis, we sought to evaluate which features of the severe emphysematous signature identified above can also be found in COPD patients with intermediate phenotype (DL_{CO} 60-80% ref.), of whom only half (53%) showed evidence of CT emphysema (Table 10 and Figure 37, Panel B). The number of DE genes between these intermediate group and patients with bronchiolitis was low ($n=77$; 40 up- and 37 down-regulated). Figure 41 shows that 37 of these 77 DE genes (48%) were also DE in the severe emphysema group described above and, interestingly, 19 of them (76.3%) were related to lymphoid follicle formation and B cell activation (Figure 41), indicating that the distinct B cell signature identified in severe emphysema is already identifiable in this intermediate group.

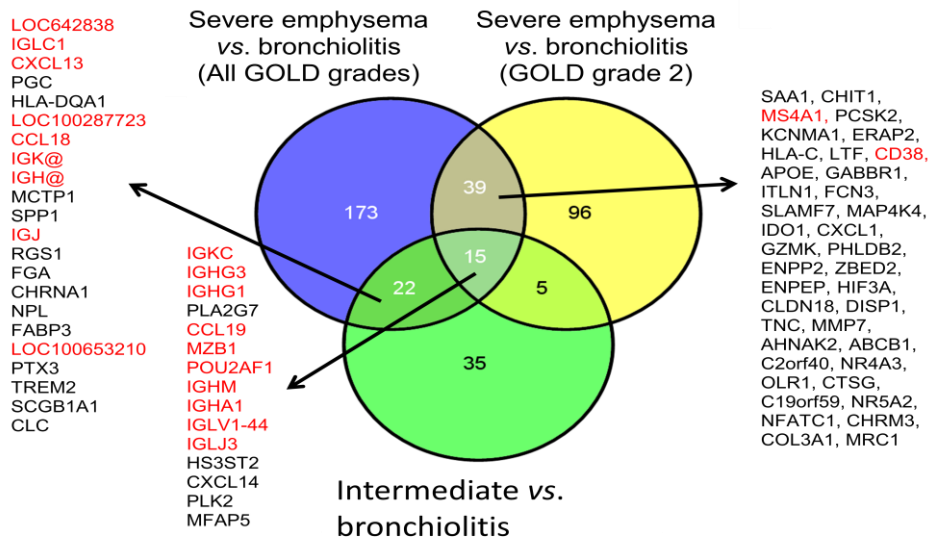


Figure 41: Venn diagram of differentially expressed genes in: (1) Blue circle: emphysema vs. bronchiolitis in patients studied (n=40), irrespective of their GOLD grade of airflow limitation; (2) Yellow circle: emphysema vs. bronchiolitis in patients with GOLD grade 2 (n=21); and, (3) Green circle: Intermediated patients vs. bronchiolitis (n=45). Figures indicate the number of genes shared by each comparison. Lists indicate individual genes (red: up-regulated genes related to B cell biology).

5.1.1.3 - Comparison 3: Moderate vs. mild emphysema

Given that the intermediate group is heterogeneous, we split it in two subgroups: those with *moderate* and those with *mild* emphysema, as described in Table 10. The number of DE genes between these two groups was 227 (156 up- and 70 down-regulated). Figure 42 shows that 45 of these 227 DE genes (19.8%) in patients with moderate emphysema were also DE in patients with severe emphysema. Genes related to lymphoid follicle formation and B cell activation (Figure 42, red font) were also identified in patients with moderate emphysema.

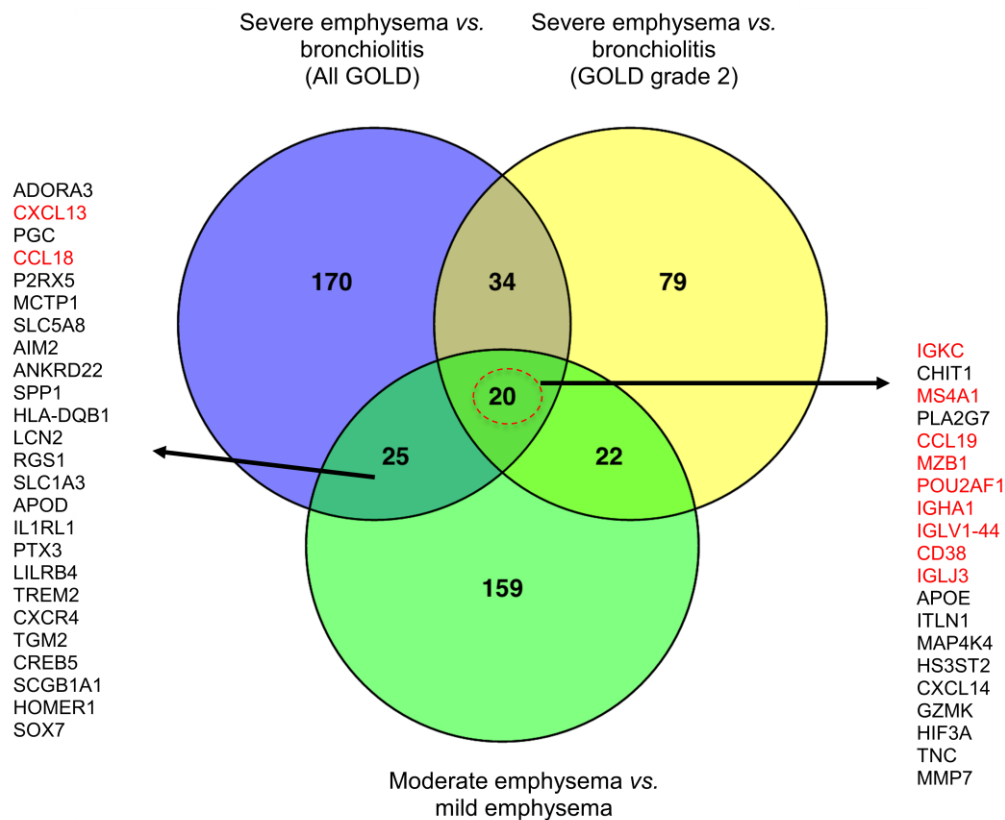


Figure 42: Venn diagram of differentially expressed genes in: (1) Blue circle: severe emphysema vs. bronchiolitis in patients studied (n=40), irrespective of their GOLD grade of airflow limitation; (2) Yellow circle: severe emphysema vs. bronchiolitis in patients with GOLD grade 2 (n=21); and, (3) Green circle: moderate emphysema vs. mild emphysema (n=23). Figures indicate the number of genes shared by each comparison. Lists indicate individual genes (red: up-regulated genes related to B cell biology).

5.1.1.4 - Comparison 4: Assessment of airflow limitation severity influence

Given the relationship observed between the severity of airflow limitation and the prevalence of emphysema (Figure 37), as well as the different airflow limitation severity observed in patients with bronchiolitis vs. severe emphysema (Table 10), to dissect the effect of the pathological abnormalities themselves (emphysema vs. bronchiolitis) on gene expression from that of their functional consequence (airflow limitation severity), we explored differences in gene transcription in patients with emphysema (n=12) or bronchiolitis (n=9) with the same degree of airflow limitation (GOLD grade 2) (Table 10). This analysis identified 155 DE genes (85 up and 70 down-regulated, Figure 41). Fifty-four of these 155 DE genes (35%, Figure 41) were also identified in the original analysis of all patients with emphysema vs. bronchiolitis (i.e.,

independently of the level of airflow limitation). Twelve of these genes (22%) were related to B cell activation and lymphoid follicle formation (Figure 41, red). Hence, these results are in keeping with our observations in the entire population discussed above and further support a prominent role of B cells in emphysema.

5.1.2 - Functional translation of transcriptomic results

To explore the functional translation of the transcriptomic B cell signature seen in emphysema (Figure 38), we perform three additional analyses. Firstly, we confirmed by qPCR the DE of 3 of the genes involved in B cell recruitment, lymphoid follicle formation and immunoglobulin production (CXCL13, CCL19, POU2AF1) [82, 246], and one acute phase protein (fibrinogen) identified using micro-arrays. For this analysis, we expanded the original population of patients discussed above with 24 additional patients in order to increase sample size, whose main clinical characteristics are shown in Table 11.

Additional tissue for qPCR validation	COPD		
Number of COPD patients	24		
Age (yrs.)	68.7		
BMI (Kg/m ²)	28.35		
Smoking exposure (pack-years)	61.04		
Smoking status (former/current)	24/0		
FEV ₁ /FVC (%)	58.93		
FEV ₁ (% reference)	69.35		
Tissue analyzed by IF	COPD E & Gold grades 3-4	COPD E & Gold grades 1-2	COPD Bronchiolitis Gold grades 1-2
Number of patients	8	4	9
Age (yrs.)	55.9±4.7	63.3±8.9	66.2±9.0
BMI (Kg/m ²)	26.0±3.2	24.1±2.38	26.3±3.8
Smoking exposure (pack-years)	45.4±22.4	48.3±13.9	51.6±22.1
FEV ₁ /FVC (%)	32.6±11.0	56.8±1	61.7±9.5
FEV ₁ (% reference)	24.0±7.1	73.0±15.5	72.6±13.2

Table 11: Clinical characteristics of additional patients included in the study for the purposes of qPCR validation of selected genes (top) and tissue immunofluorescence (IF) analysis (bottom).

As shown in Figure 43, consistent with our array results, CXCL13, CCL19, POU2AF and FGA were up-regulated in patients with any degree of emphysema detected by CT scan.

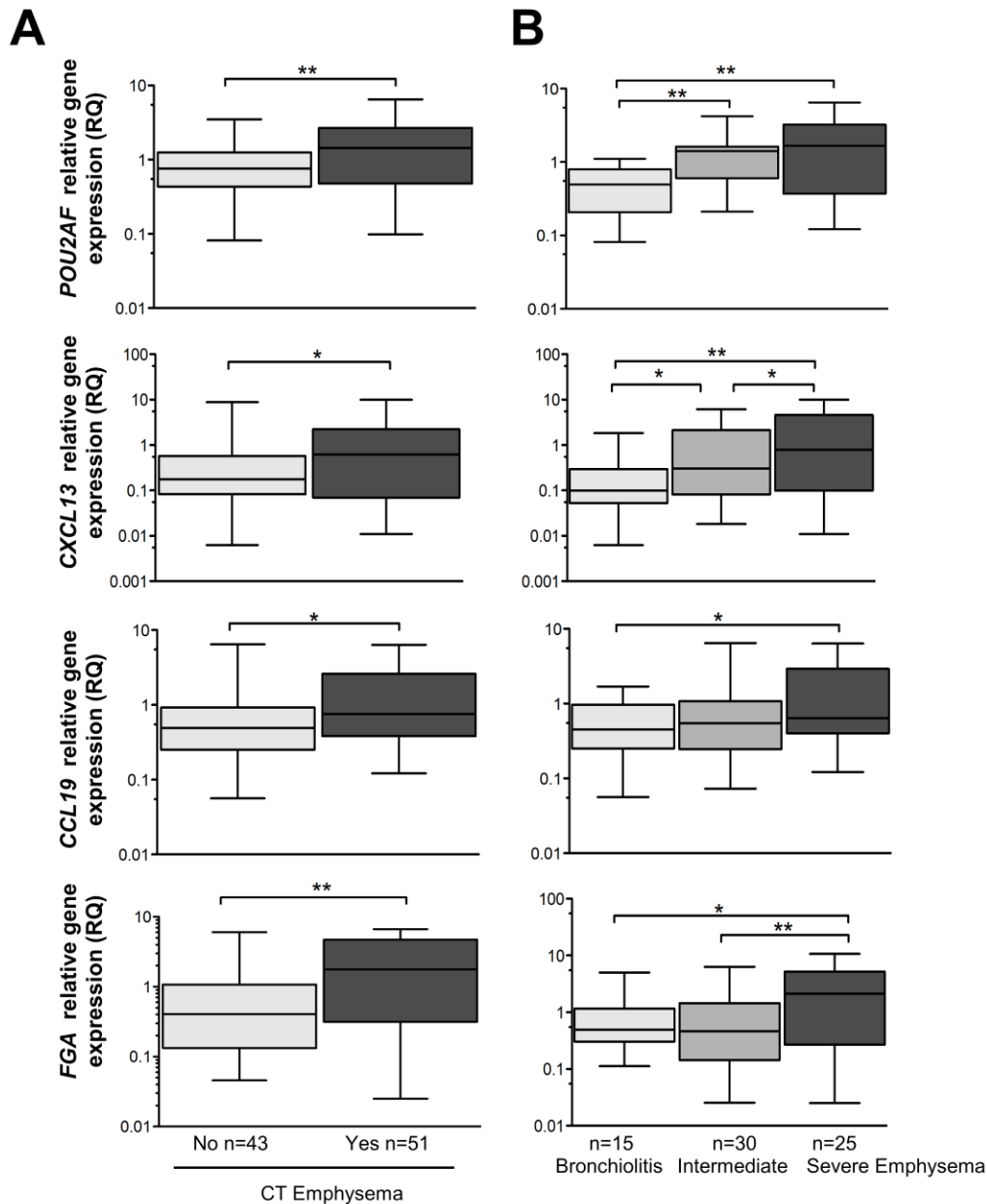


Figure 43: Validation by qPCR of emphysema related genes. Mean (\pm SD) expression level values by qPCR of POU2AF1 (Panel A), CXCL13 (Panel B), CCL19 (Panel C) and fibrinogen α chain (Panel D) in COPD patients stratified by the presence/absence of CT emphysema or by their DLCO value (% ref). * p<0.05, ** p<0.01 in the t-test.

Secondly, given that the expression of both TNFRSF17 (a B cell specific survival receptor up-regulated in differentiated B cells [247], also known as BCMA) and

CXCL13 (a major B cell chemoattractant) were up regulated in emphysema (Figure 38), we compared protein levels of BCMA ligand (BAFF) and CXCL13 in lung tissue by ELISA in patients with severe emphysema and bronchiolitis. As expected, both proteins were elevated in the former patients (Figure 44 A-B).

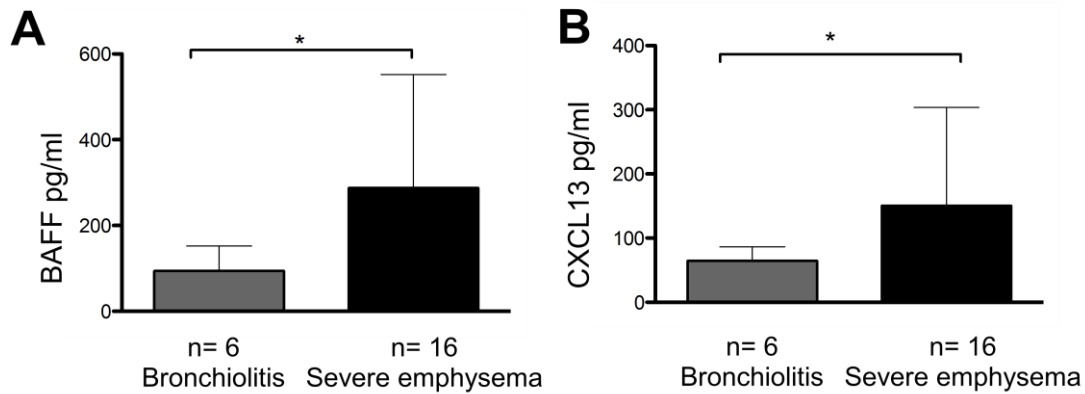


Figure 44: BAFF and CXCL13 protein content in emphysema. Mean (\pm SD) protein level measured by ELISA in lung tissue homogenates of BAFF and CXCL13 in patients with bronchiolitis or mixed disease (n= 6) and patients with emphysema (n=16). * p<0.05

Thirdly, we used immunohistochemistry techniques (anti CD20) to further delineate the role of B cells in emphysema (Figure 45). We found that, in lung tissue samples of patients with severe emphysema the area stained with anti CD20 was higher than in bronchiolitis, and increased further with airflow limitation severity (Figure 45A). Besides, we observed that in patients with emphysema (irrespective of their GOLD grade of airflow limitation) there were CD20+ B cells aggregates (i.e., lymphoid follicles) expressing mainly IgM (Figure 45 B and F) with B cells positive for the proliferation marker Ki67 (Figure 45 D and H), phosphorylated NF-kB p65 (Figure 45 E and I) indicating that these follicles include B cells that are active and IgG+ isotype switched B cells (Figure 45 C and G) [248, 249].

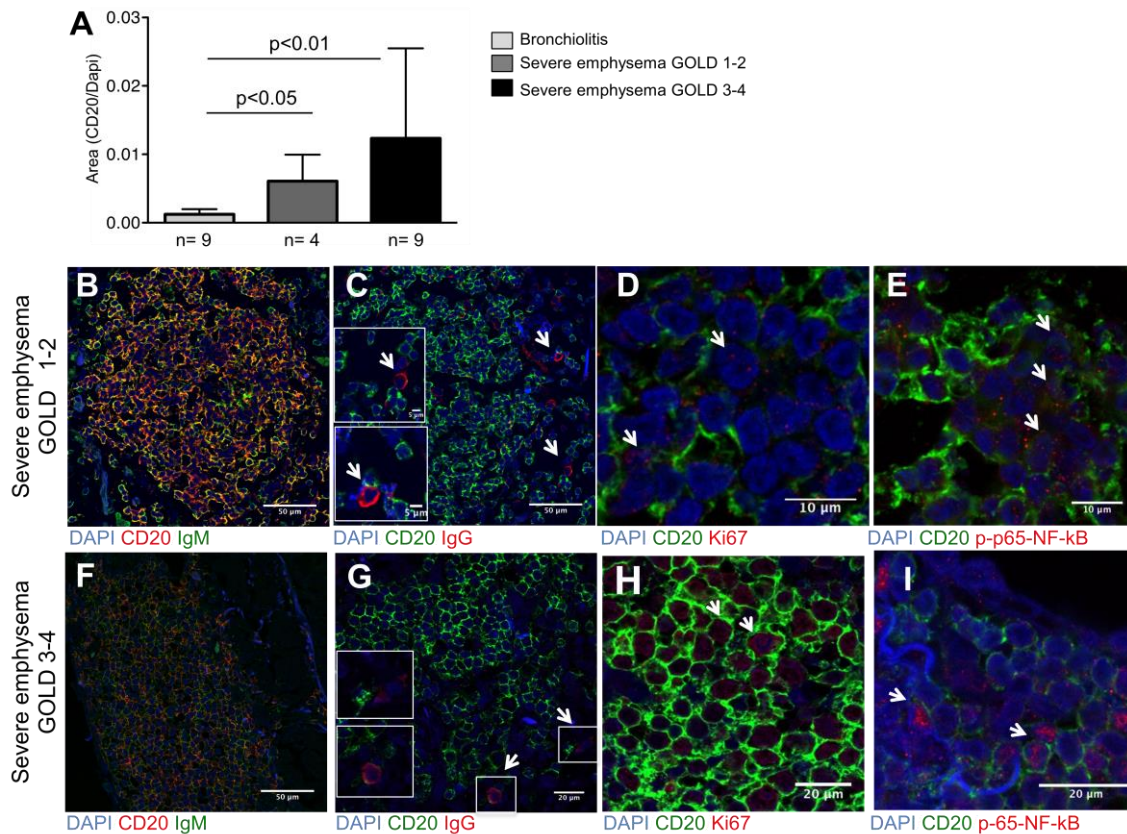


Figure 45: Panel A: % area stained with anti CD20 (over DAPI area) in patients with GOLD 1-2 with severe emphysema (E, n=5) or bronchiolitis (n=5), and in patients with GOLD 3-4, all with severe emphysema (E, n=5). Data is presented as mean±SD. Panels B-J present representative examples of confocal immunofluorescence characterization of lymphoid follicles in patients with emphysema (n=5 per group). Panels B and F, CD20 (red) and IgM (green) staining. Panels C and G CD20 (red) and IgG (green) staining, arrows point positive cells. Panels D and H-I CD20 (red) and Ki67 (green) staining, arrows point positive cells. Panels E and J CD20 (red) and NF-KB phosphorylated P65 (green) staining, arrows point positive cells.

5.2 – RESULTS IN RELATION TO OBJECTIVE 2: CELLULAR CHARACTERIZATION OF THE IMMUNE RESPONSE

5.2.1 –Study population

The main clinical characteristics of the four study groups population are summarized in Table 12. Briefly, the proportion of females was higher in non-smokers, normal lung function smokers were younger than COPD former smokers. The severity of the airflow limitation and tobacco exposure of current and former smokers with COPD was similar.

	Non Smokers n=23	Smokers n=12	COPD-FSs n=21	COPD-CS n=30
Gender (M/F)	5/18	7/5	19/2	22/8
Age	65.4 ± 12.3	59.1 ± 9.8 [†]	68.6 ± 7.0 [†]	64.8 ± 8.0
Pack/year		39.5 ± 19.9	54.86 ± 22.8	48.6 ± 19.1
BMI	27.9 ± 5.4	26.8 ± 5.3	27.7 ± 3.3	25.1 ± 3.8
FEV1 (% ref)	99.2 ± 8.1 ^{***.####}	94.9 ± 6.4 ^{++.††}	75.5 ± 17.2 ^{####.††}	77.5 ± 13.0 ^{***.++}
FEV1/FVC (%)	78.1 ± 3.9 ^{***.####}	77.1 ± 9.0 ^{+++†††}	59.7 ± 6.8 ^{####.†††}	61.8 ± 6.4 ^{***.+++}
DLCO	78.8 ± 19.4 ^{***}	77.7 ± 15.0 ⁺	71.0 ± 15.3	63.1 ± 11.3 ^{***.+}

Table 12: Clinical variables of the subjects enrolled in the cellular immune response. Comparison between non smokers and COPD current smokers is represented by *, non smokers and COPD former smokers with #, smokers and COPD current smokers with + and smokers and COPD former smokers with †. p-values are < 0,05 for one symbol, p-value < 0,005 for two symbols, p-value < ,0005 for three symbols and p-value < 0,00005 for four symbols.

5.2.2 - Characterization of the immune cell infiltrate in lung tissue

To characterize the composition of the immune infiltrate we used fresh lung tissue homogenates and analyzed by flow cytometry (as described in the methods section). The main constrain of the methodology is that we cannot evaluate the absolute changes in the number of infiltrating cells. Instead the present work analyses for each type of immune cell the changes in the proportion of the infiltrate. To do so, in each flow cytometry tube cells are stained with the hematopoietic lineage marker CD45. Then the populations of interest are referred as percentages of CD45+ cells.

Figure 46 shows that the percentage of CD45+ positive cells recovered from the lung disaggregates of the four study groups are not different. This result does not mean that the absolute infiltrate in lung tissue of the four study groups is similar; we cannot assess this because the total number of cells is not taken into account in the present analysis.

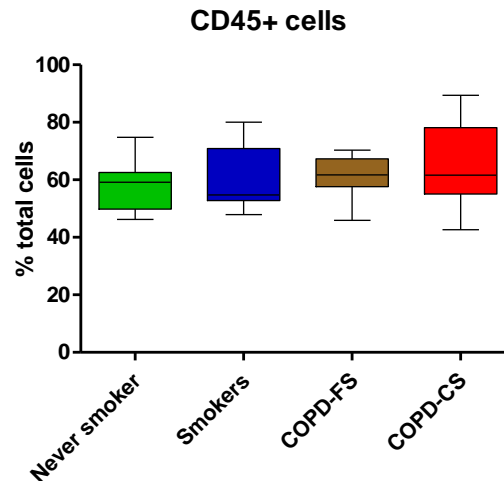


Figure 46: CD45+ cells in lung tissue homogenates by flow cytometry

To determine the percentage of Neutrophils, Macrophages, Monocytes, Mast cells, Natural killer cells (NK cells), Natural killer T cells (NKT cells), Dendritic Cells (DCs), B lymphocytes and T lymphocytes in the infiltrate we used 7 flow cytometry tubes (as described in methods). Figure 47 shows the results of lung tissue of the four study groups.

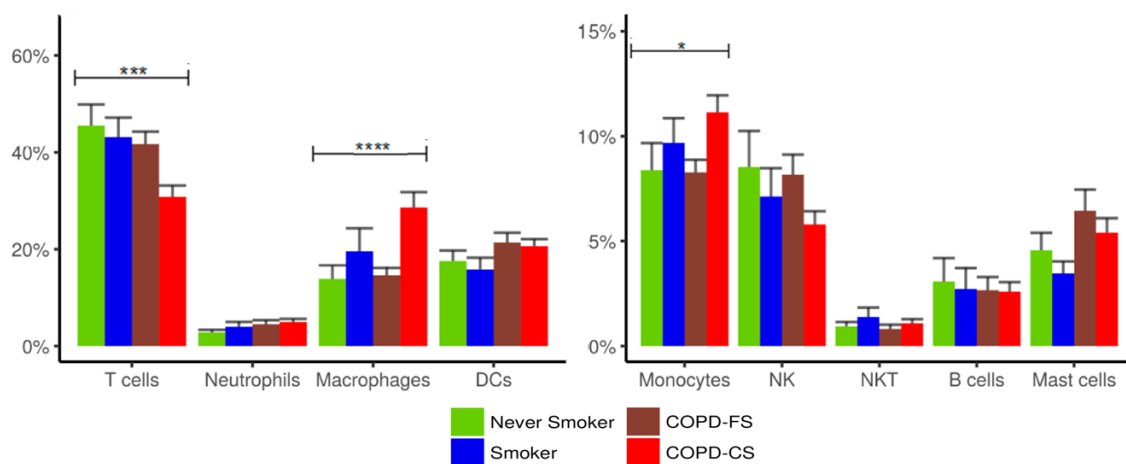


Figure 47: Abundance of the immune cell populations represented as percentage of CD45+ cells in lung tissue. P value corresponds to the result of the Kruskal–Wallis one-way analysis of variance; * p-value<0,05, ** p-value>0,005, *** p-value>0,0005, **** p-value>0,00005.

The most abundant populations were T cell lymphocytes (T-cells), macrophages (M0) and dendritic cells (DCs). Between the four study groups we observed significant differences in the percentage of lung T-cells, macrophages and monocytes (Figure 47). On reference to the decrease of T cells, the post-hoc test showed significant differences in the percentage of CD3+CD45+ T-cells in current smokers with COPD vs. non-smokers, smokers and former smokers with COPD (Figure 47). Next we assessed which T cell populations were involved in these decrease in percentages. Figure 48 shows that both CD4+CD3+CD45+ T cells and to a less extend CD8+CD3+CD45+ cells are decreased in the proportion of infiltrating cells in current-smokers with COPD.

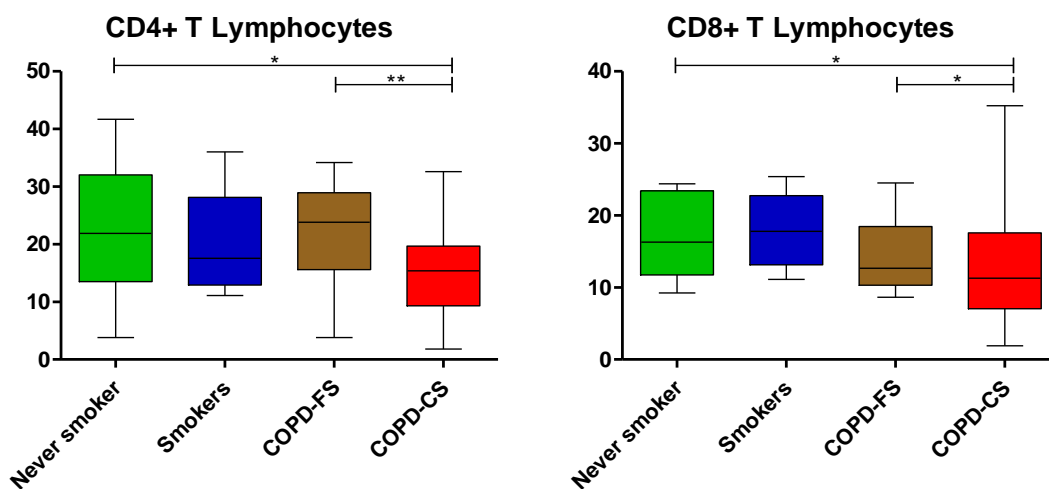


Figure 48: CD4+ and CD8+ T lymphocytes proportions in human lungs for the four studied groups. Between groups differences were assessed with a Kruskal-Wallis with a Mann-Whitney post hoc test. Asterisks indicate p values of the post-hoc test: * p-value<0,05, ** p-value>0,005.

Interestingly in never smokers the majority of TCD4+ and TCD8+ cells were CD28^{null} while active smoking reduced this percentage (Figure 49). In Smokers and COPD-CS CD4 CD28^{null} cells reduce to almost the half of the CD4 T lymphocytes (Figure 49A). For the CD8 T lymphocytes the reduction of the CD28^{null} population is higher for the Smokers (Figure 49B), although not significant.

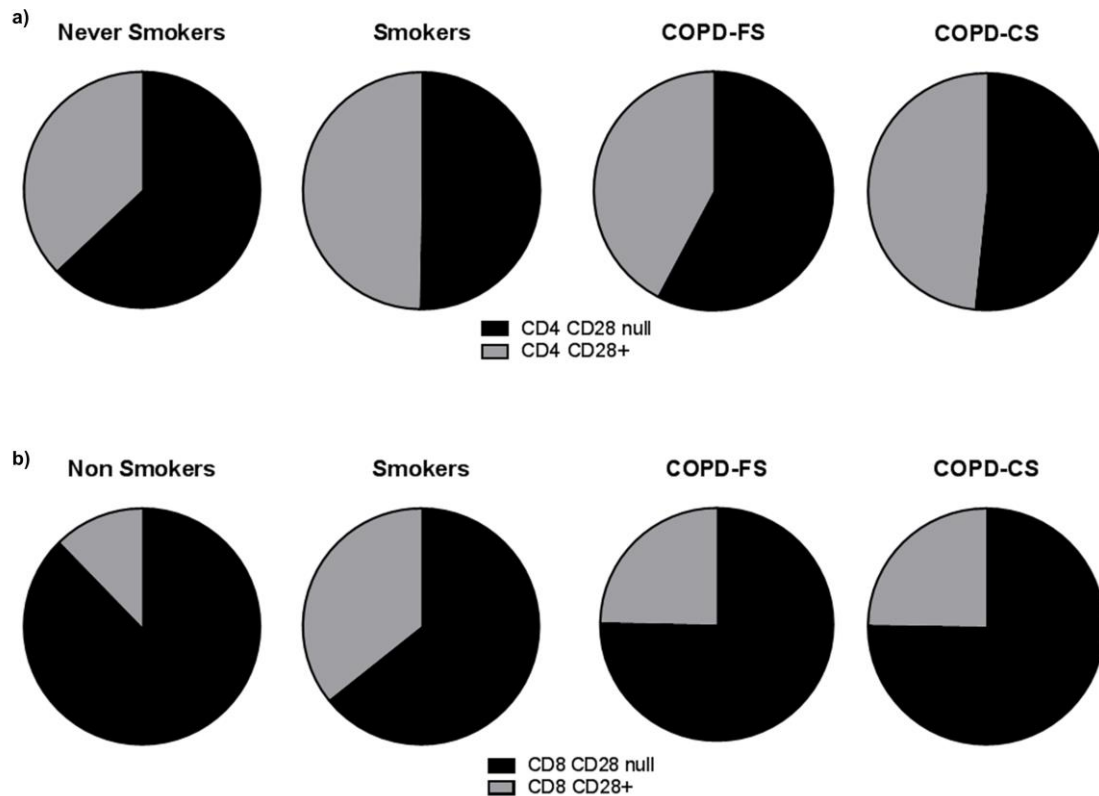


Figure 49: Expression of CD28 in a) CD4+ and b) CD8+ T lymphocytes

The observed decrease in the proportion of T cells in current smokers with COPD was mirrored by an increase in the percentage of macrophages in this group (Figure 50A). A deeper characterization of this populations showed that the increase of macrophages in current smokers with COPD is of intermediate phenotype (M1/M2, CD45+CD64+CD80+CD163+ cells (Figure 50C) and is accompanied by a decrease in the M1 pro-inflammatory macrophages CD45+CD64+CD80+cells (Figure 50B). No significant differences in the percentage of M2 macrophages were observed (Figure 50D).

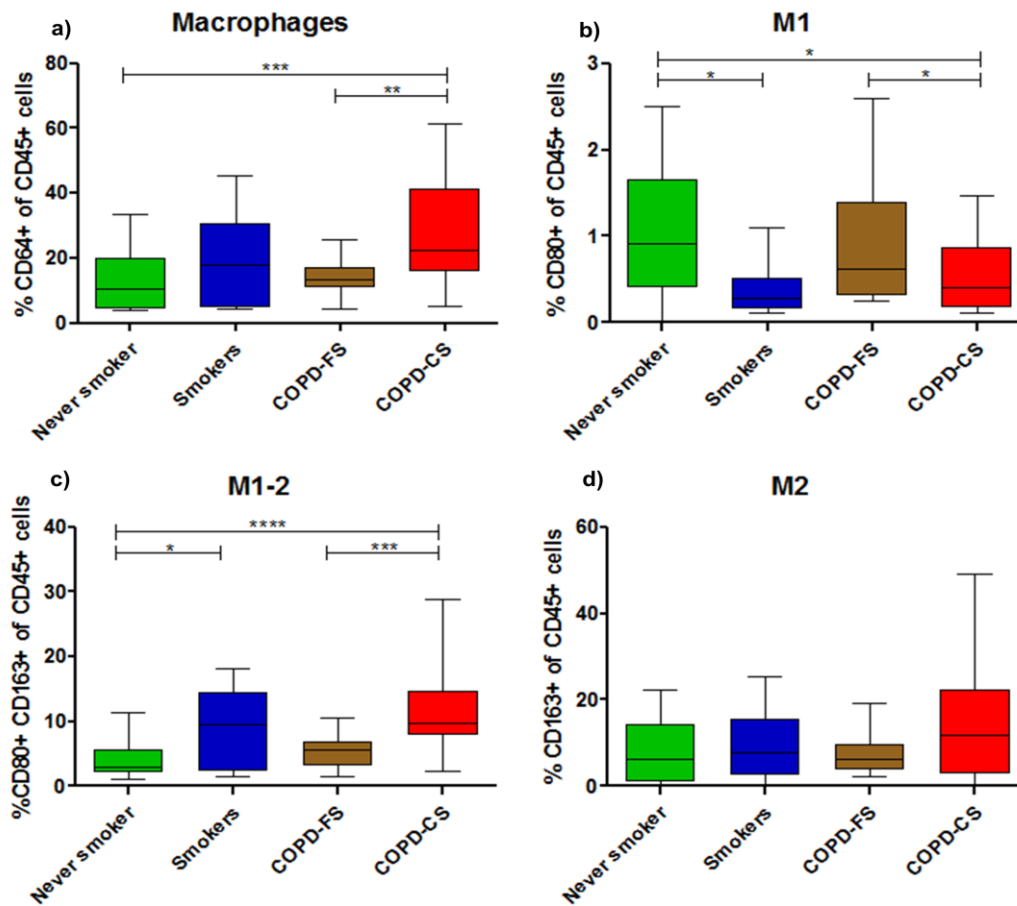


Figure 50: Macrophages and subtypes of macrophages proportions in lung tissue. * p-value<0,05, ** p-value>0,005, *** p-value>0,0005, **** p-value>0,00005.

Finally, the percentages of lung tissue monocytes were also increased in current smokers with COPD, see Figure 51.

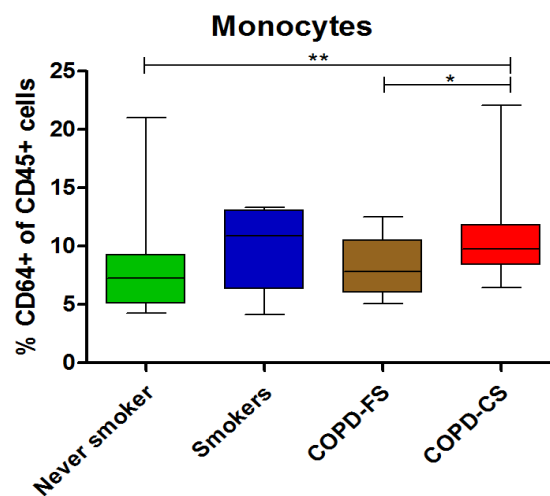


Figure 51: Lung tissue monocytes proportions. * p-value<0,05, ** p-value>0,005.

5.2.3 - Characterization of blood immune response

Next, using in whole blood the same panel of monoclonal antibodies and flow cytometry tubes was analyzed the immune cell proportion in blood of the lung tissue donors. As shown in Figure 52, the most abundant population in peripheral blood were neutrophils T cells and monocytes. The only population with significant differences between the study groups was monocytes, were an increase in current smokers without COPD vs. non-smokers, COPD former smokers and COPD current smokers was observed (Figure 52).

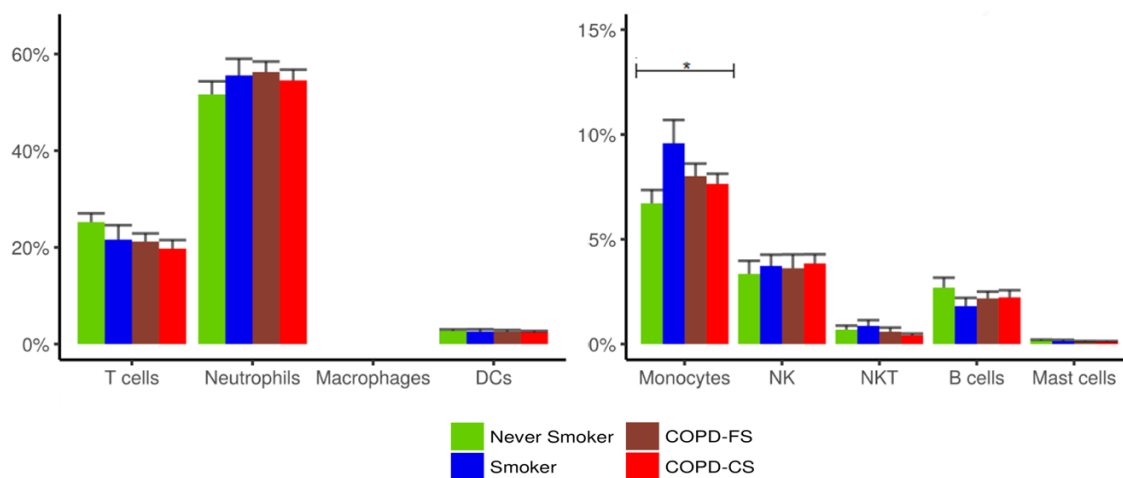


Figure 52: Abundance of the immune cell populations in blood represented as percentage of CD45+. Graphs on the left represent the most abundant populations, and in the right the less abundant. P value corresponds to the result of the Kruskal–Wallis one-way analysis of variance. * p-value<0,05.

5.2.4 - Effects of cigarette smoke vs. disease status

To evaluate if active smoking and the disease status contributed independently to the differences observed in current smokers with COPD, a two-way ANOVA for lung T-cells, M0 and Monocytes was performed (as described in methods).

As shown in Table 13, both the disease and smoking status had a significant independent effect in the proportion of T lymphocytes, and macrophages observed in lung tissue. For monocytes only smoking was responsible of the observed changes. Overall p values related to smoking were more significant to the ones related to disease status (Table 13).

	T Lymphocytes	Macrophages	Monocytes
Disease effect	-0.10 / < 0.01	0.16 / 0.03	0.049 / 0.18
Smoking effect	-0.10 / < 0.01	0.203 / <0.01	0.09 / < 0.01

Table 13: Regression coefficients and p values of the two way anova performed with the 4 study groups on relation to the contribution of disease status and smoking effect on observed percentages of T lymphocytes, macrophages and monocytes

5.2.5 –Pulmonary and systemic immune cell correlation network

To investigate if the proportion of lung tissue infiltrate is related to the systemic immune cell frequencies and main clinical parameters, we build a multi-level correlation network with all the individuals included in the study (Figure 53). A significant p value < 0.05 and a Spearman |0.3| were set as thresholds to build the network (as described in methods).

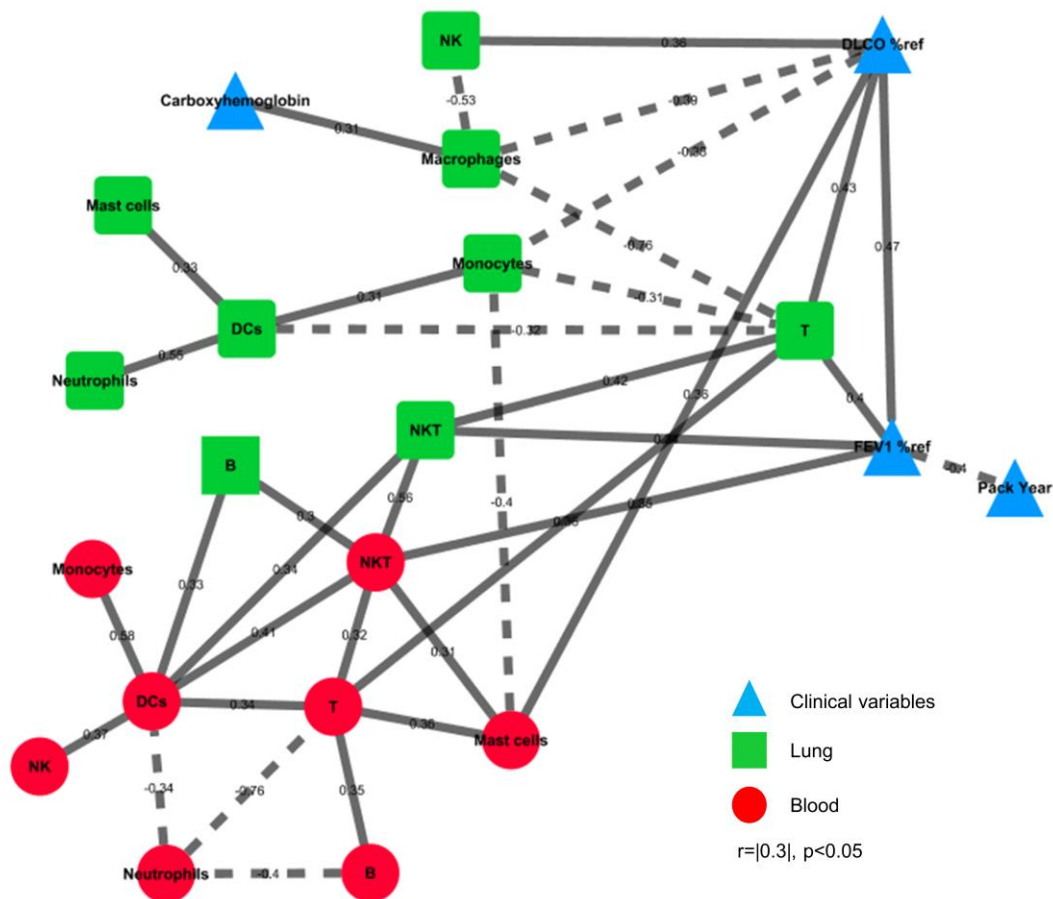


Figure 53: Correlation network of immune lung populations (green) and peripheral blood populations (red) with clinical variables (blue). Positive correlations are represented with a continuous edge while the negatives are with a discontinuous edge. P-value < 0.05 and $r > 0.3$.

The immune cell correlation network included 4 clinical variables (blue triangles): the level of post-bd FEV1 % ref. as measure of airflow limitation, the level of DLCO % ref. indicating the diffusion capacity, Pack/years as measure of cumulative tobacco exposure and the levels of carboxyhemoglobin as surrogate marker of current smoking exposure.

We observed that the two lung function variables (DLCO and FEV1) were correlated between them, and that DLCO had a higher number of correlations with immune cell populations than FEV1 (5 vs. 3). As expected, from above results (Figure 47) the proportion of lung macrophages and T cells had the highest negative correlation (-0.76), and the level of DLCO negatively correlated with lung Monocytes and Macrophages, and positively correlated with lung T and NK cells and peripheral blood Mast Cells.

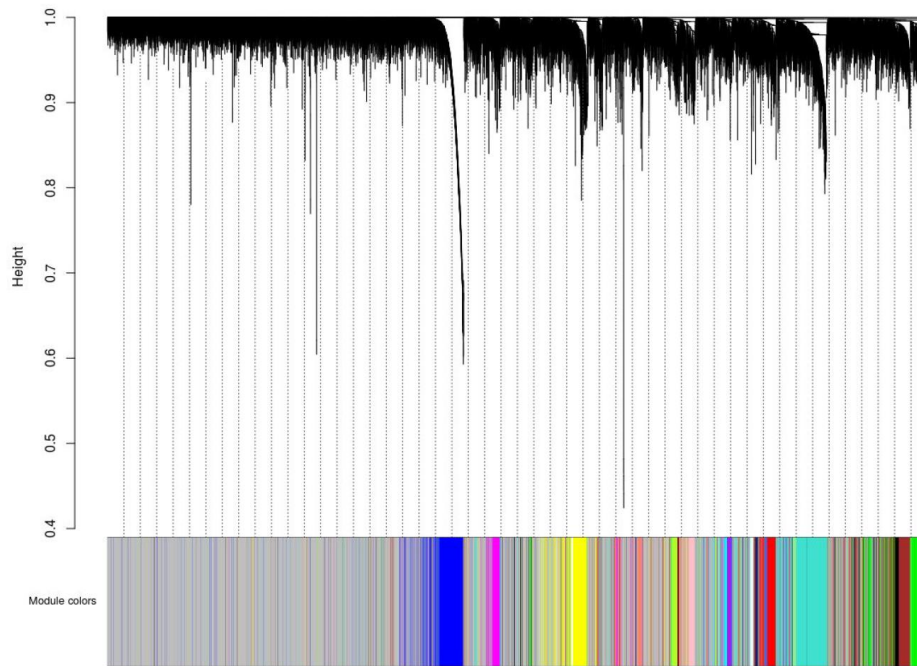
The level of FEV1 % ref. was positively correlated with lung T and NKT cells and blood NKT cells. Blood carboxyhemoglobin levels were positively correlated with the percentage of lung macrophages, which is in concordance with the smoking effect on this population described above (Table 13).

Finally, only two populations were correlated with their counterpart in blood and lung being T lymphocytes and NKTs (with $r= 0.34$ and 0.56 respectively). Showing that overall the abnormalities in lung tissue are not mirrored in the systemic compartment.

5.2.6 –Weighted gene co-expression network analysis

Next, in order to investigate the effect of the different immune lung populations on the whole lung mRNA expression, we used the WGCNA package [231, 250](as described in methods).

Briefly, the mRNA gene co-expression network was built with the array results from the whole lung tissue adjacent to the part used to determine the immune cell populations. In the co-expression network, 21 modules were identified and labeled each with a color name (Figure 54).



dark red	light yellow	grey60	midnight blue	salmon	tan	purple
76	105	121	135	156	158	198
green yellow	magenta	black	green	brown	pink	red
168	249	309	519	678	252	398
turquoise	royal blue	light green	light cyan	cyan	yellow	blue
1098	78	120	130	144	609	937

Figure 54: Gene dendrogram and identified modules (indicating the number of genes in each).

Each module contained a set of unique co-expressed genes whose expression was summarized with the module eigengene, defined as the first principal component of the expression matrix of the probes within the module. Figure 55 shows the results of the module eigengene correlation with the variables of interest.

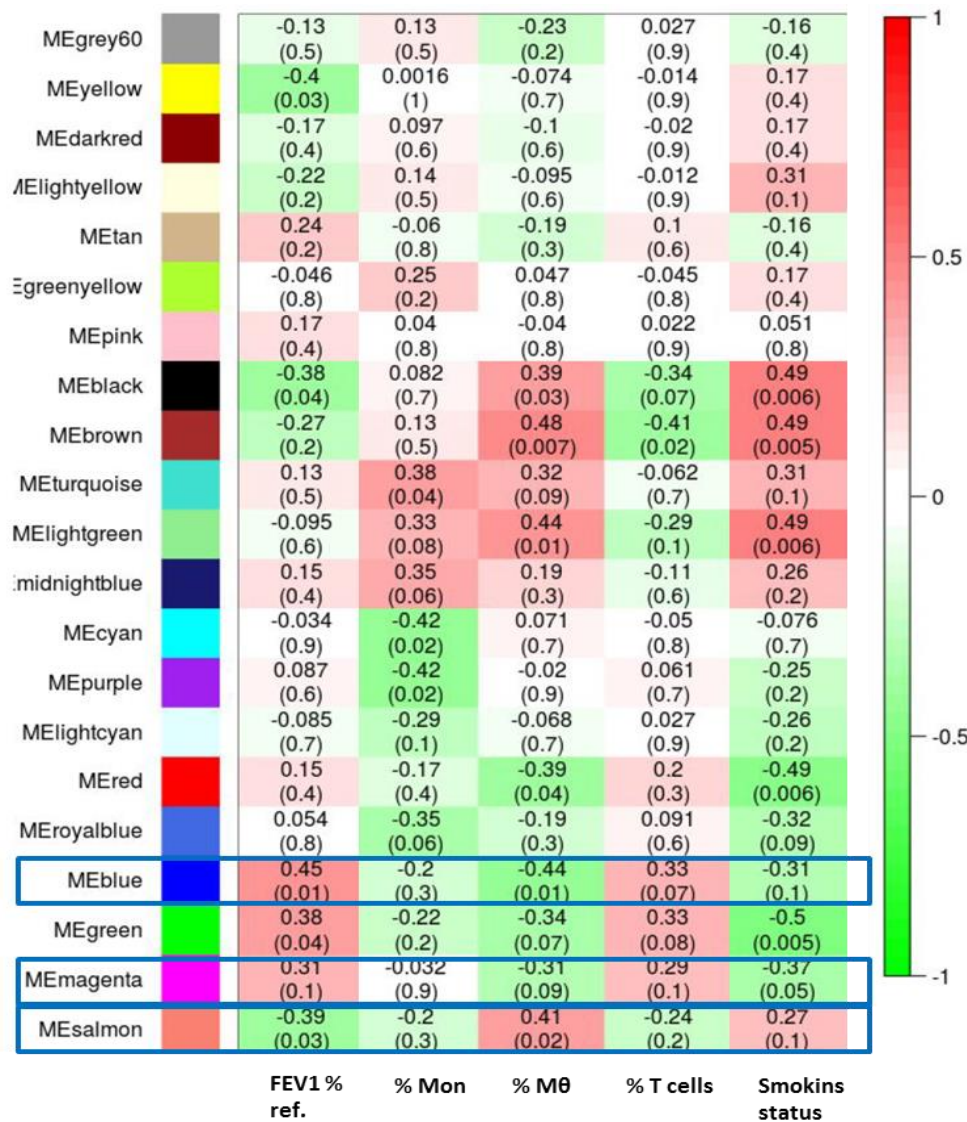


Figure 55: Heatmap representation of the coefficient and p-value of the correlation of the eigengene with the value of FEV1%, % of monocytes, macrophages, T cells and smoking status.

We observed that several modules correlated significantly with the airflow limitation, percentage of macrophages or T cells, but only 3 (Blue, Magenta and salmon) showed a significant enrichment in biological processes related with immune response or lung structure/function.

The **Blue module** had a significant positive correlation with the level of FEV1 and negative with the percentage of macrophages indicating that its genes have less expression with the presence of COPD and when the percentage of macrophages in tissue is high. Interestingly the genes contained in this module are related with cilium organization (GO:0044782, FDR=1.24027E-16, genes: SPEF2, FOXJ1, DRC1,

DNAH7, CFAP126, CCP110, DNAH5, TEKT2, CFAP53, CFAP73, TMEM231, BBOF1, CEP126, TRAF3IP1, CFAP100, KIF19, RP1, RSPH1, DNAI2, SPAG17, RSPH4A, CFAP206, DNAAF3 and ZMYND10), indicating a deregulation of the function of cilia in relation to the presence of disease and lung tissue macrophages.

The **Salmon module** had a significant negative correlation with the level of FEV1 and positive with the percentage of macrophages indicating that its genes have higher expression with the presence of COPD and when the percentage of macrophages in tissue is high. Interestingly the genes contained in this module are related with several gene ontologies that were summarized with Revigo (Table 14), belonging mainly to two categories: Extracellular matrix organization and angiogenesis. These observations indicate a deregulation of the extracellular matrix pathways (collagen, integrins and wnt signaling) with the presence of disease and a higher percentage of lung tissue macrophages.

	GO#	Description	FDR	Involved genes
Extracellular matrix organization	GO:0030198	extracellular matrix organization	9.33E-08	COL1A2, CCDC80, FBN1, SFRP2, WNT3A, DCN, COL6A3, VCAN, COL14A1, LAMA2, FAP
	GO:0043062	extracellular structure organization	9.33E-08	COL1A2, CCDC80, FBN1, SFRP2, WNT3A, DCN, COL6A3, VCAN, COL14A1, LAMA2, FAP
	GO:0001558	regulation of cell growth	4.65E-05	CXCL12, SPOCK1, SFRP2, SFRP1, SLIT3, SEMA3D, WNT3A, SERPINE2, CDKN2C
	GO:0051271	negative regulation of cellular component movement	2.22E-04	APOD, CXCL12, SFRP2, SFRP1, SEMA3D, WNT3A, DCN
	GO:1900119	positive regulation of execution phase of apoptosis	6.53E-03	PTGIS, FAP
	GO:0033138	positive regulation of peptidyl-serine phosphorylation	9.83E-03	SFRP2, GFRA2, WNT3A
	GO:0010810	regulation of cell-substrate adhesion	1.15E-02	CCDC80, APOD, SPOCK1, SFRP1
	GO:0036465	synaptic vesicle recycling	2.33E-02	DNM1, WNT3A
	GO:0000266	mitochondrial fission	2.41E-02	DNM1, DCN

	GO:0017145	stem cell division	2.60E-02	SFRP2, WNT3A
	GO:0008361	regulation of cell size	4.59E-02	CXCL12, SEMA3D, WNT3A
Angiogenesis	GO:0001525	angiogenesis	1.17E-04	APOD, ECM1, COL15A1, SFRP2, SFRP1, PTGIS, RSPO3, DCN, FAP
	GO:0030574	collagen catabolic process	1.33E-03	COL1A2, COL15A1, COL6A3, FAP
	GO:0048863	stem cell differentiation	8.55E-03	MEOX1, SFRP1, SEMA3D, WNT3A
	GO:0036342	post-anal tail morphogenesis	1.15E-02	SFRP2, WNT3A

Table 14: Gene ontology for the salmon module summarized with REVIGO in the two main process (extracellular matrix and angiogenesis), FDR and involved genes.

Finally, the **Magenta module** had a significant negative correlation with the smoking status indicating that the expression that its genes are related to current smoking. Interestingly the genes in this module are related with the presence and activity of T cells, this observation is in concordance with the results of the immune cell profiling by flow cytometry were the percentage of T cells decreases with the presence of active smoking, see Table 15.

	GO#	Description	FDR	Genes
T cell activation	GO:0042110	T cell activation	5.73E-05	CD3D, CD5, ZAP70, RASGRP1, SLA2, CD3G, TBX21, SLAMF6, SATB1
	GO:0002250	adaptive immune response	8.27E-05	SKAP1, SH2D1A, FCER1A, ZAP70, SLA2, TAP1, TBX21, SLAMF6
	GO:0002699	positive regulation of immune effector process	8.63E-05	SH2D1A, FCER1A, ZAP70, RASGRP1, TBX21, SLAMF6
	GO:0060337	type I interferon signaling pathway	6.11E-03	HLA-F, NLRC5, HLA-B
	GO:0002474	antigen processing and presentation of peptide antigen via MHC class I	6.20E-03	HLA-F, TAP1, HLA-B
	GO:0034340	response to type I interferon	6.65E-03	HLA-F, NLRC5, HLA-B
	GO:0002437	inflammatory response to antigenic stimulus	2.64E-02	FCER1A, RASGRP1

Regulation of cell killing	GO:0031341	regulation of cell killing	3.05E-03	SH2D1A, RASGRP1, SLAMF6
	GO:0032725	positive regulation of granulocyte macrophage colony-stimulating factor production	3.67E-03	FCER1A, RASGRP1
	GO:0032418	lysosome localization	4.23E-03	FCER1A, ZAP70, RASGRP1
	GO:0032604	granulocyte macrophage colony-stimulating factor production	4.79E-03	FCER1A, RASGRP1
	GO:0050848	regulation of calcium-mediated signaling	6.49E-03	FCER1A, ZAP70, SLA2
	GO:0001906	cell killing	1.01E-02	SH2D1A, RASGRP1, SLAMF6
	GO:0031349	positive regulation of defense response	1.39E-02	SH2D1A, FCER1A, RASGRP1, NLRC5, SLAMF6

Table 15: Gene ontology for the magenta module summarized with REVIGO in the two main process (extracellular matrix and angiogenesis), FDR and involved genes

5.3 – RESULTS IN RELATION TO OBJECTIVE 3: LRMSC

5.3.1 - Study population

The population of individuals of whom we have isolated LRMSC is not identical to the one described in objective 2. This is because in some cases, when the amount of tissue provided was scarce the flow cytometry could not be performed but we were able to isolate LRMSC, otherwise there are fewer individuals involved in this objective 3 because objective 2 started before.

The main clinical characteristics of the four groups are summarized in Table 16. Briefly, the proportion of females was higher in non-smokers. Normal lung function smokers were younger than COPD former smokers. The severity of the airflow limitation and tobacco exposure of current and former smokers with COPD was similar.

	No smokers n=13	Smokers n=8	COPD-FS n=12	COPD-CS n=20
Gender (m/f)	3/10	6/2	11/1	16/4
Age	65.2 ± 13.2	58.3 ± 9.6 ^{††}	71.2 ± 3.1 ^{††}	66.3 ± 7.1
Pack/year		40.2 ± 18.9	61.3 ± 21.4	42.0 ± 16.1
BMI	26.9 ± 5.3	26.7 ± 4.1	29.2 ± 3.2 ^{\$\$}	24.7 ± 4.0 ^{\$\$}
FEV1 (% ref)	101.6 ± 7.0 ^{****} ####	92.9 ± 6.8 [†]	68.1 ± 14.2 ^{####.†}	73.4 ± 16.3 ^{****}
FEV1/FVC (%)	78.9 ± 3.5 ^{****.###}	78.3 ± 10.5 ^{++.††}	58.7 ± 6.3 ^{###.††}	60.3 ± 6.8 ^{****} ++
DLCO (%)	83.0 ± 14.6 ^{***.#}	78.9 ± 11.4 ⁺	64.3 ± 11.8 [#]	60.7 ± 9.0 ^{***.+}

Table 16: Clinical variables of the subjects from which the LRMSC are obtained. Comparison between non smokers and COPD-CS is represented by *, non smokers and COPD-FSs with #, smokers and COPD-CS with +, smokers and COPD-FSs with † and COPD-CS and COPD-FSs with \$. p-values are < 0,05 for one symbol, p-value < 0,005 for two symbols, p-value < ,0005 for three symbols and p-value < 0,00005 for four symbols.

5.3.2 – LRMSC isolation procedure

There is literature on mesenchymal-like stem cells resident in peripheral organs (such as the heart), but the literature on lung mesenchymal stem cells (see introduction section 1.2.2.2 - MSC in the lung) was almost absent at the time we started this work. Now there are few papers that have described partially this population in the lungs of recipients of lung transplant [150]. But, up to date, these cells have never been assessed in COPD or in relation to smoking. For all these reasons and in order to assess the regenerative capacity of the lung of patients with COPD, we decided to evaluate the presence of cells with mesenchymal markers (CD90, CD105 and CD73) in lung tissue.

The proof of concept experiment was to stain fresh lung tissue homogenates (used in objective 2) with fluorescently conjugated monoclonal antibodies for the mesenchymal stem cell markers and analyzed it by flow cytometry.

The flow cytometry gating strategy was based on the selection of CD45-CD34- cells, excluding in this manner the endothelial and fibroblast populations, then the presence of CD90, CD73 and CD105 was assessed. Figure 56 shows that we were indeed able to identify a minority of cells that stained with these markers.

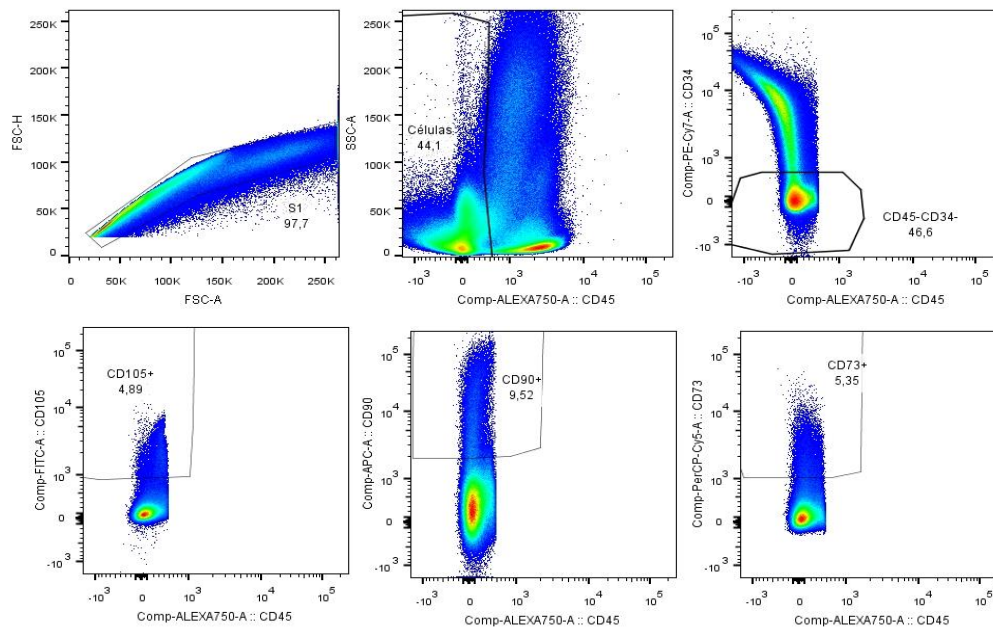


Figure 56: Flow cytometry detection of LRMSC, proportions of CD105+, CD90+ and CD73+ cell in lung tissue homogenates. The gates were fixed with and FMO with the CD45 and CD34.

After being able to identify these cells by flow cytometry, in order to characterize them properly, the next step was to set up the isolation and expansion procedure. Following the literature reported for cardiac resident mesenchymal stem cells [153, 154, 159] an explant based culture method was established in the lab with minor modifications (without thrombin and cardiotrophin in the SCM). The key isolation features are that the cells are let diffuse from the tissue, adhere to the fibroblast cell layer that is formed on the dish 15-20 days after the culture start, and then when removed from the plate with mild trypsinization and plated in poly-D-lysine coated wells these cells form spheres. Spheres remain floating while the other cell populations adhere to the plastic. After 3-4 days, spheres are recovered and plated in conventional tissue culture plates where they adhere to plastic adopting a spindle morphology and rapidly expand. We term these cells sphere derived cells (SDC). Confluent SDC are harvested and re-plated on poly-D-

lysine coated culture plates to generate the secondary spheres. Figure 57 shows a scheme of the procedure with representative images of each step.

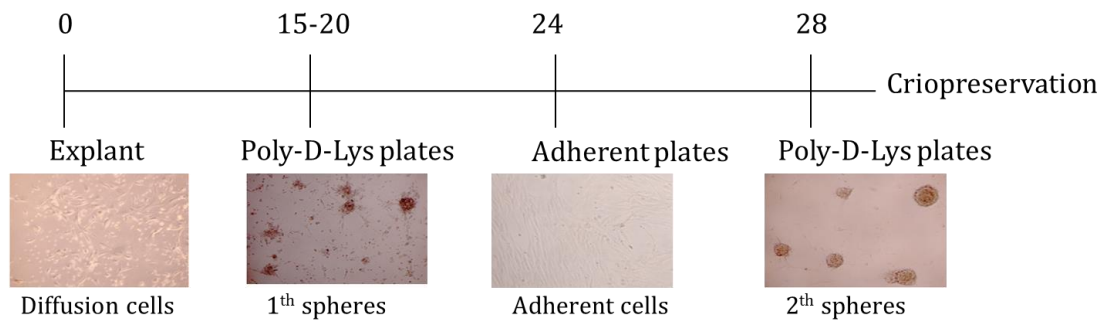


Figure 57: LRMSC cell isolation procedure set up.

This isolation procedure was performed in 59 subjects and was successful in 46 (78% of overall success rate). Table 17 shows the culture success statics per group, we did not observe significant differences. Failures are related to lack of expansion of the cells, usually related of poor sphere formation, not to contamination or other culture incidences.

	1 st Spheres	2 nd Spheres
Never Smokers; n=13	92.3% (12/13)	84.6% (11/13)
Smokers; n=8	87.5% (7/8)	75% (6/8)
COPD-FSs; n=12	83.3% (10/12)	66.7% (8/12)
COPD-CS; n=20	75% (15/20)	70% (14/20)

Table 17: Success rate of the LRMSC culture, percentage of samples were first or secondary spheres assembly properly.

5.3.3 - Characterization of LRMSC

Due to the lack of information on LRMSC characteristics and function, an extensive initial characterization of isolated cells was performed including: analysis of cell surface markers, mRNA expression, differentiation capacity, localization in the lung and immunomodulatory capacity. The results of the characterization are described below per type of analysis for the whole group of isolated LRMSC in comparison to control BM-MSK cell lines.

5.3.3.1 - Cell surface characterization by flow cytometry

Flow cytometry analysis with cell surface mesenchymal stem cell markers was performed at all phases of the culture. The progressive enrichment in the fraction of CD45-CD90+CD73+ cells achieved the 80% in second spheres. Figure 58 shows the comparison of cell surface markers in second spheres (n=44) in front of the 3 control BM-MSC cell lines (cell lines provided by Carlos Rio, Hospital Son Espases, Mallorca).

The only significant difference observed between LRMSC and BM-MSC is an increase in the expression of EGFR in LRMSC. This could be due to the presence of EGF in the LRMSC cell culture media which is absent for BM-MSC. Moreover, under the light contrast microscopy LRMSC in the SDC culture step have the same spindle morphology which makes them indistinguishable from BM-MSC.

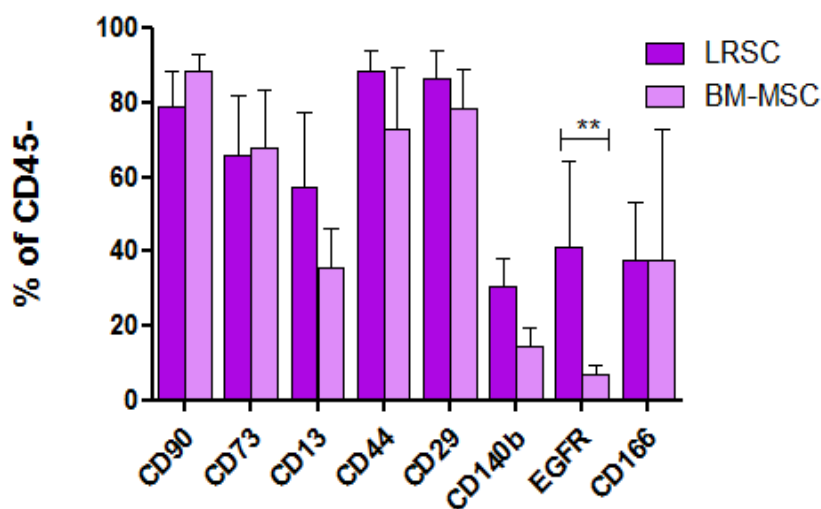


Figure 58: Flow cytometry markers of the LRMSC and BM-MSC. Mean \pm sd and Mann-Whitney test, **p-value<0,005.

5.3.3.2 –Transcriptomics profile comparison

In order to assess the expression of MSC features by LRMSC, total RNA from second spheres of a representative group of individuals (n=28) was isolated and profiled using Affimetrix microarrays. RNA was also isolated from the whole lung tissue from which MSC were isolated, from the blood of the same individuals and also from the three control MSC cell lines.

The principal component analysis (PCA) of the microarray results (Figure 59) shows that the expression profile of LRMSC is similar (closer in the PCA dimensions) to that

of BM-MSc and different from the transcriptomics profile of the lung tissue of whom they are isolated, and also very different from the profile of blood.

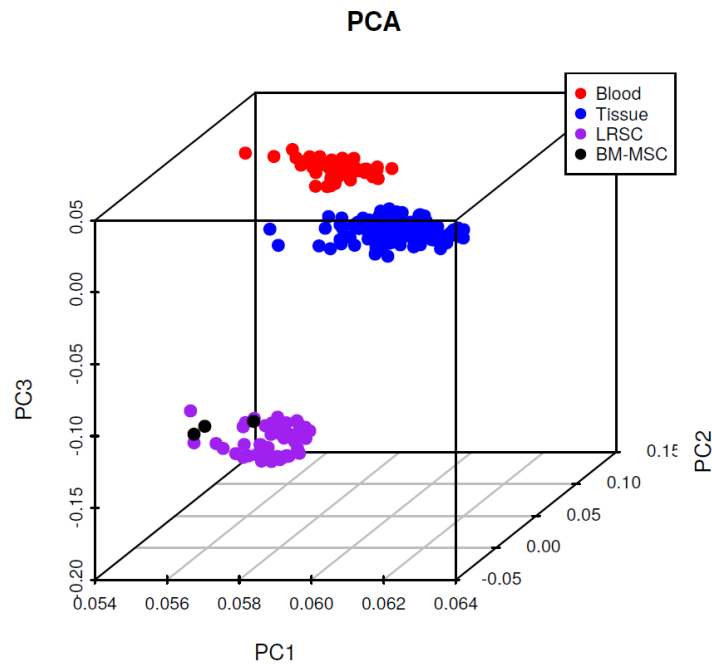


Figure 59: PCA of lung tissue, peripheral blood, BM-MSc and LRMSc mRNA

The PCA restricted to the BM-MSc and the four groups of MSC shows that the LRMSc have features that differentiate them from BM-MSc as LRMSc cluster together a part from BM-MSc in spite of their different group of origin, see Figure 60.

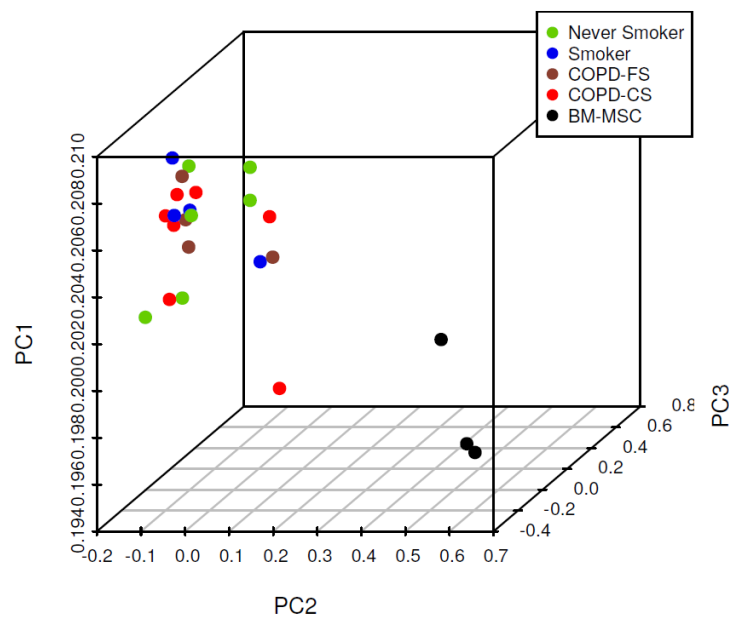


Figure 60: PCA of the LRMSc divided into the 4 studied groups and the BM-MSc

5.3.3.2.1 - Rohart test

In the literature other cell lineages have been describe to share the same surface markers than MSC. Because of that and in order to characterize cells as of MSC lineage the Rohart bioinformatic test was performed. This test, using as input the microarray raw data, gives a prediction score per sample that classifies it as MSC origin or not (above or below 0.5 of resulting score).

Using this test only two LRMSC cell lines were scored as non-MSC (0,37 and 0,47), see Figure 61. The three positive control cell lines had the highest scores and the blood and tissue samples that were included as negative controls, were not classified as of MSC lineage.

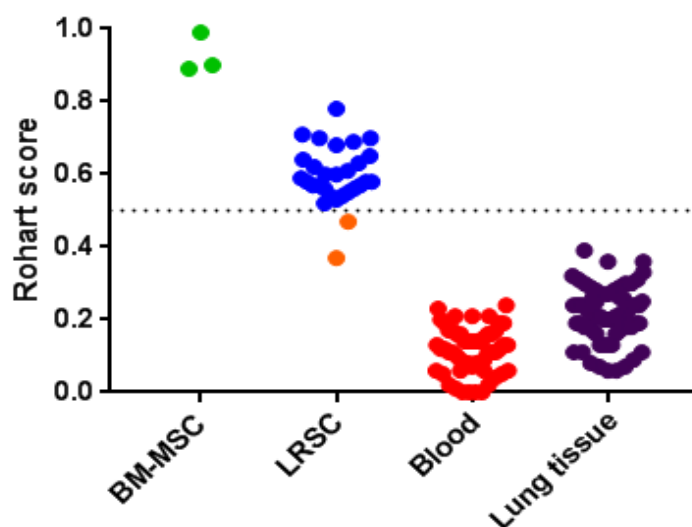


Figure 61: Rohart test score for the prediction of the mesenchymal cells. The orange dots of the LRMSC (blue) represent the LRMSC without a good Rohart predictive score.

The differential expression between BM-MSC and LRMSC of the genes included in the Rohart test has been analyzed. Only 4 genes were differentially expressed, 3 had a reduce expression in LRMSC (ABI3BP, ITGA11, KIAA1199) and one was increased (APCDD1). ABI3BP and ITGA11 are adhesion proteins of the extracellular matrix described in BM-MSC [251-253]. KIAA1199 is an activator of the Wnt/ β -cathening signaling that promote the EMT through an increase of the MMPs [254, 255] and APCDD1 is an inhibitor of the same pathway, described to be increase after adipogenic differentiation [254, 255]. This 4 genes support the Rohart score lower for the LRMSC than for the BM-MSC point to more differentiated phenotype for their tissue origin.

5.3.3.2.2 – Expression of stemness related genes

Finally the differential gene expression between LRMSC, BM-MSC and lung tissue was performed using RankProd. In Figure 62 each circle represents a comparison between two groups and the overlapping areas are the common genes differentially express in both comparisons. The overlapping area between the comparison of the LRMSC with BM-MSC and LRMSC with lung represents the specific signature for the LRMSC (1117 genes). In the same way it was defined the signature for the BM-MSC (365 genes) and mesenchymal genes (2629 genes) were defined as the common genes for the LRMSC and BM-MSC in front of lung tissue.

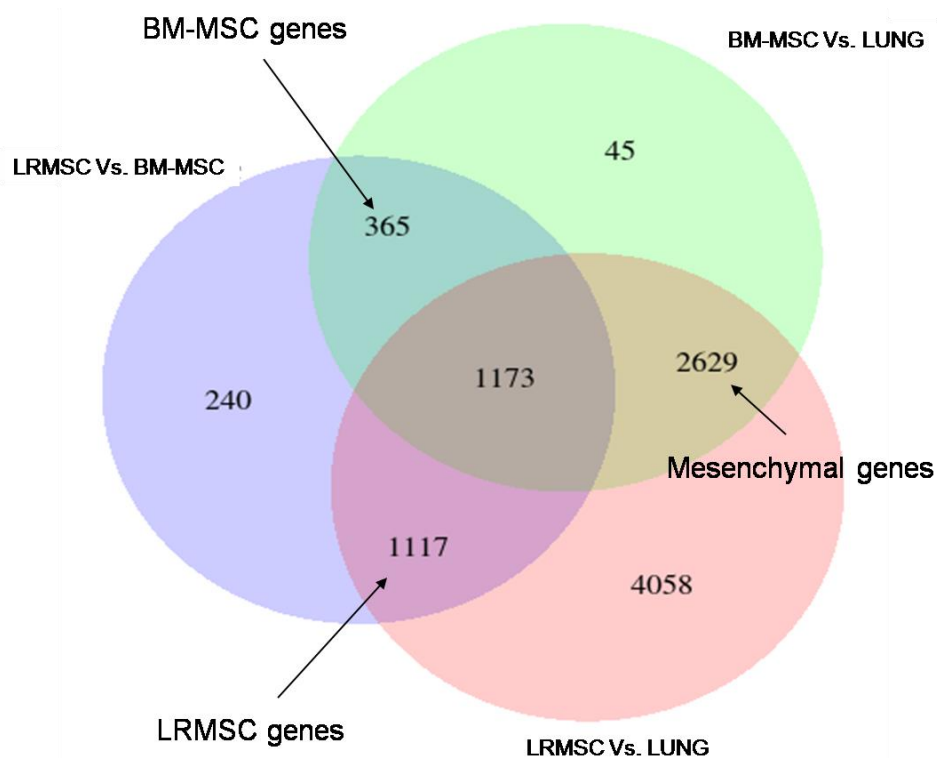


Figure 62: Venn diagram of the differentially express genes between LRMSC, BM-MSC and lung tissue analyzed by RankProd.

The gene signature for the LRMSC (1117 genes) was analyzed to identify the ontologies in which these genes are involved, see Table 18. Several process related to lung development, neurogenesis, TGF- β signaling and extracellular matrix organization appeared among these ontologies, Table 18 marked in purple. These ontologies support the lung resident and mesenchymal origin of the LRMSC.

Category	Term	N° Genes	FDR
REACTOME_PATHWAY	R-HSA-191273:R-HSA-191273	9	0.0002
REACTOME_PATHWAY	R-HSA-1650814:R-HSA-1650814	15	0.0006
REACTOME_PATHWAY	R-HSA-2426168:R-HSA-2426168	11	0.0023
GOTERM_BP_DIRECT	GO:0006695~cholesterol biosynthetic process	10	0.0051
GOTERM_BP_DIRECT	GO:0006351~transcription, DNA-templated	151	0.0054
GOTERM_BP_DIRECT	GO:0048704~embryonic skeletal system morphogenesis	10	0.0063
GOTERM_BP_DIRECT	GO:0048286~lung alveolus development	9	0.0116
GOTERM_BP_DIRECT	GO:0009952~anterior/posterior pattern specification	14	0.0134
GOTERM_BP_DIRECT	GO:0050918~positive chemotaxis	9	0.0143
GOTERM_BP_DIRECT	GO:0043065~positive regulation of apoptotic process	33	0.0149
GOTERM_BP_DIRECT	GO:0008284~positive regulation of cell proliferation	45	0.0236
GOTERM_BP_DIRECT	GO:0001657~ureteric bud development	9	0.0253
KEGG_PATHWAY	hsa04350:TGF-beta signaling pathway	14	0.0190
KEGG_PATHWAY	hsa04360:Axon guidance	18	0.0204
GOTERM_BP_DIRECT	GO:0045892~negative regulation of transcription, DNA-templated	47	0.0301
GOTERM_BP_DIRECT	GO:0045666~positive regulation of neuron differentiation	13	0.0342
GOTERM_BP_DIRECT	GO:0008285~negative regulation of cell proliferation	39	0.0366
GOTERM_BP_DIRECT	GO:0045669~positive regulation of osteoblast differentiation	11	0.0434
GOTERM_BP_DIRECT	GO:0006355~regulation of transcription, DNA-templated	115	0.0454
GOTERM_BP_DIRECT	GO:0030198~extracellular matrix organization	23	0.0480
GOTERM_BP_DIRECT	GO:0030155~regulation of cell adhesion	9	0.0569
GOTERM_BP_DIRECT	GO:0010628~positive regulation of gene expression	28	0.0583

Table 18: Gene ontologies in which LRMSC are involve, purple rows represents the ontologies of interest.

5.3.3.3 - Differentiation capacity

BM-MSC are defined as cells with the capacity to differentiate into the three mesodermal lineages: adipocytes, osteocytes and chondrocytes. To characterize the differentiation capacity, 2 lines LRMSC of each study group was cultured under the appropriate differentiating stimulus. The LRMSC tested differentiated toward de adipogenic lineage (Figure 63A and C), osteogenic lineage (Figure 63B and D) and to chondrocytes (Figure 63E).

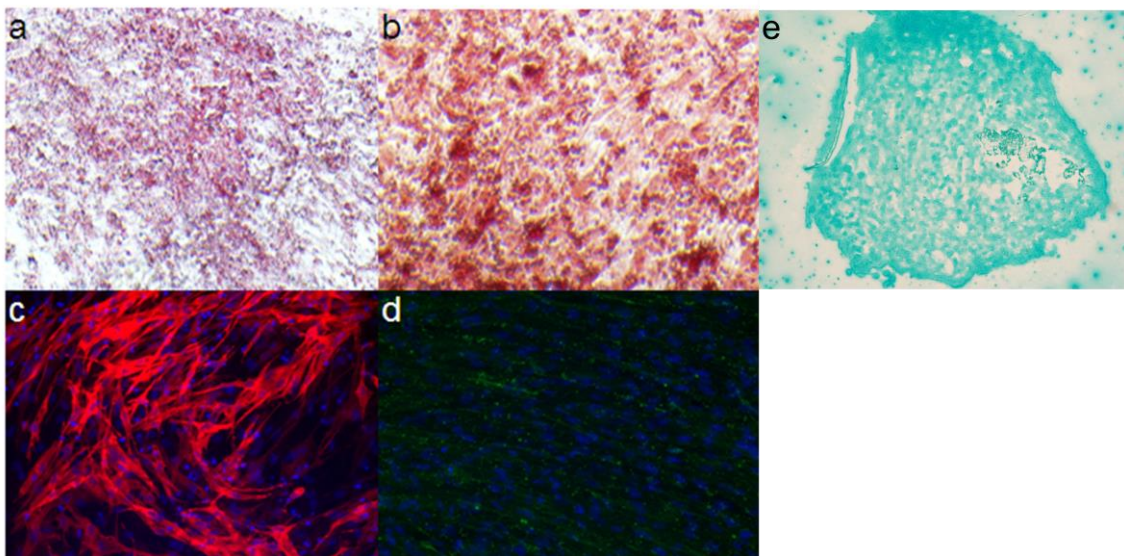


Figure 63: Differentiation capacity of the LRMSC toward adipocytes stained by a) oil red and c) Anti-FABP-4; osteocytes stained by b) alizarin red and d) anti-osteocalcin; and towards chondrocytes stained by alcian blue. Representative staining of n=8 differentiations.

5.3.3.4 – Senescence status

In order to be able to perform functional assays the senescence status was determined by the β -Galactosidase activity in several passages. Until passage nine LRMSC did not show any senescence staining (Figure 64 B and C). This was assessed in two lines of each study group, and in concordance with these results, functional experiments were performed with the cells at passage 6.

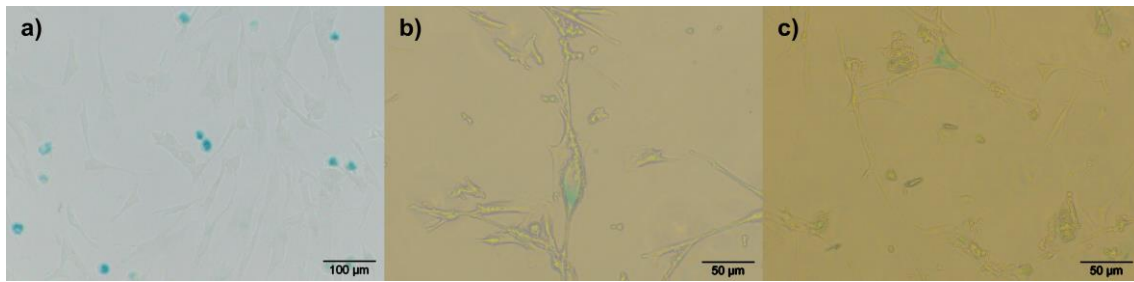


Figure 64: Senescence determination assay based on the β -galactosidase activity; a) positive control, b) and c) LRMSC at passage 9.

5.3.3.5 - Localization in the lung

Triple immunostaining with CD45, CD73 and CD90 was performed over lung tissue sections. A 8x8 field mosaic at 63x objective was made to ensure a significant area with a good resolution for localize the LRMSC. This methodology allow the screening of a bigger area of the tissue and the possibility of analyze specific areas with a deeper zoom, see Figure 65.

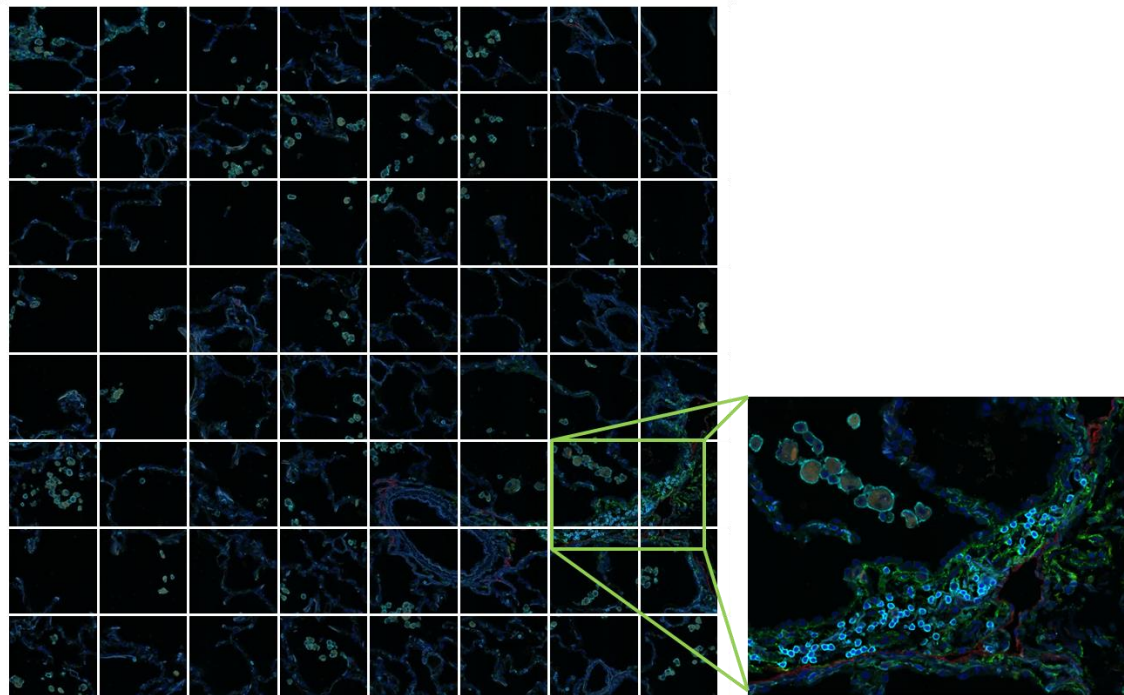


Figure 65: 8x8 field mosaic at 63x objective

LRMSC were identify as CD45- CD90+ CD73+ cells, represented in Figure 66 by the yellow (green-CD73 and red-CD90 without the cyan-CD45) staining. Mosaics were made in 5 non smokers, 5 smokers, 5 COPD-FSs and 3 current smokers. CD90+ CD73+ cells were identify in all the analyzed tissue with no significant differences between

groups. CD90+ CD73+ cells were present in the vascular endothelium Figure 66A alveolar wall Figure 66 B and C, and in the lung parenchyma Figure 66 D and E.

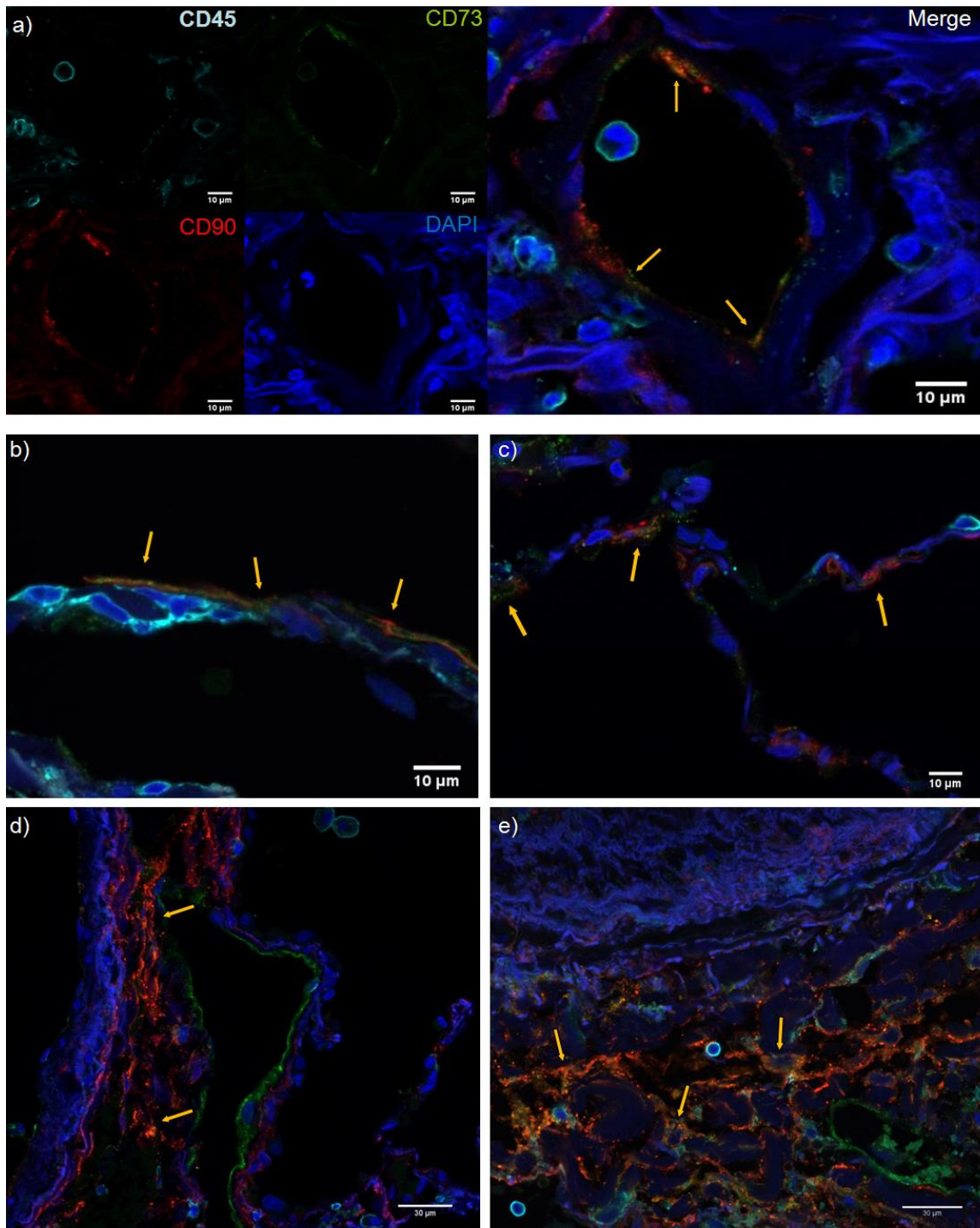


Figure 66: Immunofluorescence staining of LRMSC in lung tissue for CD45 in cyan, CD73 in green and CD90 in red. Representative image of a) vascular endothelium b) and c) alveolar wall and d) and e) lung parenchyma

To confirm that this CD90+ CD73+ cells are the LRMSC another staining were made. CD105 was analyzed as typical MSC marker and appears to colocalize in the vassal

endothelium with the CD90, see Figure 67A. To confirm that these cells are not endothelial cell the expression of the CD31 was analyzed in Figure 67B where it can be seen some co-localization of CD90 and CD31 (yellow arrows), but not in the endothelium where there is only expression of the CD31 (green arrow).

From the microarray analysis 3 genes with maximum differential expression between LRMSC and lung tissue (MMP3, MMP1 and CLGN) were selected for confirmation, see Figure 67C, D and E. MMP3 appeared not very specific staining, without co-localization with the others markers. MMP1 seems to colocalize with the CD73 only in cells surrounded by CD45 which usually are macrophages (cyan arrows). CLGN appeared to not colocalize with the CD73.

Finally a fibroblast marker, FoxF1 was analyzed, see Figure 67F. FoxF1 seems to co-localize with the CD90 in a similar structure than the CD90 and CD73, see Figure 66 D and E, indicating that these areas enrich on CD90+ CD73 cells could be fibroblast. It seems difficult to localize the LRMSC with only 3 markers, the CD90+ CD73+ CD45-cells with the confirmation of the CD105+ would be close, but there is also the need of excluding the CD31+ for the endothelial cells and the FoxF1 for the fibroblast.

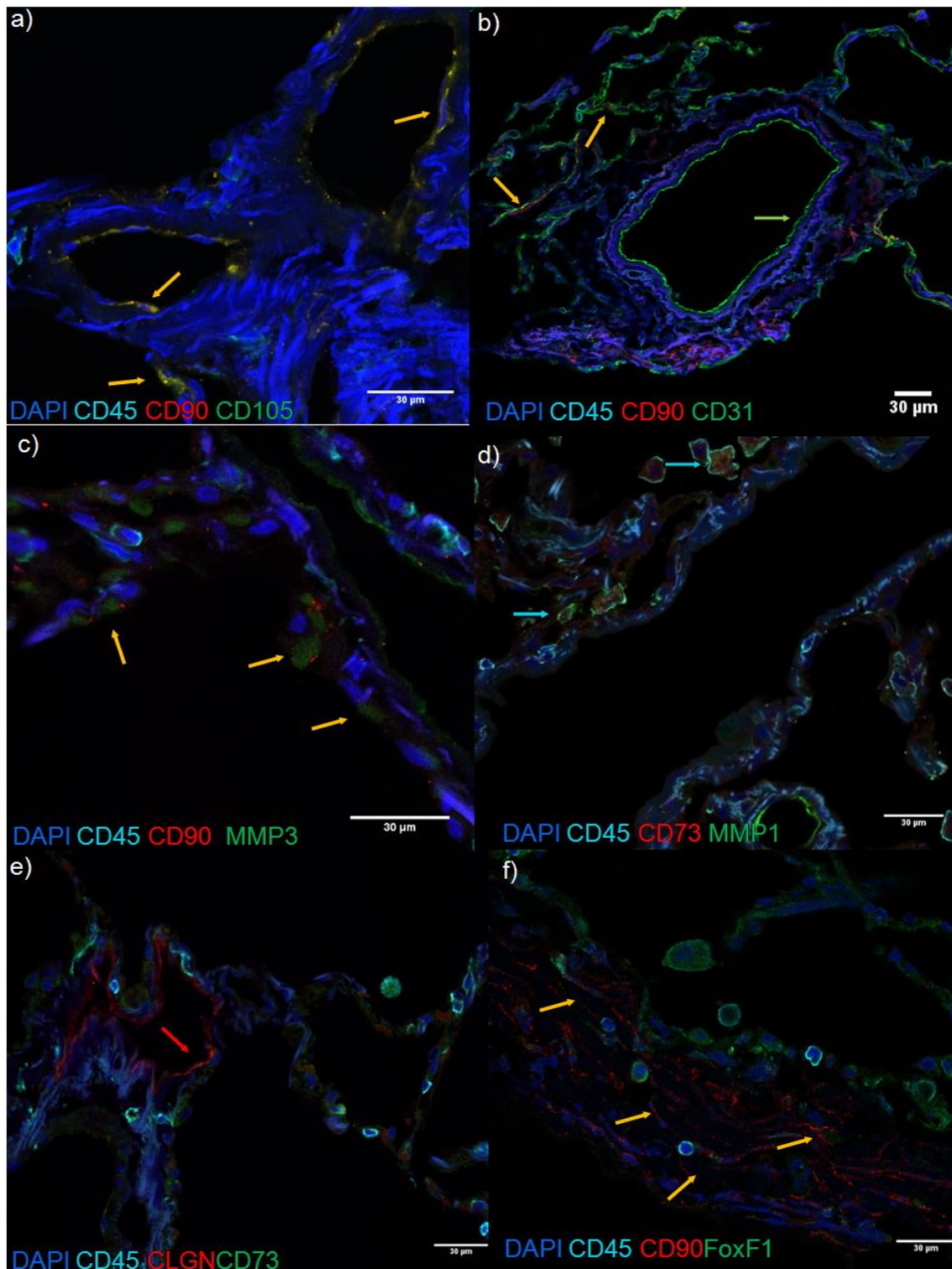


Figure 67: Additional staining for the LRMSC confirmation, maintaining the CD45 and the CD90 or CD73 the following markers are analyzed; a) CD105, b) CD31, c) MMP3, d) MMP1, e) CLGN and f) FoxF1

5.3.3.6 - Immunomodulatory capacity

A final characteristic of MSC is their immunomodulatory capacity, usually this is tested *in vitro* co-culturing them with stimulated T and B cells, and the read out is the suppression of the T and B cell proliferation.

Accordingly, in order to compare the LRMSC immunomodulatory properties, B and T lymphocytes were isolated from a single buffy coat donor, labeled with CFSE, stimulated in an antigen unspecific manner, and co-cultured in triplicates with either LRMSC or control BM-MS. As negative controls three lines of lung fibroblasts were include in the experiment. At 4 or 7 days the proliferation of T and B cells was assessed by determination of the CFSE level and co-staining with CD3, CD4, CD8 and 7-AAD or CD19 and 7-AAD.

The percentage of proliferation was determined comparing to the level of proliferation observed at 4 or 7 days when T and B cells were not stimulated. The positive controls were the B and T cells stimulated but not co-cultured with MSC. This experiment was performed with 29 LRMSC cell lines, 2 BM-MS. C lines and 3 fibroblast lines at the same time.

Both LRMSC and BM-MS. C similarly and significantly reduce the percentage of lymphocytes that proliferate (Figure 68). The percentage of reduction on proliferation is higher for the B cells and T CD4+ cells, and lower for the T CD8+ cells, while lung fibroblasts were not able to reduce the proliferation of any type of lymphocytes.

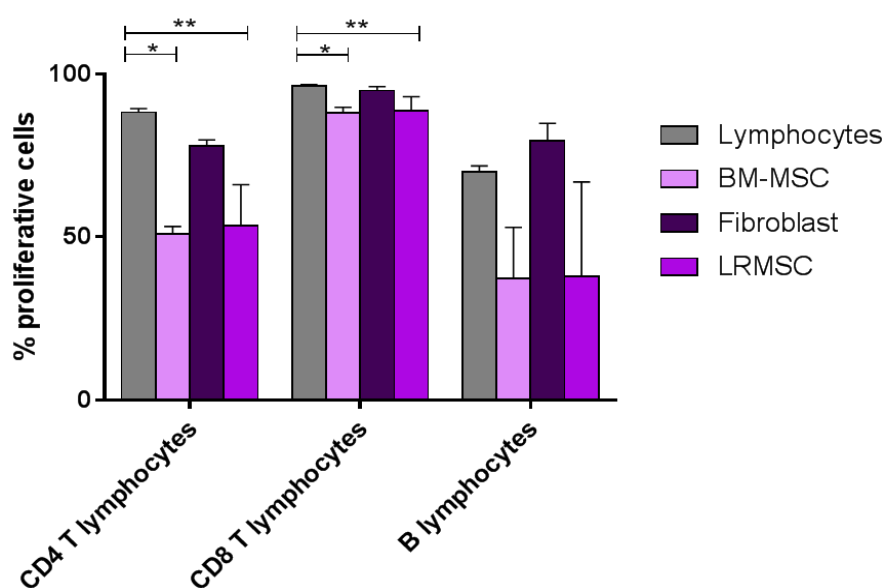


Figure 68: Immunomodulatory capacity of BM-MS. C, LRMSC and fibroblast in co-culture with B lymphocytes, CD4+ T lymphocytes and CD8+ T lymphocytes.

For T cells, we determined the number of cells that reached a determined number of divisions (1 to 6) in all the experimental conditions (Figure 69). When T CD4 cells are stimulated with CD3+CD28 without any co-culture around 40% of the cells reach the 4th and 5th divisions and around 20% stops in the first two divisions. For T CD8 cells the situation is similar but the percentage of cells between the 4th to 6th divisions is higher (around 60%).

When cells are co-cultured with BM-MSC or LRMSC we observe an opposite proliferation curve, with 40% of T CD4 cells in the first two divisions and only 10 % in the 4th or 5th division. For T CD8 cells the situation is similar and most of the proliferation is stop at the 3rd or 4th division.

With fibroblasts, while the final percentage of proliferation is similar to what observed with T CD4 or T CD8 cells alone, there is a difference in the division number that these lymphocytes reached, being stop in the 3rd and 4th division for T CD4 cells and 4th and 5th division for T CD8 cells. Meaning that fibroblast also interfered, although to a less extend in the proliferation of T lymphocytes.

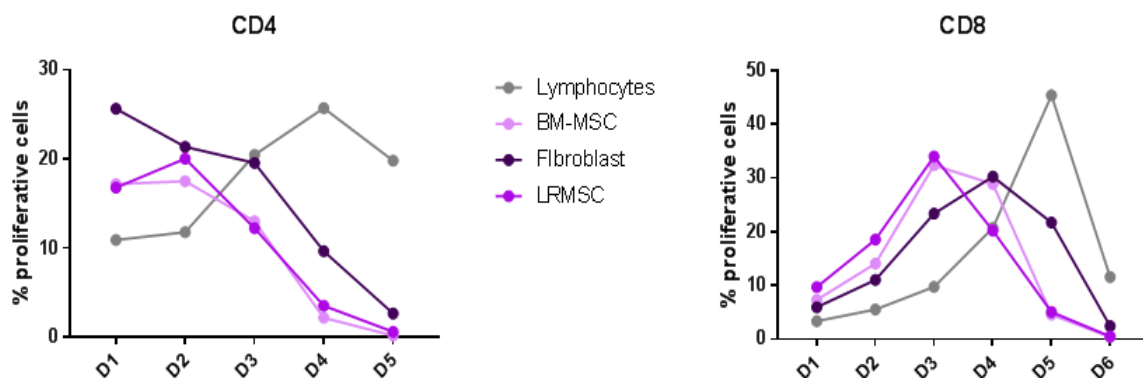


Figure 69: Percentage of proliferative CD4 or CD8 T lymphocytes in each division.

The proliferation of B lymphocytes in divisions could not be analyzed because of the small number of cells remaining in each division.

5.3.4 - LRMSC differences between study groups

5.3.4.1 –LRMSC quantification in lung homogenates

First, we assessed if there were differences in the percentage of LRMSC observed by flow cytometry in the lung tissue homogenates of the different study groups. We observed no significant differences in the proportion of CD90+CD73+CD45-CD34- cells in lung tissue (Figure 70).

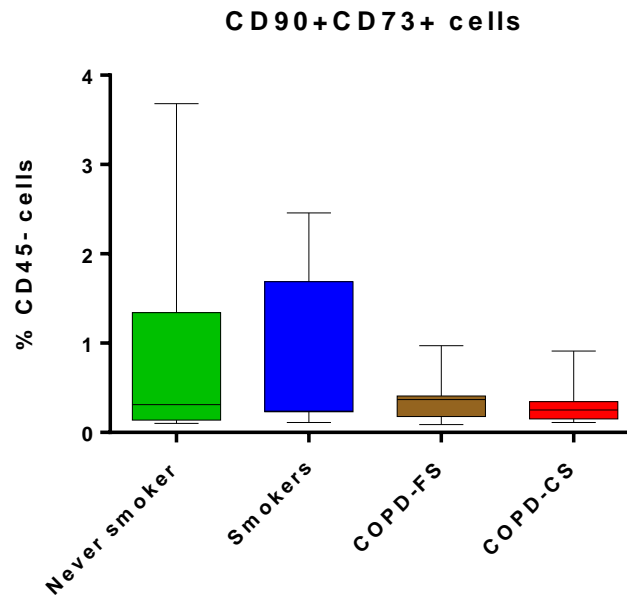


Figure 70: Flow cytometry quantification of CD90+ CD73+ cells in lung tissue homogenates express as % of CD45- cells. Kruskal-wallis –value=0,65.

5.3.4.2 - Proliferation capacity

We assessed if the LRMSC from different groups had a different proliferation capacity seeding the same number of cells of each donor ($5 \cdot 10^3$ and 10^4) in a 96 well plate in triplicate and determined the DNA content of each well by fluorimetry in three consecutive days. The ratio of increase between the two consecutive days was analyzed (Figure 71), no differences in the proliferative capacity of LRMSC between the four studied groups were observed.

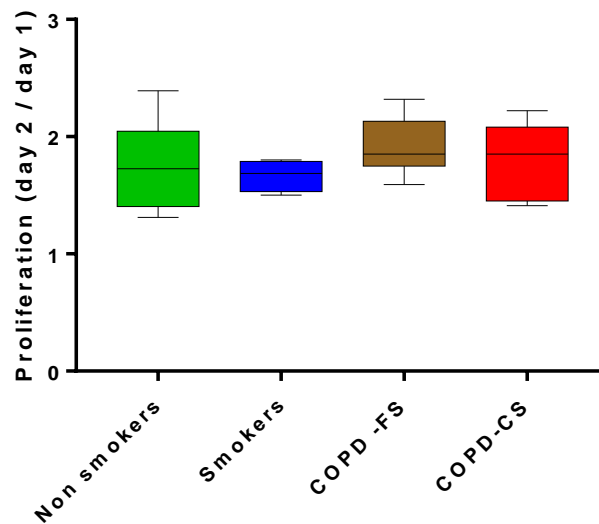


Figure 71: Proliferation capacity determined by fluorescent determination of the DNA content and express as the ratio between day 2 and the first day.

5.3.4.3 –Telomere length

Telomere length was determined at passage 6 for all the cell lines with the qPCR described by Cawthon *et al.* [232]. No differences in the R/T difference were observed for the 4 study groups, see Figure 72.

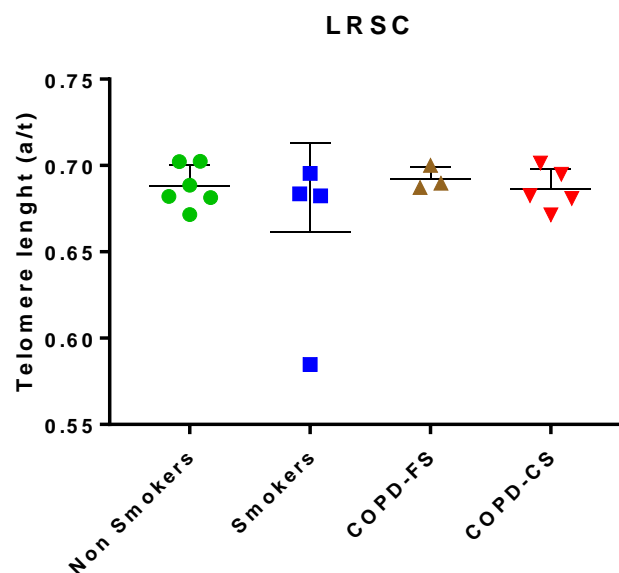


Figure 72: Telomere length for the LRMSC for the four studied groups.

5.3.4.4– Differences in the MSC Rohart score

We compared if the LRMSC of the four study groups received a different Rohart score (Figure 73) and we did not find any differences between study groups.

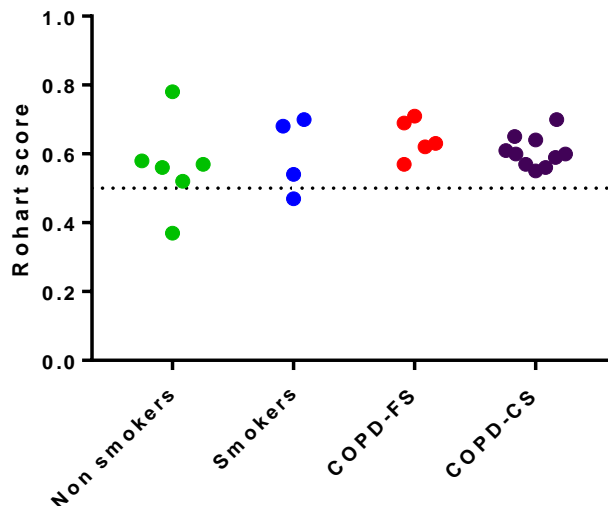


Figure 73: Rohart score for the LRMSC for the four studied groups.

5.3.4.5 –Differences in gene expression

Transcriptomic differences by pairs were analyzed by Limma. No differences were statistically significant at $FDR < 0.05$, this can be due to the small sample size of the compared populations. Just for this reason we selected as suggestive of differential expression those genes with a nominal p value < 0.01 per comparison (Figure 74). To simplify the interpretation, all the COPD are grouped together without separation in function of their smoking status. In the Venn diagram the overlapping area between COPD vs. Never Smokers and COPD vs. Smokers identify the genes related to a COPD signature in the LRMSC. In the same way the never smokers signature and the smokers related signature was identified. As a result of this analysis we observed 7 COPD related genes, 30 genes related with never smokers and 32 with smokers.

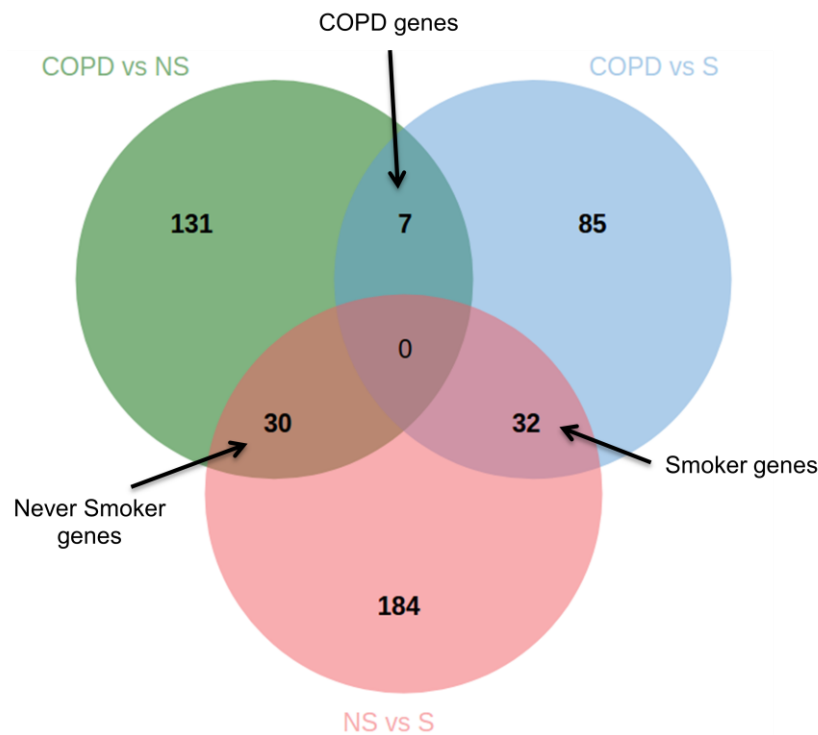


Figure 74: Venn diagram of the differentially express genes (Limma<0,01) between Never Smokers, Smokers, and COPD.

Next we compared the differentially express genes between COPD-CS and COPD-FS to identify genes characteristics of the active smoking inside the disease. There were only 5 with a nominal p value <0.01: ZSWIM7, neurobeachin, PLD3 (phospholipase D3), synapin III and FRZB (frizzled-related protein). This last gene has been previously described as Wnt inhibitor and to inhibit EMT in the lung [256].

5.3.4.6 - Immunomodulatory capacity

We compared the percentage of proliferation reduction on T CD4, T CD8 and B cells for LRMSC of the four studied groups (Never smokers=7, Smokers=4, COPD-FS=6, COPD-CS=9) (Figure 75). An impaired reduction of the proliferation of T CD8 cells was observed for COPD-CS. A tendency of a higher reduction in the proliferation was observed for the B lymphocytes in co-culture with the never smokers LRMSC, but it didn't reach statistical significance.

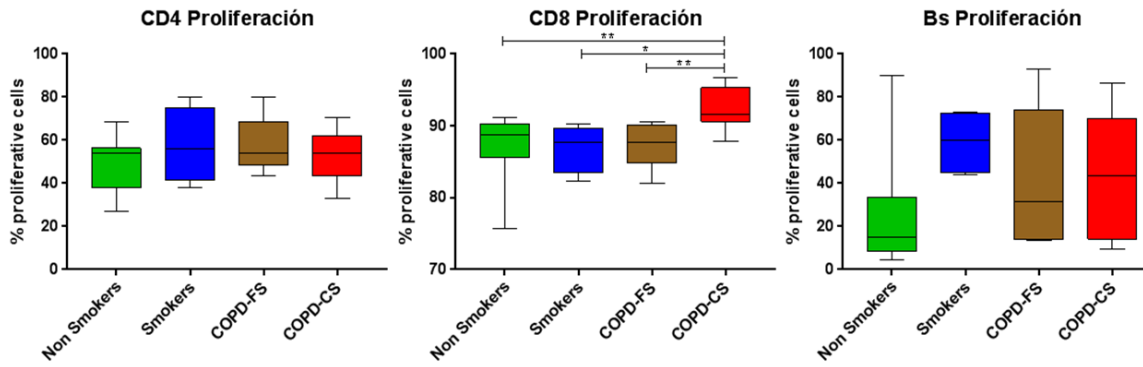


Figure 75: Proliferative capacity of the a) CD4 T lymphocytes, b) CD8 T lymphocytes and the c) B lymphocytes in co-culture with the LRMSC of the four studied groups, experiment was performed in triplicate. P value corresponds to the result of the Kruskal–Wallis followed by a Mann-Whitney post-hoc test; * p-value<0,05, ** p-value>0,005.

Next, T CD8 cell proliferation was analyzed by the percentage of cells in each division (as described above) Figure 76. COPD-CS arrest the proliferation in the 4th division while in the rest of groups the proliferation was arrested at the 3rd division.

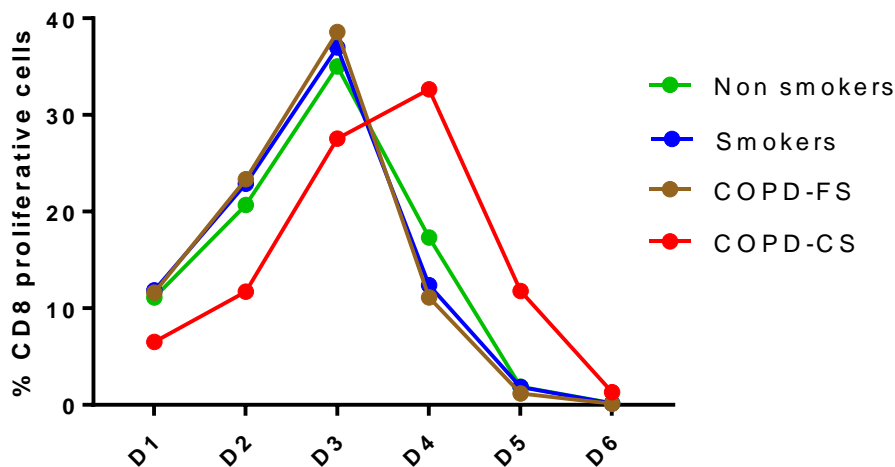


Figure 76: Percentage of proliferating cells in each division (mean) for the LRMSC of the 4 studied groups.

Finally, a correlation of the percentage of CD8 proliferative cells with several clinical variables was performed, see Figure 77. The percentage of CD8 proliferative T lymphocytes was negatively correlated with the level of FEV1% ref., DLCO % ref. and the KCO % ref. meaning that the reduced immunomodulatory capacity is associated with more severe disease status.

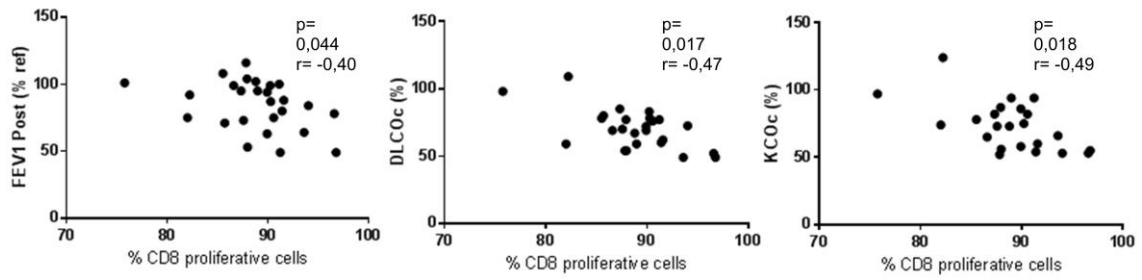


Figure 77: Correlation of the CD8 T lymphocytes with the FEV1, DLCO and KCO

No other clinical correlation was observed with the percentage of proliferation for B or T CD4 cells.

6 - DISCUSSION

6 - DISCUSSION

The discussion of the results of this PhD dissertation is organized in two parts: (1) the discussion of the results per objective; and (2) a general discussion that aims at integrating the main findings of each of the three objectives.

6.1 – OBJECTIVE 1. MOLECULAR IMMUNE RESPONSE

This part of the PhD dissertation describes and contrasts the transcriptomic signature in lung tissue of emphysema and bronchiolitis in patients with COPD. Main results reveal that emphysema is associated with a prominent immune response and a distinct B cell signature, which is not present in patients with bronchiolitis.

6.1.1 - Comparison with previous studies

Hogg *et al.* elegantly showed that the number of neutrophils, macrophages, CD4 cells, CD8 cells, B cells and lymphoid follicles increased in the airways and lung parenchyma of COPD with more severe airflow limitation [257]. Our results extend these observations by contrasting the inflammatory response in COPD patients with emphysema and bronchiolitis, with or without the same degree of airflow limitation.

A large body of experimental and clinical evidence supports the concept that emphysema can be an autoimmune disease triggered by cigarette smoking [44, 47]. This includes the fact that emphysema develops in mice after tobacco smoking- sensitized T cell transfer [70], that oligoclonal T and B cells can be isolated from the lung parenchyma of these patients [66], that they have both circulating [72] and tissue [71] auto-antibodies, and that lymphoid follicles have been repeatedly identified in the lung parenchyma of both animal models and patients with severe COPD [82, 246, 257], most likely with emphysema according to our observations herein (Figure 37). The results of this PhD dissertation, also support that there may be an autoimmune component of emphysema because I observed a distinct B cell signature in emphysema, but not in bronchiolitis.

Finally, lung transcriptomics in COPD has also been investigated already by several previous studies [258-260]. The results of this Thesis complement and extend them

because: (i) previous analysis studied a smaller number of individuals [261] or included patients with mild airflow limitation only [82, 246, 257] whereas the current Thesis includes a much larger number of individuals with a wide range of functional severity; (ii) I used network analysis to provide an integrated perspective of the lung immune response in these patients [183, 191] and I validated experimentally the role of B cells in emphysema; (iii) my analysis is the first to compare lung transcriptome in patients with severe emphysema or bronchiolitis, as well as to investigate differential gene expression in patients with mild and moderate emphysema and the effects of airflow limitation severity. The latter is particularly relevant given the relationship observed between the prevalence of emphysema and the severity of airflow limitation in my (Figure 37) and previous studies [262]; and, finally (iv) previous studies included current and former smokers, thus potentially confounding results by the well-described effects of active smoking on gene transcription [258, 263]. To avoid it, this Thesis studied former smokers only.

6.1.2 - Interpretation of findings

The results of this Thesis show that, as hypothesized, the molecular signature of emphysema and bronchiolitis in COPD are distinct. The former, but not the latter, is characterized by a prominent B cell molecular signature, as supported by the following observations: (i) DE genes up-regulated in severe emphysema (comparison 1) were enriched in ontologies related to the immune response and, specifically, in genes present in memory B cells. Some of these B cell-related genes were DE also in patients with intermediate characteristics (comparison 2) as well as in patients with moderate (*vs.* mild) emphysema (comparison 3) and in patients matched for the degree of airflow limitation (comparison 4). Moreover, immunohistochemistry identified the presence of CD20+IgM+ lymphoid follicles, active B cells (NF-KB p-p65+), proliferation (Ki-67+) and IgG+ cells in lung tissue of patients with emphysema, irrespectively of the severity of airflow limitation; (ii) the emphysema transcriptomic signature was validated *in silico* using GSEA and the dataset of Campbell *et al.* where emphysematous regions of the lungs were carefully selected by micro CT and laser dissection [224]; (iii) B cell related DE genes were hubs in the emphysema co-expression network (Figure 38) and were also correlated with innate immune receptors like AIM2. This was not the case in the bronchiolitis network, where the main B cell related hubs (CXCL13, LTB) were

absent (Figure 3); *(iv)* CXCL13 expressed by B cells is a key driver of lymphoid follicle formation, both in animal models and lung tissue of COPD patients [82, 246]. Our results therefore confirm that CXCL13 mRNA and protein levels are up-regulated in patients with emphysema, and expand previous results by showing that both B cell recruitment and the expression of genes controlling immunoglobulin transcription (CXCL13, CCL19 and POU2AF1) correlated with the severity of emphysema, as assessed by the DL_{CO} value; and, *(v)* in emphysema I found up-regulation of TNFRSF17 (BCMA), a BAFF receptor specific of activated B cells [247], and increased tissue levels of BAFF protein, in keeping with previous findings [81]. It is possible, therefore, that BAFF signaling through BCMA might contribute to increased activated B cell survival in emphysema. This may explain also the elevated immunoglobulin mRNA levels observed in our study. Overall, these findings are in agreement with recent observations showing expression of BAFF in the B cells of the lymphoid follicles in severe COPD [264, 265].

Considering all these findings together, in this PhD Thesis I propose the following pathogenic hypothesis for emphysema (Figure 78): *(i)* signals involving NF- κ B activation (e.g., smoking, airway infection, among others) lead to epithelial cell activation and increased production of BAFF, CCL19 and CXCL13 [264, 265]; *(ii)* this recruits CD27+IgM+ B cells into the lung; *(iii)* there, these cells respond to foreign and/or self antigens [44] and form lymphoid follicles, where B active cells divide and isotype switching occurs; and, *(iv)* the survival of these B cells is promoted in part by BCMA signaling that results in the production of key mediators of the immune response network observed in emphysema which in turn maintain the B cell loop.

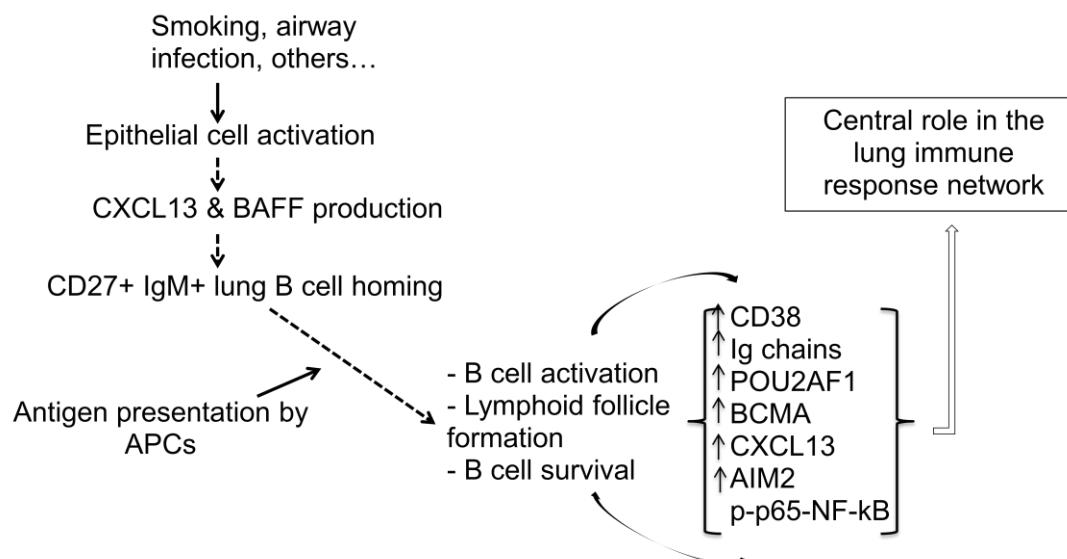


Figure 78: Diagram illustrating the proposed lung acquired immune response network in emphysema.

6.1.3 - Potential clinical implications

In keeping with previous observations [262], the results of this PhD Thesis clearly show that emphysema is almost invariably present in COPD patients with severe-very severe airflow limitation, whereas it occurs only in about half of the patients with mild-moderate disease (Figure 37). A simple explanation for this observation is that the occurrence of emphysema is a late event in the natural history of COPD. However, a recent report indicates that there are different vital lung function trajectories that can lead to COPD in adult life [266]. Further, our results here show that the molecular signature of emphysema and bronchiolitis is different, even in patients with the same degree of airflow limitation (GOLD grade 2). Hence, since there are no longitudinal studies that investigate the natural history of emphysema in COPD, an equally plausible explanation is that emphysema and bronchiolitis are different diseases which may co-occur (or not) in a given patient with COPD, hence challenging the concept that COPD is a single disease [267, 268].

It has been suggested that emphysema can be an autoimmune disease triggered by cigarette smoking [44, 47]. The results of this Thesis provide further support to this hypothesis⁷ by identifying a core functional molecular B cell related signature in patients with emphysema. Whether the antigen(s) eliciting this B cell response is a self (e.g. matrix degradation products) and/or external antigen(s) (bacteria, viruses) is unclear. Yet their identification may open new prophylactic and therapeutic strategies

for COPD patients. Selective depletion of B cells with the use of rituximab, a genetically engineered chimeric anti-CD20 monoclonal antibody, has been shown to be effective in several diseases where B-lymphocytes play a key pathogenic role, such as CD20+ B cell non-Hodgkin's and relapsing rheumatoid arthritis [269]. Following the results of this study, its potential role in emphysema merits further research.

6.1.4 – Potential Limitations

First, I used the term “bronchiolitis” generically to encompass all the structural abnormalities that can occur in the airways COPD patients, and not necessarily to indicate the presence of inflammation. Second, because the observational nature of this part of the PhD Thesis, functional evidences based on animal models or longitudinal human studies are required to validate their real clinical relevance. Third, this Thesis did not compare different lung tissue samples (with or without emphysema) obtained from the same individual, as Campbell *et al.* did [224]. To address this limitation, I used GSEA to contrasts our results in their dataset, as discussed below. Fourth, although I studied a considerable number of patients, subgroup analyses involve relatively small samples. Finally, the lung tissue samples analyzed do not always correspond to those areas with most severe CT emphysema, since this are not always accessible.

6.2 – OBJECTIVE 2. CELLULAR IMMUNE RESPONSE

This part of the PhD Thesis characterizes the cellular immune response network in lung tissue and peripheral blood of mild/moderated patients with COPD, never smokers and smokers with normal lung function, and correlated it with expression changes in whole lung tissue.

Main results reveal an increase in the proportion of lung macrophages and decrease in T cells related both to smoking status and disease. These immune cell alterations are not mirrored in peripheral blood, but are related to pathological process in the lung.

6.2.1 - Comparison with previous studies

It is important to start by highlighting that I have not evaluated changes in the absolute number of lung infiltrating cells, as most of the previous studies do; instead I have analyzed simultaneously the proportion of different immune cell populations. To my knowledge this is the first study that analyzes the cellular composition of both lung tissue and peripheral blood samples and integrates the results using networks. This limits the comparison of our results with previous studies.

It is well known, that lung tissue from severe airflow limitation COPD patients is characterized by an increased adaptive immune cell mediators (determined by Immunohistochemistry in lung tissue), including T CD8+ cytotoxic lymphocytes [59-61], T CD4+ lymphocytes polarized toward a TH1 response [18, 64] and B cell lymphoid follicles [18, 65]. In the lung tissue homogenate samples studied, I did not found differences in the proportion of B cells, but I observed a decrease in the proportion of T cells. These differences can be due to the fact that this Thesis included only patients with mild/moderated severe airflow limitation and the fact that I do not have absolute cell number counts.

A previous study with lung tissue homogenates, reported a decrease in the proportion of T CD4+ cells with an increase of CD8+ T cells in mild/moderated COPD [270]. At variance with this study, in this PhD dissertation there is not a significant increase in the proportion of T CD8+ cells, but I extend the study with the involvement of active smoking in the lung immune response, what could be the responsible of the divergences

with this study is related with current smoking. Unreported viral infections or differences in the smoking status can be responsible of these divergences.

With respect to lung tissue macrophages, an increase in their numbers in BAL and lung tissue and their correlation with the level of airway obstruction has been previously reported [34, 35]. My observations in this Thesis reproduce this previous observation in a much larger sample size, and complement it by showing that the increase in the proportion of macrophages is related both to current smoking and COPD in an independent manner.

Recent reports using IHC in lung tissue slides reported the increase of polarized macrophage markers (iNOS for M1 and CD206 for M2) both in relation to smoking and airflow limitation severity [271]. In agreement, we observe a higher proportion of intermediate phenotype macrophages with co-expression of both M1 and M2 markers, in relation to current smoking exposure in patients with COPD [272]. But at variance, the non-smokers population studied expressed also M1, M2 or M1-M2 markers, although I did not evaluate differences in the intensity of the staining.

With respect to the blood immune cell composition in COPD, previous reports showed differences related to a low grade systemic inflammation reflected by elevated levels of some pro-inflammatory cytokines and leukocytes [273-276]. I did not find significant changes in the blood of the study groups, so a main observation of this Thesis is the lack of correlation between the lung and blood immune cell populations.

Finally, several studies have investigated the differences at transcriptomic level in whole lung tissue [277-279]. The main limitation of these studies is that the cellular composition of the lung is not known at the time the transcriptomic profiling is done. The present transcriptomic co-expression analysis overcomes this limitation and identifies 3 modules that are related to the percentage of macrophages, T cells or monocytes in lung tissue.

6.2.2 - Interpretation of findings

The results of this Thesis show that the infiltrate present in mild moderated COPD comprises mostly macrophages and T lymphocytes. These two lung cell populations have a strong negative correlation between them indicating that an increase in the

proportion of macrophages is accompanied by a decrease in T lymphocytes and *vice versa*.

The increase in relation to current smoking and COPD of intermediated phenotype macrophages can reflect an attempt of the lung tissue to resolve the damage inflicted by smoking in these “early” stages of the disease. This attempt is not successful as macrophages do not reach the full M2 profile. Concomitant with this observation, the percentage of the M1 population decreases; this seems also an attempt to limit the “damage” avoiding a further burden of the inflammatory response.

The lung tissue mRNA co-expression analysis performed here identified two modules related to the percentage of macrophages. Their genes involve changes in the extracellular matrix and in the cilium function. Abnormalities in both processes have been previously related to COPD [280, 281], but not associated with the percentage of macrophages. Further functional experiments are required in order to identify the exact mechanism underlying this association, but can be related with the abnormal efferocytosis [46].

With respect to the observed reduction in the proportion of T lymphocytes, it affects CD4⁺ T cells and to a less extent CD8⁺ T lymphocytes. When I considered the level of the CD28 co-receptor, I observed that most of the lung T lymphocytes lack of it and never smokers had the highest proportion of CD28^{null} T cells, both for CD4 and CD8 T lymphocytes.

Interestingly, even if in COPD current smokers the proportion of T cells decreases, this decrease is in the proportion of CD28^{null} cells, and accordingly there is a relative increase in the proportion of the CD28⁺ T lymphocytes. In summary, the reduction in the proportion of T lymphocytes in the lungs of current smokers with COPD is related to the terminally differentiated population, not to the active population. Reduction in the proliferation of T lymphocytes had been previously described [282] and could be the reason for our reduction of the CD28^{null} population in early stages of the disease.

High levels of T CD4⁺CD28^{null} cells have been reported in the lung of very severe COPD patients [73], but up to date no information on its presence in milder stages of the disease was reported. The results of this Thesis seem to be opposite since I observed that never smokers had the highest proportion of CD28^{null} cells and there is an increase of the CD28⁺ cells in smokers and COPD. Our mRNA co-expression analysis confirm

these results as correlate the effect of tobacco smoke with genes related to T cell activation (salmon module). These differences could be related to the stage of the disease, as in early stages the tobacco had the main contribution to the pathogenesis (described in section 5.2.4) what could induce the decrease on activated T cells [282] while on more severe stages the COPD pathogenesis imposes an active T cell response [283]. Increase in this terminally differentiated or end-stage cytotoxic T lymphocyte population (CTL, T CD8+CD28^{null}) has been observed in aging [284] and COPD [74]. The results of this Thesis are in agreement with these observations, as seems that the proportion of CD28+ cells is increased in relation to current tobacco consumption what can be considered as ongoing damage that could lead to the expansion and conversion into the CTL with disease severity and also with age.

The cellular correlation network observed here shows that carboxyhemoglobin levels correlate with the macrophage lung proportions. The strong effect of the tobacco smoke exposure in immune cell populations in the lung was also reported by the two way ANOVA analysis, and it is stronger and in the same direction of the effect disease. This observation suggests that the immunological mechanisms of response to smoke are common in normal lung function smokers and mild COPD patients, at least at the level of cellular populations. The perpetuating mechanism in the initial phases of COPD might be related to changes in the functionality or absolute numbers of the immune cells rather than changes in the percentage of infiltrating populations.

Finally, I observed that changes observed in lung tissue were not reflected in blood, suggesting that these two compartments are affected by the disease in different manners, thus the blood is not a good surrogate of the immune cell composition changes ongoing in the lung.

6.2.3 - Potential limitations

First, all the included patients had lung cancer. In theory, this can be a confounding factor but, if it is, it will affect all samples analyzed. Second, we used flow cytometry for the characterization of the immune cell populations, so we could not define absolute numbers. Instead, we have described the proportions of the total CD45+ hematopoietic immune infiltrate in relation to tobacco smoke and COPD.

6.2.4 - Potential clinical implications

The results of this part of the Thesis suggest that the pharmacological modulation of the macrophage infiltration directed to the lung compartment in incipient stages of airflow limitation might have a beneficial effect in patients with COPD. Tobacco cessation is key element in order to maintain the balance of immune cell populations in the lung.

6.3 – OBJECTIVE 3. REGENERATIVE CAPACITY

This part of the PhD Thesis investigated, for the first time, a population of lung resident mesenchymal-like stem cells (LRMSC) in the lungs of patients with COPD. To do so, I developed an isolation/expansion methodology based in their sphere forming capacity. Main results show that LRMSC express BM-MSc surface markers and stemness related genes, had multi-lineage differentiation potential and immunomodulatory properties. I did not found differences in the proportion of LRMSC cells between groups, but these cells present differences in the immunomodulatory capacity in relation to COPD and current smoking.

6.3.1 - Comparison with previous studies

MSC cells residing in other organs have been previously reported (see introduction section 1.2.2.1 - Mesenchymal stem cells), although there are few studies obtaining tissue resident MSC in disease organs [285-287]. Specifically in the lung, previous studies have identify CD105+ CD90+ and CD73+ cells with some mesenchymal properties in BAL [144] and human lung tissue of healthy individuals [144, 148-150]. The results of this Thesis supports those of previous reports, adds a new methodology for the "in-vitro" expansion of the LRMSC while maintaining their stemness related properties, and characterizes this population of LRMSC in patients with COPD.

The current established MSC definition is not able to differentiate MSC and closely related populations, such as fibroblast [149, 288, 289]. The present Thesis used several markers to characterize the LRMSC, including cell surface markers, transcriptional levels and the immunomodulatory capacity, for these reasons it represents an advance in the state of the art of the field. This, unfortunately, implies that I cannot compare the findings of this Thesis with previous reports in lung tissue because all the molecular markers that I used have not been previously assessed/reported. Furthermore the type of samples used to obtain the cell population are crucial in both fibroblasts and MSC, as they had been described to maintain specific properties from their tissue of origin [290-293]. This means that I cannot compare the results seen with MSC of BAL origin.

6.3.2 - Interpretation of findings

The 3D culture methodology established maintains the stemness related properties while the conventional 2D adherent step allows the expansion of the cells. Furthermore this 2-step methodology is a convenient cell culture technique to expand *in vitro* the stem cells avoiding MSC exhaustion and increase in size.

The LRMSC population identified in this Thesis fulfills the mesenchymal defining criteria [145, 146, 288], as they are: adherent to plastic, express the expected surface markers (CD105+ CD90+ and CD73+), and have tri-lineage differentiation capacity. Despite that, these properties are not enough to differentiate a mesenchymal cell from a fibroblast, as even the expression of some stemness related transcripts had been described in fibroblast [288, 294, 295]. The Rohart test confirmed that the described cells are putative MSC, residing in the lung.

In addition, it has been shown that the described LRMSC have immunomodulatory capacities, as they inhibit the proliferation of both T and B cells in co-culture system to the same extend that BM-MSc, while lung fibroblast have a reduce capacity. However, our LRMSC population shows a huge variability with several of them having similar immunomodulatory capacity than our control lung fibroblast. This is the case for example of the immunomodulation of B cells were two groups of LRMSC in COPD appear, one arresting the proliferation of activated B cells and a second promoting it. These differences were not related to the currently assessed clinical parameters, but deserve further investigation.

Interestingly LRMSC from lung tissue of current smokers with COPD showed an impaired immunomodulation of T CD8+ cells. This result is in agreement with the effect of tobacco smoking in changes of the percentages of immune cells in relation to both COPD and smoking. Interestingly the proliferation of T CD8+ cells was in relation to the levels of FEV1 % ref., DLCO % ref. and KCOc % ref. indicating that further functional defects in LRMSC in relation to the lung function of the donor should be investigated.

The mechanism by which exert their immunomodulatory capacity is still unclear but it involves both cell to cell contact mechanisms and soluble factors [296, 297]. This immunomodulation could be exert directly over lymphocytes or indirectly by affecting APCs, predominantly DCs [298]. In the present study they proven to act directly on T

and B cells, but an effect on antigen presenting cells cannot be excluded, as it has not been assessed.

MSC are sensitive of the microenvironment and the surrounding cytokines could activate the MSC toward an anti-inflammatory (M2) response or to a pro-inflammatory (M1) response, like the macrophages [140, 299, 300]. IFN γ priming is necessary for initial activation of the MSC but LPS or fibrinogen activate TLR4 polarizing the MSC toward a pro-inflammatory phenotype [300, 301], while poli (I:C) or progesterone activates the TLR3 inducing an anti-inflammatory response [302, 303].

Direct cell to cell contact immunomodulation is exerted mainly by interactions with the MHC II that without the necessary co-stimulatory molecules and the expression of FAS ligand leading to lymphocyte anergy [304, 305]. The soluble mediators of the immunomodulation are mainly cytokines (IL6, IL8, IL10, IFN γ , IL4, IL1ra and TGF β), indoleamine 2,3-dioxygenase (IDO), lipids mediators such prostaglandin (PGE2), chemokines (RANTES and CCL10), or HLA molecules (HLA-G).

Taking into account all this complex regulation, the observed differences in the reduction of the proliferation of T and B lymphocytes could be due to the original microenvironment of their lung. This deserves further investigation as could be a possible explanation for the LRMSC from COPD-CS impair immunomodulatory activity over CD8 T lymphocytes.

The regenerative potential of MSC diminishes with age leading to functional impairments of adult stem cells [306, 307]. Accelerated aging of stem cells is a plausible hypothesis to link stem cell exhaustion and age-related diseases, such as COPD. For this reason I assessed if telomere length of LRMSC in COPD patients was compromised, or related to age of the donor. In this respect I did not observed differences, but the limited age range (60-80 years) studied and the small number of individuals in the study can interfere with this results.

The telomere loss during *in vitro* expansion has been described as one of the responsible of the senescence status and the reduction of proliferation until complete stop [308-310]. As the need of an *in vitro* isolation steps may compromise the proliferative potential of the cultured cells, the telomere length had been determined in passage 5 without signs of senescence for all the cells. and.

6.3.3 - Potential limitations

An important aspect of this part of the Thesis is that the methodology for the isolation of the LRMSC makes a heterogeneous culture. Cells are obtained from lung tissue explants without a sorting step and subsequent cell passages enrich the culture in the LRMSC but there is always a remnant of contaminating cells. Another potential limitation is that this Thesis focused in one lung stem cell population, several others have been reported and might have a deeper impact on the regeneration itself, so further investigation is deserved.

6.4 INTEGRATIVE DISCUSSION

The general hypothesis of this PhD dissertation was that the clinical heterogeneity and complexity of COPD is associated with different types of immune response, as well as to differences in lung regeneration and/or repair capacity. By and large, results show that, as discussed below, the immune response in COPD is indeed heterogeneous and associated to different clinical features.

I showed that the lung immune response of patients with bronchiolitis (i.e., absence of emphysema) *vs.* those with severe emphysema is different both in magnitude and network structure. The presence of severe emphysema is highly related with the severity of the airflow limitation, this and the relatively low number of the individuals profiled per group are the main limitations of the work. Despite of that, the differential expression changes reported in relation to severity of emphysema have been recently reproduced in two larger and independent studies [311, 312]. Indicating that emphysema related genes harbor molecular drivers of COPD severity and represent potential therapeutic targets. Furthermore, when I studied the stages of the disease with mild/moderated severe airflow limitation, I observed that the immune response is still heterogeneous, but main players are in relation to active tobacco consumption and related to the presence of macrophages and T cells. Interestingly the proportion of macrophages and the current smoking status are related to pathobiological changes in the whole lung mRNA in processes as cilium and extracellular matrix organization that are later observed as deregulated in severe emphysema, opening a door for future functional studies in this direction.

For the first time, to my knowledge, I reported that cellular immune related differences observed in the lung tissue are not mirrored in blood suggesting that the extra pulmonary effects of the disease represent a different pathobiological entity. These results are in concordance with that the recent study of Nunez *et al.* [313] showed that soluble inflammatory markers are not correlated in the BAL and blood.

Finally, this Thesis is the first that characterizes LRMSC in COPD. No differences in proportion of these cells, or their extracellular markers were observed. But interestingly, in keeping with results of the immune response profiling, differences in the immunomodulatory capacity of T CD8 cells in relation to smoke were observed. This

finding links the immune cell alterations with the regenerative capacity in COPD, which was the ultimate goal of this PhD Thesis.

7 - CONCLUSIONS

7.1 - GENERAL CONCLUSION

The lung immune response is heterogeneous and associated with both the lung regenerative capacity and the clinical heterogeneity/complexity of COPD.

7.2 - SPECIFIC CONCLUSIONS

1. The lung tissue molecular signature of emphysema and bronchiolitis in COPD are different. Results in emphysema support a pathogenic role of the acquired immune response, highlight the need of identifying the antigen(s) triggering this response and open new therapeutic possibilities, ranging from the avoidance/elimination of this antigen(s) to the pharmacological manipulation of this B -cell response.
2. In COPD patients with mild/moderate airflow limitation the cellular pulmonary and systemic immune response are not related. In these disease stages main immune cell alterations are common to the effects of current tobacco consumption and relate to alterations in the proportion and type of macrophages and relate to functional changes in the transcriptomic profile of the lung.
3. LRMSC are present in the lung of patients with COPD in a similar proportion to controls, but *in vitro* have an impaired immunomodulatory capacity related to active smoking. Further functional *in vivo* experiments are required in order to assess their regenerative capacity and to explore potential molecular targets to, eventually, revert it back to normal for therapeutic purposes.

8 - BIBLIOGRAPHY

8 - BIBLIOGRAPHY

1. Vogelmeier, C.F., et al., *Global Strategy for the Diagnosis, Management, and Prevention of Chronic Obstructive Lung Disease 2017 Report: GOLD Executive Summary*. Arch Bronconeumol, 2017. **53**(3): p. 128-149.
2. Rabe, K.F., et al., *Global strategy for the diagnosis, management, and prevention of chronic obstructive pulmonary disease: GOLD executive summary*. Am J Respir Crit Care Med, 2007. **176**(6): p. 532-55.
3. Eisner, M.D., et al., *Lifetime environmental tobacco smoke exposure and the risk of chronic obstructive pulmonary disease*. Environ Health, 2005. **4**(1): p. 7.
4. Gall, E.T., et al., *Indoor air pollution in developing countries: research and implementation needs for improvements in global public health*. Am J Public Health, 2013. **103**(4): p. e67-72.
5. Balmes, J., et al., *American Thoracic Society Statement: Occupational contribution to the burden of airway disease*. Am J Respir Crit Care Med, 2003. **167**(5): p. 787-97.
6. Bush, A., *COPD: a pediatric disease*. COPD, 2008. **5**(1): p. 53-67.
7. Tirimanna, P.R., et al., *Prevalence of asthma and COPD in general practice in 1992: has it changed since 1977?* Br J Gen Pract, 1996. **46**(406): p. 277-81.
8. Lopez, A.D., et al., *Chronic obstructive pulmonary disease: current burden and future projections*. Eur Respir J, 2006. **27**(2): p. 397-412.
9. Murray, C.J. and A.D. Lopez, *Alternative projections of mortality and disability by cause 1990-2020: Global Burden of Disease Study*. Lancet, 1997. **349**(9064): p. 1498-504.
10. Ko, F.W. and D.S. Hui, *Outdoor air pollution: impact on chronic obstructive pulmonary disease patients*. Curr Opin Pulm Med, 2009. **15**(2): p. 150-7.
11. Fletcher, C. and R. Peto, *The natural history of chronic airflow obstruction*. Br Med J, 1977. **1**(6077): p. 1645-8.
12. Smith, C.A. and D.J. Harrison, *Association between polymorphism in gene for microsomal epoxide hydrolase and susceptibility to emphysema*. Lancet, 1997. **350**(9078): p. 630-3.
13. DeMeo, D.L., et al., *Familial aggregation of FEF(25-75) and FEF(25-75)/FVC in families with severe, early onset COPD*. Thorax, 2004. **59**(5): p. 396-400.
14. Lange, P., B. Celli, and A. Agustí, *Lung-Function Trajectories and Chronic Obstructive Pulmonary Disease*. N Engl J Med, 2015. **373**(16): p. 1575.
15. Agustí, A.G., *COPD, a multicomponent disease: implications for management*. Respir Med, 2005. **99**(6): p. 670-82.
16. *Definition and classification of chronic bronchitis for clinical and epidemiological purposes. A report to the Medical Research Council by their Committee on the Aetiology of Chronic Bronchitis*. Lancet, 1965. **1**(7389): p. 775-9.

17. Cosio, M.G., K.A. Hale, and D.E. Niewoehner, *Morphologic and morphometric effects of prolonged cigarette smoking on the small airways*. Am Rev Respir Dis, 1980. **122**(2): p. 265-21.
18. Hogg, J.C., et al., *The nature of small-airway obstruction in chronic obstructive pulmonary disease*. N Engl J Med, 2004. **350**(26): p. 2645-53.
19. Mullen, J.B., et al., *Reassessment of inflammation of airways in chronic bronchitis*. Br Med J (Clin Res Ed), 1985. **291**(6504): p. 1235-9.
20. Hogg, J.C., P.T. Macklem, and W.M. Thurlbeck, *Site and nature of airway obstruction in chronic obstructive lung disease*. N Engl J Med, 1968. **278**(25): p. 1355-60.
21. Snider, G.L., *Distinguishing among asthma, chronic bronchitis, and emphysema*. Chest, 1985. **87**(1 Suppl): p. 35S-39S.
22. Majo, J., H. Ghezzi, and M.G. Cosio, *Lymphocyte population and apoptosis in the lungs of smokers and their relation to emphysema*. Eur Respir J, 2001. **17**(5): p. 946-53.
23. Tudor, R.M., et al., *Oxidative stress and apoptosis interact and cause emphysema due to vascular endothelial growth factor receptor blockade*. Am J Respir Cell Mol Biol, 2003. **29**(1): p. 88-97.
24. Tudor, R.M., et al., *State of the art. Cellular and molecular mechanisms of alveolar destruction in emphysema: an evolutionary perspective*. Proc Am Thorac Soc, 2006. **3**(6): p. 503-10.
25. Ngan, D.A., et al., *The possible role of granzyme B in the pathogenesis of chronic obstructive pulmonary disease*. Ther Adv Respir Dis, 2009. **3**(3): p. 113-29.
26. Abboud, R.T. and S. Vimalanathan, *Pathogenesis of COPD. Part I. The role of protease-antiprotease imbalance in emphysema*. Int J Tuberc Lung Dis, 2008. **12**(4): p. 361-7.
27. Laurell, C.B. and S. Eriksson, *The electrophoretic α 1-globulin pattern of serum in α 1-antitrypsin deficiency*. 1963. COPD, 2013. **10 Suppl 1**: p. 3-8.
28. Matzinger, P., *The danger model: a renewed sense of self*. Science, 2002. **296**(5566): p. 301-5.
29. Sun, W., R. Wu, and J.A. Last, *Effects of exposure to environmental tobacco smoke on a human tracheobronchial epithelial cell line*. Toxicology, 1995. **100**(1-3): p. 163-74.
30. Churg, A., et al., *Acute cigarette smoke-induced connective tissue breakdown requires both neutrophils and macrophage metalloelastase in mice*. Am J Respir Cell Mol Biol, 2002. **27**(3): p. 368-74.
31. Stone, P.J., et al., *Elastin and collagen degradation products in urine of smokers with and without chronic obstructive pulmonary disease*. Am J Respir Crit Care Med, 1995. **151**(4): p. 952-9.

32. Parker, L.C., L.R. Prince, and I. Sabroe, *Translational mini-review series on Toll-like receptors: networks regulated by Toll-like receptors mediate innate and adaptive immunity*. Clin Exp Immunol, 2007. **147**(2): p. 199-207.
33. Richards, G.A., et al., *Spirometric abnormalities in young smokers correlate with increased chemiluminescence responses of activated blood phagocytes*. Am Rev Respir Dis, 1989. **139**(1): p. 181-7.
34. Molet, S., et al., *Increase in macrophage elastase (MMP-12) in lungs from patients with chronic obstructive pulmonary disease*. Inflamm Res, 2005. **54**(1): p. 31-6.
35. Shapiro, S.D., *The macrophage in chronic obstructive pulmonary disease*. Am J Respir Crit Care Med, 1999. **160**(5 Pt 2): p. S29-32.
36. Hautamaki, R.D., et al., *Requirement for macrophage elastase for cigarette smoke-induced emphysema in mice*. Science, 1997. **277**(5334): p. 2002-4.
37. Snider, G.L., *Experimental studies on emphysema and chronic bronchial injury*. Eur J Respir Dis Suppl, 1986. **146**: p. 17-35.
38. Peleman, R.A., et al., *The cellular composition of induced sputum in chronic obstructive pulmonary disease*. Eur Respir J, 1999. **13**(4): p. 839-43.
39. Galdston, M., et al., *Interactions of neutrophil elastase, serum trypsin inhibitory activity, and smoking history as risk factors for chronic obstructive pulmonary disease in patients with MM, MZ, and ZZ phenotypes for alpha-antitrypsin*. Am Rev Respir Dis, 1977. **116**(5): p. 837-46.
40. Linden, M., et al., *Airway inflammation in smokers with nonobstructive and obstructive chronic bronchitis*. Am Rev Respir Dis, 1993. **148**(5): p. 1226-32.
41. Lane, N., et al., *Regulation in chronic obstructive pulmonary disease: the role of regulatory T-cells and Th17 cells*. Clin Sci.(Lond), 2010. **119**(2): p. 75-86.
42. Steinman, L., *State of the art. Four easy pieces: interconnections between tissue injury, intermediary metabolism, autoimmunity, and chronic degeneration*. Proc Am Thorac Soc, 2006. **3**(6): p. 484-6.
43. Schaefer, L., et al., *The matrix component biglycan is proinflammatory and signals through Toll-like receptors 4 and 2 in macrophages*. J Clin Invest, 2005. **115**(8): p. 2223-33.
44. Cosio, M.G., M. Saetta, and A. Agusti, *Immunologic aspects of chronic obstructive pulmonary disease*. N Engl J Med, 2009. **360**(23): p. 2445-54.
45. Widgerow, A.D., *Cellular resolution of inflammation--catabasis*. Wound Repair Regen, 2012. **20**(1): p. 2-7.
46. Noguera, A., et al., *An investigation of the resolution of inflammation (catabasis) in COPD*. Respir Res, 2012. **13**: p. 101.
47. Faner, R., T. Cruz, and A. Agusti, *Immune response in chronic obstructive pulmonary disease*. Expert Rev Clin Immunol, 2013. **9**(9): p. 821-33.
48. Lambrecht, B.N., J.B. Prins, and H.C. Hoogsteden, *Lung dendritic cells and host immunity to infection*. Eur Respir J, 2001. **18**(4): p. 692-704.
49. Marshak-Rothstein, A., *Toll-like receptors in systemic autoimmune disease*. Nat Rev Immunol, 2006. **6**(11): p. 823-35.

50. Butcher, E.C. and L.J. Picker, *Lymphocyte homing and homeostasis*. Science, 1996. **272**(5258): p. 60-6.
51. Freeman, C.M., J.L. Curtis, and S.W. Chensue, *CC chemokine receptor 5 and CXC chemokine receptor 6 expression by lung CD8+ cells correlates with chronic obstructive pulmonary disease severity*. Am J Pathol, 2007. **171**(3): p. 767-76.
52. Grumelli, S., et al., *An immune basis for lung parenchymal destruction in chronic obstructive pulmonary disease and emphysema*. PLoS Med, 2004. **1**(1): p. e8.
53. Bratke, K., et al., *Function-associated surface molecules on airway dendritic cells in cigarette smokers*. Am.J.Respir Cell Mol.Biol., 2008. **38**(6): p. 655-660.
54. Demedts, I.K., et al., *Accumulation of dendritic cells and increased CCL20 levels in the airways of patients with chronic obstructive pulmonary disease*. Am J Respir Crit Care Med, 2007. **175**(10): p. 998-1005.
55. Giancotti, F.G. and E. Ruoslahti, *Integrin signaling*. Science, 1999. **285**(5430): p. 1028-32.
56. Calabrese, F., et al., *Marked alveolar apoptosis/proliferation imbalance in end-stage emphysema*. Respir Res, 2005. **6**: p. 14.
57. Hodge, S., et al., *Alveolar macrophages from subjects with chronic obstructive pulmonary disease are deficient in their ability to phagocytose apoptotic airway epithelial cells*. Immunol Cell Biol, 2003. **81**(4): p. 289-96.
58. Vandivier, R.W., P.M. Henson, and I.S. Douglas, *Burying the dead: the impact of failed apoptotic cell removal (efferocytosis) on chronic inflammatory lung disease*. Chest, 2006. **129**(6): p. 1673-82.
59. Saetta, M., et al., *CD8+ T-lymphocytes in peripheral airways of smokers with chronic obstructive pulmonary disease*. Am J Respir Crit Care Med, 1998. **157**(3 Pt 1): p. 822-6.
60. Saetta, M., et al., *CD8+ve cells in the lungs of smokers with chronic obstructive pulmonary disease*. Am J Respir Crit Care Med, 1999. **160**(2): p. 711-7.
61. O'Shaughnessy, T.C., et al., *Inflammation in bronchial biopsies of subjects with chronic bronchitis: inverse relationship of CD8+ T lymphocytes with FEV1*. Am J Respir Crit Care Med, 1997. **155**(3): p. 852-7.
62. Imai, K., et al., *Correlation of lung surface area to apoptosis and proliferation in human emphysema*. Eur Respir J, 2005. **25**(2): p. 250-8.
63. Kasahara, Y., et al., *Endothelial cell death and decreased expression of vascular endothelial growth factor and vascular endothelial growth factor receptor 2 in emphysema*. Am J Respir Crit Care Med, 2001. **163**(3 Pt 1): p. 737-44.
64. Turato, G., et al., *Airway inflammation in severe chronic obstructive pulmonary disease: relationship with lung function and radiologic emphysema*. Am J Respir Crit Care Med, 2002. **166**(1): p. 105-10.
65. van der Strate, B.W., et al., *Cigarette smoke-induced emphysema: A role for the B cell?* Am J Respir Crit Care Med, 2006. **173**(7): p. 751-8.

66. Sullivan, A.K., et al., *Oligoclonal CD4+ T cells in the lungs of patients with severe emphysema*. Am J Respir Crit Care Med, 2005. **172**(5): p. 590-6.
67. Shapiro, S.D., *End-stage chronic obstructive pulmonary disease: the cigarette is burned out but inflammation rages on*. Am J Respir Crit Care Med, 2001. **164**(3): p. 339-40.
68. Richmond, I., et al., *Bronchus associated lymphoid tissue (BALT) in human lung: its distribution in smokers and non-smokers*. Thorax, 1993. **48**(11): p. 1130-4.
69. Rose, N.R. and C. Bona, *Defining criteria for autoimmune diseases (Witebsky's postulates revisited)*. Immunol Today, 1993. **14**(9): p. 426-30.
70. Taraseviciene-Stewart, L., et al., *An animal model of autoimmune emphysema*. Am J Respir Crit Care Med, 2005. **171**(7): p. 734-42.
71. Feghali-Bostwick, C.A., et al., *Autoantibodies in patients with chronic obstructive pulmonary disease*. Am J Respir Crit Care Med, 2008. **177**(2): p. 156-63.
72. Lee, S.H., et al., *Anti-elastin autoimmunity in tobacco smoking-induced emphysema*. Nat Med, 2007. **13**(5): p. 567-9.
73. Hoetzenecker, K., et al., *High levels of lung resident CD4+CD28null cells in COPD: implications of autoimmunity*. Wien Klin Wochenschr, 2013. **125**(5-6): p. 150-5.
74. Hodge, G., et al., *Role of increased CD8/CD28(null) T cells and alternative co-stimulatory molecules in chronic obstructive pulmonary disease*. Clin Exp Immunol, 2011. **166**(1): p. 94-102.
75. Thewissen, M., et al., *Analyses of immunosenescent markers in patients with autoimmune disease*. Clin Immunol, 2007. **123**(2): p. 209-18.
76. Harrison, O.J., et al., *Airway infiltration of CD4+ CCR6+ Th17 type cells associated with chronic cigarette smoke induced airspace enlargement*. Immunol Lett, 2008. **121**(1): p. 13-21.
77. Demoor, T., et al., *CCR7 modulates pulmonary and lymph node inflammatory responses in cigarette smoke-exposed mice*. J Immunol, 2009. **183**(12): p. 8186-94.
78. Pons, J., et al., *Blunted gamma delta T-lymphocyte response in chronic obstructive pulmonary disease*. Eur Respir J, 2005. **25**(3): p. 441-6.
79. Chang, Y., et al., *CD8 positive T cells express IL-17 in patients with chronic obstructive pulmonary disease*. Respir Res, 2011. **12**: p. 43.
80. Shan, M., et al., *Lung myeloid dendritic cells coordinately induce TH1 and TH17 responses in human emphysema*. Sci Transl Med, 2009. **1**(4): p. 4ra10.
81. Polverino, F., et al., *A novel insight into adaptive immunity in chronic obstructive pulmonary disease: B cell activating factor belonging to the tumor necrosis factor family*. Am J Respir Crit Care Med, 2010. **182**(8): p. 1011-9.
82. Litsiou, E., et al., *CXCL13 production in B cells via Toll-like receptor/lymphotoxin receptor signaling is involved in lymphoid neogenesis in*

- chronic obstructive pulmonary disease*. Am J Respir Crit Care Med, 2013. **187**(11): p. 1194-202.
83. Wiegman, C.H., et al., *Oxidative stress-induced mitochondrial dysfunction drives inflammation and airway smooth muscle remodeling in patients with chronic obstructive pulmonary disease*. J Allergy Clin Immunol, 2015. **136**(3): p. 769-80.
 84. Rangasamy, T., et al., *Genetic ablation of Nrf2 enhances susceptibility to cigarette smoke-induced emphysema in mice*. J Clin Invest, 2004. **114**(9): p. 1248-59.
 85. Balaban, R.S., S. Nemoto, and T. Finkel, *Mitochondria, oxidants, and aging*. Cell, 2005. **120**(4): p. 483-95.
 86. Crystal, R.G., *Airway basal cells. The "smoking gun" of chronic obstructive pulmonary disease*. Am J Respir Crit Care Med, 2014. **190**(12): p. 1355-62.
 87. Crystal, R.G., et al., *Airway epithelial cells: current concepts and challenges*. Proc Am Thorac Soc, 2008. **5**(7): p. 772-7.
 88. Rock, J.R., S.H. Randell, and B.L. Hogan, *Airway basal stem cells: a perspective on their roles in epithelial homeostasis and remodeling*. Dis Model Mech, 2010. **3**(9-10): p. 545-56.
 89. Hajj, R., et al., *Basal cells of the human adult airway surface epithelium retain transit-amplifying cell properties*. Stem Cells, 2007. **25**(1): p. 139-48.
 90. Mercer, R.R., et al., *Cell number and distribution in human and rat airways*. Am J Respir Cell Mol Biol, 1994. **10**(6): p. 613-24.
 91. Shaykhiev, R. and R.G. Crystal, *Basal cell origins of smoking-induced airway epithelial disorders*. Cell Cycle, 2014. **13**(3): p. 341-2.
 92. Boers, J.E., A.W. Ambergen, and F.B. Thunnissen, *Number and proliferation of basal and parabasal cells in normal human airway epithelium*. Am J Respir Crit Care Med, 1998. **157**(6 Pt 1): p. 2000-6.
 93. Liu, X. and J.F. Engelhardt, *The glandular stem/progenitor cell niche in airway development and repair*. Proc Am Thorac Soc, 2008. **5**(6): p. 682-8.
 94. Barkauskas, C.E., et al., *Type 2 alveolar cells are stem cells in adult lung*. J Clin Invest, 2013. **123**(7): p. 3025-36.
 95. Kotton, D.N. and E.E. Morrisey, *Lung regeneration: mechanisms, applications and emerging stem cell populations*. Nat Med, 2014. **20**(8): p. 822-32.
 96. Breeze, R.G. and E.B. Wheeldon, *The cells of the pulmonary airways*. Am Rev Respir Dis, 1977. **116**(4): p. 705-77.
 97. Lumsden, A.B., A. McLean, and D. Lamb, *Goblet and Clara cells of human distal airways: evidence for smoking induced changes in their numbers*. Thorax, 1984. **39**(11): p. 844-9.
 98. AUERBACH, O., et al., *Changes in bronchial epithelium in relation to cigarette smoking and in relation to lung cancer*. N Engl J Med, 1961. **265**: p. 253-67.
 99. Dye, J.A. and K.B. Adler, *Effects of cigarette smoke on epithelial cells of the respiratory tract*. Thorax, 1994. **49**(8): p. 825-34.

100. Kennedy, S.M., et al., *Increased airway mucosal permeability of smokers. Relationship to airway reactivity.* Am Rev Respir Dis, 1984. **129**(1): p. 143-8.
101. Blanpain, C. and E. Fuchs, *Stem cell plasticity. Plasticity of epithelial stem cells in tissue regeneration.* Science, 2014. **344**(6189): p. 1242281.
102. Didon, L., et al., *RFX3 modulation of FOXJ1 regulation of cilia genes in the human airway epithelium.* Respir Res, 2013. **14**: p. 70.
103. Rock, J.R., et al., *Notch-dependent differentiation of adult airway basal stem cells.* Cell Stem Cell, 2011. **8**(6): p. 639-48.
104. Pilette, C., et al., *Reduced epithelial expression of secretory component in small airways correlates with airflow obstruction in chronic obstructive pulmonary disease.* Am J Respir Crit Care Med, 2001. **163**(1): p. 185-94.
105. Shaykhiev, R., et al., *Cigarette smoking reprograms apical junctional complex molecular architecture in the human airway epithelium in vivo.* Cell Mol Life Sci, 2011. **68**(5): p. 877-92.
106. AUERBACH, O., et al., *Changes in the bronchial epithelium in relation to smoking and cancer of the lung; a report of progress.* N Engl J Med, 1957. **256**(3): p. 97-104.
107. Aarbiou, J., et al., *Human neutrophil defensins and secretory leukocyte proteinase inhibitor in squamous metaplastic epithelium of bronchial airways.* Inflamm Res, 2004. **53**(6): p. 230-8.
108. Araya, J., et al., *Squamous metaplasia amplifies pathologic epithelial-mesenchymal interactions in COPD patients.* J Clin Invest, 2007. **117**(11): p. 3551-62.
109. Faner, R., et al., *Abnormal lung aging in chronic obstructive pulmonary disease and idiopathic pulmonary fibrosis.* Am J Respir Crit Care Med, 2012. **186**(4): p. 306-313.
110. Ghadially, R., et al., *The aged epidermal permeability barrier. Structural, functional, and lipid biochemical abnormalities in humans and a senescent murine model.* J Clin Invest, 1995. **95**(5): p. 2281-90.
111. Fulop, T., et al., *Aging, immunity, and cancer.* Discov Med, 2011. **11**(61): p. 537-50.
112. Aoshiba, K. and A. Nagai, *Senescence hypothesis for the pathogenetic mechanism of chronic obstructive pulmonary disease.* Proc Am Thorac Soc, 2009. **6**(7): p. 596-601.
113. Decramer, M., W. Janssens, and M. Miravitlles, *Chronic obstructive pulmonary disease.* Lancet, 2012. **379**(9823): p. 1341-51.
114. Buro-Auremma, L.J., et al., *Cigarette smoking induces small airway epithelial epigenetic changes with corresponding modulation of gene expression.* Hum Mol Genet, 2013. **22**(23): p. 4726-38.
115. Berdasco, M. and M. Esteller, *DNA methylation in stem cell renewal and multipotency.* Stem Cell Res Ther, 2011. **2**(5): p. 42.
116. Talikka, M., et al., *Genomic impact of cigarette smoke, with application to three smoking-related diseases.* Crit Rev Toxicol, 2012. **42**(10): p. 877-89.

117. Staudt, M.R., et al., *Airway Basal stem/progenitor cells have diminished capacity to regenerate airway epithelium in chronic obstructive pulmonary disease*. *Am J Respir Crit Care Med*, 2014. **190**(8): p. 955-8.
118. Bakke, P.S., et al., *Candidate genes for COPD in two large data sets*. *Eur Respir J*, 2011. **37**(2): p. 255-63.
119. Castaldi, P.J., et al., *The COPD genetic association compendium: a comprehensive online database of COPD genetic associations*. *Hum Mol Genet*, 2010. **19**(3): p. 526-34.
120. Potten, C.S. and M. Loeffler, *Stem cells: attributes, cycles, spirals, pitfalls and uncertainties. Lessons for and from the crypt*. *Development*, 1990. **110**(4): p. 1001-20.
121. Bertoncello, I. and J.L. McQualter, *Lung stem cells: do they exist?* *Respirology*, 2013. **18**(4): p. 587-95.
122. Rando, T.A., *The immortal strand hypothesis: segregation and reconstruction*. *Cell*, 2007. **129**(7): p. 1239-43.
123. Lajtha, L.G., *Stem cell concepts*. *Differentiation*, 1979. **14**(1-2): p. 23-34.
124. Morrison, S.J. and J. Kimble, *Asymmetric and symmetric stem-cell divisions in development and cancer*. *Nature*, 2006. **441**(7097): p. 1068-74.
125. Fuchs, E. and J.A. Segre, *Stem cells: a new lease on life*. *Cell*, 2000. **100**(1): p. 143-55.
126. Bjornson, C.R., et al., *Turning brain into blood: a hematopoietic fate adopted by adult neural stem cells in vivo*. *Science*, 1999. **283**(5401): p. 534-7.
127. Forbes, S.J., et al., *Adult stem cell plasticity: new pathways of tissue regeneration become visible*. *Clin Sci (Lond)*, 2002. **103**(4): p. 355-69.
128. Seruya, M., et al., *Clonal population of adult stem cells: life span and differentiation potential*. *Cell Transplant*, 2004. **13**(2): p. 93-101.
129. Gerson, S.L., *Mesenchymal stem cells: no longer second class marrow citizens*. *Nat Med*, 1999. **5**(3): p. 262-4.
130. Pittenger, M.F., et al., *Multilineage potential of adult human mesenchymal stem cells*. *Science*, 1999. **284**(5411): p. 143-7.
131. Epperly, M.W., et al., *Bone marrow origin of myofibroblasts in irradiation pulmonary fibrosis*. *Am J Respir Cell Mol Biol*, 2003. **29**(2): p. 213-24.
132. Hashimoto, N., et al., *Bone marrow-derived progenitor cells in pulmonary fibrosis*. *J Clin Invest*, 2004. **113**(2): p. 243-52.
133. Fine, A., *Marrow cells as progenitors of lung tissue*. *Blood Cells Mol Dis*, 2004. **32**(1): p. 95-6.
134. Morrison, S.J. and A.C. Spradling, *Stem cells and niches: mechanisms that promote stem cell maintenance throughout life*. *Cell*, 2008. **132**(4): p. 598-611.
135. Ahmed, M. and C. Ffrench-Constant, *Extracellular Matrix Regulation of Stem Cell Behavior*. *Curr Stem Cell Rep*, 2016. **2**: p. 197-206.

136. Lane, S.W., D.A. Williams, and F.M. Watt, *Modulating the stem cell niche for tissue regeneration*. Nat Biotechnol, 2014. **32**(8): p. 795-803.
137. Scadden, D.T., *The stem-cell niche as an entity of action*. Nature, 2006. **441**(7097): p. 1075-9.
138. Nelson, C.M. and M.J. Bissell, *Of extracellular matrix, scaffolds, and signaling: tissue architecture regulates development, homeostasis, and cancer*. Annu Rev Cell Dev Biol, 2006. **22**: p. 287-309.
139. Rozario, T. and D.W. DeSimone, *The extracellular matrix in development and morphogenesis: a dynamic view*. Dev Biol, 2010. **341**(1): p. 126-40.
140. Waterman, R.S., et al., *A new mesenchymal stem cell (MSC) paradigm: polarization into a pro-inflammatory MSC1 or an Immunosuppressive MSC2 phenotype*. PLoS One, 2010. **5**(4): p. e10088.
141. Anderson, D.J., F.H. Gage, and I.L. Weissman, *Can stem cells cross lineage boundaries?* Nat Med, 2001. **7**(4): p. 393-5.
142. Ying, Q.L., et al., *Changing potency by spontaneous fusion*. Nature, 2002. **416**(6880): p. 545-8.
143. Lagasse, E., et al., *Purified hematopoietic stem cells can differentiate into hepatocytes in vivo*. Nat Med, 2000. **6**(11): p. 1229-34.
144. Lama, V.N., et al., *Evidence for tissue-resident mesenchymal stem cells in human adult lung from studies of transplanted allografts*. J Clin Invest, 2007. **117**(4): p. 989-96.
145. Bernardo, M.E., F. Locatelli, and W.E. Fibbe, *Mesenchymal stromal cells*. Ann N Y Acad Sci, 2009. **1176**: p. 101-17.
146. Morikawa, S., et al., *Prospective identification, isolation, and systemic transplantation of multipotent mesenchymal stem cells in murine bone marrow*. J Exp Med, 2009. **206**(11): p. 2483-96.
147. Djouad, F., et al., *Mesenchymal stem cells inhibit the differentiation of dendritic cells through an interleukin-6-dependent mechanism*. Stem Cells, 2007. **25**(8): p. 2025-32.
148. Ricciardi, M., et al., *Comparison of epithelial differentiation and immune regulatory properties of mesenchymal stromal cells derived from human lung and bone marrow*. PLoS One, 2012. **7**(5): p. e35639.
149. Sabatini, F., et al., *Human bronchial fibroblasts exhibit a mesenchymal stem cell phenotype and multilineage differentiating potentialities*. Lab Invest, 2005. **85**(8): p. 962-71.
150. Rolandsson, S., et al., *Primary mesenchymal stem cells in human transplanted lungs are CD90/CD105 perivascularly located tissue-resident cells*. BMJ Open Respir Res, 2014. **1**(1): p. e000027.
151. Rohart, F., et al., *A molecular classification of human mesenchymal stromal cells*. PeerJ, 2016. **4**: p. e1845.
152. Sinclair, K.A., et al., *Mesenchymal Stromal Cells are Readily Recoverable from Lung Tissue, but Not the Alveolar Space, in Healthy Humans*. Stem Cells, 2016.

153. Messina, E., et al., *Isolation and expansion of adult cardiac stem cells from human and murine heart*. *Circ Res*, 2004. **95**(9): p. 911-21.
154. Chimenti, I., et al., *Isolation and expansion of adult cardiac stem/progenitor cells in the form of cardiospheres from human cardiac biopsies and murine hearts*. *Methods Mol Biol*, 2012. **879**: p. 327-38.
155. Davis, D.R., et al., *Isolation and expansion of functionally-competent cardiac progenitor cells directly from heart biopsies*. *J Mol Cell Cardiol*, 2010. **49**(2): p. 312-21.
156. Davis, D.R., et al., *Validation of the cardiosphere method to culture cardiac progenitor cells from myocardial tissue*. *PLoS One*, 2009. **4**(9): p. e7195.
157. Pavlova, S.V., et al., *Characteristics of cardiac cell cultures derived from human myocardial explants*. *Bull Exp Biol Med*, 2013. **156**(1): p. 127-35.
158. Li, T.S., et al., *Cardiospheres recapitulate a niche-like microenvironment rich in stemness and cell-matrix interactions, rationalizing their enhanced functional potency for myocardial repair*. *Stem Cells*, 2010. **28**(11): p. 2088-98.
159. Cho, H.J., et al., *Generation of human secondary cardiospheres as a potent cell processing strategy for cell-based cardiac repair*. *Biomaterials*, 2013. **34**(3): p. 651-61.
160. Cho, H.J., et al., *Secondary sphere formation enhances the functionality of cardiac progenitor cells*. *Mol Ther*, 2012. **20**(9): p. 1750-66.
161. Bartosh, T.J., et al., *Aggregation of human mesenchymal stromal cells (MSCs) into 3D spheroids enhances their antiinflammatory properties*. *Proc Natl Acad Sci U S A*, 2010. **107**(31): p. 13724-9.
162. Ylostalo, J.H., et al., *Unique characteristics of human mesenchymal stromal/progenitor cells pre-activated in 3-dimensional cultures under different conditions*. *Cytotherapy*, 2014. **16**(11): p. 1486-500.
163. Bartosh, T.J. and J.H. Ylostalo, *Preparation of anti-inflammatory mesenchymal stem/precursor cells (MSCs) through sphere formation using hanging-drop culture technique*. *Curr Protoc Stem Cell Biol*, 2014. **28**: p. Unit 2B.6.
164. Potapova, I.A., et al., *Mesenchymal stem cells support migration, extracellular matrix invasion, proliferation, and survival of endothelial cells in vitro*. *Stem Cells*, 2007. **25**(7): p. 1761-8.
165. Chimenti, I., et al., *Human Lung Spheroids as In Vitro Niches of Lung Progenitor Cells With Distinctive Paracrine and Plasticity Properties*. *Stem Cells Transl Med*, 2016.
166. Schweitzer, K.S., et al., *Adipose stem cell treatment in mice attenuates lung and systemic injury induced by cigarette smoking*. *Am J Respir Crit Care Med*, 2011. **183**(2): p. 215-25.
167. Rojas, M., et al., *Bone marrow-derived mesenchymal stem cells in repair of the injured lung*. *Am J Respir Cell Mol Biol*, 2005. **33**(2): p. 145-52.

168. Ortiz, L.A., et al., *Mesenchymal stem cell engraftment in lung is enhanced in response to bleomycin exposure and ameliorates its fibrotic effects*. Proc Natl Acad Sci U S A, 2003. **100**(14): p. 8407-11.
169. Mei, S.H., et al., *Mesenchymal stem cells reduce inflammation while enhancing bacterial clearance and improving survival in sepsis*. Am J Respir Crit Care Med, 2010. **182**(8): p. 1047-57.
170. Islam, M.N., et al., *Mitochondrial transfer from bone-marrow-derived stromal cells to pulmonary alveoli protects against acute lung injury*. Nat Med, 2012. **18**(5): p. 759-65.
171. Li, X., et al., *Mitochondrial transfer of induced pluripotent stem cell-derived mesenchymal stem cells to airway epithelial cells attenuates cigarette smoke-induced damage*. Am J Respir Cell Mol Biol, 2014. **51**(3): p. 455-65.
172. Badri, L., et al., *Epithelial interactions and local engraftment of lung-resident mesenchymal stem cells*. Am J Respir Cell Mol Biol, 2011. **45**(4): p. 809-16.
173. Loebinger, M.R., et al., *Mesenchymal stem cell delivery of TRAIL can eliminate metastatic cancer*. Cancer Res, 2009. **69**(10): p. 4134-42.
174. Le Blanc, K., et al., *Mesenchymal stem cells for treatment of steroid-resistant, severe, acute graft-versus-host disease: a phase II study*. Lancet, 2008. **371**(9624): p. 1579-86.
175. Manning, E., et al., *Interleukin-10 delivery via mesenchymal stem cells: a novel gene therapy approach to prevent lung ischemia-reperfusion injury*. Hum Gene Ther, 2010. **21**(6): p. 713-27.
176. D'Agostino, B., et al., *Mesenchymal stem cell therapy for the treatment of chronic obstructive pulmonary disease*. Expert Opin Biol Ther, 2010. **10**(5): p. 681-7.
177. Serrano-Mollar, A., et al., *Safety and Tolerability of Alveolar Type II Cell Transplantation in Idiopathic Pulmonary Fibrosis*. Chest, 2016. **150**(3): p. 533-43.
178. Faner, R., et al., *Network medicine, multimorbidity and the lung in the elderly*. Eur Respir J, 2014. **44**(3): p. 775-88.
179. Silverman, E.K. and J. Loscalzo, *Network medicine approaches to the genetics of complex diseases*. Discov Med, 2012. **14**(75): p. 143-52.
180. Wolkenhauer, O., et al., *The road from systems biology to systems medicine*. Pediatr Res, 2013. **73**(4 Pt 2): p. 502-7.
181. Kitano, H., *Computational systems biology*. Nature, 2002. **420**(6912): p. 206-10.
182. Clermont, G., et al., *Bridging the gap between systems biology and medicine*. Genome Med, 2009. **1**(9): p. 88.
183. Barabási, A.L., N. Gulbahce, and J. Loscalzo, *Network medicine: a network-based approach to human disease*. Nat Rev Genet, 2011. **12**(1): p. 56-68.
184. Kohl, P., et al., *Systems biology: an approach*. Clin Pharmacol Ther, 2010. **88**(1): p. 25-33.

185. Agustí, A. and J. Vestbo, *Current controversies and future perspectives in chronic obstructive pulmonary disease*. Am J Respir Crit Care Med, 2011. **184**(5): p. 507-13.
186. Wild, C.P., *Complementing the genome with an "exposome": the outstanding challenge of environmental exposure measurement in molecular epidemiology*. Cancer Epidemiol Biomarkers Prev, 2005. **14**(8): p. 1847-50.
187. Wild, C.P., *The exposome: from concept to utility*. Int J Epidemiol, 2012. **41**(1): p. 24-32.
188. Bousquet, J., et al., *Integrated care pathways for airway diseases (AIRWAYS-ICPs)*. Eur Respir J, 2014. **44**(2): p. 304-23.
189. Divo, M., et al., *Comorbidities and risk of mortality in patients with chronic obstructive pulmonary disease*. Am J Respir Crit Care Med, 2012. **186**(2): p. 155-61.
190. Bousquet, J., et al., *Systems medicine and integrated care to combat chronic noncommunicable diseases*. Genome Med, 2011. **3**(7): p. 43.
191. Diez, D., A. Agustí, and C.E. Wheelock, *Network analysis in the investigation of chronic respiratory diseases. From basics to application*. Am J Respir Crit Care Med, 2014. **190**(9): p. 981-8.
192. Barabási, A.L., *Network medicine--from obesity to the "diseasome"*. N Engl J Med, 2007. **357**(4): p. 404-7.
193. Goh, K.I., et al., *The human disease network*. Proc Natl Acad Sci U S A, 2007. **104**(21): p. 8685-90.
194. Agusti, A., P. Sobradillo, and B. Celli, *Addressing the complexity of chronic obstructive pulmonary disease: from phenotypes and biomarkers to scale-free networks, systems biology, and P4 medicine*. Am J Respir Crit Care Med, 2011. **183**(9): p. 1129-37.
195. Barabási, A.L. and E. Bonabeau, *Scale-free networks*. Sci Am, 2003. **288**(5): p. 60-9.
196. Vázquez, A., et al., *The topological relationship between the large-scale attributes and local interaction patterns of complex networks*. Proc Natl Acad Sci U S A, 2004. **101**(52): p. 17940-5.
197. Menche, J., et al., *Disease networks. Uncovering disease-disease relationships through the incomplete interactome*. Science, 2015. **347**(6224): p. 1257601.
198. Sharma, A., et al., *A disease module in the interactome explains disease heterogeneity, drug response and captures novel pathways and genes in asthma*. Hum Mol Genet, 2015. **24**(11): p. 3005-20.
199. Menche, J., et al., *A diVIsive Shuffling Approach (VIStA) for gene expression analysis to identify subtypes in Chronic Obstructive Pulmonary Disease*. BMC Syst Biol, 2014. **8 Suppl 2**: p. S8.
200. McDonald, V.M., et al., *Multidimensional assessment and tailored interventions for COPD: respiratory utopia or common sense?* Thorax, 2013. **68**(7): p. 691-4.

201. Vanfleteren, L.E., et al., *Clusters of comorbidities based on validated objective measurements and systemic inflammation in patients with chronic obstructive pulmonary disease*. *Am J Respir Crit Care Med*, 2013. **187**(7): p. 728-35.
202. Van Remoortel, H., et al., *Risk factors and comorbidities in the preclinical stages of chronic obstructive pulmonary disease*. *Am J Respir Crit Care Med*, 2014. **189**(1): p. 30-8.
203. Grosdidier, S., et al., *Network medicine analysis of COPD multimorbidities*. *Respir Res*, 2014. **15**: p. 111.
204. Pozo-Rodríguez, F., et al., *Clinical audit of COPD patients requiring hospital admissions in Spain: AUDIPOC study*. *PLoS One*, 2012. **7**(7): p. e42156.
205. Pozo-Rodríguez, F., et al., *[Clinical audit of patients admitted to hospital in Spain due to exacerbation of COPD (AUDIPOC study): method and organisation]*. *Arch Bronconeumol*, 2010. **46**(7): p. 349-57.
206. López-Campos, J.L., et al., *European COPD Audit: design, organisation of work and methodology*. *Eur Respir J*, 2013. **41**(2): p. 270-6.
207. Faner, R., et al., *Molecular and clinical disease of comorbidities in exacerbated COPD patients*. *Eur Respir J*, 2015. **46**(4): p. 1001-10.
208. Faner, R. and A. Agustí, *Network analysis: a way forward for understanding COPD multimorbidity*. *Eur Respir J*, 2015. **46**(3): p. 591-2.
209. Xie, L., et al., *An increased ratio of serum miR-21 to miR-181a levels is associated with the early pathogenic process of chronic obstructive pulmonary disease in asymptomatic heavy smokers*. *Mol Biosyst*, 2014. **10**(5): p. 1072-81.
210. Ezzie, M.E., et al., *Gene expression networks in COPD: microRNA and mRNA regulation*. *Thorax*, 2012. **67**(2): p. 122-31.
211. Turan, N., et al., *A systems biology approach identifies molecular networks defining skeletal muscle abnormalities in chronic obstructive pulmonary disease*. *PLoS Comput Biol*, 2011. **7**(9): p. e1002129.
212. Vestbo, J., et al., *Evaluation of COPD Longitudinally to Identify Predictive Surrogate End-points (ECLIPSE)*. *Eur Respir J*, 2008. **31**(4): p. 869-73.
213. Agustí, A., et al., *Persistent systemic inflammation is associated with poor clinical outcomes in COPD: a novel phenotype*. *PLoS One*, 2012. **7**(5): p. e37483.
214. Agustí, A. and W. Macnee, *The COPD control panel: towards personalised medicine in COPD*. *Thorax*, 2013. **68**(7): p. 687-90.
215. Faner, R., et al., *Systemic inflammatory response to smoking in chronic obstructive pulmonary disease: evidence of a gender effect*. *PloS one*, 2014. **9**(5): p. e97491.
216. Yoo, S., et al., *Integrative analysis of DNA methylation and gene expression data identifies EPAS1 as a key regulator of COPD*. *PLoS Genet*, 2015. **11**(1): p. e1004898.
217. Agustí, A., et al., *Lungs, bone marrow, and adipose tissue. A network approach to the pathobiology of chronic obstructive pulmonary disease*. *Am J Respir Crit Care Med*, 2013. **188**(12): p. 1396-406.

218. Villena, C., et al., *The CIBERES Pulmonary Biobank Consortium: an opportunity for cooperative international respiratory research*. Eur.Respir J., 2011. **37**(1): p. 204-206.
219. Roca, J., et al., *Spirometric reference values from a Mediterranean population*. Bull Eur Physiopathol Respir, 1986. **22**(3): p. 217-24.
220. Roca, J., et al., *Single-breath carbon monoxide diffusing capacity prediction equations from a Mediterranean population*. Am Rev Respir Dis, 1990. **141**(4 Pt 1): p. 1026-32.
221. Breitling, R., et al., *Rank products: a simple, yet powerful, new method to detect differentially regulated genes in replicated microarray experiments*. FEBS Lett, 2004. **573**(1-3): p. 83-92.
222. Huang, d.W., B.T. Sherman, and R.A. Lempicki, *Systematic and integrative analysis of large gene lists using DAVID bioinformatics resources*. Nat Protoc, 2009. **4**(1): p. 44-57.
223. Subramanian, A., et al., *Gene set enrichment analysis: a knowledge-based approach for interpreting genome-wide expression profiles*. Proc Natl Acad Sci U S A, 2005. **102**(43): p. 15545-50.
224. Campbell, J.D., et al., *A gene expression signature of emphysema-related lung destruction and its reversal by the tripeptide GHK*. Genome Med, 2012. **4**(8): p. 67.
225. Benita, Y., et al., *Gene enrichment profiles reveal T-cell development, differentiation, and lineage-specific transcription factors including ZBTB25 as a novel NF-AT repressor*. Blood, 2010. **115**(26): p. 5376-84.
226. Fuller, T.F., et al., *Weighted gene coexpression network analysis strategies applied to mouse weight*. Mamm Genome, 2007. **18**(6-7): p. 463-72.
227. *Computing., R.C.T.R.F.f.S., R: A language and environment for statistical computing.* . 2016.
228. Shannon, P., et al., *Cytoscape: a software environment for integrated models of biomolecular interaction networks*. Genome Res, 2003. **13**(11): p. 2498-504.
229. Irizarry, R.A., et al., *Exploration, normalization, and summaries of high density oligonucleotide array probe level data*. Biostatistics, 2003. **4**(2): p. 249-64.
230. Miller, J.A., et al., *Strategies for aggregating gene expression data: the collapseRows R function*. BMC bioinformatics, 2011. **12**: p. 322.
231. Langfelder, P. and S. Horvath, *WGCNA: an R package for weighted correlation network analysis*. BMC bioinformatics, 2008. **9**: p. 559.
232. Cawthon, R.M., *Telomere length measurement by a novel monochrome multiplex quantitative PCR method*. Nucleic Acids Res, 2009. **37**(3): p. e21.
233. Faner, R., et al., *Network Analysis of Lung Transcriptomics Reveals a Distinct B-Cell Signature in Emphysema*. Am J Respir Crit Care Med, 2016. **193**(11): p. 1242-53.

234. Barjaktarevic, I., et al., *Diffusing capacity for carbon monoxide correlates best with tissue volume from quantitative CT scanning analysis*. Chest, 2015. **147**(6): p. 1485-93.
235. McDonough, J.E., et al., *Small-airway obstruction and emphysema in chronic obstructive pulmonary disease*. N Engl J Med, 2011. **365**(17): p. 1567-75.
236. Galbán, C.J., et al., *Computed tomography-based biomarker provides unique signature for diagnosis of COPD phenotypes and disease progression*. Nat Med, 2012. **18**(11): p. 1711-5.
237. Ernst, J.A., et al., *Isolation and characterization of the B-cell marker CD20*. Biochemistry, 2005. **44**(46): p. 15150-8.
238. Abbas, A.R., et al., *Immune response in silico (IRIS): immune-specific genes identified from a compendium of microarray expression data*. Genes Immun, 2005. **6**(4): p. 319-31.
239. Beste, M.T., et al., *Molecular network analysis of endometriosis reveals a role for c-Jun-regulated macrophage activation*. Sci Transl Med, 2014. **6**(222): p. 222ra16.
240. Tang, D., et al., *PAMPs and DAMPs: signal Os that spur autophagy and immunity*. Immunol Rev, 2012. **249**(1): p. 158-75.
241. Gauffre, A., et al., *Nuclear localization of the Epstein-Barr virus/C3d receptor (CR2) in the human Burkitt B lymphoma cell, Raji*. Mol Immunol, 1992. **29**(9): p. 1113-20.
242. Gruber, T.A., et al., *Activation-induced cytidine deaminase accelerates clonal evolution in BCR-ABL1-driven B-cell lineage acute lymphoblastic leukemia*. Cancer Res, 2010. **70**(19): p. 7411-20.
243. van Keimpema, M., et al., *FOXP1 directly represses transcription of proapoptotic genes and cooperates with NF- κ B to promote survival of human B cells*. Blood, 2014. **124**(23): p. 3431-40.
244. Mackay, F., et al., *BAFF AND APRIL: a tutorial on B cell survival*. Annu Rev Immunol, 2003. **21**: p. 231-64.
245. Bradbury, L.E., et al., *The CD19/CD21 signal transducing complex of human B lymphocytes includes the target of antiproliferative antibody-1 and Leu-13 molecules*. J Immunol, 1992. **149**(9): p. 2841-50.
246. Bracke, K.R., et al., *Role of CXCL13 in cigarette smoke-induced lymphoid follicle formation and chronic obstructive pulmonary disease*. Am J Respir Crit Care Med, 2013. **188**(3): p. 343-355.
247. O'Connor, B.P., et al., *BCMA is essential for the survival of long-lived bone marrow plasma cells*. J Exp Med, 2004. **199**(1): p. 91-8.
248. Kraal, G., I.L. Weissman, and E.C. Butcher, *Germinal centre B cells: antigen specificity and changes in heavy chain class expression*. Nature, 1982. **298**(5872): p. 377-9.
249. Posey, J.E., V.L. Brandt, and D.B. Roth, *Paradigm switching in the germinal center*. Nat Immunol, 2004. **5**(5): p. 476-7.

250. Malki, K., et al., *Integrative mouse and human mRNA studies using WGCNA nominates novel candidate genes involved in the pathogenesis of major depressive disorder*. Pharmacogenomics, 2013. **14**(16): p. 1979-90.
251. Hodgkinson, C.P., et al., *Abi3bp regulates cardiac progenitor cell proliferation and differentiation*. Circ Res, 2014. **115**(12): p. 1007-16.
252. Hodgkinson, C.P., et al., *Abi3bp is a multifunctional autocrine/paracrine factor that regulates mesenchymal stem cell biology*. Stem Cells, 2013. **31**(8): p. 1669-82.
253. Zhang, W.M., et al., *Analysis of the human integrin alpha11 gene (ITGA11) and its promoter*. Matrix Biol, 2002. **21**(6): p. 513-23.
254. Yiew, N.K.H., et al., *A novel role for the Wnt inhibitor APCDD1 in adipocyte differentiation: Implications for diet-induced obesity*. J Biol Chem, 2017. **292**(15): p. 6312-6324.
255. Jia, S., et al., *KIAA1199 promotes migration and invasion by Wnt/ β -catenin pathway and MMPs mediated EMT progression and serves as a poor prognosis marker in gastric cancer*. PLoS One, 2017. **12**(4): p. e0175058.
256. Guo, Y., et al., *Frzb, a secreted Wnt antagonist, decreases growth and invasiveness of fibrosarcoma cells associated with inhibition of Met signaling*. Cancer Res, 2008. **68**(9): p. 3350-60.
257. Hogg, J.C., et al., *The nature of small-airway obstruction in chronic obstructive pulmonary disease*. N.Engl.J.Med, 2004. **350**(26): p. 2645-2653.
258. Bosse, Y., et al., *Molecular signature of smoking in human lung tissues*. Cancer Res, 2012. **72**(15): p. 3753-63.
259. Savarimuthu Francis, S.M., et al., *Genes and gene ontologies common to airflow obstruction and emphysema in the lungs of patients with COPD*. PloS one, 2011. **6**(3): p. e17442.
260. Spira, A., et al., *Gene expression profiling of human lung tissue from smokers with severe emphysema*. Am J Respir Cell Mol Biol, 2004. **31**(6): p. 601-10.
261. Golpon, H.A., et al., *Emphysema lung tissue gene expression profiling*. Am J Respir Cell Mol Biol, 2004. **31**(6): p. 595-600.
262. Agusti, A., et al., *Characterisation of COPD heterogeneity in the ECLIPSE cohort*. Respir Res., 2010. **11**: p. 122.
263. Spira, A., et al., *Effects of cigarette smoke on the human airway epithelial cell transcriptome*. Proc Natl Acad Sci U S A, 2004. **101**(27): p. 10143-8.
264. Seys, L.J., et al., *Role of B Cell-Activating Factor in Chronic Obstructive Pulmonary Disease*. Am J Respir Crit Care Med, 2015. **192**(6): p. 706-18.
265. Polverino, F., et al., *B Cell-Activating Factor. An Orchestrator of Lymphoid Follicles in Severe Chronic Obstructive Pulmonary Disease*. Am J Respir Crit Care Med, 2015. **192**(6): p. 695-705.
266. Lange, P., et al., *Lung-Function Trajectories Leading to Chronic Obstructive Pulmonary Disease*. N Engl J Med, 2015. **373**(2): p. 111-22.

267. Agustí, A., *The path to personalised medicine in COPD*. Thorax, 2014. **69**(9): p. 857-64.
268. Vanfleteren, L.E., et al., *Moving from the Oslerian paradigm to the post-genomic era: are asthma and COPD outdated terms?* Thorax, 2014. **69**(1): p. 72-9.
269. Edwards, J.C., et al., *Efficacy of B-cell-targeted therapy with rituximab in patients with rheumatoid arthritis*. N Engl J Med, 2004. **350**(25): p. 2572-81.
270. Forsslund, H., et al., *Distribution of T-cell subsets in BAL fluid of patients with mild to moderate COPD depends on current smoking status and not airway obstruction*. Chest, 2014. **145**(4): p. 711-22.
271. Natoli, G. and S. Monticelli, *Macrophage activation: glancing into diversity*. Immunity, 2014. **40**(2): p. 175-7.
272. Bazzan, E., et al., *Dual polarization of human alveolar macrophages progressively increases with smoking and COPD severity*. Respir Res, 2017. **18**(1): p. 40.
273. Jin, Y., et al., *Treg/IL-17 ratio and Treg differentiation in patients with COPD*. PLoS One, 2014. **9**(10): p. e111044.
274. Agustí, A., et al., *Persistent systemic inflammation is associated with poor clinical outcomes in COPD: a novel phenotype*. PLoS One, 2012. **7**(5): p. e37483.
275. Gan, W.Q., et al., *Association between chronic obstructive pulmonary disease and systemic inflammation: a systematic review and a meta-analysis*. Thorax, 2004. **59**(7): p. 574-80.
276. Agustí, A., *Systemic effects of chronic obstructive pulmonary disease: what we know and what we don't know (but should)*. Proc Am Thorac Soc, 2007. **4**(7): p. 522-5.
277. Gower, A.C., et al., *Transcriptomic studies of the airway field of injury associated with smoking-related lung disease*. Proc Am Thorac Soc, 2011. **8**(2): p. 173-9.
278. Chesné, J., et al., *Systematic analysis of blood cell transcriptome in end-stage chronic respiratory diseases*. PLoS One, 2014. **9**(10): p. e109291.
279. Zeskind, J.E., M.E. Lenburg, and A. Spira, *Translating the COPD transcriptome: insights into pathogenesis and tools for clinical management*. Proc Am Thorac Soc, 2008. **5**(8): p. 834-41.
280. Wang, I.M., et al., *Gene expression profiling in patients with chronic obstructive pulmonary disease and lung cancer*. Am J Respir Crit Care Med, 2008. **177**(4): p. 402-11.
281. Ning, W., et al., *Comprehensive gene expression profiles reveal pathways related to the pathogenesis of chronic obstructive pulmonary disease*. Proc Natl Acad Sci U S A, 2004. **101**(41): p. 14895-900.
282. Hernandez, C.P., et al., *Effects of cigarette smoke extract on primary activated T cells*. Cell Immunol, 2013. **282**(1): p. 38-43.

283. Lambers, C., et al., *T cell senescence and contraction of T cell repertoire diversity in patients with chronic obstructive pulmonary disease*. Clin Exp Immunol, 2009. **155**(3): p. 466-75.
284. Sharma, G., N.A. Hanania, and Y.M. Shim, *The aging immune system and its relationship to the development of chronic obstructive pulmonary disease*. Proc Am Thorac Soc, 2009. **6**(7): p. 573-80.
285. van den Berge, S.A., M.E. van Strien, and E.M. Hol, *Resident adult neural stem cells in Parkinson's disease--the brain's own repair system?* Eur J Pharmacol, 2013. **719**(1-3): p. 117-27.
286. Iqbal, S.A., et al., *Identification of mesenchymal stem cells in perinodular fat and skin in Dupuytren's disease: a potential source of myofibroblasts with implications for pathogenesis and therapy*. Stem Cells Dev, 2012. **21**(4): p. 609-22.
287. Moossavi, S., et al., *Host-microbiota interaction and intestinal stem cells in chronic inflammation and colorectal cancer*. Expert Rev Clin Immunol, 2013. **9**(5): p. 409-22.
288. Dominici, M., et al., *Minimal criteria for defining multipotent mesenchymal stromal cells. The International Society for Cellular Therapy position statement*. Cytotherapy, 2006. **8**(4): p. 315-7.
289. Wetzig, A., et al., *Differential marker expression by cultures rich in mesenchymal stem cells*. BMC Cell Biol, 2013. **14**: p. 54.
290. Jüngel, A., C. Ospelt, and S. Gay, *What can we learn from epigenetics in the year 2009?* Curr Opin Rheumatol, 2010. **22**(3): p. 284-92.
291. Rinn, J.L., et al., *Anatomic demarcation by positional variation in fibroblast gene expression programs*. PLoS Genet, 2006. **2**(7): p. e119.
292. Slany, A., et al., *Plasticity of fibroblasts demonstrated by tissue-specific and function-related proteome profiling*. Clin Proteomics, 2014. **11**(1): p. 41.
293. Chang, H.Y., et al., *Diversity, topographic differentiation, and positional memory in human fibroblasts*. Proc Natl Acad Sci U S A, 2002. **99**(20): p. 12877-82.
294. Haniffa, M.A., et al., *Mesenchymal stem cells: the fibroblasts' new clothes?* Haematologica, 2009. **94**(2): p. 258-63.
295. Whetton, A.D. and G.J. Graham, *Homing and mobilization in the stem cell niche*. Trends Cell Biol, 1999. **9**(6): p. 233-8.
296. Yagi, H., et al., *Mesenchymal stem cells: Mechanisms of immunomodulation and homing*. Cell Transplant, 2010. **19**(6): p. 667-79.
297. Ben-Ami, E., S. Berrih-Aknin, and A. Miller, *Mesenchymal stem cells as an immunomodulatory therapeutic strategy for autoimmune diseases*. Autoimmun Rev, 2011. **10**(7): p. 410-5.
298. Kyurkchiev, D., et al., *Secretion of immunoregulatory cytokines by mesenchymal stem cells*. World J Stem Cells, 2014. **6**(5): p. 552-70.

299. Betancourt, A.M., *New Cell-Based Therapy Paradigm: Induction of Bone Marrow-Derived Multipotent Mesenchymal Stromal Cells into Pro-Inflammatory MSC1 and Anti-inflammatory MSC2 Phenotypes*. Adv Biochem Eng Biotechnol, 2013. **130**: p. 163-97.
300. Romieu-Mourez, R., et al., *Cytokine modulation of TLR expression and activation in mesenchymal stromal cells leads to a proinflammatory phenotype*. J Immunol, 2009. **182**(12): p. 7963-73.
301. Copland, I.B., et al., *The effect of platelet lysate fibrinogen on the functionality of MSCs in immunotherapy*. Biomaterials, 2013. **34**(32): p. 7840-50.
302. Zhao, X., et al., *Progesterone enhances immunoregulatory activity of human mesenchymal stem cells via PGE2 and IL-6*. Am J Reprod Immunol, 2012. **68**(4): p. 290-300.
303. Ryan, J.M., et al., *Interferon-gamma does not break, but promotes the immunosuppressive capacity of adult human mesenchymal stem cells*. Clin Exp Immunol, 2007. **149**(2): p. 353-63.
304. Gur-Wahnon, D., et al., *The induction of APC with a distinct tolerogenic phenotype via contact-dependent STAT3 activation*. PLoS One, 2009. **4**(8): p. e6846.
305. Augello, A., et al., *Bone marrow mesenchymal progenitor cells inhibit lymphocyte proliferation by activation of the programmed death 1 pathway*. Eur J Immunol, 2005. **35**(5): p. 1482-90.
306. Wagner, W., et al., *Aging and replicative senescence have related effects on human stem and progenitor cells*. PLoS One, 2009. **4**(6): p. e5846.
307. Liu, Q., et al., *Defective proliferative potential of MSCs from pediatric myelodysplastic syndrome patients is associated with cell senescence*. Int J Clin Exp Pathol, 2015. **8**(10): p. 13059-66.
308. Baxter, M.A., et al., *Study of telomere length reveals rapid aging of human marrow stromal cells following in vitro expansion*. Stem Cells, 2004. **22**(5): p. 675-82.
309. Bonab, M.M., et al., *Aging of mesenchymal stem cell in vitro*. BMC Cell Biol, 2006. **7**: p. 14.
310. Choi, M.R., et al., *Genome-scale DNA methylation pattern profiling of human bone marrow mesenchymal stem cells in long-term culture*. Exp Mol Med, 2012. **44**(8): p. 503-12.
311. Obeidat, M., et al., *Integrative Genomics of Emphysema Associated Genes Reveals Potential Disease Biomarkers*. Am J Respir Cell Mol Biol, 2017.
312. Morrow, J.D., et al., *Functional interactors of three genome-wide association study genes are differentially expressed in severe chronic obstructive pulmonary disease lung tissue*. Sci Rep, 2017. **7**: p. 44232.
313. Nunez, B., et al., *Lack of Correlation Between Pulmonary and Systemic Inflammation Markers in Patients with Chronic Obstructive Pulmonary Disease: A Simultaneous, Two-Compartmental Analysis*. Arch Bronconeumol, 2016. **52**(7): p. 361-7.

9 - ANNEX I: PUBLISHED ARTICLES

1. Faner R, **Cruz T**, Agusti A. Immune response in chronic obstructive pulmonary disease. *Expert Rev Clin Immunol* 2013; **9**(9): 821-33. (JCR 3.648)
2. Faner R, Gonzalez N, **Cruz T**, Kalko SG, Agusti A. Systemic inflammatory response to smoking in Chronic Obstructive Pulmonary Disease: evidence of a gender effect. *PLoS ONE* 2014; **9**(5): e97491. (JCR 3.73)
3. Faner R, **Cruz T**, López-Giraldo A, Agusti A. Network medicine, multimorbidity and the lung in the elderly. *European Respiratory Journal* 2014; **44**(3): 775-88. (JCR 6.355)
4. Agusti A, Lopez-Giraldo A, **Cruz T**, Faner R. Relevance of systems biology to respiratory medicine. *BRN Reviews* 2015.
5. Faner R, **Cruz T**, Casserras T, et al. Network Analysis of Lung Transcriptomics Reveals a Distinct B Cell Signature in Emphysema. *American Journal of Respiratory and Critical Care Medicine* 2016; **193**: 1242-53. (JCR 12.996)
6. Faner R, Sobradillo P, Noguera A, **Cruz T**, et al. The inflammasome pathway in stable COPD and acute exacerbations. *ERJ Open Res* 2016; **2**(3).

AGRADECIMIENTOS:

En primer lugar me gustaría agradecer a mis directores de tesis Rosa y Álvaro por la oportunidad que me han dado de comenzar en el mundo de la ciencia. A Rosa por enseñarme todo lo que he aprendido del laboratorio, analizar datos y plantear los experimentos sin irse por las ramas, directa al grano. A Álvaro por darme la oportunidad de formar parte de este grupo, su dirección y todo el tiempo que me ha dedicado.

Gracias a mis compañeras de laboratorio Gemma y Tamara que me han ayudado en buena parte de este trabajo y sin las cuales no hubiera sido posible. Sobre todo gracias por aguantarme en los no tan buenos momentos que he pasado durante estos 5 años de tesis. También agradecer a la nueva incorporación durante esta última etapa Sandra, para finalizar los experimentos y de soporte moral durante la escritura de esta tesis y suministro de kinder buenos.

Por supuesto gracias a Guillaume, el bioinformático del grupo y cerebro pensante detrás de todos esos scripts de R que a mí me traían por la calle de la amargura. Gracias a su enorme paciencia por ayudarme con la estadística de cada cosa que le pedía y por explicarme como realizar los análisis.

A pesar de que esta Tesis está escrita en primera persona, son todos ellos igual de participes en el resultado final que se presenta aquí. Gracias porque sin ellos esta Tesis no hubiese sido posible.

A la gente del servicio de inmunología por ser nuestro gran recurso adyacente y es que cuando falta algo siempre tenemos ahí a la "NASA". En el plano personal, porque no son solo las innumerables preguntas dentro del laboratorio, sino también las risas y buenos momentos fuera de él.

Gracias al Dr. Rojas por haberme dado la oportunidad de realizar una estancia en su laboratorio en Pittsburgh y tener la primera experiencia americana. A la gente del laboratorio por enseñarme todas las técnicas con ratones, la ayuda con las gestiones y por acogerme durante esos tres meses haciendo que el tiempo se pasase volando.

Por último fuera del laboratorio pero no por ello menos importante.

Gracias a mi familia, porque ellos son los primeros que han confiado en mi desde el principio y me han dado la oportunidad de estudiar lo que he querido. Sin ellos nada de esto hubiese sido posible.

Finalmente, gracias a todos mis amigos que han estado a mi lado durante este tiempo. Gracias por estar a mi lado cuando las cosas no salían tan bien, por apoyarme y animarme; y bueno por todos los buenos ratos, risas, consejos y por hacerme sentir en Barcelona como en casa.